



Mars Science Laboratory Telecommunications System Design

*Andre Makovsky, Peter Plott, and
Jim Taylor*



November 2009

**Jet Propulsion Laboratory
California Institute of Technology**

DESCANSO

**Deep Space Communications and Navigation Systems
Center of Excellence**

Design and Performance Summary Series

Mars Science Laboratory (MSL) Rover, wheels downward, descending on the sky crane.



DESCANSO Design and Performance Summary Series

Article 14

Mars Science Laboratory Telecommunications System Design

Andre Makovsky

Peter Ilott

Jim Taylor

Jet Propulsion Laboratory

California Institute of Technology

Pasadena, California

National Aeronautics and

Space Administration

Jet Propulsion Laboratory

California Institute of Technology

Pasadena, California

November 2009

This research was carried out at the Jet Propulsion Laboratory, California Institute of Technology, under a contract with the National Aeronautics and Space Administration.

Reference herein to any specific commercial product, process, or service by trade name, trademark, manufacturer, or otherwise, does not constitute or imply endorsement by the United States Government or the Jet Propulsion Laboratory, California Institute of Technology.

Copyright 2009 California Institute of Technology.
Government sponsorship acknowledged.

DESCANSO DESIGN AND PERFORMANCE SUMMARY SERIES

Issued by the Deep Space Communications and Navigation Systems
Center of Excellence
Jet Propulsion Laboratory
California Institute of Technology

Joseph H. Yuen, Editor-in-Chief

Previously Published Articles in This Series

Article 1—“Mars Global Surveyor Telecommunications”
Jim Taylor, Kar-Ming Cheung, and Chao-Jen Wong

Article 2—“Deep Space 1 Telecommunications”
Jim Taylor, Michela Muñoz Fernández, Ana I. Bolea Alamañac, and Kar-Ming Cheung

Article 3—“Cassini Orbiter/Huygens Probe Telecommunications”
Jim Taylor, Laura Sakamoto, and Chao-Jen Wong

Article 4—“Voyager Telecommunications”
Roger Ludwig and Jim Taylor

Article 5—“Galileo Telecommunications”
Jim Taylor, Kar-Ming Cheung, and Dongae Seo

Article 6—“Odyssey Telecommunications”
Andre Makovsky, Andrea Barbieri, and Ramona Tung

Article 7—“Deep Space 1 Navigation: Extended Missions”
Brian Kennedy, Shyam Bhaskaran, J. Edmund Riedel, and Mike Wang

Article 8—“Deep Space 1 Navigation: Primary Mission”
Brian Kennedy, J. Edmund Riedel, Shyam Bhaskaran, Shailen Desai, Don Han, Tim McElrath,
George Null, Mark Ryne, Steve Synnott, Mike Wang, and Robert Werner

Article 9—“Deep Impact Flyby and Impactor Telecommunications”
Jim Taylor and David Hansen

Article 10—“Mars Exploration Rover Telecommunications”
Jim Taylor, Andre Makovsky, Andrea Barbieri, Ramona Tung,
Polly Estabrook, and A. Gail Thomas

Article 11—“ Mars Exploration Rover Navigation”
Louis A. D’Amario

Article 12 —“Mars Reconnaissance Orbiter Telecommunications”
Jim Taylor, Dennis K. Lee, and Shervin Shambayati

Article 13 —“Dawn Telecommunications”
Jim Taylor

Article 14 —“Mars Science Laboratory Telecommunications System Design”
Andre Makovsky, Peter Ilott, and Jim Taylor

Foreword

This Design and Performance Summary Series, issued by the Deep Space Communications and Navigation Systems Center of Excellence (DESCANSO), is a companion series to the DESCANSO Monograph Series. Authored by experienced scientists and engineers who participated in and contributed to deep-space missions, each article in this series summarizes the design and performance of major systems, such as communications and navigation, for each mission. In addition, the series illustrates the progression of system design from mission to mission. Lastly, the series collectively provides readers with a broad overview of the mission systems described.

Joseph H. Yuen
DESCANSO Leader

Acknowledgements

This article was made possible by access to information and documents provided by members of the Mars Science Laboratory (MSL) spacecraft development and test team. We made particular use of material from the Mission Plan, as prepared for the 2009 mission by Bobak Ferdowsi and John Gilbert. Much of the information on spacecraft configuration, the science payload, and subsystems *other* than telecommunications came from the excellent project review information in the project's DocuShare library, maintained by Marie-Ann Carroll.

Some of the spacecraft and mission descriptive material, including this article's cover art, appears on the MSL public webpage. The authors are also grateful to the MSL Mission outreach office and the staff of the MSL development project for helping us assemble information for the current mission (2011 launch).

Table of Contents

Foreword	v
Acknowledgements	vi
Table of Contents	vii
List of Figures	ix
List of Tables	xii
1. Mission and Spacecraft Summary	1
1.1 Mission Description	4
1.2 Launch/Arrival Period Selection	5
1.2.1 Cruise Mission Phase Telecom Trades.....	6
1.2.2 EDL and Surface Mission Phase Telecom Trades	7
1.3 Launch Phase and Initial Acquisition	10
1.4 Cruise Phase.....	20
1.5 Approach Phase.....	21
1.6 EDL Phase	21
1.6.1 DTE to Entry, MRO after Entry.....	26
1.6.2 Full-DTE EDL Communications.....	28
1.6.3 Surface Phase.....	29
1.7 Flight System Description	35
1.7.1 Engineering Subsystems and Functions.....	38
1.7.2 Payload (Science Instruments).....	40
2 Telecom Subsystem Overview	42
2.1 Telecom for Launch, Cruise, and into EDL	43
2.2 Surface Operations	46
2.2.1 X-Band.....	46
2.2.1.1 Downlink (DTE)	46
2.2.1.2 Uplink (DFE).....	46
2.2.2 UHF.....	46
2.3 X-Band Flight Subsystem Description.....	47
2.3.1 X-Band Interfaces with MSL Control and Data Systems.....	47
2.3.2 X-Band Key Hardware Components.....	49
2.3.2.1 Cruise Stage X-Band Telecom Components	49
2.3.2.1.1 Medium-gain Antenna	49
2.3.2.2 Parachute Cone X-Band Telecom Components.....	51
2.3.2.2.1 Waveguide Transfer Switches (P-WTS-1 and P-WTS-2)	51
2.3.2.2.2 Parachute Low-Gain Antenna	51
2.3.2.2.3 Tilted Low-Gain Antenna	53
2.3.2.3 Descent Stage X-Band Telecom Components	53
2.3.2.3.1 Descent Low-Gain Antenna.....	54
2.3.2.3.2 Descent Stage Waveguide Transfer Switches	56
2.3.2.3.3 Traveling Wave Tube Amplifier.....	57
2.3.2.3.4 X-Band Diplexer	57
2.3.2.3.5 Transmit Low-Pass Filter	57
2.3.2.3.6 Exciter Low-Pass Filter	58
2.3.2.3.7 Receiver Low-Pass Filter	58
2.3.2.3.8 Waveguide	59
2.3.2.3.9 Descent Stage SDST	59
2.3.2.4 Rover X-Band Telecom Components.....	59

2.3.2.4.1	Rover Waveguide Transfer Switches.....	60
2.3.2.4.2	Rover Low-Gain Antenna.....	60
2.3.2.4.3	High-Gain Antenna	62
2.3.2.4.4	Rover Diplexer.....	63
2.3.2.4.5	Rover Small Deep Space Transponder	66
2.3.2.4.6	Rover Receiver Low-Pass Filter	69
2.3.2.4.7	Solid State Power Amplifier	69
2.3.3	<i>Functional Redundancy (Rover as Backup to Descent Stage)</i>	70
2.3.4	<i>Encoding Modes/Frame Sizes</i>	71
2.4	UHF Flight Subsystem Description	71
2.4.1	<i>UHF Interfaces with MSL Control and Data Systems</i>	71
2.4.1	<i>UHF Key Hardware Components</i>	72
2.4.1.1	Parachute Cone UHF Telecom Components.....	72
2.4.1.1.1	Parachute UHF (PUHF) Antenna	72
2.4.1.2	Descent Stage UHF Telecom Components	73
2.4.1.3	Rover UHF Telecom Components.....	75
2.5	Terminal Descent Sensor (Landing Radar) Description.....	83
2.6	MSL Telecom Hardware Mass and Power Summary	86
2.6.1	<i>X-Band Mass</i>	86
2.6.2	<i>X-Band Spacecraft Power Consumption</i>	86
2.6.3	<i>UHF Mass and Power Consumption</i>	87
2.6.4	<i>TDS Power</i>	88
3	Ground Systems	89
3.1	X-Band Operations: the Deep Space Network.....	89
3.2	EDL Operations: EDL Data Analysis (EDA).....	92
4	Telecom Subsystem Link Performance	95
4.1	X-Band	95
4.1.1	<i>Cruise Link Performance</i>	95
4.1.2	<i>EDL (X-Band) Performance</i>	99
4.1.3	<i>Surface Performance (X-Band)</i>	104
4.2	UHF	107
4.2.1.1	EDL (UHF).....	107
4.2.1.2	Surface (UHF Relay)	112
5	Flight Operations (Plans)	113
5.1	Mission Operations System Approach	113
5.2	Initial Surface Ground Operations.....	114
5.3	Tactical Operations after First 90 Sols	114
5.4	UHF Telecom Constraints	118
5.5	X-Band Telecom Constraints	119
5.6	Surface Relay Link Strategy and Operations	119
5.6.1	<i>Orbiter Relay Support Strategy</i>	119
5.6.2	<i>Surface Initial Commanding Strategy</i>	120
5.6.3	<i>Surface Initial Communications Strategy</i>	120
5.6.4	<i>Surface Communications Operations</i>	120
6	MSL Telecom Topics in Follow-up Article	122
	Abbreviations and Acronyms	123
	References.....	133

List of Figures

Figure 1-1. Artist’s conception of Mars Science Laboratory on Mars.....	1
Figure 1-2. Medium-gain antenna.....	2
Figure 1-3. Exploded view of the five major stages of the MSL spacecraft (flight system).....	3
Figure 1-4. MSL cruise trajectories, SPE angle, and Earth–spacecraft range.....	4
Figure 1-5. MSL & Juno launch periods.....	8
Figure 1-6. EDL coverage after entry for Mars Reconnaissance Orbiter and Odyssey.....	10
Figure 1-7. Atlas V 541 Launch Vehicle.....	11
Figure 1-8. Launch Phase Illustration.....	12
Figure 1-9. Ground tracks for optimal launch windows (type I trajectory).....	14
Figure 1-10: Ground tracks for optimal launch windows (type II trajectory).....	15
Figure 1-11. Station elevation angle, type I open.....	16
Figure 1-12. Station elevation angle, type II open.....	16
Figure 1-13. Canberra DSS range to spacecraft for 48 hours after injection.....	18
Figure 1-14. Canberra space loss to spacecraft, type II open trajectory.....	18
Figure 1-15. Type II (solid) & type I (dashed) trajectories and SPE angle launch to arrival for various launch dates.....	19
Figure 1-16. Timeline: Cruise Stage separation to entry interface.....	23
Figure 1-17. EDL timeline: entry interface to backshell separation.....	23
Figure 1-18. Banking maneuver along anti-velocity vector.....	24
Figure 1-19. EDL timeline: backshell separation to fly-away.....	25
Figure 1-20. Overview of TDS requirements during EDL.....	26
Figure 1-21: Sabot, shown during ground parachute deployment test.....	28
Figure 1-22. Example DTE views during EDL (2009 launch data, Gale site).....	29
Figure 1-23. MSL geometry during surface operations.....	30
Figure 1-24. Earth rise vs. date, for different MSL landing sites.....	31
Figure 1-25. Earth set time for different MSL landing latitudes.....	31
Figure 1-26. Earth visibility duration vs. date (MSL surface mission).....	32
Figure 1-27. Time (min) per sol MRO is above 10 deg elevation vs. MSL latitude.....	33
Figure 1-28. Maximum elevation of MRO passes vs. sol (MSL at Equator) for better of the AM passes and both of the PM passes for 120 sols (based on 2009 launch data).....	34
Figure 1-29 Maximum elevation of MRO passes vs. sol (MSL at Equator) better of the AM passes and only the better PM pass for 60 sols (based on 2009 launch data).....	34
Figure 1-30. Percentage of time spent by MRO between 10-deg steps in elevation.....	35
Figure 1-31. External view of the MSL rover.....	37
Figure 2-1. MSL X-band block diagram.....	42
Figure 2-2. UHF block diagram.....	44
Figure 2-3. X-band and UHF sequence during EDL.....	45
Figure 2-4. Telecom LVDS and 1553B interfaces.....	48
Figure 2-5. MGA uplink gain.....	50

Figure 2-6. MGA downlink gain.	50
Figure 2-7. Locations of the low-gain antennas.	51
Figure 2-8. PLGA X-Band uplink gain with spacecraft mock-up, RCP, 4/30/09.	52
Figure 2-9. PLGA X-Band downlink gain with spacecraft mock-up, RCP, 4/17/09.	53
Figure 2-10. Descent Stage X-band layout.	54
Figure 2-11. Telecom plate assembly.	54
Figure 2-12. DLGA and DLGA adapter overview.	55
Figure 2-13. GRASP model for DLGA scattering study.	56
Figure 2-14. MSL DLGA downlink pattern modeled from GRASP model.	56
Figure 2-15. Rover telecom internal layout showing overall placement of the X-band and UHF components.	59
Figure 2-16. Rover detailed internal layout.	60
Figure 2-17. WIPL-D model of RLGA on rover deck.	61
Figure 2-18: RLGA patterns modeled by WIPL-D (includes ground-plane effects).	61
Figure 2-19. Free-space uplink gain comparison between MER RLGA and MSL RLGA.	62
Figure 2-20. HGA and gimbal assembly.	62
Figure 2-21. HGA Uplink Directivity showing first several sidelobes.	64
Figure 2-22. Detail of the uplink main lobe HGA directivity.	64
Figure 2-23. HGA downlink directivity showing first several sidelobes.	65
Figure 2-24. Detail of HGA main lobe downlink directivity.	65
Figure 2-25. Group III small deep space transponder.	66
Figure 2-26. MSL SSPA block diagram.	70
Figure 2-27. PUHF antenna mounted on parachute cone.	72
Figure 2-28. PUHF antenna radiation pattern.	73
Figure 2-29. DUHF antenna mounted on descent stage.	74
Figure 2-30. DUHF antenna pattern as mounted on descent stage.	74
Figure 2-31. UHF hardware in rover WEB.	75
Figure 2-32. RUHF antenna mounted on rover.	76
Figure 2-33. MSL RUHF Quadrafil helix antenna.	76
Figure 2-34. WIPL-D model for RUHF pattern analysis.	77
Figure 2-35. Surface RUHF antenna pattern, Rx.	78
Figure 2-36. Surface RUHF antenna pattern, Tx.	78
Figure 2-37. RUHF pattern study for sky crane.	79
Figure 2-38. RUHF pattern analysis results for sky crane.	80
Figure 2-39. Electra-Lite FM-002.	81
Figure 2-40. System overview block diagram of the TDS.	84
Figure 2-41. TDS antenna locations and pointing directions.	85
Figure 3-1. Canberra Deep Space Communications Complex (CDSCC) showing 70-m and 34-m stations.	90
Figure 3-2. Block diagram of DSS-24 station at Goldstone.	91
Figure 3-3. MER EDA computer array.	93
Figure 4-1. Required ranging cycle time as a function of Pr/No.	96

Figure 4-2. MSL X-band uplink data rates during cruise, type II day 1.	97
Figure 4-3. MSL X-band downlink data rates during cruise, type II day 1.	98
Figure 4-4. MSL X-band ranging Pr/No during cruise, type II day 1.	99
Figure 4-5. Configuration example of EDAs at DSN for EDL support.	101
Figure 4-6. EDA analysis example showing missed tone cases.	102
Figure 4-7. DTE Pt/No Gale site, 2009 launch.	103
Figure 4-8. DTE Doppler Gale site, 2009 launch.	103
Figure 4-9. DTE Doppler rates Gale site, 2009 launch.	104
Figure 4-10. X-band uplink data rates, Mars surface.	105
Figure 4-11. X-band downlink rates, Mars surface.	106
Figure 4-12. X-band downlink Pt/No via RLGA.	107
Figure 4-13. Range variations to MRO for Gale (2009 launch), three orbiter phasings.	109
Figure 4-14. View angle variations to MRO for Gale (2009 launch), three orbiter phasings.	110
Figure 4-15. Received power at MRO for Gale (2009 launch), three Orbiter phasings.	110
Figure 4-16. Received power at Odyssey for Gale (2009 Launch), three orbiter phasings.	111
Figure 5-1. MSL surface operations MOS overview.	113
Figure 5-2. Functional architecture of MSL MOS.	115
Figure 5-3. Subsystems and functions of MSL MOS.	116
Figure 5-4. MSL tactical process during surface ops (at top level).	117
Figure 5-5. Estimated sol-by-sol return data volume through MRO.	118

List of Tables

Table 1-1. 2011 launch and 2012 arrival dates for type I and type II trajectories.....	2
Table 1-2. MSL major mission phases.	5
Table 1-3. Launch period / window durations.....	11
Table 1-4. Legend for Launch Vehicle and Launch Phase figures.	12
Table 1-5. Trajectory correction maneuvers planned during Cruise.....	21
Table 1-6. Periods of UHF or DTE dropouts between CSS and landing.	27
Table 1-7: Orbital elements for relay orbiters.	32
Table 1-8. Comparison between MSL and MER.	36
Table 2-1. Acronyms and abbreviations in X-band telecom block diagram.	43
Table 2-2. Acronyms and abbreviations in UHF telecom block diagram.	45
Table 2-3. MGA RF characteristics.....	49
Table 2-4. Transmit low-pass filter RF characteristics.....	58
Table 2-5: Receive low-pass filter RF characteristics.	58
Table 2-6. Rover HGA RF characteristics.....	63
Table 2-7. SDST receive functional characteristics.....	68
Table 2-8. SDST exciter characteristics at 880f1.	69
Table 2-9. SSPA key characteristics.	70
Table 2-10. TDS high level characteristics.	84
Table 2-11. X-band telecom mass summary.....	86
Table 2-12. X-band telecom spacecraft power consumption.....	87

1. Mission and Spacecraft Summary

The Mars Science Laboratory (MSL) mission has the primary objective of placing a mobile science laboratory on the surface of Mars to assess the biological potential of the landing site, characterize the geology of the landing region, investigate planetary processes that influence habitability, and characterize the broad spectrum of surface radiation. MSL will conduct fundamentally new observations of Mars geology using advanced micro-imagery and spectrometry, while assessing the radiation environment and studying the surface environments. The MSL mission aims to achieve these objectives in a manner that will offer the excitement and wonder of space exploration to the public. Figure 1-1 shows how the Rover is expected to look on the surface of Mars, with its instrument arm deployed.

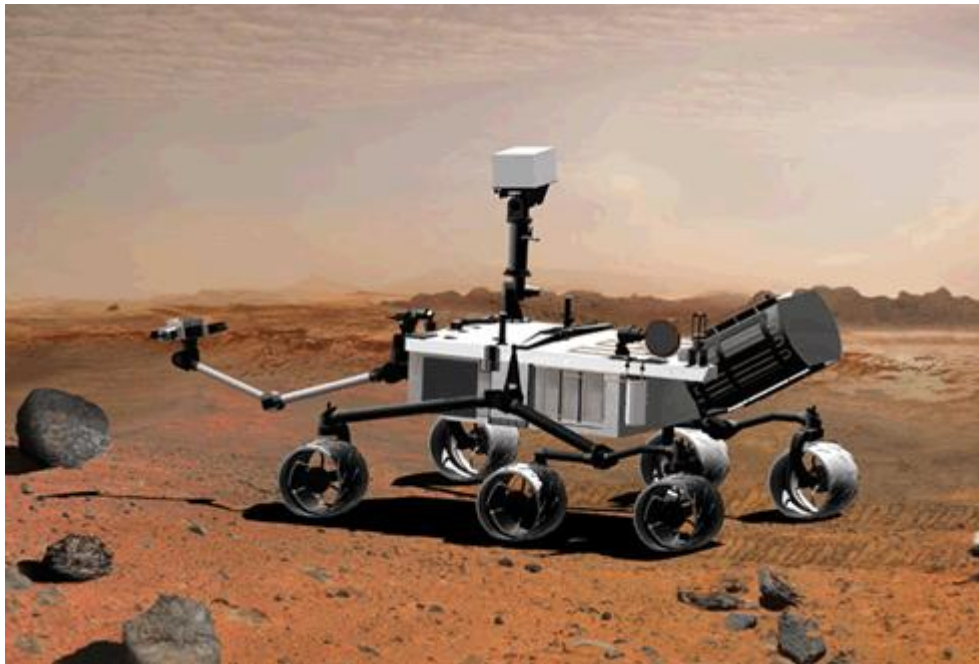


Figure 1-1. Artist's conception of Mars Science Laboratory on Mars.

The MSL will be launched during the 2011 Mars opportunity, with launch dates now planned between mid-October and early December 2011 and possible arrival dates at Mars in August 2012. Geometries that enable communications during the entry, descent, and landing (EDL) phase are a mission design driver.

The MSL cruise trajectory has not yet been finalized [1], but it will include both type I and type II trajectories. A type I Earth–Mars interplanetary trajectory carries the spacecraft less than 180 deg around the Sun; a type-II trajectory carries the spacecraft 180 deg or more around the Sun [2].

Table 1-1 lists examples for the opening and closing of the trajectory launch periods. (The type II opening is somewhat variable because it is driven by the launch period of the Juno mission and by the EDL communications requirements.)

Table 1-1. 2011 launch and 2012 arrival dates for type I and type II trajectories.

Cruise Trajectory	Launch date	Arrival date
Type 1 open	12/02/11	8/11/12
Type 1 close	12/24/11	8/16/12
Type II open	10/20/11	8/28/12
Type II close	11/14/11	8/28/12

MSL’s telecom capability, which will employ a non-directive low gain antenna (LGA), depends on the spacecraft orientation and the distance between Earth and the spacecraft. The cruise stage has a solar array (on a surface surrounding the horn of the medium-gain antenna [MGA]). The MGA and the other antennas are described in more detail in Section 2. In Figure 1-2, the array is the flat blue surface at the top in the to-left drawing. This array powers the cruise loads and charges the batteries. Therefore, the cruise-stage orientation to the Sun is driven by power and thermal subsystem constraints. The solar array normal must be pointed near the Sun line, at a Sun-view angle that optimizes the solar cell power output, which can be affected by being heated too much. On the other hand, the telecom link would be optimal if the antenna bore sight (and, hence, the spacecraft $-Z$ axis) were pointed towards Earth.

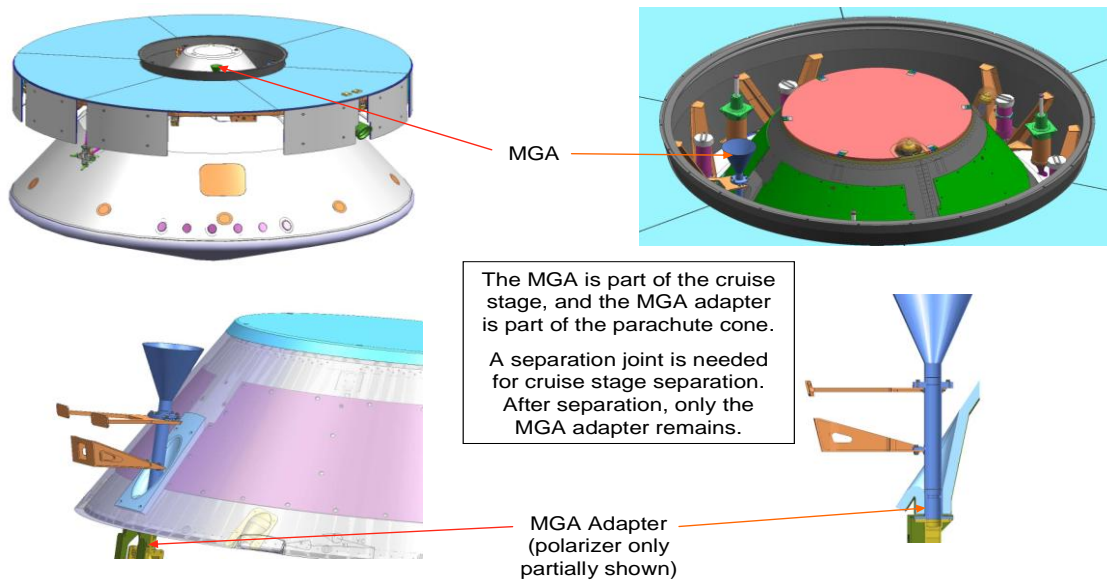


Figure 1-2. Medium-gain antenna.

Figure 1-3 shows the array and the MGA edge-on in the cruise stage at the top. The $-Z$ axis is toward the top of the figure. The competing power and telecom needs are major factors in the design trades in cruise stage orientation that must be made. The telecom and power/thermal constraints are linked by the Sun–Probe–Earth (SPE) angle [3].

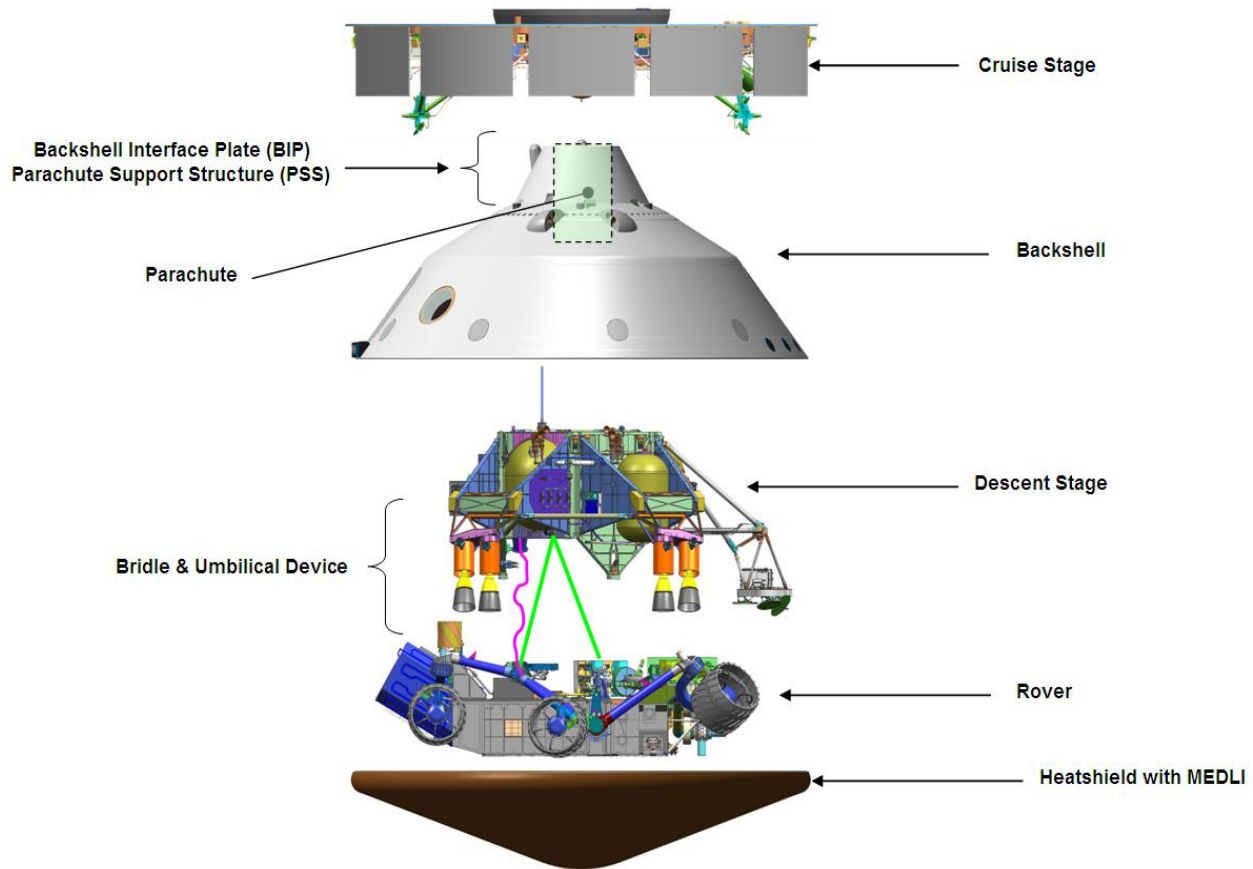


Figure 1-3. Exploded view of the five major stages of the MSL spacecraft (flight system).

Figure 1-4 shows the spacecraft-Earth range on the left vertical axis and the SPE angle on the right vertical axis. The range (sometimes called distance) is shown in astronomical units (AU), with 1 AU being approximately 150 million kilometers. The type II trajectory initially has very high SPE angles, especially for launches near the opening of the launch period. Large SPE angles are a challenge for telecom, even at relatively short ranges. A broad-beam antenna has a poor pattern due to spacecraft obstructions at angles greater than about 80 degrees (deg) off boresight¹.

¹ Boresight refers to a direction in which an antenna's gain is the maximum. A fixed antenna, such as an MSL LGA, is defined in terms of the spacecraft axis (or axes) direction along which it is mounted. That direction, for example the $-Z$ axis for the parachute LGA (PLGA) and the anti-velocity vector for the tilted LGA (TLGA) to be discussed, is loosely referred to as the boresight.

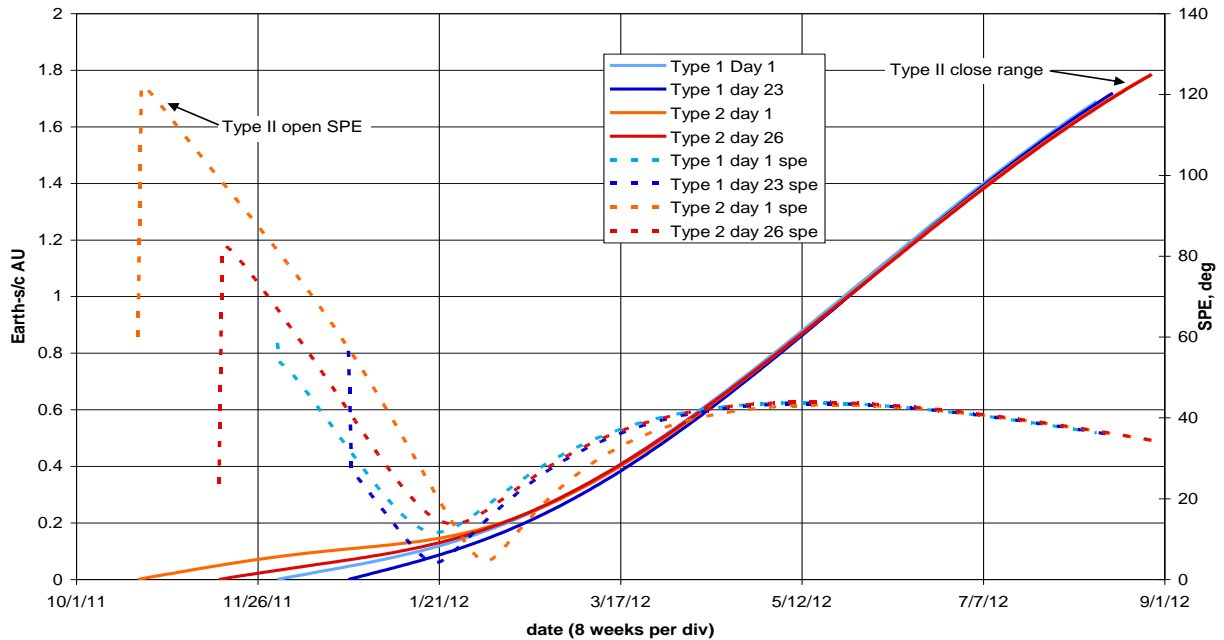


Figure 1-4. MSL cruise trajectories, SPE angle, and Earth-spacecraft range.

1.1 Mission Description

The MSL mission has four major phases:

- Launch.
- Cruise/Approach.
- Entry, Descent, and Landing (EDL).
- Surface Operations.

Table 1-2 provides more detail regarding these phases. Prior to EDL, time references are in terms of the familiar Earth hours and days. On the surface of Mars, all planning and rover activity is in terms of sols (Martian days)².

² One sol, in terms of Earth time, is approximately 24 hours, 39 minutes, and 35 seconds long. A sol is equivalent to about 1.027 Earth days. A sol is divided into 24 (Martian) hours, each of which is 60 (Martian) minutes, and so forth, analogous to the time units on Earth.

Table 1-2. MSL major mission phases.

Mission Phase	Description	Expected Duration
Launch	The launch phase is defined to begin at the point where the spacecraft transfers to internal power prior to launch. It is complete (after spacecraft separation from the launch vehicle's upper stage) when the spacecraft reaches a thermally stable, positive energy balance, commandable configuration	Less than 1 day
Cruise	The cruise phase begins when the launch phase ends, and it ends 45 days prior to atmospheric entry (E-40 days).	250 to 320 days
Approach	The approach phase is defined to begin at 45 days prior to atmospheric entry (E-45 days) and ends when the spacecraft reaches the Mars atmospheric entry interface point. That point is defined at a Mars radius of 3522.2 km.	45 days
EDL	Entry-descent-landing (EDL) begins when the spacecraft reaches the entry interface point (Mars radius of 3522.2 km) and ends when the rover reaches a thermally stable, positive energy balance, commandable configuration on the surface.	About 10 minutes
Surface	The surface mission begins when EDL ends, and it ends when the mission is declared complete. The design of the rover must provide for a surface mission duration of at least one Mars year (669 sols, equivalent to 687 Earth days).	Prime mission: 669 sols (with possible additional extensions)

1.2 Launch/Arrival Period Selection

There are four landing sites on Mars under consideration (Mawrth Vallis (Valley), Gale Crater, Eberswalde Crater, and Holden Crater), spanning latitudes between 27 deg S and 25 deg N.

With these sites, the parameter limits that drive the launch and arrival periods can be summarized as a set of constraints [4].

- Spacecraft injected mass = 4050 kilograms (kg).
- Launch-specific energy (C3) capability < 20.1 km²/s² (Atlas V 541, instantaneous launch window).
- Atmospheric entry velocity < 5.9 km/s (not a hard constraint due to EDL heating performance study results).
- Declination of launch asymptote < 40 deg.
- Arrival no later than 30 days before the start of solar conjunction.
- Launch eclipse duration ≤ 65 minutes (Note: exceeded for type II for launch after 11/3).
- Early cruise SPE angle constraints:
 - Launch vehicle separation attitude (SEP to SEP + 18 days):
 - Angle between -Z axis and Sun ≤ 64.0 deg and ≥ 20.0 deg.
 - Angle between -Z axis and Earth ≤ 68.8 deg.
- EDL communications strategy constraints:

- Relay:
 - Mars Reconnaissance Orbiter (MRO) local mean solar time (LMST) node as close to nominal value (3:00 p.m.) as possible.
 - Odyssey LMST node at 3:00 p.m. because of propellant issues related to orbiter lifetime.
 - View angle to orbiters (MRO/Odyssey) ≤ 135 deg.
 - MRO/Odyssey elevation at landing + 1 min ≥ 10 deg.
- Direct to Earth (DTE):
 - View angle to Earth ≤ 75 deg.
 - Earth elevation at landing + 1 min $\geq 10^\circ$.
- > 20-day launch period (varies with trajectory type and EDL communications constraints).
- Declination of launch asymptote < 28.5 deg (for Atlas 541; the Atlas V 551 could help this situation).
- Atmospheric entry velocity < 5.6 km/s.
- EDL communications strategy constraints:
 - Full ultra high frequency (UHF) EDL coverage via MRO and Odyssey from Entry³ to Landing + 1 minute. (Relay coverage is not possible for all of EDL due to geometric constraints from cruise stage separation (CSS) until entry.)
 - Full DTE EDL coverage (For type I only possible for Mawrth Vallis).

1.2.1 Cruise Mission Phase Telecom Trades

An example of the significant decisions involving telecom yet to be made in mission design 2 years before launch is the one involving cruise trajectory type (I vs. II), launch window, power subsystem constraints, and LGA pattern.

- Type I vs. type II trajectory: The type II trajectory has very large initial SPE angles (as shown in Figure 1-4), greater than 120 degrees at the start of the launch window. At the other end of cruise, the EDL geometry of the type II is much preferred compared to the type I, as it offers better UHF coverage opportunities (for example).
- Launch period: With a 2011 launch, Juno's launch period, driven by the complex trajectory to get the Juno spacecraft into orbit around Jupiter, overlaps MSL's launch period.
- Solar array and antenna pointing: Power output and thermal considerations require the solar array to be pointed within an optimum range of angles from the Sun. Too

³ Entry defined as the point where the entry vehicle is at a radius of 3522.2 km from nominal Mars center. Entry is also considered at a time beginning 600 seconds after nominal cruise state separation.

far from the Sun, not enough power⁴; too close to the Sun, too much heating. This range of angles tends to force the PLGA angle to Earth to be too far off boresight in the days and weeks just after launch.

- Solar array pointing (thermal constraint): While Sun-Earth distance remains short, the solar array should be pointed not too close to the Sun, to avoid overheating the solar panels and losing efficiency.

The following question was asked: How far off boresight can we point the PLGA and still have acceptable communications-link performance? Based on PLGA gain pattern measurements with the spacecraft mock-up, we estimate a mission design constraint of 80-deg offpoint from PLGA boresight. The measured PLGA patterns described in Section 2 (Figure 2-8 and Figure 2-9) can be compared with this 80-deg constraint.

1.2.2 EDL and Surface Mission Phase Telecom Trades

Telemetry during EDL is transmitted via the MSL UHF subsystem and the spacecraft (sometimes called relay assets) orbiting Mars and by DTE at X-band to the Deep Space Network (DSN). The UHF relay transmits real-time EDL data in a continuous stream at a rate of 8 kilobits per second (kbps) in bit stream mode⁵. The UHF bit stream broadcast by MSL during EDL will be received by multiple orbiters that have their UHF relay radios set to operating in a compatible listen-only bit stream mode. The data for DTE is in the form of semaphores, the so-called multiple frequency shift keying (MFSK) tones. As with the Phoenix and Mars Exploration Rover (MER) landers, the possibility exists to monitor the UHF signal from a large Earth-located ground station, such as the Green Bank radio telescope in West Virginia.

The relay communications assets available to MSL are the MRO as primary and the Odyssey orbiter as backup. It is also possible to use the European Mars Express (MEX) orbiter in a limited capacity if either the primary or backup (or both) orbiters becomes unavailable; however, this would have to be planned in advance to enable MEX to phase for the MSL EDL. The MSL mission is not currently pursuing this option.

Due the limitations of geometry during EDL, simultaneous coverage by both an orbiter for UHF and an Earth station for DTE is unlikely for the entire EDL phase. The mission strategy is to ensure DTE coverage during the period from CSS until at least atmospheric entry. During this period relay, coverage is difficult or impossible to achieve, particularly for UHF immediately after CSS. Ideally, we will have at a minimum a substantial overlap of X-band and UHF coverage during entry, where the relay link will begin to be viable. During hypersonic entry, we expect to lose UHF coverage due to plasma blackout (lasting between 25 and 100 seconds). DTE coverage during this period is, therefore, desirable. The descent stage will continue to transmit X-band DTE MFSK tones all the way to landing.

⁴ The capacity of the rover's radioisotope-thermoelectric generator (RTG) power source, while adequate with a battery for peak loads during surface operations, is insufficient to fully power the spacecraft during cruise. The solar array augments the RTG during cruise.

⁵ Bit stream mode is a non-acknowledged transmission mode that includes no Proximity-1 protocol formatting and no data retransmission mechanisms. After a successful landing there will be an opportunity to transmit EDL a superset of the real-time data that is stored on-board MSL during the event. The post-landing transmission could use the Proximity-1 mode.

The 2011 launch has two possible types of trajectories, each of which offers advantages and disadvantages for telecom coverage. The type I trajectory launch period is from 10/22/11 to 11/14/11. The type II trajectory launch period is from 11/25/11 to 12/18/11. Figure 1-5 illustrates the candidate October - December 2011 MSL type II and type I launch periods and their relation to the candidate Juno launch period⁶.

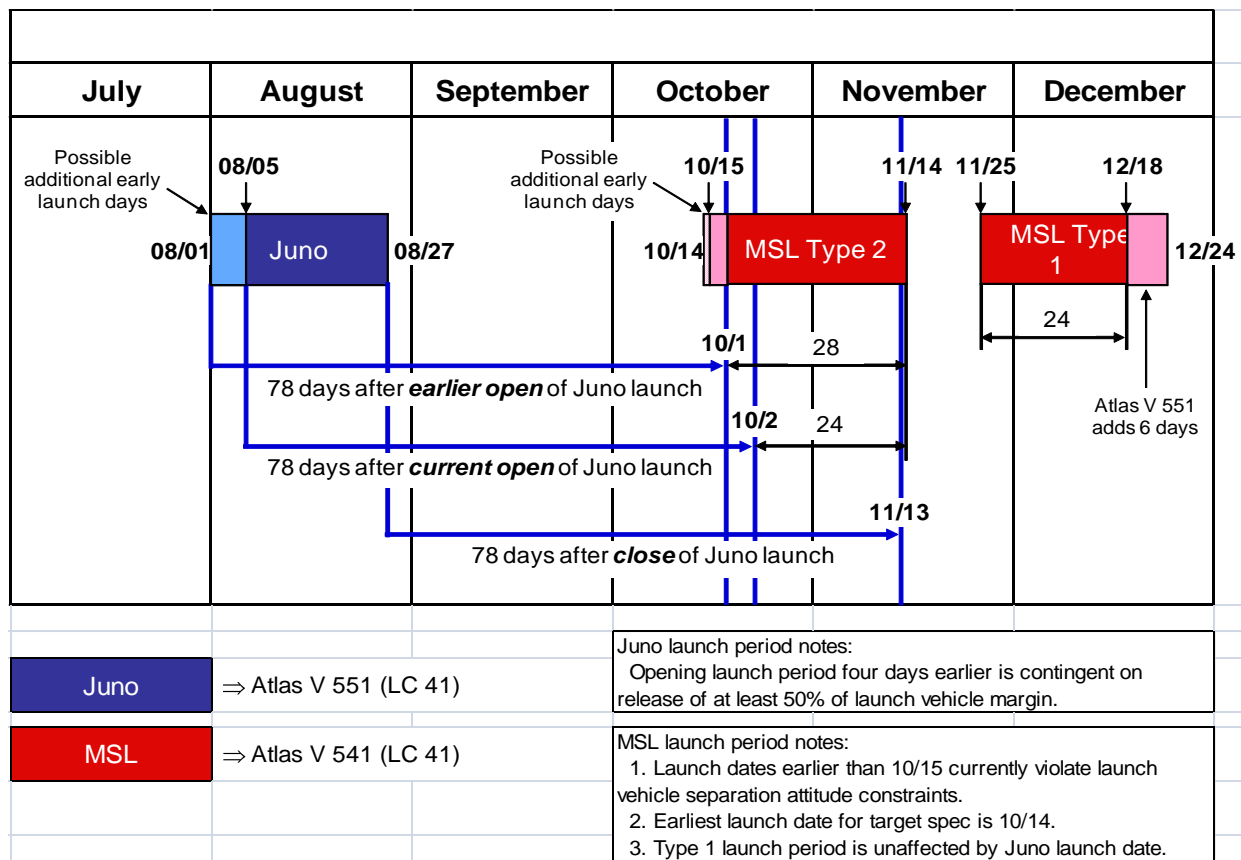


Figure 1-5. MSL & Juno launch periods.

For the 2011 launch opportunity, and to simplify the preliminary verification of EDL communications coverage, the following actions were performed in the trajectory selection process by Mission Design:

- For MRO relay coverage:
 - Check that there is a line of sight between MSL and MRO at the Entry interface and at landing + 1 minute.
 - Assume that MRO can be phased anywhere in its orbit for optimal coverage of MSL EDL.
 - Check that the orbiter elevation is greater than 10 deg at landing and landing + 1 minute.

⁶ The type I period could open 10/18/11 if Juno launches early, and the Atlas pad turnaround of 78 days is met. The Atlas launch vehicle team requires a minimum 78-day period at the pad to support either a type I or type II MSL launch

- Check that the angle from the MSL anti-velocity vector to the orbiter at entry is less than 135 deg.
- Similarly for DTE coverage (directly to Earth):
 - Check that there is a line of sight between MSL and Earth at the Entry interface and at landing.
 - Check that Earth elevation is greater than 10° at landing.
 - Check that the angle from the MSL anti-velocity vector to Earth at entry is less than 75 deg.

Orbiter coverage is strongly desired since it can provide return link telemetry at a rate of 8 kbps⁷, versus the MFSK tones (at a maximum rate of a new tone every 10 seconds) available with DTE EDL communications. Each MFSK tone carries one of 256 messages represented as a “subcarrier frequency” (the frequency spacing between carrier and subcarrier). A tone provides notification of an event (e.g., “parachute deploy”). In addition, signal processing recovers frequency characteristics of the signal (such as Doppler-shift due to deceleration), which can be used to help reconstruct events during EDL. UHF, by contrast, can provide a large amount of real-time engineering telemetry. The maximum planned data latency is 1 second on UHF transmitted telemetry during EDL. This data latency will ensure that the ground receives as complete a history of events as possible, in case a reconstruction is needed.

Figure 1-6 illustrates the quality of the coverage during the post entry phase of EDL for the two main relay assets and, for DTE, for the four primary landing sites and the two types of trajectories. In the figure, green shading indicates good coverage for the full duration of EDL for the indicated link type, yellow indicates coverage for only part of the EDL, and red indicates little or no coverage. We see that DTE coverage for the type I trajectory is complete (that is, all the way until landing) only for the northern site, Mawrth Vallis. This is due to the Earth setting below the horizon for the southern sites (red shading). On the other hand, for the type II trajectory, we can expect only partial coverage from Odyssey for the southern sites (yellow shading), though MRO coverage is still available. This is primarily due to orbital phasing and survivability limitations for Odyssey. For either trajectory, only the Mawrth site offers complete EDL telecom coverage after atmospheric entry for DTE and both orbiters.

⁷ Parts of the post entry phase of EDL could support relay data rates greater than 8 kbps, but the single rate of 8 kbps is baselined to simplify planning.

EDL Coverage Summary					
Launch Period	Asset	Mawrth (24.0N)	Gale (4.5S)	Eberswalde (23.9S)	Holden (26.4S)
Type 2	MRO	Green	Green	Green	Green
	ODY	Green	Yellow	Yellow	Yellow
	DTE*	Green	Green	Green	Green
Type 1	MRO	Green	Green	Green	Green
	ODY	Green	Green	Green	Green
	DTE*	Green	Pink	Pink	Pink

*Drop outs are possible between landing – 60 s and landing – 20 s due to parachute and powered descent dynamics.

Figure 1-6. EDL coverage after entry for Mars Reconnaissance Orbiter and Odyssey.

Section 2 of this article contains more detailed information regarding the EDL communications geometry and the rationale behind the 135-deg Orbiter and the 75-deg Earth angles from the anti-velocity vector for relay and DTE coverage.

1.3 Launch Phase and Initial Acquisition

The Launch phase begins when the spacecraft transfers to internal power on the launch pad. It ends when the spacecraft is declared stable, healthy, ready to accept commands, and when the launch telemetry has been played back. The major activities in the Launch phase include: the liftoff and boost phase of the launch vehicle; insertion into a circular parking orbit; a coast period, followed by additional launch vehicle upper stage burns necessary to inject the spacecraft onto a trajectory to Mars; separation of the spacecraft from the launch vehicle; initial acquisition by the DSN; verification of the initial spacecraft health and operating conditions; and the verified execution of a minimal set of post-launch commands. Table 1-3 shows the launch window durations for different phases of the launch periods. The window duration for a type II trajectory falls from 90 minutes on 11/13/2011 to zero (no window) on 11/14/2011.

Table 1-3. Launch period / window durations.

Launch Period	Launch Date	Launch Day	Launch Window Duration (min)
Type II	10/14/2001	Open	~90 min
	10/29/2011	Middle	~120 min
	11/13/2011	Close – 1 day	~90 min
	11/14/2011	Close	No Window
Type I	11/25/2011	Open	~95 min
	12/3/2011	Intermediate	~70 min
	12/10/2011	Intermediate	~60 min
	12/18/2011	Close	~15 min

In June 2006, the Atlas V 541 was selected as the launch vehicle for MSL. The Atlas 541, shown in Figure 1-7 represents a 5-meter (m) fairing, the addition of four solid-rocket motors to the central booster, and a single-engine Centaur upper-stage. Ref. [5] provides more details on the launch vehicle. Figure 1-8 illustrates the launch events.

Table 1-4 provides a legend for the acronyms used in these two figures.

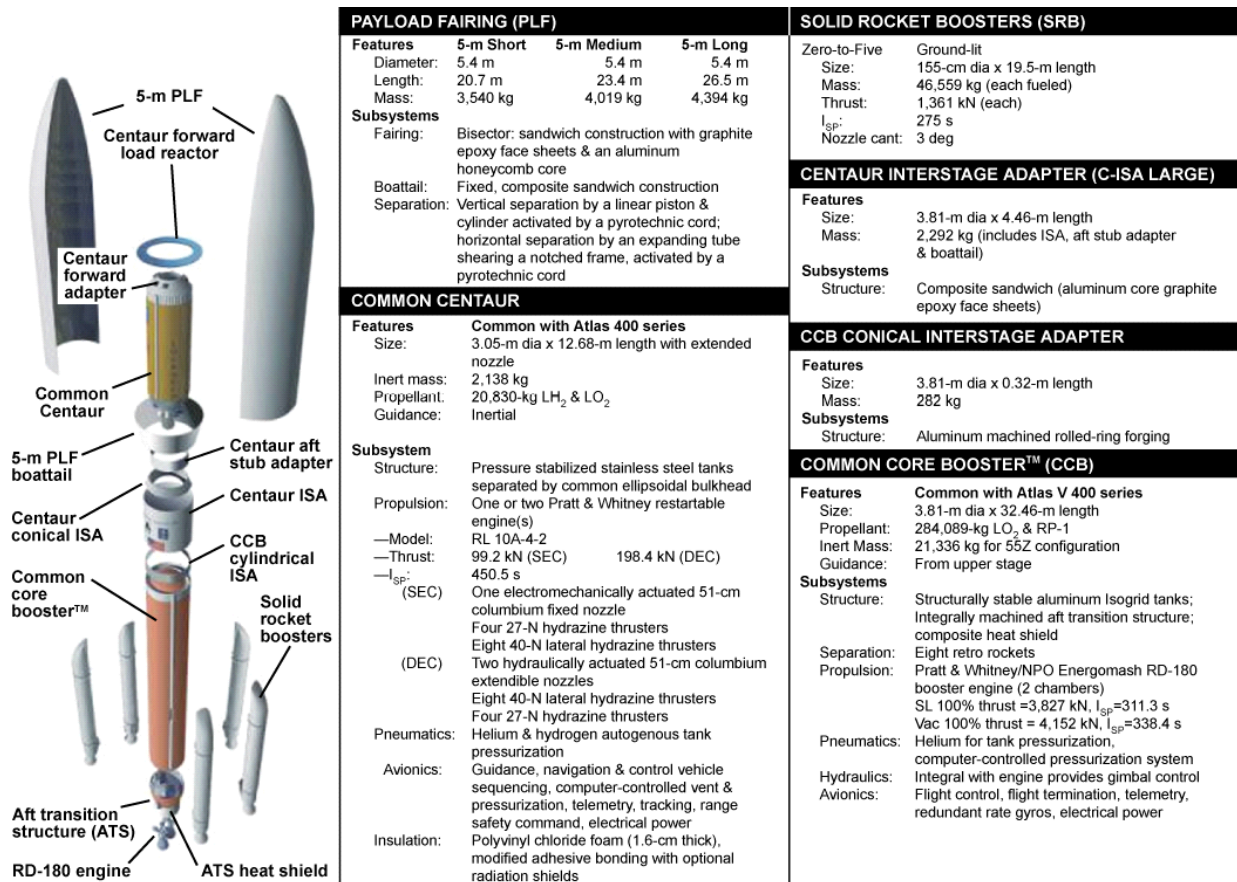


Figure 1-7. Atlas V 541 Launch Vehicle.

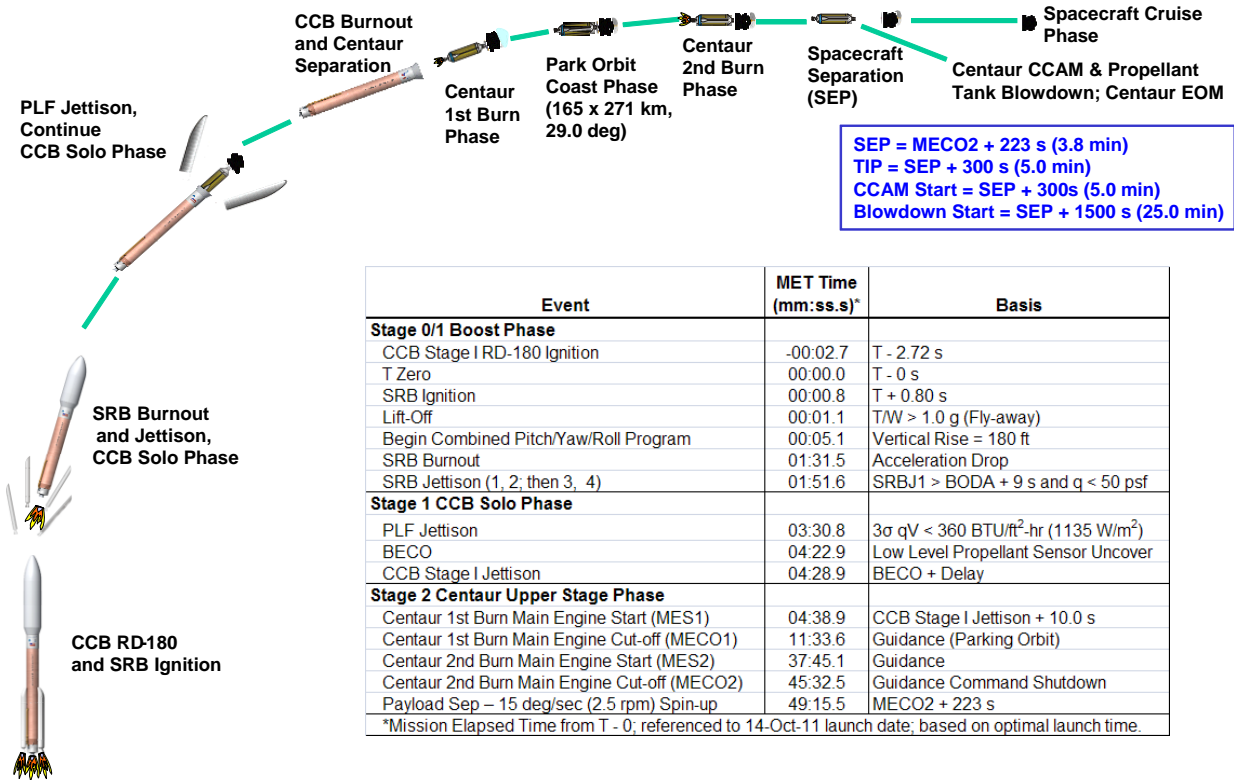


Figure 1-8. Launch Phase Illustration.

Table 1-4. Legend for Launch Vehicle and Launch Phase figures.

ATS	aft transition structure	MECO	main engine cutoff
BECO	booster engine cutoff	MES	main engine start
BODA	burnout detection algorithm	NPO	NPO Energomash is a Russian manufacturer
CCAM	collision and contamination avoidance maneuver	PLF	payload fairing
CCB	common core booster	RP	rocket propellant or refined petroleum (kerosene)
C-ISA	Centaur interstage adapter	SEC	Single-Engine Centaur
DEC	Dual-Engine Centaur	SEP	Separation
EOM	end of mission	SRB	solid rocket boosters
ISA	interstage adapter	SRBJ	solid rocket booster jettison
LH2	liquid hydrogen	TIP	target interface point
LO2	liquid oxygen	T/W	Ratio of thrust and weight on pad

Depending on the specific launch date, there might or might not be an eclipse of the Sun by the Earth after launch vehicle separation. The traveling wave tube amplifier (TWTA) is scheduled to be powered on at eclipse exit⁸. The TWTA will start the X-band downlink after a 4-minute warm up period.

The plots in Figure 1-9 (for a type I trajectory) and Figure 1-10 (for a type II trajectory) show the ground tracks for the first 24 hours after launch based on the optimum launch windows. Each ground track begins south and east of the launch site in Florida, goes through TIP and then SEP. Enter and exit Earth occultation times are indicated.

For both trajectory types, the first DSN site to view the spacecraft after launch, called the “initial acquisition” site, is Canberra, Australia. An important mission consideration is whether the spacecraft is in view of the initial acquisition site when it separates from the launch vehicle. Because separation data is very important for launch-phase performance assessment, the MSL mission might contract with a non-DSN network that has a station with line-of-sight at separation time. The Universal Space Network (USN) is a likely candidate.

Figure 1-11 and Figure 1-12 show the station elevation angles for the first 48 hours after injection for trajectories of type I and type II assuming a launch on the first (“open”) launch date for that type. Because the initial trajectory is slightly south of the Equator for type I, the Canberra site, which has higher elevation angles, is favored. The opposite is true for the initial type II trajectory, for which Goldstone, California, and Madrid, Spain (both northern sites) are favored.

The figures show two minimum-elevation coverage ‘masks’, the higher (10 deg) for transmitting and the lower (6 deg) for receiving. Stations are not allowed to transmit below 10 deg (in order to limit the radio frequency (RF) power flux density that hits the Earth). Depending on the terrain in the vicinity of the station, a station does not have line-of-sight to receive below approximately 6 deg elevation; this is, therefore, taken as the mask. For navigation, with both receiving and transmitting required, the minimum mask is 10 deg.

⁸ There is nothing in terms of spacecraft power subsystem capability about associating MSL TWTA power-on with eclipse exit. However, this time allows for a reasonable interval after the initial ascent for the microwave circuitry to vent residual gases to vacuum before experiencing high power radio frequency (RF) energy, thus adhering to the TWTA maker’s recommendation for a period of hard vacuum before generation of RF power for the first time after launch. This added time reduces the possibility of RF breakdown or arcing in the waveguides or the TWTA itself.

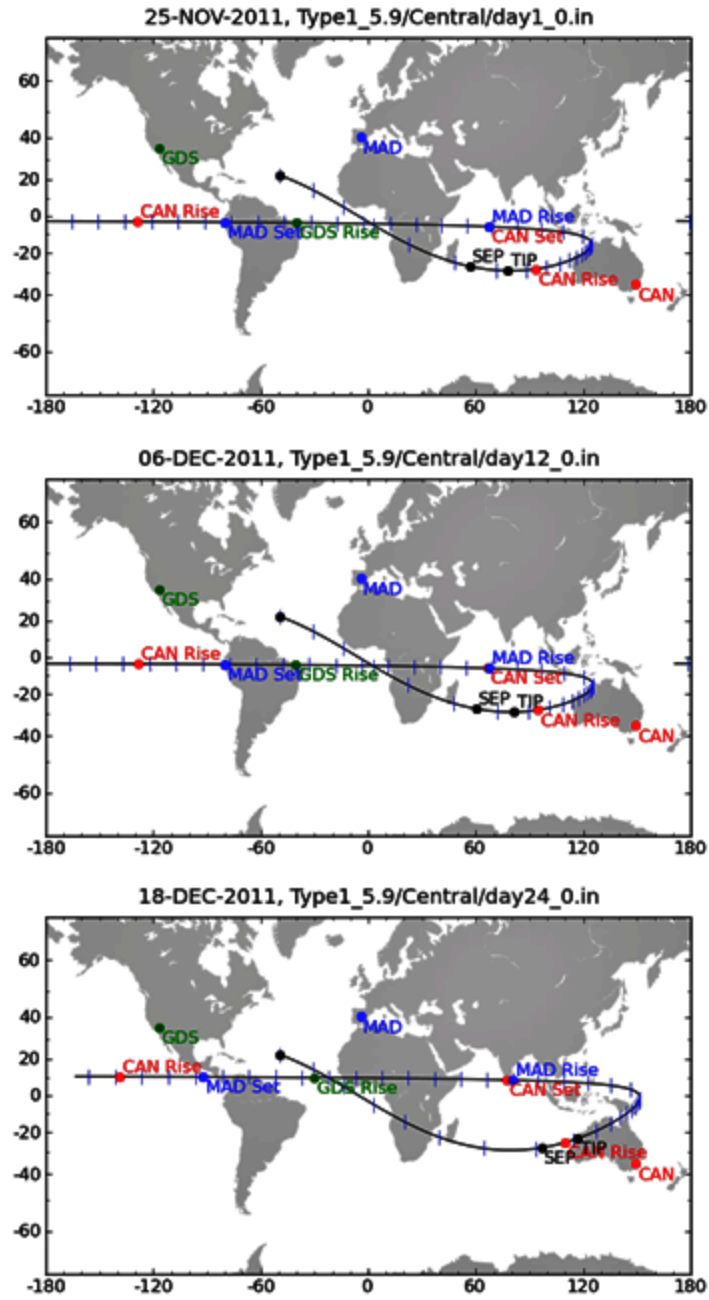


Figure 1-9. Ground tracks for optimal launch windows (type I trajectory).

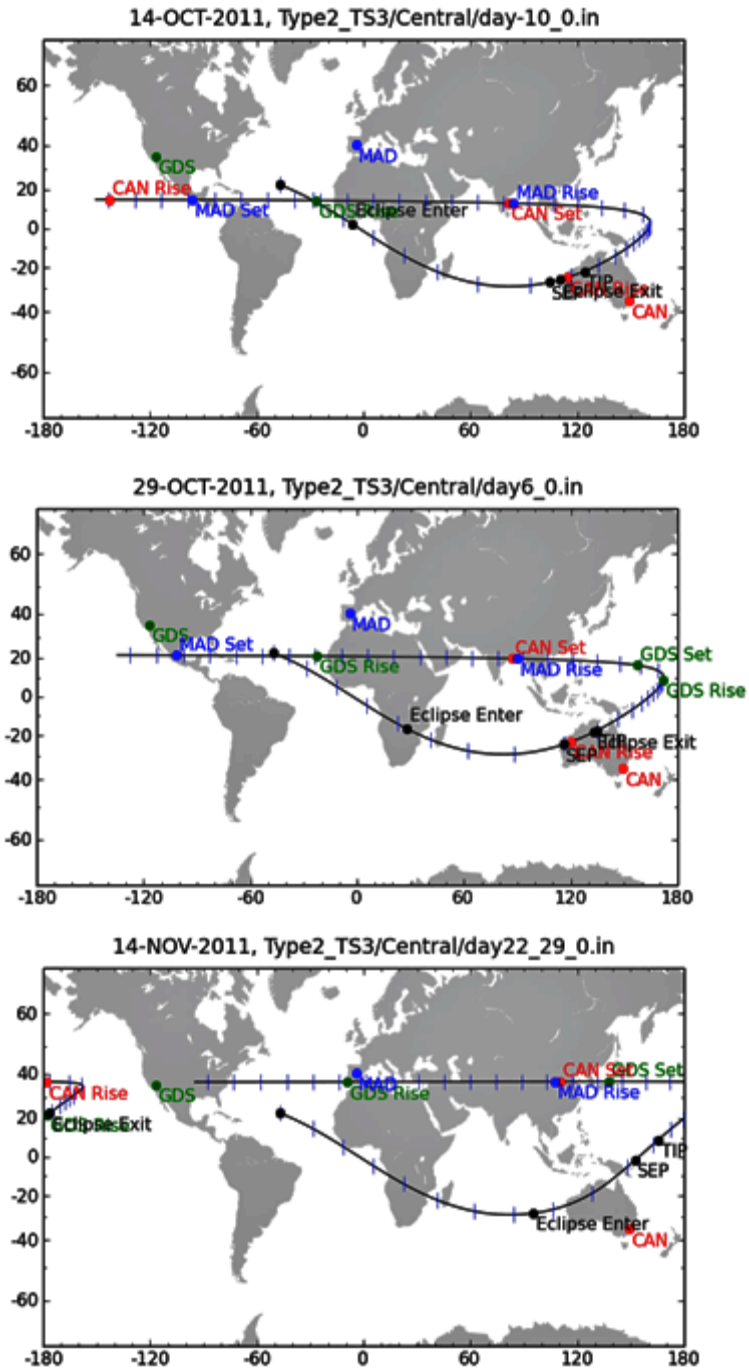


Figure 1-10: Ground tracks for optimal launch windows (type II trajectory).

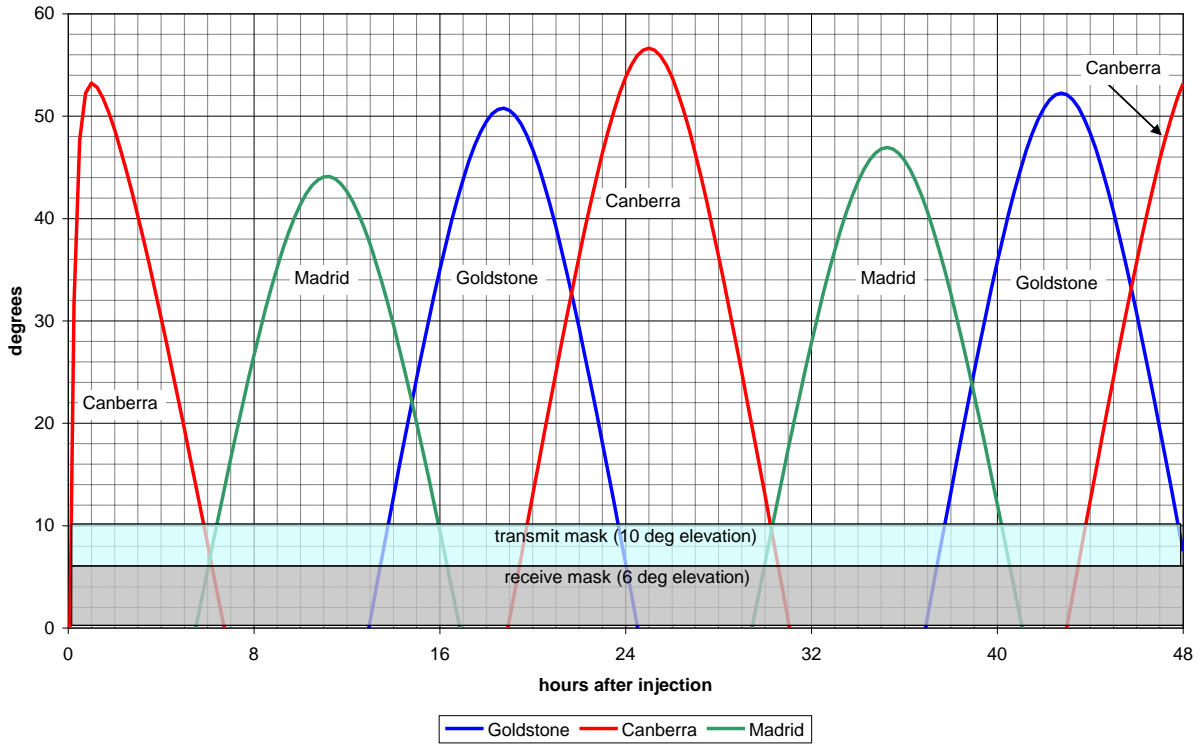


Figure 1-11. Station elevation angle, type I open.

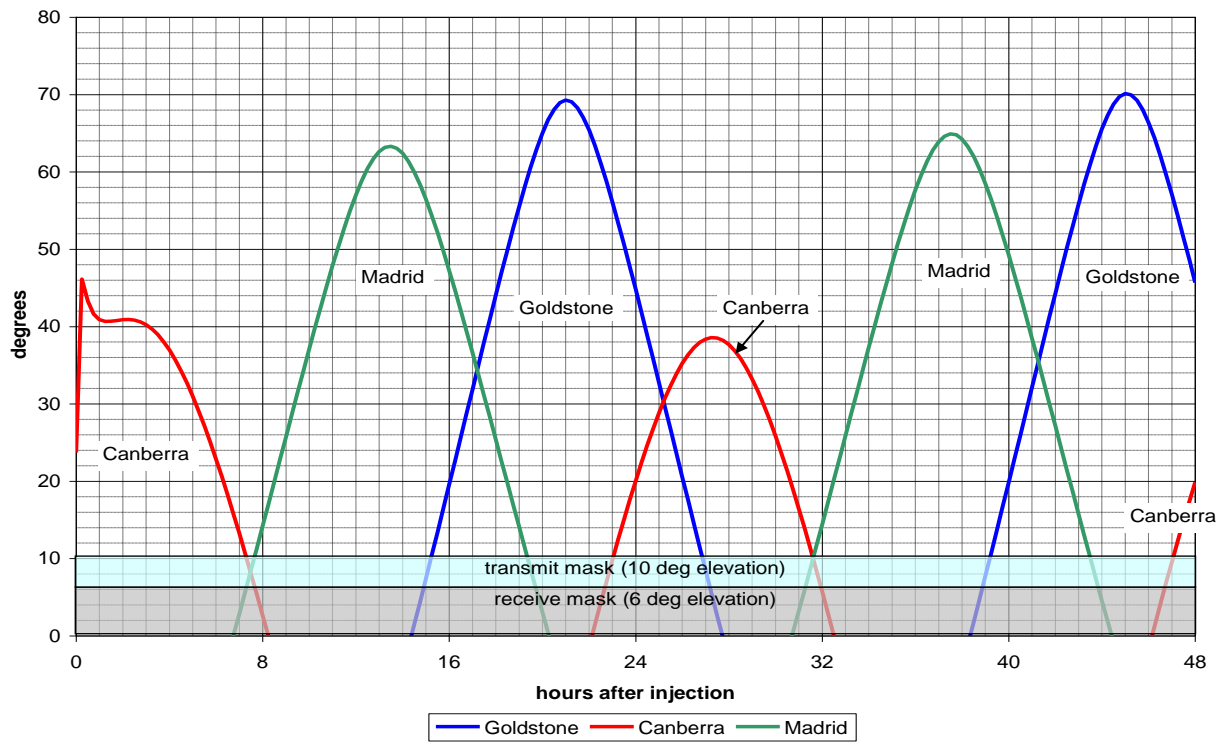


Figure 1-12. Station elevation angle, type II open.

Figure 1-13 presents the minimum-maximum envelope of spacecraft-Earth ranges for the first 48 hours for type I and type II trajectories. The four curves are window-open and window-close for both type I and type II trajectories. The purpose of this figure is to show how fast the spacecraft is moving away. By the third deep space station (DSS) pass (~ 16 hours past injection), the spacecraft is already at Moon-distance (~ 380,000 km).

With antenna pointing angles constant, the communications capability falls off with the square of the distance between transmitter and receiver. This decrease in capability is called space loss, and it is an important factor in the link budget or design control table that defines performance at a given point in time. As a number, the space loss goes as $1/(\text{range squared})$ and in decibels (dB) as $-20*\log(\text{range})$. Figure 1-14 shows how the space loss increases, as a function of time (in hours), almost 40 dB in the first 24 hours, then about another 5 dB in the next 24 hours.

After 48 hours (Figure 1-13), depending on date within the launch window, the range will be between 660,000 and 840,000 km for a type I trajectory and between 640,000 and 720,000 km for a type II trajectory. Because of the logarithmic character in space loss, the span of the signal strength due to range differences for these four cases at 48 hours is approximately 3 dB.

Like other deep-space missions, MSL will operate under tracking station strong-signal constraints that are unique to the initial acquisition portion of the mission to accommodate a 40-dB change in signal level during initial acquisition day. As one possible example, MSL could initially use the uplink and downlink DSN configurations as follows (Section 3 includes a block diagram for a 34-m tracking station, showing the elements involved in these configurations):

- Uplink: The station transmitter operated at 200 watts (W, normal is 20 kilowatts [kW]) for the first three passes, then operated at the normal power level.
- Downlink: The station microwave system is configured to receive the opposite polarization from that transmitted for the first pass. For MSL, this means the initial acquisition 34-m station will receive in the left circular polarization (LCP) configuration. Since the distance is so close and the signal so strong, polarization leakage would still provide a strong enough signal to close the link.

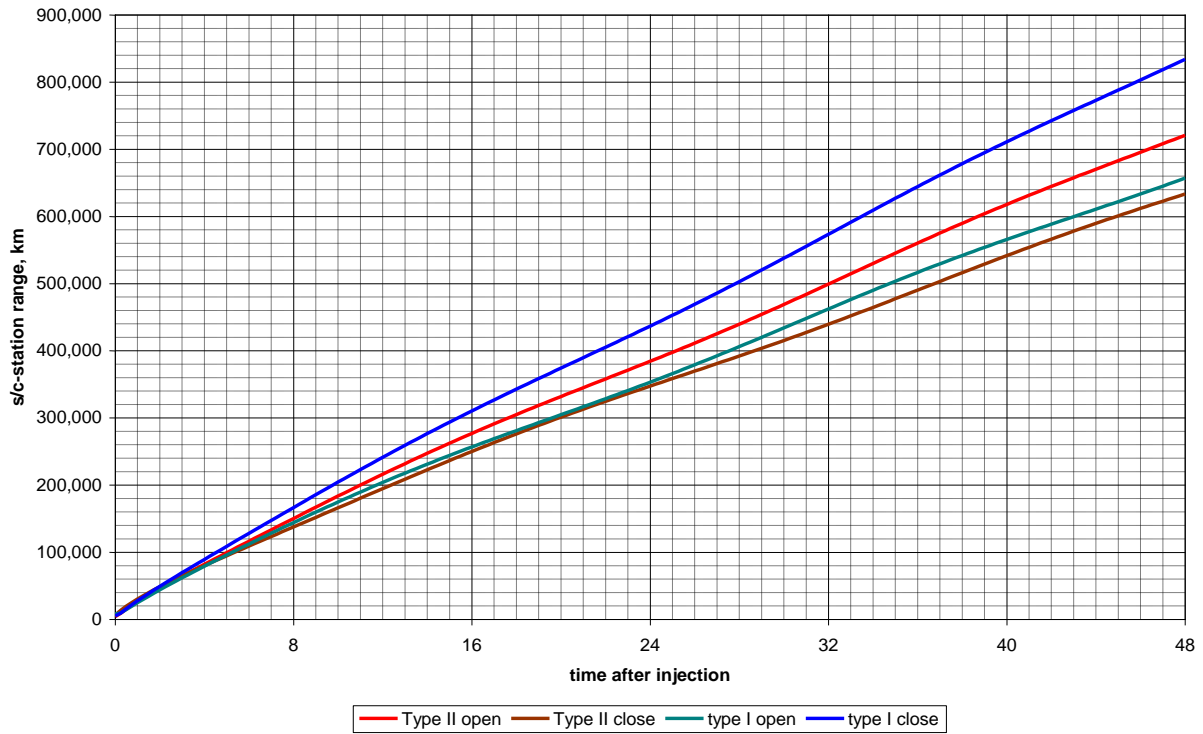


Figure 1-13. Canberra DSS range to spacecraft for 48 hours after injection.

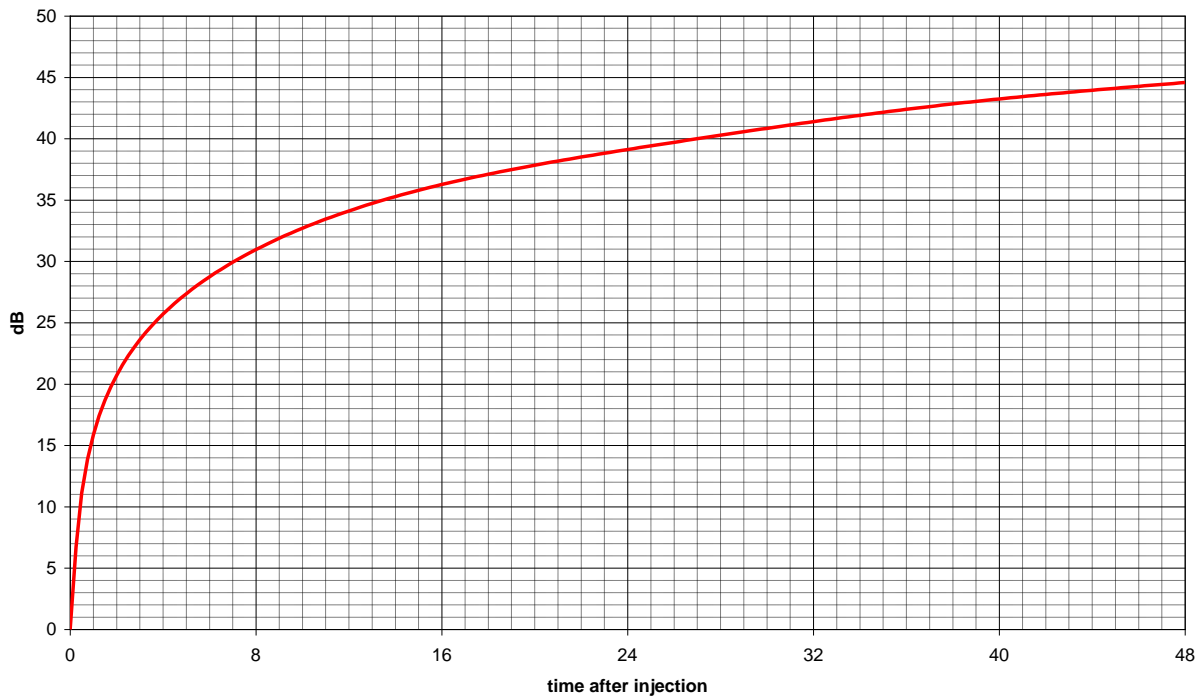


Figure 1-14. Canberra space loss to spacecraft, type II open trajectory.

Figure 1-15 shows the SPE angles for the type II (solid lines) and type I (dashed line) trajectories as a function of the time after launch for different launch dates during the two different launch periods. The SPE angle at arrival is approximately 34 deg for arrivals in August 2012.

Because of both the antenna pointing angle (related to SPE angle) and the Figure 1-14 range increase rate, the type II open (earliest launch date) is the most demanding from a telecom point of view, in particular for the first 15 days after launch and leading up to the first trajectory correction maneuver (TCM).

Analysis of telecom link performance has shown that planned off-Earth angles during early cruise should be constrained to 80 deg. The reason for this constraint can be seen in the gain patterns (see Figure 2-8 and Figure 2-9) of the PLGA. Beyond 80 – 85 deg, the uncertainty in the measured gain pattern increases dramatically due to antenna-test-range errors and spacecraft mockup differences from the actual spacecraft.

The type II trajectory produces SPE angles higher than 120 deg starting within a day after launch and remaining above 80 deg for more than a month. One of the mission design issues will be to limit the off-Earth pointing while maintaining sufficient solar array power.

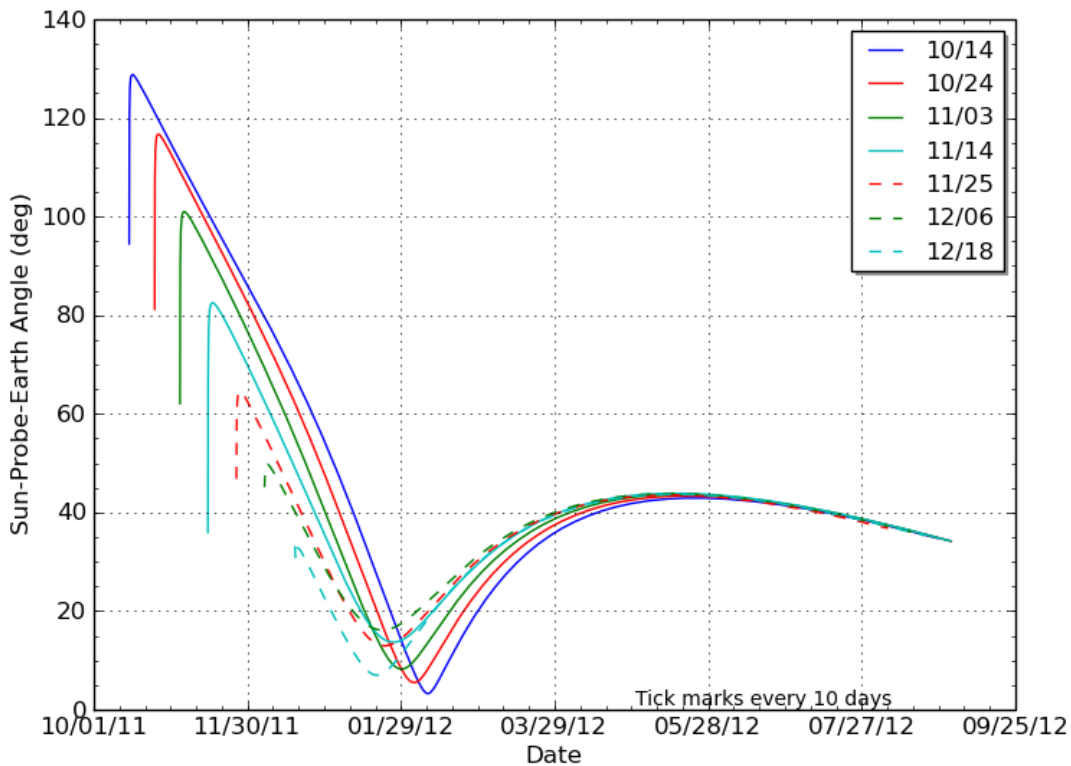


Figure 1-15. Type II (solid) & type I (dashed) trajectories and SPE angle launch to arrival for various launch dates.

1.4 Cruise Phase

Similar to the Mars Exploration Rover (MER) mission [6],⁹ the interplanetary trajectory attitude control plan for MSL has the cruise stage spinning at 2 revolutions per minute (rpm) until shortly before entry into the Martian atmosphere. The cruise antennas (a medium gain antenna and a low gain antenna) have their boresights co-aligned with the spacecraft $-Z$ axis. The $-Z$ axis is closely aligned with the spin axis of the spacecraft. In Figure 1-3, the $-Z$ axis is a line from bottom to top and in the plane of the drawing. Due to mass imbalances, the center of mass will be slightly offset from the $-Z$ axis and there will be a small wobble as the spacecraft spins. Because of the spinning, the worst-case antenna gain around the axis of revolution will certainly occur at least once every revolution (every 15 seconds); therefore that worst-case value is modeled for link prediction.

The major activities in the Cruise phase include: checkout and maintenance of the spacecraft in its flight configuration; monitoring and characterization/calibration of the spacecraft and payload subsystems (and associated parameter updates); attitude maintenance turns; navigation activities for determining and correcting the vehicle's flight path (for example TCMs); and preparation for EDL and surface operations. Three forms of navigation data that involve the telecom links are:

- Two-way Doppler, provided whenever the spacecraft receiver is in lock with an uplink carrier.
- Turnaround ranging, provided if the spacecraft ranging channel is on and the uplink carrier is modulated with the ranging signal (and the spacecraft receiver is in lock with the uplink).
- Delta differential one-way ranging (DOR), provided when the spacecraft transmits a one-way downlink and the spacecraft DOR tones are on. Two tracking stations are, alternately and in coordination, tracking the spacecraft and a quasar so as to fix the angular location of the spacecraft relative to the quasar.

The MSL mission is planning as many as six TCMs, though the last few might be cancelled if the trajectory remains good for entry without them (see Table 1-5 for more detailed TCM information).

The propulsion system can execute axial and lateral propulsive velocity corrections in the spacecraft reference frame. A vector mode maneuver is one that combines the axial and lateral segments so that the vector sum produces the desired inertial change in velocity (the "delta V") in magnitude and direction. This is a powerful maneuver-implementation mode that spinning spacecraft such as MSL can accomplish without executing a turn. A no-turn vector mode maneuver reduces operational risk by eliminating the estimation and control of a new attitude with potentially unknown characteristics. Additionally, the existing attitude is part of the nominal plan, well characterized, provides adequate spacecraft power, and supports ground communication. The downside to vector mode maneuvers is mainly higher propellant costs, especially for large "delta V" corrections [7].

⁹ The MER program included two rovers, launched in 2003 and landing on Mars on January 4 and January 24, 2004. Both rovers have been operating successfully for more than 5 years.

Table 1-5. Trajectory correction maneuvers planned during Cruise.

TCM	Time	OD Data Cutoff*	Description
TCM-1	L + 15 days	L + 10 days	Correct injection errors; remove part of injection bias for planetary protection; partial retargeting to entry aimpoint for desired landing site; aimpoint biased for planetary protection; may involve turn.
TCM-2	L + 120 days	L + 115 days	Correct TCM-1 errors; remove part of injection bias for planetary protection; partial retargeting to entry aimpoint for desired landing site; aimpoint biased for planetary protection; vector-mode maneuver.
TCM-3	E– 60 days	E – 65 days	Correct TCM-2 errors; target to entry aimpoint for desired landing site; vector-mode maneuver
TCM-4	E– 8 days	E – 8.5 days	Correct TCM-3 errors; vector-mode maneuver
TCM-5	E– 2 days	E – 2.5 days	Correct TCM-4 errors; final entry targeting maneuver required to achieve EFPA delivery accuracy requirement, vector-mode maneuver.
TCM-5X	E– 1 days	E – 1.5 days	Contingency maneuver for failure to execute TCM-5; vector mode maneuver.
TCM-6	E – 9 hours	E – 14 hours	Contingency maneuver; final opportunity to target entry aimpoint; vector-mode maneuver
	* Time measured from launch (L) or entry (E); OD = orbit determination; EFPA = entry flight path angle.		

1.5 Approach Phase

The Approach phase is defined to begin 60 days prior to entry into the Martian atmosphere and to end when the spacecraft reaches the atmospheric entry interface point, defined as a radius of 3522.2 km from the center of Mars. The principal activities during the Approach phase include the acquisition and processing of navigation data needed to make decisions on the need for the final three TCMs (and to support their development if it's required) and the spacecraft activities leading up to the separation from the cruise stage and start of EDL.

From a Telecom point of view, Approach is just late cruise in terms of range, antennas, link performance, etc. The same Cruise stage configurations and station configurations are in use.

1.6 EDL Phase

After a 5-day final approach, Entry Descent and Landing (EDL) is divided into three stages, lasting a total of 21 minutes. Figure 1-16 through Figure 1-19 are pictorials of the various stages of EDL.

- First stage (15 minutes) includes:
 - EDL start, ending with cruise stage separation.

- Exo-atmospheric, ending with switch to the tilted low-gain antenna (TLGA), bypassing the descent-stage diplexer¹⁰, and reaching the reference entry interface.
- Second stage (5 minutes) includes:
 - Entry, including a period of potential UHF blackout due to plasma generation.
 - Parachute descent, including heat shield separation and using the landing radar, formally called the terminal descent sensor (TDS) and described in Section 2.
- Third stage (less than 1 minute) includes:
 - Powered descent phase, including backshell separation with switch to X-band descent low gain antenna (DLGA) and the UHF descent UHF (DUHF) antennas.
 - Sky crane phase (during which the descent stage acts as a sky crane to lower the rover shortly before it lands), including touchdown and electrical bridle cut.
 - Flyaway of the sky crane.

Figure 1-16 and Figure 1-17 show, respectively, the spacecraft events connected with the first two stages. Figure 1-19 shows the final stage.

The pre-EDL (PEDL) spacecraft maneuvers for EDL will start approximately 10 minutes before Entry, with cruise stage separation (CSS). Unlike with MER, the spacecraft remains pointed toward Earth during the separation.

After CSS, the spacecraft will despin from the 2 rpm that existed throughout cruise. After approximately 1 minute, the spacecraft will perform the turn to entry (TTE) maneuver. At this point, the attitude of the entry body is no longer optimal for Earth communications.

Prior to reaching the entry interface point, the cruise balance masses (CBM) are separated from the spacecraft, as shown in the second from last sketch in Figure 1-16, moving the center of mass of the entry body to induce the proper angle of attack to enable aerodynamic lift.

At this time in mission design, the nominal angle of attack is between 15 and 19 deg. The angle of attack will vary up to ± 2.5 deg from the design value until shortly before parachute deploy. The TLGA antenna is mounted at 17.5 deg with respect to the $-Z$ axis of the spacecraft.

¹⁰The descent stage diplexer is bypassed to prevent coronal discharge within the diplexer during the repressurization during entry. Since receive capability is no longer required during entry, diplexer bypass has no effect on telecommunications.

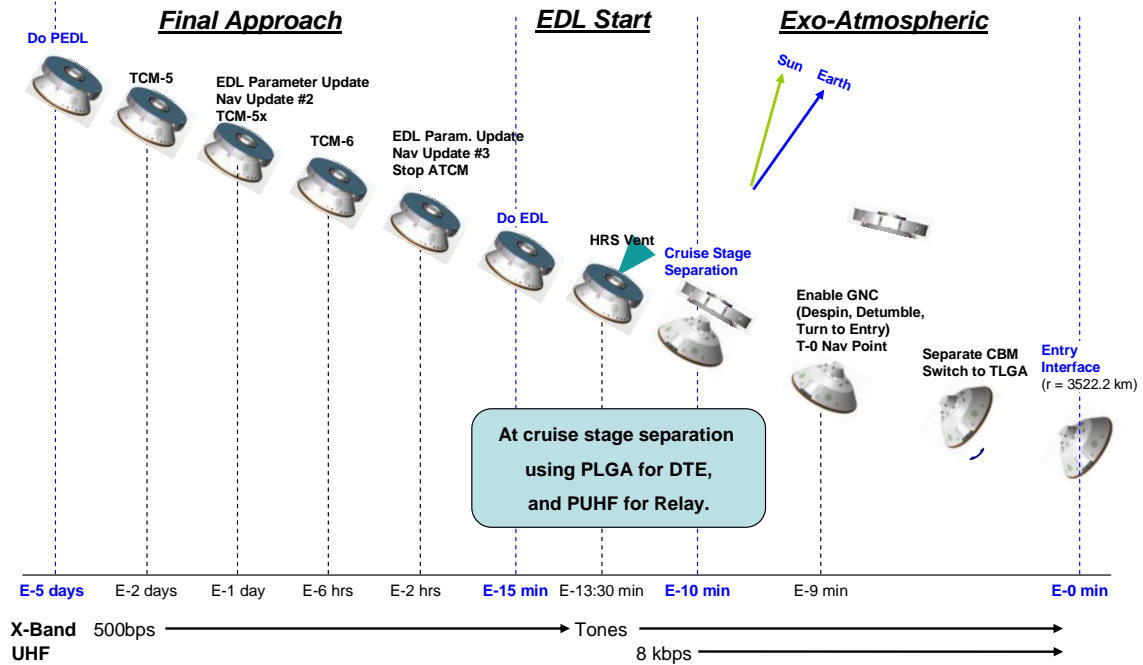


Figure 1-16. Timeline: Cruise Stage separation to entry interface.

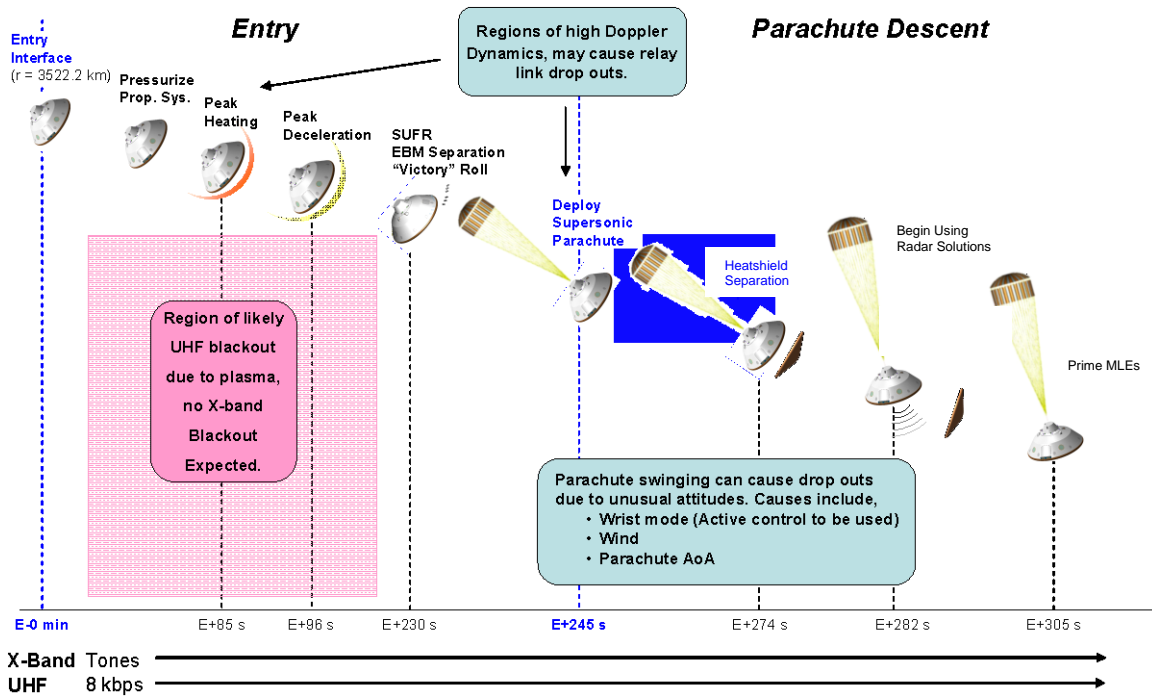


Figure 1-17. EDL timeline: entry interface to backshell separation.

After entry, the vehicle will perform banking maneuvers to achieve a smaller landing ellipse (guided entry). These banking maneuvers are performed using repeated short (about 20 millisecond) firings of the reaction control system (RCS) thrusters. As shown in Figure 1-18, where Mars is at the bottom, a “lift up” maneuver tilts the heat shield slightly above the velocity vector and a “lift down” maneuver tilts it slightly below. During this time, the angle of attack (AoA) is in the range of 15 to 19 deg. The MSL TLGA is nominally aligned with the anti-velocity vector to minimize variations of off-boresight angles during banking. The result of this alignment is that the variations in off-boresight angle would be expected to be roughly equal on either side of the antenna’s boresight, rather than skewed to one side of boresight.

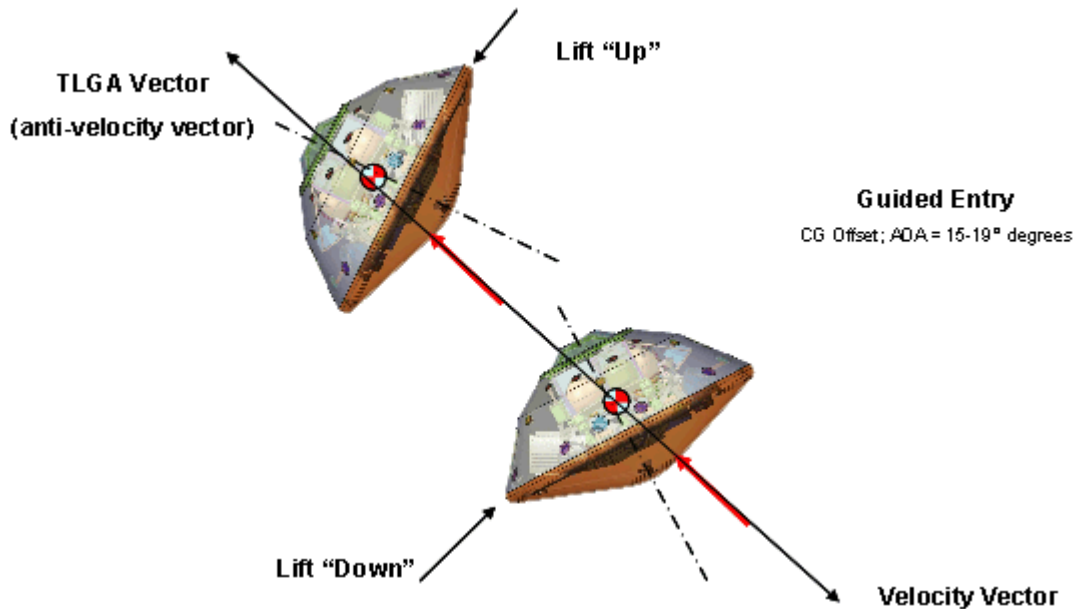


Figure 1-18. Banking maneuver along anti-velocity vector.

During the period of peak heating (Figure 1-17, centered at ~ E +85 s), it is also likely that the UHF signal will experience a dropout due to plasma shielding (see Section 4). Next comes the period of peak deceleration, which causes challenging Doppler dynamics for signal acquisition and tracking.

Figure 1-19 shows the last portion of EDL, starting with parachute deployment and followed by heat shield separation, radar activation, and backshell separation (BSS). At this point, the vehicle will start its power descent phase, during which the descent stage, acting as a sky-crane, will lower the rover using a bridle approximately 7 m long. After rover touchdown, the descent stage will fly-away in open loop and set down (uncontrolled) sufficiently far from the rover landing site to avoid the possibility of damage to the rover or contamination of the area around the rover landing site.

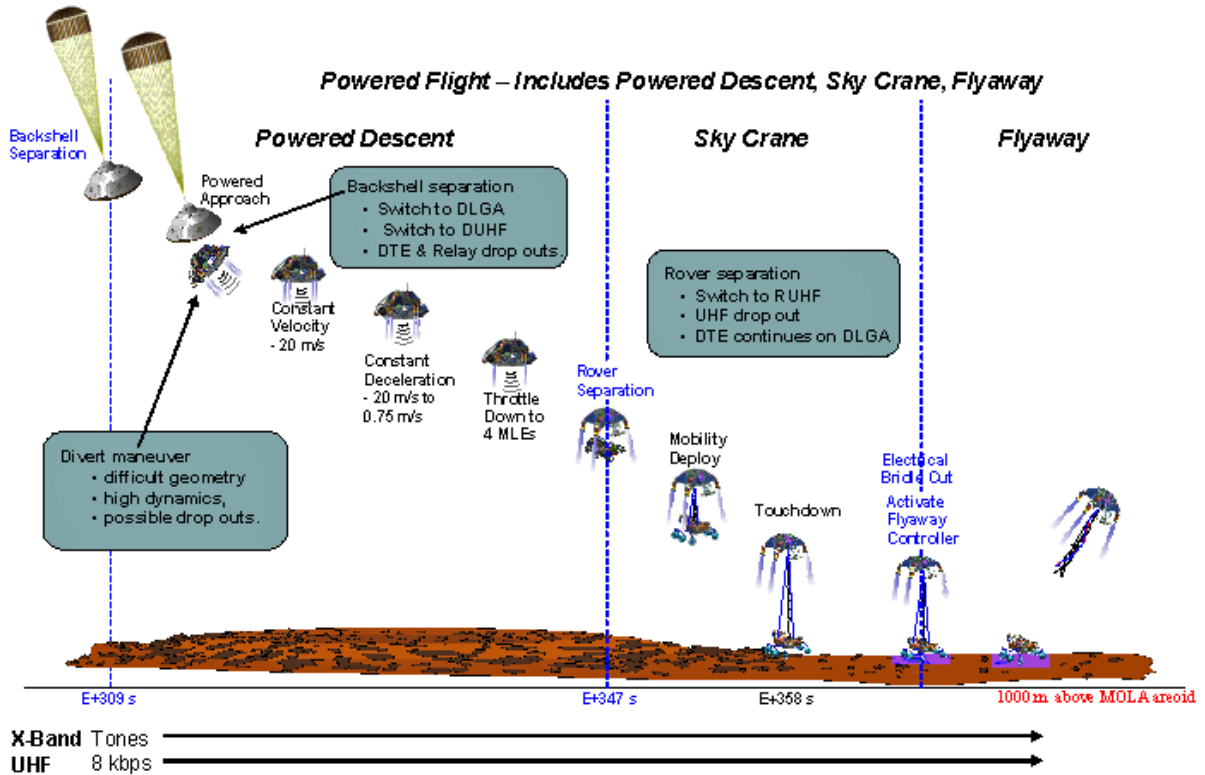


Figure 1-19. EDL timeline: backshell separation to fly-away.

While slowing on the parachute, the system will prepare the propulsion subsystem, separate the heat shield, and begin using the TDS to acquire a landing solution. (Note: A change from the 2009 mission plan is that the mobility deployment of the wheels will now occur during the sky crane maneuver in the final seconds before touchdown).

To achieve a soft controlled landing, the EDL system must be able to accurately measure altitude and three-axis velocity (i.e., horizontal and vertical velocity) beginning at several kilometers and continuing all the way down to a few meters above the surface. The TDS is designed to provide these measurements starting at heat shield jettison all the way to rover touchdown.

Figure 1-20 provides a brief overview of the TDS requirements during the EDL phase of the MSL mission. Section 2 includes a description of the TDS.

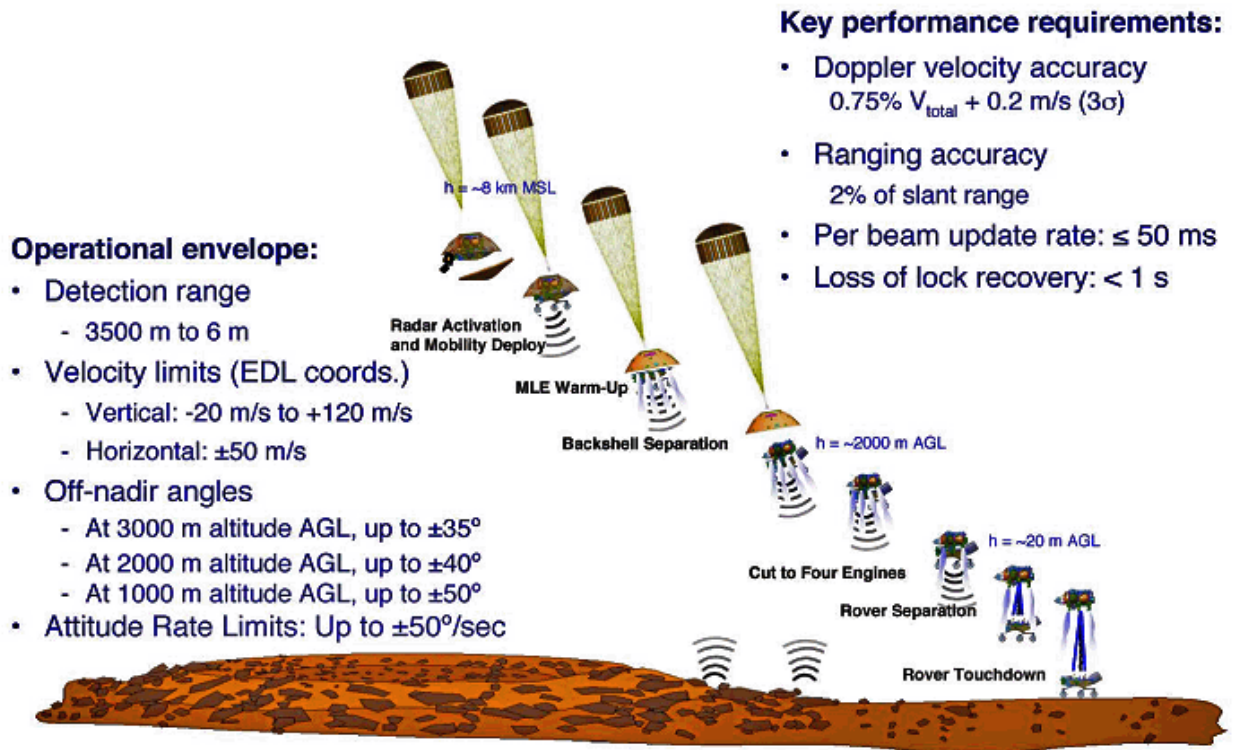


Figure 1-20. Overview of TDS requirements during EDL.

1.6.1 DTE to Entry, MRO after Entry

Communications during EDL, sufficient to allow a reasonable chance to determine what happened (using data reconstruction) in the event of an EDL failure, has been mandated by Headquarters at the National Aeronautics and Space Administration (NASA) since the Mars Polar Lander failure of 1998.

Due to limitations on the range and view angles to the Mars orbiters (“relay assets”), relay during EDL cannot cover the entire time from CSS to landing + 1 minute. Since the majority of important events occur after entry, the orbiters will be phased in their orbits to optimize a relay link from entry to landing + 1 minute. The mission design baseline is that DTE should provide the coverage during the period from CSS to entry, a time when, by comparison to the after-entry period, relatively few events occur. Nevertheless DTE coverage from CSS to landing + 1 minute is desirable. The period of maximum heating is expected to create a plasma envelope sufficient to produce a link dropout at UHF relay frequencies (but not at X-band), making DTE via a plasma-penetrating frequency highly desirable during this period.

In addition to the plasma blackout period, there are several short intervals during EDL when link dropouts for both relay and DTE are expected. Table 1-6 lists the most important dropout periods, the cause for each dropout, and the dropout’s expected duration.

Table 1-6. Periods of UHF or DTE dropouts between CSS and landing.

Event	Cause	Estimated LOS
CSS	Switch to PLGA, CSS shock, CS blocks antenna	~ 1 second
Turn to Entry	Switch to TLGA	~ 1 second
Plasma blackout (UHF only)	Plasma envelope cuts off UHF link	25 to 100 sec
Parachute deploy (X-Band only)	Sabot may cause X-Band blockage, resulting in loss of MFSK tone(s). Note we stay on the TLGA due to possible damage of the PLGA from sabot impact.	Worst case: entire phase (~ 75 sec)
Backshell Deploy	Change to DUHF & DLGA Blockage	~ 1 – 6 sec
Rover sep & Sky Crane (UHF Only)	Change to RUHF, UHF Blockage	~ 1 – 5 sec

The red highlighted row of the table mentions a temporary blockage of the X-band DTE from the parachute deployment sabot¹¹. Figure 1-21 shows the MSL sabot in action during deployment of a parachute mass model from its canister during a ground test. The sabot is the device about a third of the way from the bottom of the picture. It is partially wrapped in a capture bag, a loose web of straps designed to keep it contained. The parachute mass model is at the top of the picture. The movement of the sabot during parachute deployment can be quite violent, and there is a concern that when the sabot falls back to the top of the parachute canister it could impact and damage the PLGA. At backshell deployment, a steep-angled and very dynamic maneuver is performed by the powered descent vehicle to “divert” the spacecraft away from the parachute and backshell. This maneuver will briefly create high Doppler rates and unusual attitudes that might cause a dropout in addition to the blockage and UHF antenna switch shown in the table.

¹¹ The term sabot referred originally to a device used in a firearm to hurl a projectile, such as a bullet, that is smaller than the bore diameter, or requires the projectile to be held in a precise position.

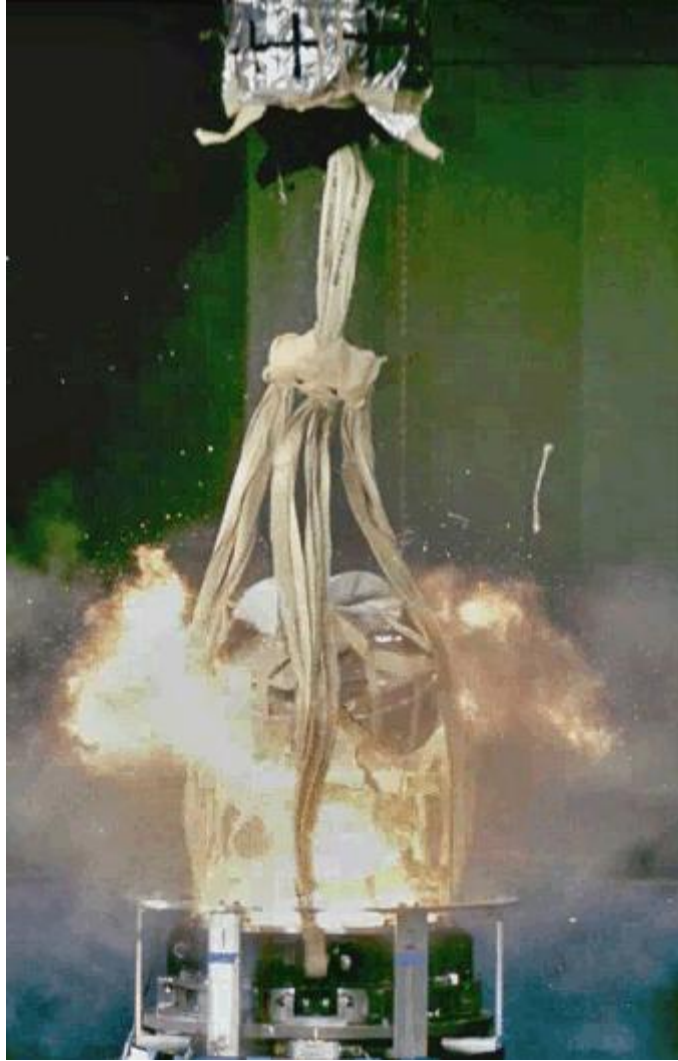


Figure 1-21: Sabot, shown during ground parachute deployment test.

1.6.2 Full-DTE EDL Communications

As discussed previously, full-DTE EDL communications is considered desirable as backup to the relay link after entry until landing + 1 minute. This so-called full-DTE coverage is not guaranteed for both trajectory types and all landing sites. While the type II trajectory does offer full-DTE coverage for the four primary landing sites, only the northern landing site (Mawrth Vallis at 24 deg N) has full-DTE coverage for the type I trajectory. The actual duration after entry for DTE varies considerably from a couple of minutes after entry to close to landing + 1 minute, depending on the landing site and the actual launch date. The current baseline for using the X-band EDL antennas is to use the PLGA (which points along the spacecraft $-Z$ axis from CSS to entry), and then the TLGA (which points along the average tilt angle and, therefore, close to the anti-velocity vector after turn to entry) at entry. Figure 1-22 illustrates the view angles for the antennas during EDL using data from the 2009 launch analysis for the more southerly Gale Crater landing site (at 4.5 deg S). The figure, with data for only one candidate landing site and for the 2009 launch, is for illustration purposes only. The 2011 launch trajectories will offer similar view angles. A plot of the $-Z$ axis views would show considerably greater variation after

entry due to the guided entry maneuvers (banking turns); however, using the TLGA minimizes these variations.

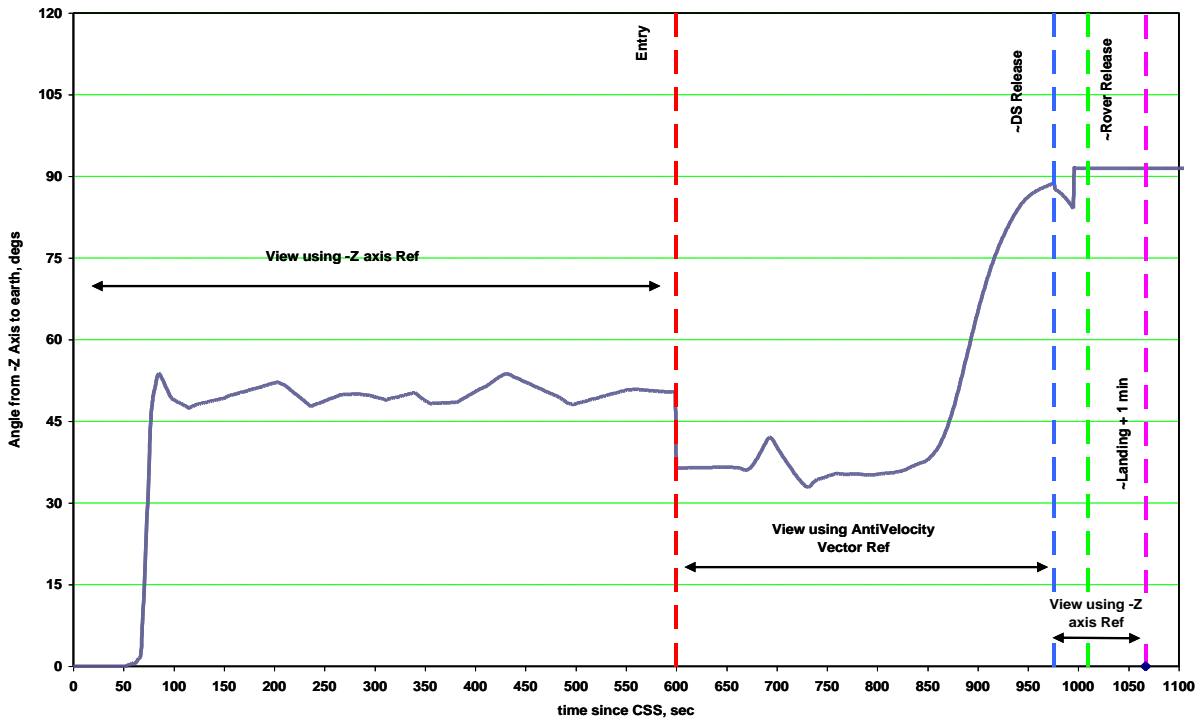


Figure 1-22. Example DTE views during EDL (2009 launch data, Gale site).

1.6.3 Surface Phase

The lifetime requirement for MSL is one Martian year on the surface. One Martian year is 687 24-hr Earth days or 669 Martian sols. The Earth geometry during the surface mission is shown in Figure 1-23. The Mars-Earth range (blue curve, left axis) varies between 0.6 and 2.4 astronomical units (AU). MSL will be landing at an Earth-Mars range between 1.7 and 1.8 AU.

On Mars, the rise and set times of the Earth vary with the date and the latitude of the landing site. The four candidate landing site names and latitudes are included in Figure 1-6. The landing site has not yet been selected; therefore, the three figures that follow Figure 1-23 give only a rough idea of the operational environment: Figure 1-24 shows how the Earth rise time varies by approximately 5 hours during 1 Martian year. Figure 1-25 shows that the Earth set-time has a similar variation. The rise and set times are in Mars local true solar time (LTST) [8]¹².

¹² Because the orbit of Mars around the Sun is not perfectly circular and the planet does not rotate about an axis perpendicular to its orbit plane, there is a seasonally variable discrepancy between the even advance of an artificially defined Mean Solar Time and of the True Solar Time corresponding to the actual planet-centered position of the Sun in its sky. By analogy with the 24 time zones on Earth, Mars Mean Solar time is defined on the Mars prime meridian as Mars Time Coordinated, or MTC, by analogy to the terrestrial UTC (Universal Time Coordinated). Again by analogy with the Earth, local solar time at the selected location is defined in terms of similarly constructed "Mars time zones". These Mars time zones are exactly 15 deg wide and centered on successive 15-deg multiples of

The duration per day that the Earth is visible (assuming a 10-deg land mask and zero rover tilt) is shown in Figure 1-26. This duration (8 to 13 hours) is for the Earth, not for any one DSN site on the rotating Earth. Disregarding any constraints in DSN scheduling and uplink/downlink operations, the figure shows the maximum possible time per day available to uplink commands (via a direct from Earth [DFE]) link and to get telemetry data (via a DTE link).

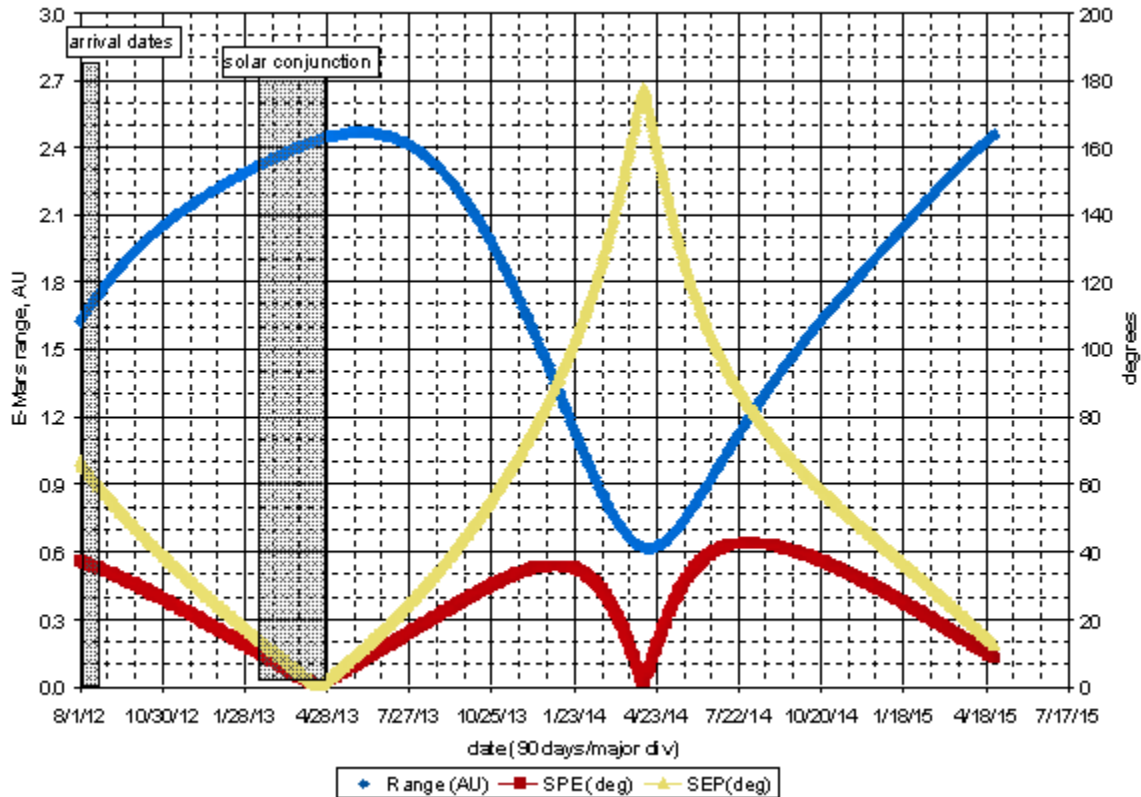


Figure 1-23. MSL geometry during surface operations.

longitude, at 0 deg, 15 deg, 30 deg, etc. For more detail on Mars Solar Time, see [8] (<http://www.giss.nasa.gov/tools/mars24/help/index.html>)

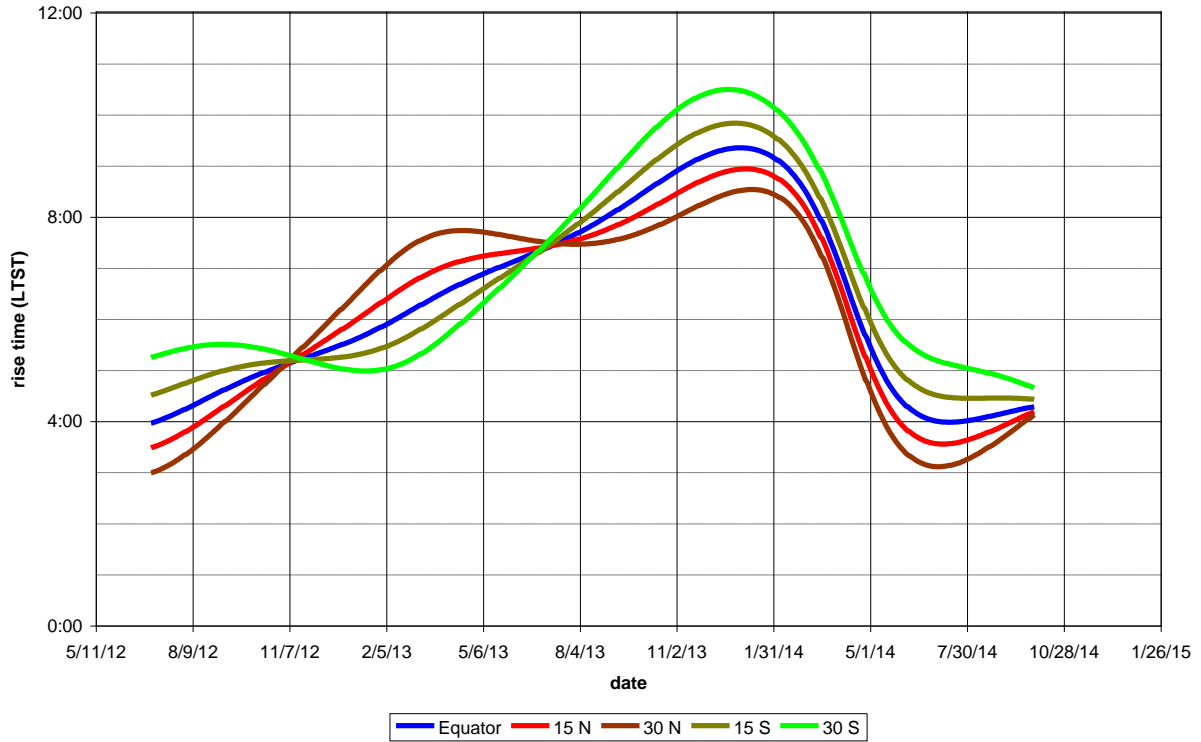


Figure 1-24. Earth rise vs. date, for different MSL landing sites.

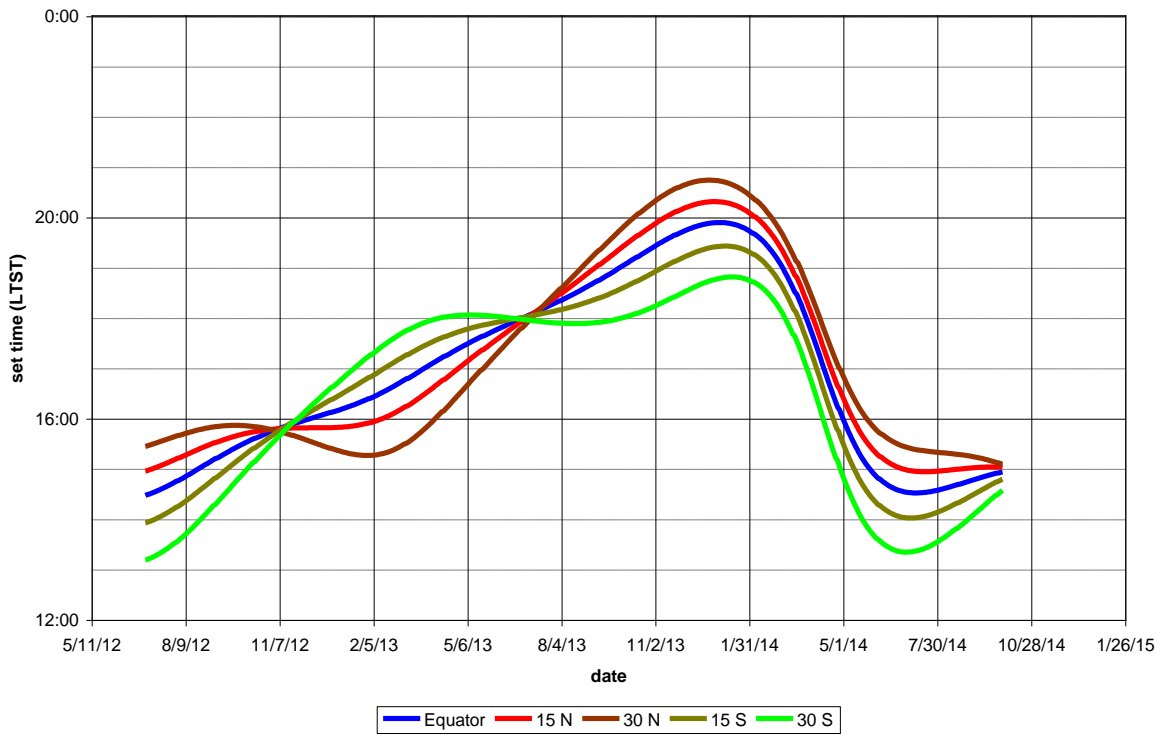


Figure 1-25. Earth set time for different MSL landing latitudes.

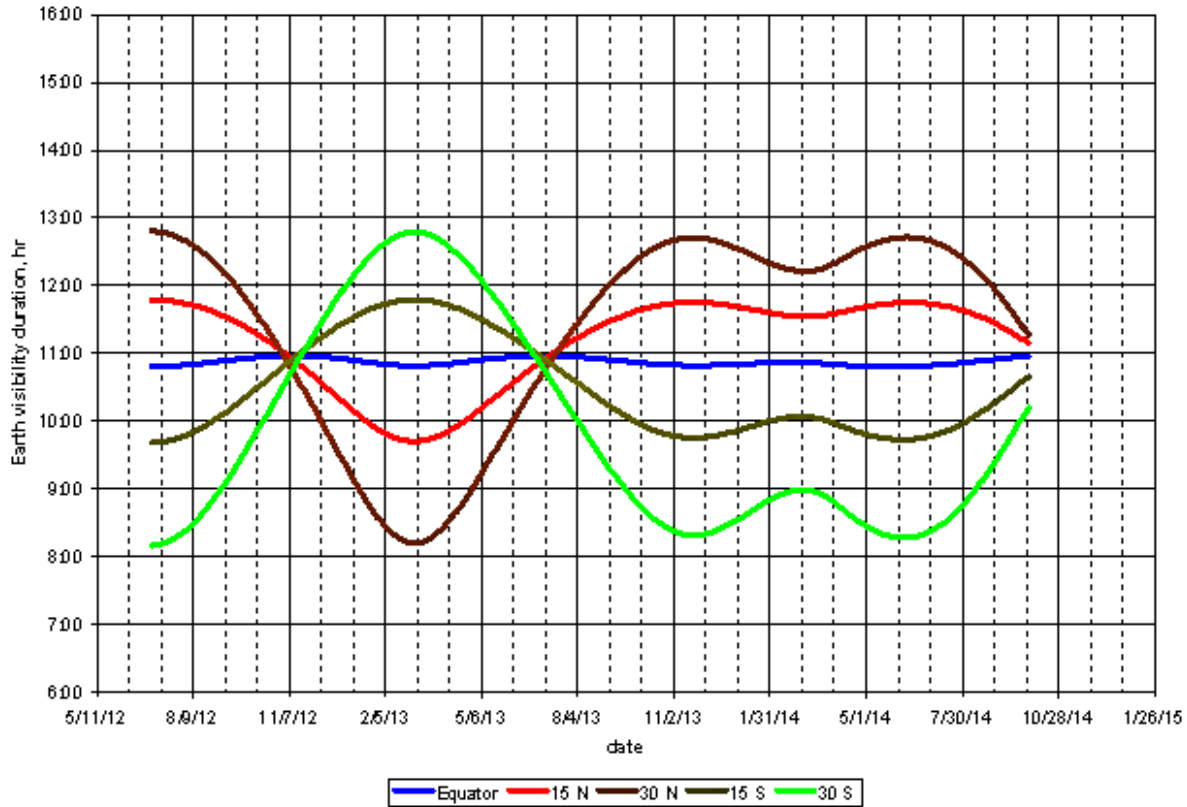


Figure 1-26. Earth visibility duration vs. date (MSL surface mission).

MSL will be able to relay data with the Mars Reconnaissance Orbiter (MRO) and Odyssey¹³. Table 1-7 summarizes their classical orbital elements¹⁴.

Table 1-7: Orbital elements for relay orbiters.

Parameter	Odyssey	MRO
Semi-Major Axis (km)	3788.1479	3648.606
Eccentricity	0.0108616	0.012176
Inclination (deg)	92.894	92.655
Longitude of Ascending Node	235.4908	-10.695
Argument of Periapsis (deg)	267.5309	-90.003
Epoch	01-Jan-2006 00:01:00	07-Dec-2006 01:00:00

¹³ Collectively, Odyssey and MRO are referred to as the Mars Relay assets available during the MSL surface mission. Odyssey was launched in 2001 and MRO in 2005.

¹⁴ See http://en.wikipedia.org/wiki/Orbital_elements for definitions of Orbital Elements as used in celestial mechanics. Exactly six parameters are necessary to unambiguously define an arbitrary and unperturbed orbit. In the Table, the epoch defines a reference time when the sixth parameter, the mean anomaly (the position of the orbiter along its ellipse) is equal to zero.

Figure 1-27 shows the amount of time per sol that MRO is above an elevation of 10 deg vs. the latitude of the rover’s landing site. With MSL near the Martian Equator, the time MRO is above 10-deg elevation is approximately 13 minutes total, divided between two passes per sol.

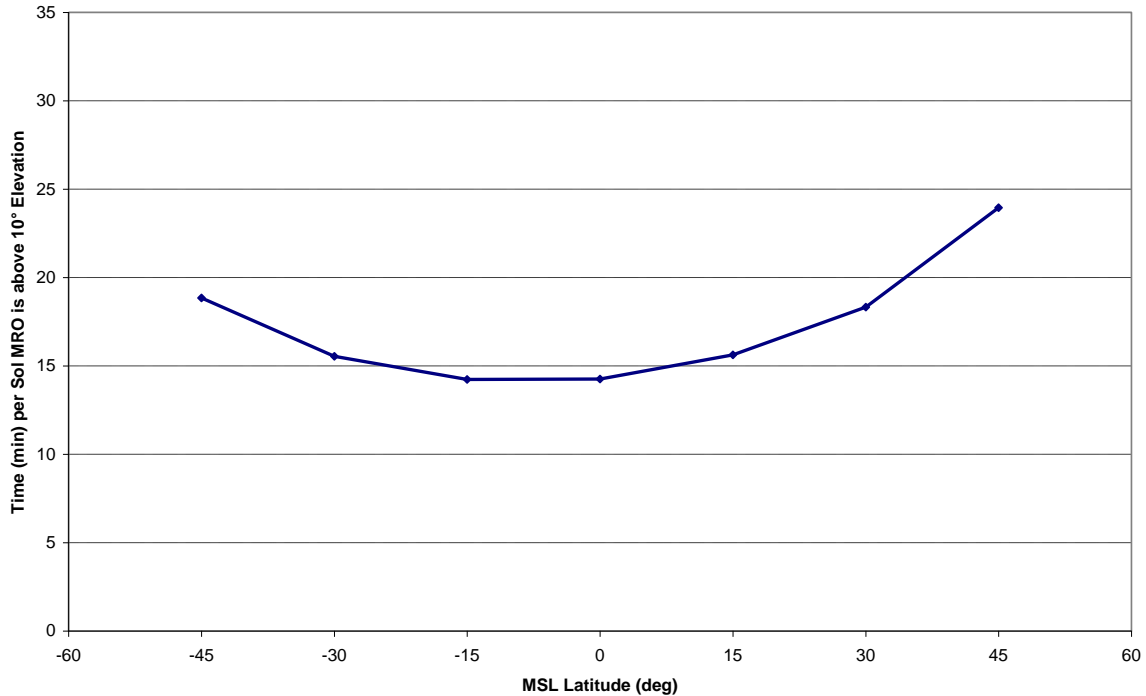


Figure 1-27. Time (min) per sol MRO is above 10 deg elevation vs. MSL latitude.

The next two plots (Figure 1-28 and Figure 1-29) show a different periodicity in maximum elevation of a pass between MSL and MRO for the case of MSL at the Martian Equator. Figure 1-28 covers 120 sols, and Figure 1-29 covers 60 sols. Both figures have the required 10-deg minimum elevation angle to MRO. Within these constraints, the left vertical axis indicates how the maximum elevation angle to MRO varies over the 120-sol or the 60-sol duration. Both these plots are based on 2009 launch data; however, the general performance bounds are the same for the 2011 launch.

Figure 1-28 shows the maximum elevation angle considering three of the four possible passes per sol: the better of the two morning or “AM” passes (in blue) and both of the evening or “PM” passes (in red). This figure shows the first 120 sols of the surface mission. Generally, the higher the elevation angle, the longer the pass.

Figure 1-29 looks quite different because it shows the maximum elevation angle considering only two passes per sol: the better AM pass (in blue) and the better PM pass (in red). Also this figure shows only the first 60 sols.

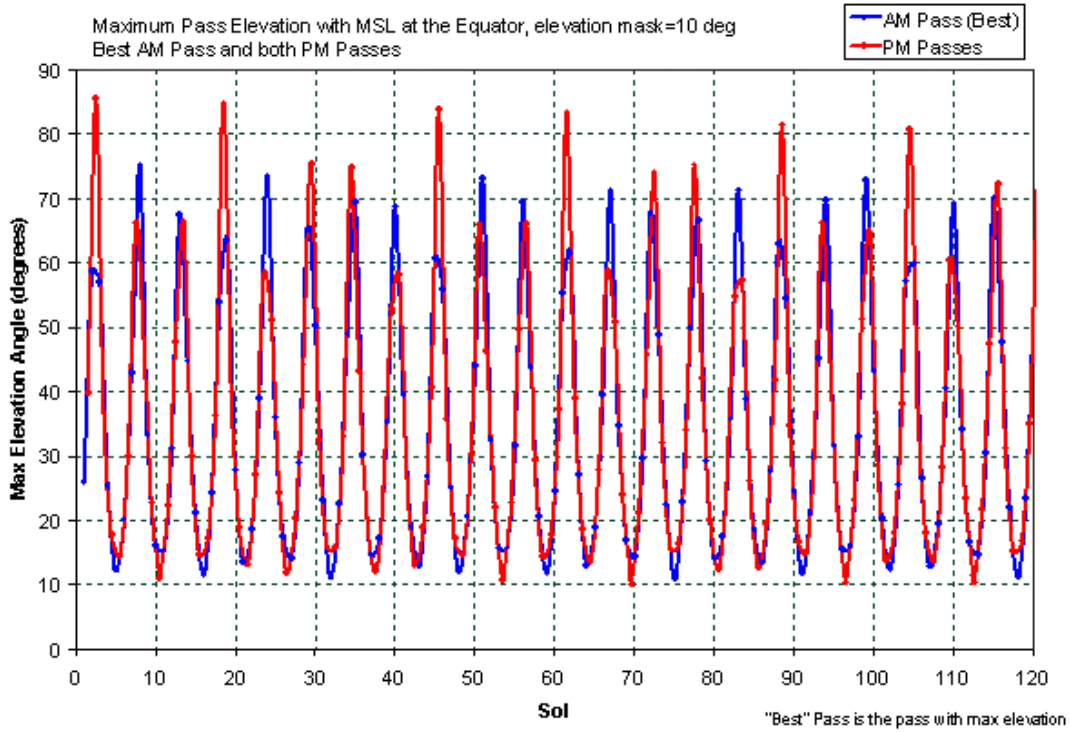


Figure 1-28. Maximum elevation of MRO passes vs. sol (MSL at Equator) for better of the AM passes and both of the PM passes for 120 sols (based on 2009 launch data).

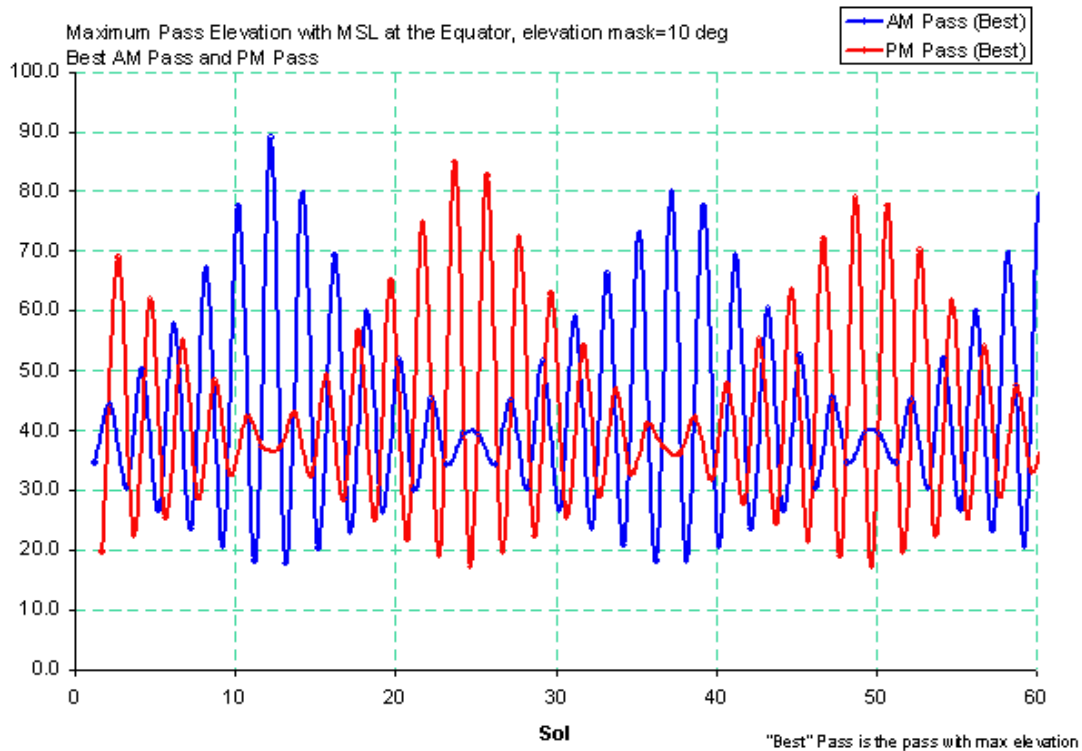


Figure 1-29 Maximum elevation of MRO passes vs. sol (MSL at Equator) better of the AM passes and only the better PM pass for 60 sols (based on 2009 launch data).

Figure 1-30 gives the breakdown of visibility time for each 10-deg elevation step. For a landing site between 45 deg S and 45 deg N (which includes all four candidate sites), the percentage of time is approximately independent of latitude. It is seen that more than half the time is spent between 10 deg and 20 deg elevation and that the time spent progressively decreases until it is just one quarter of one percent for elevation between 80 and 90 deg. This implies that, on average, a broader antenna pattern, which provides significant coverage at low elevation angles, is advantageous, while high gain in the zenith direction is generally not useful.

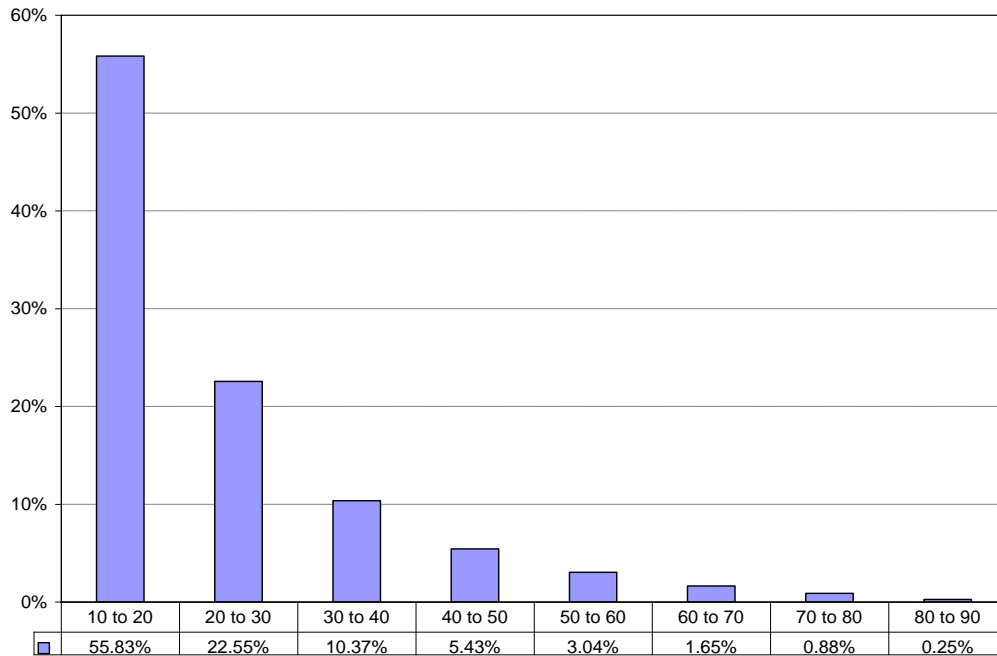


Figure 1-30. Percentage of time spent by MRO between 10-deg steps in elevation.

1.7 Flight System Description

The flight system (Figure 1-3) consists of an Earth-Mars cruise spacecraft, entry-descent-landing (EDL) system, and a mobile science rover with an integrated instrument package. In the figure, the MSL EDL instrumentation (MEDLI) [9] is an instrumentation suite installed in the heat shield of the Mars Science Laboratory's (MSL) Entry Vehicle that will gather data on the atmosphere and on aerothermal, Thermal Protection System (TPS), and aerodynamic characteristics of the MSL Entry Vehicle during entry and descent providing engineering data for future Mars missions.

During cruise, the spacecraft is spin-stabilized (2 rpm); the spin is about the Z axis. In Figure 1-3, the -Z axis is in the plane of the figure, extending at the top center of the figure.

The EDL system consists of a mid-1970s Viking-derived aeroshell structure and propulsion system for a precision guided entry and soft landing. The soft landing is new for MSL and

contrasts with the airbag designs that were used by the mid-1990s the Mars Pathfinder (MPF) mission[10]¹⁵ and the early 2000s MER mission.

Table 1-8 provides a top-level comparison of MSL and MER. MER telecommunication, including telecom subsystem mass and power draw, is described in [6]. The MSL telecom subsystem, including mass and power draw, is described in Section 2.

Table 1-8. Comparison between MSL and MER.

	MSL	MER
LV/Launch Mass	Atlas V/4000 kg	Delta II/1050 kg
Design Mission Life	1 yr cruise/1 Martian year surface	7 month cruise/3 month surface
Telecom Redundancy	Significant telecom redundancy/Single Mission- One rover. Telecom includes a small deep space transponder (SDST) and a TWTA on the Descent Stage and an SDST and a solid-state power amplifier (SSPA) on the rover (for X-Band). The rover also has two UHF radios.	Limited telecom redundancy/Dual Mission 2 rovers. Each rover has 1 SDST and 2 SSPAs (X-Band), and one UHF radio
Payload	10 instruments (84 kg)	5 instrument (~9 kg)
Sample Acquisition	Arm + rock abrasion tool (RAT) + Powdering Corer + Scoop	Arm + RAT
EDL System	Guided Entry/Sky Crane	MPF Heritage/Airbags
Heat-shield Diameter	4.5 m	2.65 m
EDL Comm	Partial UHF + partial DTE or full DTE	DTE + partial UHF
Rover Mass	850 kg (allocation)	170 kg (actual)
Rover Range	>20 km designed	1km (design) and >10 km (actual)
Surface Power	MM RTG/2500 Whr/sol	Solar/<900 Whr/sol
Surface Comm	X-Band DTE + UHF	X-Band DTE + UHF

Figure 1-31 is a view of the MSL rover in its fully deployed configuration.

¹⁵ Mars Pathfinder, launched in December 1996 and landed July 1997, consisted of a lander and the Sojourner rover. MPF was originally designed as a technology demonstration of a way to deliver an instrumented lander and a free-ranging robotic rover to the surface. It accomplished this goal. Both vehicles outlived their design lives on Mars, the Pathfinder lander by nearly three times and the rover by 12 times.

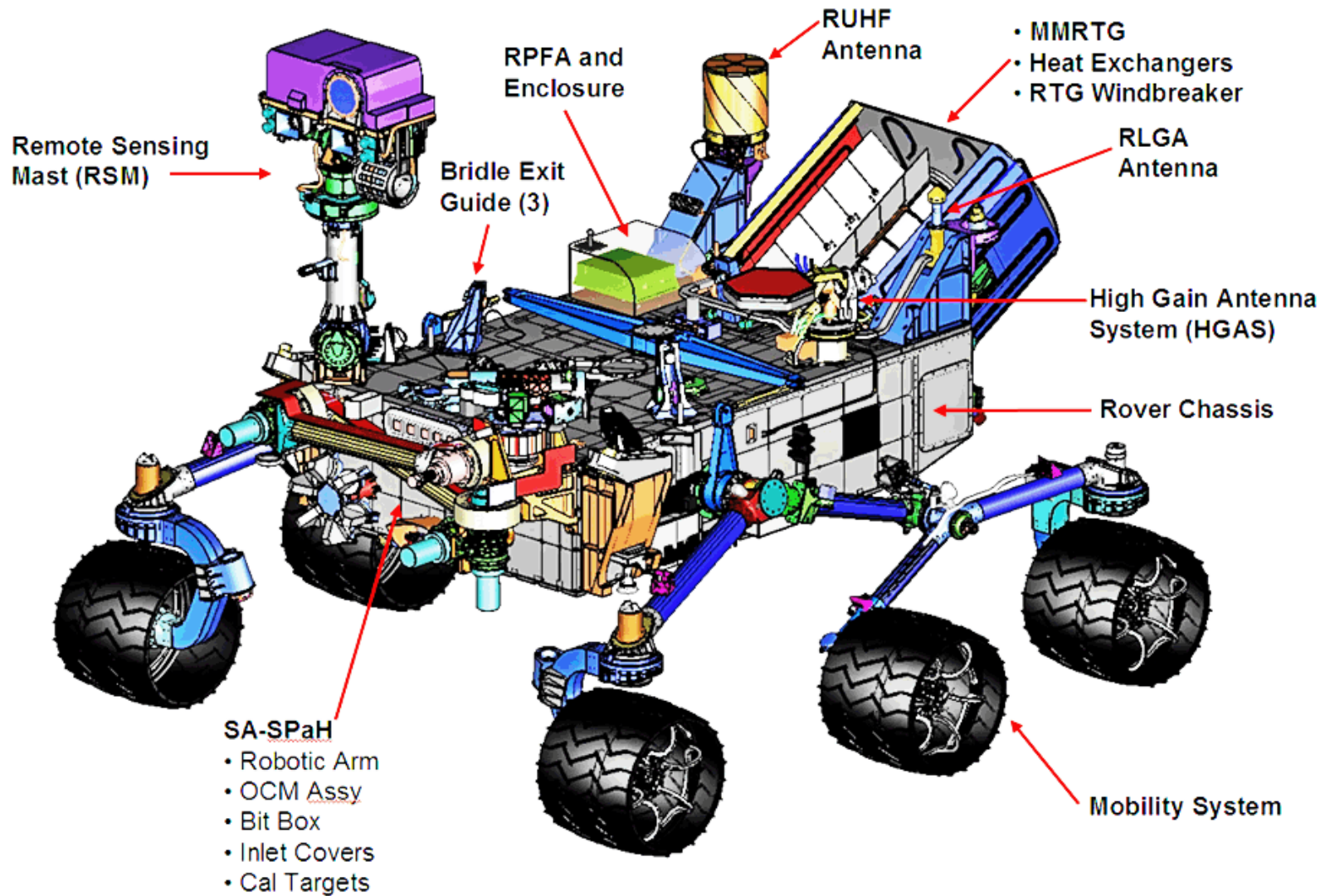


Figure 1-31. External view of the MSL rover.

1.7.1 Engineering Subsystems and Functions

The following description of the engineering subsystems related to telecom is from the Mission Plan [11].

Chassis. The chassis is the central part of the rover, accommodating the flight system elements. In addition to the structural integration of components, the structural system serves as a significant part of the thermal control of the vehicle, with insulation, thermal coupling of the payload mounting panel and the Multi-Mission Radioisotope Thermoelectric Generator (MMRTG) heat exchangers. The chassis core forms the shell of the warm electronics box (WEB); panels internal to this are used to mount the flight system avionics and payload avionics. Similar to MER, the active telecom components (SDST, SSPA, and Electra UHF radio) are in the WEB.

Mobility. The rover is a scaled version of the six-wheel drive, four-wheel steering system from MER, utilizing the rocker-bogie configuration. Based on the center of mass, the vehicle is required to withstand a tilt of at least 50 deg in any direction without overturning. During descent, this number will be slightly higher, as the mast is not deployed. Fault protection will limit the rover from exceeding 30-deg tilts. The design of the rocker-bogie allows traverse over (meaning the wheel moves over) objects approximately as large as the wheel diameter. Each wheel has cleats and is independently actuated and geared, providing for climbing in soft sand and scrambling over rocks. Each front and rear wheel can be independently steered, allowing the vehicle to turn in place as well as execute arcing turns

Power (surface operations). Rover power is primarily provided by the MMRTG, which is required to generate a constant 110 W at the start of the prime mission (though the current best estimate predicted by the Department of Energy [DOE] is approximately 114 W at the start of the 2009 mission surface phase), decaying to approximately 108 W at the end of the mission. The values for the 2011 mission would be somewhat lower.

Peak power from the rover activities easily exceeds this, however, and the rover has two 20 amp-hour (A-hr) batteries (“nameplate” output at delivery) to allow for all activities. The 2009 launch requirements for performance of the battery are that it should provide as much as 555 W-hr per sol for 670 cycles, given a starting condition of 100 percent state of charge (SOC). Such a deep discharge (555 W-hr) was not intended to occur more than once per sol. In light of the 2009 to 2011 launch slip, and after review of the surface power situation, the 555 W-hr figure is considered not sufficient. Consequently, among other changes, a larger battery capacity might be required. Mounting solar panels on the top of the deck is also under consideration. At the posting of this article, the power situation is still under review and analysis.

Guidance, Navigation, and Control (GNC). During cruise, EDL, and surface operations, the telecom antenna orientation relative to Earth depends on GNC. The MSL Cruise Guidance and Control Subsystem makes extensive use of heritage hardware and flight software algorithms from the MER and MPF missions. Three-axis inertial attitude and spin rate are determined onboard in real time using an internally redundant star scanner and one of two 4-head Sun sensors. During cruise, the flight system is spin-stabilized about the spacecraft Z axis at 2 rpm. Eight thrusters arranged in two clusters are used as actuators to control spin rate, “turn” the spacecraft (by precessing the spacecraft spin axis), and perform axial or lateral trajectory correction maneuvers (TCMs).

From the perspective of navigation, the onset of EDL and the events leading up to it are of critical importance to mission success. The EDL system differs from those used for other mission functions in that it does not require an interactive, ground-generated mission plan. During the entire phase, the vehicle acts autonomously, based on pre-loaded software and parameters. On MSL, the landing radar is book kept as part of GNC.

Thermal control (surface operations). The MSL is capable of landing between 45 deg N and 45 deg S and, accordingly, the thermal control system must be designed to accommodate a wide variety of climates and temperatures. Across these latitudes, Mars surface temperatures can reach as high as +40 deg C and as low as -127 deg C (the freezing point of carbon dioxide [CO₂] at Martian atmospheric pressures), with daily thermal cycles of up to 145°C. At any latitude, the thermal system is designed to achieve a minimum of 6 hours per sol at which the rover avionics mounting plate (RAMP) and, specifically, the Payload Mounting Module (PMP) will stay at 20°C or higher. In extreme cases (for example, at latitudes beyond 30 deg, such as winter at 45 S), the RAMP temperature must be maintained above -40 deg C throughout the sol. In addition, the thermal design also limits the daily thermal cycle to ± 30 deg C. The majority of the Martian year, at any latitude, the thermal system will be warming the rover. The thermal system will achieve this in several ways: passively, through the dissipation of internal components; by electrical heaters strategically placed on key components; and by using the rover heat rejection system (HRS). The HRS is a set of redundant integrated pump assemblies and a fluid loop that runs throughout the WEB that serves to minimize thermal gradients across the rover. The fluid loop actually serves the additional purpose of rejecting heat when the rover has become too warm, but it also can gather waste heat from the MMRTG, by pumping fluid through two heat exchangers mounted alongside the MMRTG. (Because MSL has a surface cooling loop that was not present on MER, the MSL hardware temperatures should vary less than they do on MER.)

Rover Avionics. The avionics are responsible for the command, data handling, power regulation, power distribution, and pyro functions for all mission phases (including cruise and EDL). Rover avionics serve these functions during the surface phase. At the heart of the avionics are the Rover Compute Elements (RCEs), redundant computers operated one at a time, with the spare held in cold backup (except during EDL where the redundant computer acts as a hot backup). Each RCE contains a central processor (a radiation hardened PowerPC 750 architecture system) communicating with peripheral devices using other cards connected on a compact peripheral component interconnect (cPCI) backplane interface and providing central memory storage for mission data and telemetry of 32 gigabits via a non-volatile memory/camera (NVMCAM) card. In addition to the RCEs, power switching and analog input/output are provided by the redundant Rover power and analog modules (RPAMs) connected to the RCEs via MIL-STD-1553 [12] data bus connection^{16,17}.

Flight software. The software in the main computer of the rover executes a control loop that monitors the status of the flight system during all phases, checks for the presence of commands

¹⁶ One hardware element of the avionics that must remain powered on the surface is the MSL remote engineering unit (MREU) in the RPAM. The MREU in each RPAM is redundantly connected to the two Electra Lite transponders (ELTs). An ELT may receive a “hail” from an Orbiter requesting the rover to wake up.

¹⁷ MIL-STD 1553 is a standard published by the United States Department of Defense that defines the mechanical, electrical and functional characteristics of a serial data bus.

to execute, maintains a buffer of telemetry for transmission, performs communication functions, and checks the overall health of the spacecraft. Central control of the entire flight system is under control of the flight software running in the RCE (the same architecture as was used for the MER mission). On the surface, activities such as imaging, driving, or instrument operations are performed under commands transmitted in a command sequence to the rover from the flight team. The rover generates constant engineering, housekeeping, and analysis (EH&A) telemetry and episodic event reports (EVRs) that are stored for eventual transmission.

It is possible that other activities will generate or be affected by radio frequency interference while the Rover is communicating. The flight software will ensure that incompatible activities do not run during a communication window.

Communications behavior. The rover telecom subsystem is used to send and receive command sequences, data, telemetry, and flight-software updates. The behavior of the telecom subsystem is controlled by the interaction of flight software, ground sequences, and a set of parameter tables that define the state of telecom hardware and that control the settings and timing of telecommunications windows. Communication windows will be sequenced whenever it is desired to communicate with the rover. Windows must fit within scheduled DSN availability and expected relay orbiter passes. A window is defined as an interval of time that contains all the activities directly associated with preparation and execution of a communication session. During surface operations, the ground system will coordinate with the DSN and the MRO project to determine a set of desired communication windows.

Communication information is stored in two tables on the rover: the primary table and the high-priority table. The primary table can hold as many as 256 communication windows and is used for standard operations. A high-priority table can be used in the event of Rover anomaly resolution or for other purposes. When communication windows are loaded into the high-priority table, they take precedence over any windows defined in the primary table. This allows new communication windows to effectively replace selected onboard windows, should the need arise, without affecting the entire set of previously planned communication events.

1.7.2 Payload (Science Instruments)

The rover carries the largest science payload suite to date, with instruments sponsored by NASA and others contributed by international partners. The following, also from the Mission Plan [11], is a summary/listing of the MSL science instrumentation.

The instruments are roughly divided into four categories:

- 1) Remote Sensing (2):
 - Mastcam: Multi-spectral, stereo imaging, as well as video.
 - ChemCam: (Chemistry and Mineralogy) Remote spectroscopy of rocks and soils from laser ablation; remote microscopic imagery.
- 2) In-Situ (2):
 - Mars Hand Lens Imager (MAHLI): Color microscopic imager.
 - Alpha-Particle X-ray Spectrometer (APXS): spectroscopy of soil and rocks using X-ray fluorescence and particle-induced X-ray emission.

- 3) Analytical (2):
- CheMin: Mineralogical analysis of acquired samples of rock and soil using X-ray diffraction.
 - Sample Analysis at Mars (SAM): Chemical and isotopic analysis of acquired samples of rock, soil, or atmosphere (including organics) using a mass spectrometer, gas chromatographs, and a tunable laser spectrometer.
- 4) Environmental (4):
- Radiation Assessment Detector (RAD): Detect and measure natural high-energy radiation.
 - Mars Descent Imager (MARDI): High-resolution color video of descent.
 - Dynamic Albedo of Neutrons (DAN): Detect and analyze hydrogen in the near-subsurface of Mars.
 - Rover Environmental Monitoring Station (REMS): To monitor the meteorology and ultraviolet (UV) environment near the rover.

2 Telecom Subsystem Overview

During the mission phases of initial acquisition after launch, the X-band will be used for TCMs (as described in the MSL Telecom Functional Design Document . [13]), all cruise and some EDL, and surface communications.

Figure 2-1 is a block diagram of the X-band telecom subsystem. Table 2-1 contains definitions of the abbreviations and acronyms in the figure.

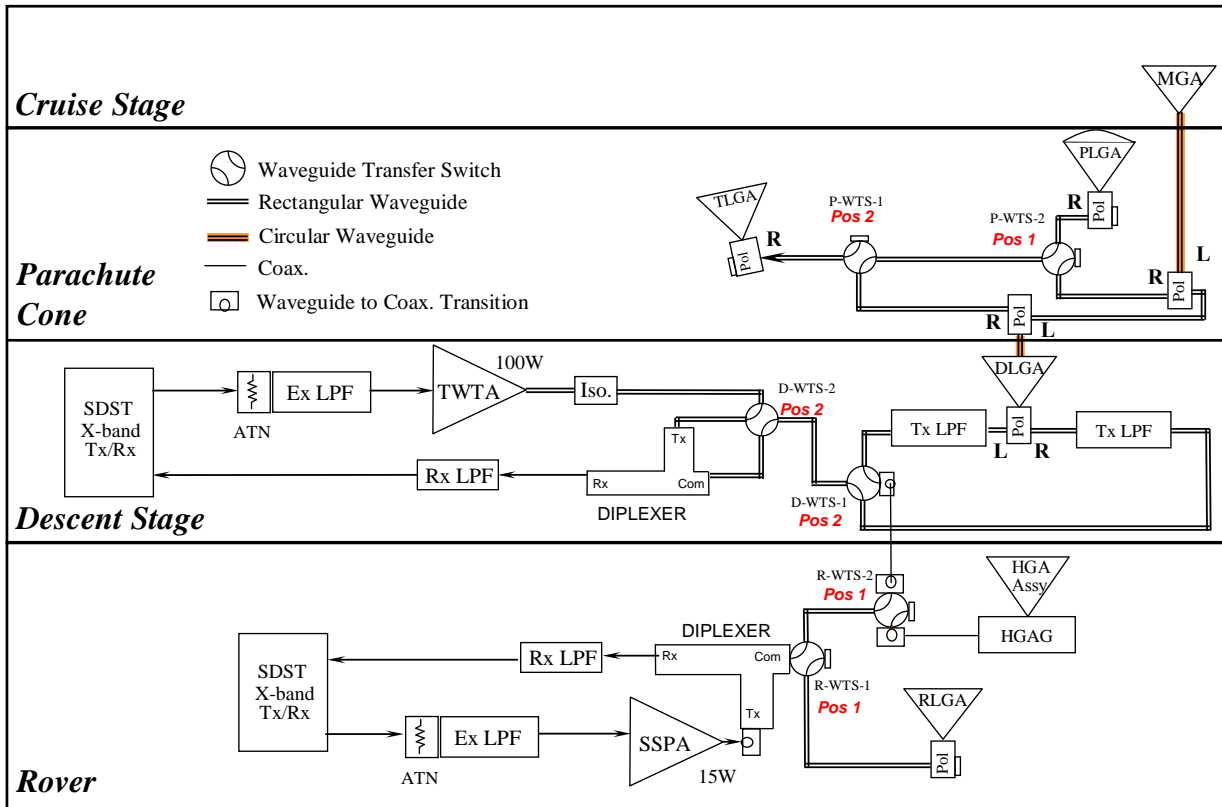


Figure 2-1. MSL X-band block diagram.

Table 2-1. Acronyms and abbreviations in X-band telecom block diagram.

Term	Definition	Term	Definition	Term	Definition
Assy	Assembly	L	Left circular polarization	RLGA	Rover low gain antenna
ATN	Attenuator	LPF	Low pass filter	SDST	Small deep space transponder
Com	Common	MGA	Medium gain antenna	SSPA	Solid state power amplifier
D-	Descent	Pol	Polarizer	TLGA	Tilted low gain antenna
Ex	Exciter	P-	Parachute	TWTA	Traveling wave tube amplifier
HGA	High gain antenna	R-	Rover	Tx	Transmit
HGA G	High gain antenna gimbal	R	Right circular polarization	W	Watt
Iso	Isolator	Rx	Receive	WTS	Waveguide transfer switch

All stages have X-band antennas, and there is active X-band telecom equipment on two stages (the descent stage and the rover). The red **Pos1** and **Pos2** in Figure 2-1 define the WTS positions at launch. The four layers in the diagram are called slices.

2.1 Telecom for Launch, Cruise, and into EDL

The descent stage and the rover each have a small deep space transponder (SDST) [14] and a transmitter (a 100-W output TWTA on the descent stage and a 15 W output SSPA on the rover). During cruise, the nominal path is to use the radio on the descent stage; there is, however, a backup switching arrangement where RF signals can be routed to and from the rover. Being able to use either the TWTA or the SSPA (albeit at a significantly lower link performance, with the extra line losses and the reduced power from the SSPA) provides functional redundancy during cruise.

The MGA and PLGA antennas used during cruise and the first part of EDL are shown in the top two slices of Figure 2-1 The MGA provides greater gain and a smaller beamwidth; the PLGA provides a larger beamwidth, but less gain. At any given time, one antenna is selected; the selected antenna it receives uplink from the DSN and transmits downlink to the DSN.

During the EDL phase, the PLGA, the TLGA, and the DLGA are the X-Band antennas used; EDL is downlink only. At the atmospheric entry interface, the diplexer in the descent stage is bypassed to avoid critical-pressure, high-power coronal discharge. This has an added advantage of decreasing the transmit line loss somewhat.

When EDL starts, CSS occurs, and the top slice (the cruise stage) is ejected along with the MGA.

During the banking maneuvers (Figure 1-18), the TLGA provides the best downlink to the Earth. The original plan was to switch back to the PLGA just before parachute deployment, after the so-called “Straighten Up and Fly Right” (SUFR) maneuver, when the $-Z$ axis and the antivelocety vector are more co-aligned. However, because there is a good chance the parachute sabot will

impact the PLGA at parachute deployment, it was decided to stay on the TLGA to maximize the likelihood of continuing the DTE link during parachute descent.

When backshell separation occurs, the second slice (parachute cone) breaks away, taking the TLGA with it. For the remainder of the powered descent, we use the DLGA. Note that there is no switching needed to be on the DLGA. Because the DLGA serves as part of the waveguide run up to the parachute cone hardware, the DLGA naturally begins radiating when the backshell is ejected.

The powered descent vehicle phase concludes with rover separation and sky-crane operations. Upon touchdown, the bridle is cut and the descent stage flies away. At Rover separation, we lose the descent stage SDST, the TWTA, and the DLGA. However, the separated descent stage SDST and TWTA continue to transmit through the DLGA until the stage crashes on the surface at the end of the “fly-away phase.” The rover X-band system (the rover SDST and SSPA) is not scheduled to transmit until after the end of EDL.

The UHF block diagram is shown in Figure 2-2.

Table 2-2 defines the terms used in the figure.

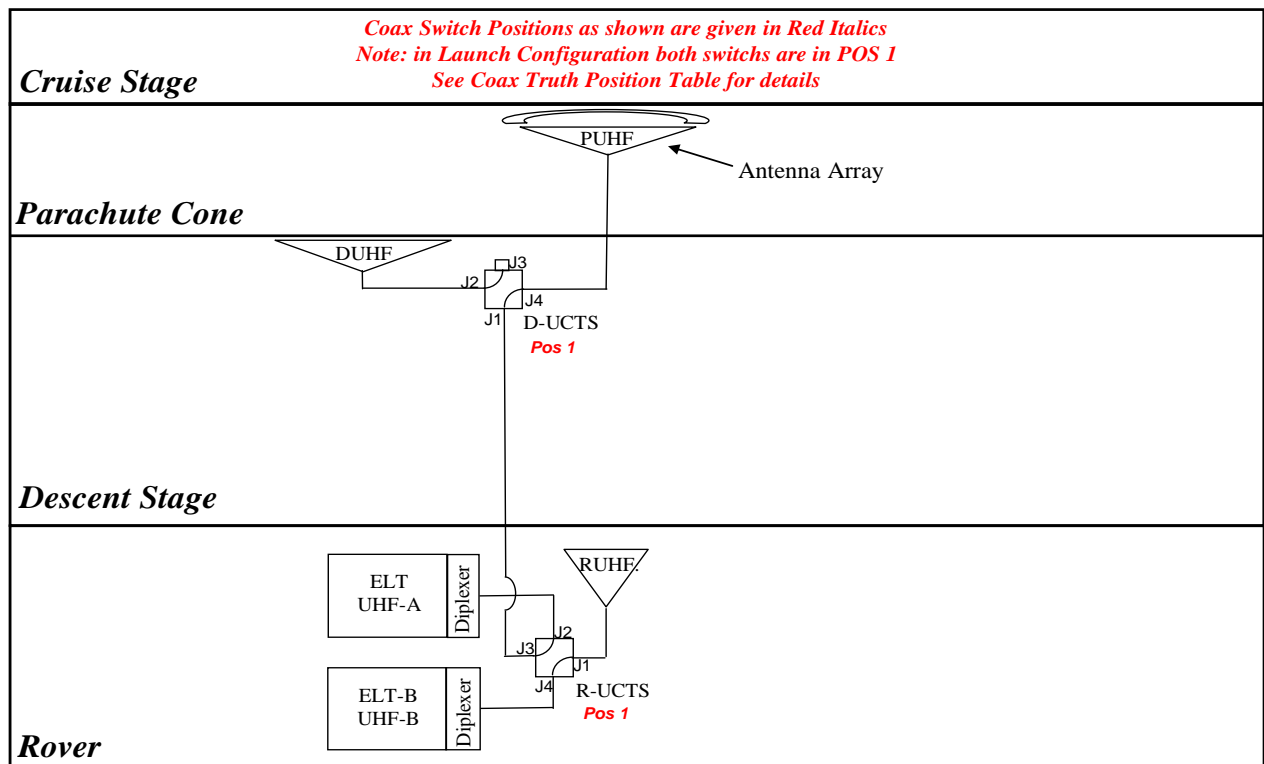


Figure 2-2. UHF block diagram.

Table 2-2. Acronyms and abbreviations in UHF telecom block diagram.

Term	Definition	Term	Definition	Term	Definition
DUHF	Descent UHF antenna	J-	Jack (connector)	R-	Rover
D-	Descent	Pos	Position	RUHF	Rover UHF antenna
ELT	Electra Lite transponder	PUHF	Parachute UHF antenna	UCTS	UHF coaxial transfer switch

The UHF radio is the Electra Lite Transponder (ELT), which is derived from the Electra UHF transponder (EUT) used on the MRO. Except for checkouts during cruise, the first use of the UHF is in the EDL phase, after cruise stage separation.

During EDL, all three UHF antennas are used: the PUHF from CSS until backshell deployment, the DUHF during powered descent, and the RUHF during and after the sky-crane stage (for the period from post landing + 1 minute through end of the surface mission).

The descent UHF coaxial transfer switch (D-UTCS) selects between the DUHF and the PUHF antennas. The rover UHF coaxial transfer switch (R-UTCS) selects between the Rover UHF antenna (RUHF) and either of the descent antennas.

During surface operations, UHF is the primary mode of returning large volumes of data to the Earth (via orbiter relay).

This complex series of EDL telecom events (involving multiple successive configurations of both X-band and UHF) is shown in Figure 2-3. Refer back to Figure 1-16, Figure 1-17, and Figure 1-19 for pictorials of the EDL events at the spacecraft level.

The DSDST is the SDST on the descent stage.

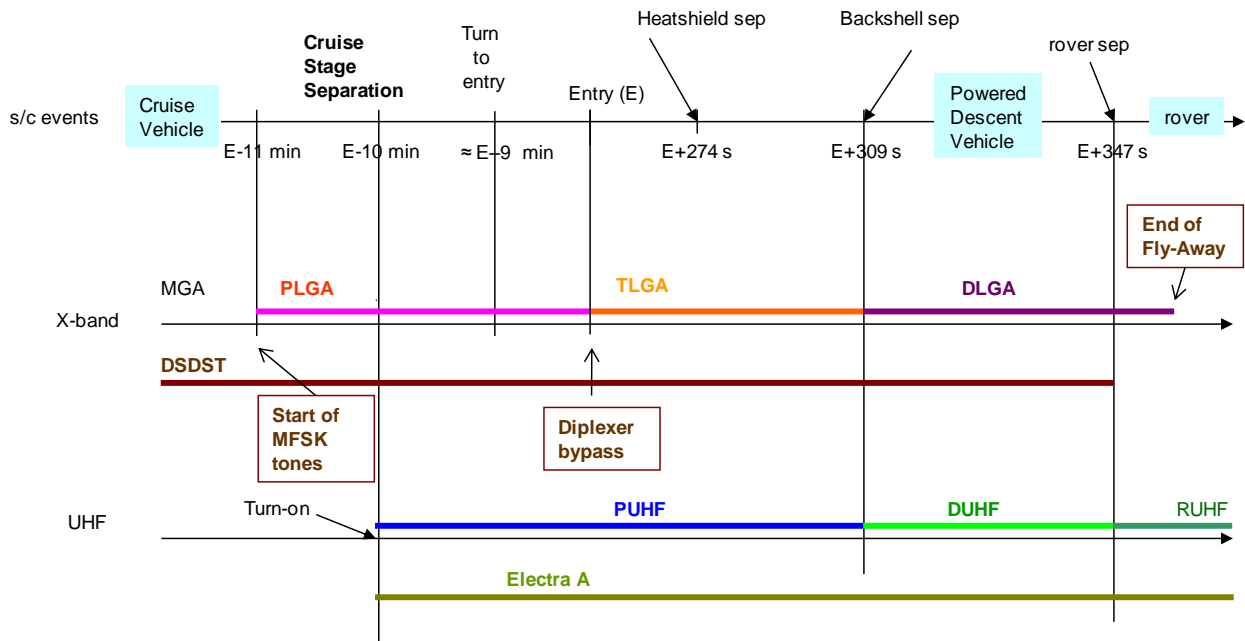


Figure 2-3. X-band and UHF sequence during EDL.

2.2 Surface Operations

The surface telecom system uses three antennas: two for X-band DTE/DFE and a UHF antenna for relay to an orbiting asset. Figure 1-31 shows the X-band and UHF antennas mounted on the rover deck.

The X-band antennas are the Rover low-gain antenna (RLGA) and the high-gain antenna (HGA). The HGA is used for either DTE commanding or DFE telemetry, while the RLGA is used primarily for low-rate (contingency) DFE commanding. The downlink signal level achievable using the RLGA is too low for all but special DTE applications.

The HGA sits on a 2 degree-of-freedom gimbal, with 5-deg system pointing accuracy (including rover attitude knowledge), and is 0.28 m in diameter. Table 2-4 shows that the downlink gain is about 4 dB lower and the uplink gain about 3 dB lower, at 5 deg off boresight.

2.2.1 X-Band

2.2.1.1 Downlink (DTE)

The SSPA transmits 15 W and receives its RF input signal from the rover SDST. The basic telecom requirement for surface operations on the HGA is to provide a downlink capability of at least at 160 bits per second (bps) to a 34-m station or 800 bps to a 70-m station.

2.2.1.2 Uplink (DFE)

Current DFE planning is to use the HGA for the typical daily uplink of commands, taking approximately 15 minutes for a total volume of 225 kilobits (kb). Typical uplink rates to the HGA will be 1 kbps or 2 kbps. The 15 minutes provides some margin for possible station transmitter delays and for packaging of commands into groups.

In safe mode, commands from the Earth will be received via the RLGA. The RLGA has a broad pattern and does not have pointing capability like the HGA. The RLGA does, however, have the capability for uplink (command) communications (15 bits per second at max range).

2.2.2 UHF

The primary data path for surface operations is via the UHF relay system, using the Mars orbiting assets (MRO or Odyssey¹⁸). MSL has baselined the primary relay communications to be via MRO, with two passes a day primarily used to return data from the surface.

Communications through Odyssey could also be planned for additional data return or if MRO was unavailable, as long as there was DSN time for data return from Odyssey and sufficient energy to support UHF operations with Odyssey during the sol.

The UHF subsystem has a pair of redundant Electra-Lite radios. The Electra-Lite radio is a smaller version of the Electra radio flown on MRO. The MSL Electra-Lite/MRO Electra link can function using an adaptive data rate scheme; that is, the data rate can automatically adjust to variations in signal strength due to antenna patterns, angles, and proximity between MRO and MSL throughout the overflight. In this mode of operations, it is the MRO radio that controls the

¹⁸ The Mars Explorer (MEX) orbiter is also compatible with the Electra lite radio, may also be available as a redundant relay path. MEX was launched in 2003 by the European Space Agency.

return data rate, based on its own receiver power telemetry. The MRO radio commands the lander radio to change data rates on the fly. Forward rates will not be adjusted in this scheme. Section 2.4.1 includes UHF frame and coding options.

A single quad-helix antenna designed especially for MSL, the RUHF, is mounted to the rover deck and used with either redundant radio.

The MSL/MRO relay link can also be used in a safe mode. The Electra-Lite radio can communicate a wake-up signal (via low-voltage differential signaling [LVDS]) to the rover avionics upon hearing a “hail” forward link¹⁹ from MRO. This is most useful in a contingency mode, where the rover is effectively asleep with the ELT waiting for a communications possibility. The MSL mission intends to rely on this function as a fault response mode only. For example, a fault response would occur if the spacecraft lost its clock timing and did not know when relay passes were to occur.

The UHF functionality of the Odyssey and MEX orbiters is similar to that of the MRO UHF. However, these radios do not have the adaptive data rate capability.

In some cases, an X-band DTE/DFE link of reasonable duration is not possible, particularly if the Earth-visibility is limited (for example, winter seasons if the MSL landing site is at an extreme north or south latitude). A forward UHF link could be used in these cases to command the rover. Commanding via Odyssey and MRO has been demonstrated with the MER and Phoenix missions. MER was launched in 2003, with the primary Mars surface mission in 2004 and extended surface operations continuing with both rovers. Phoenix was launched in 2007, and the landed mission extended from May to November 2008.

2.3 X-Band Flight Subsystem Description

2.3.1 X-Band Interfaces with MSL Control and Data Systems

Figure 2-4 shows the data and control interfaces of the transponders. Some interfaces, as defined below, are the same for UHF and X-band transponders.

The main interface for all data transfer functions to both the SDST radios is the MSAP²⁰ delivered Telecommunications Interface (MTIF) card, which is the MSL telecommunications interface between the Avionics subsystem, the SDST, and Electra Lite. The data transfer functions, include:

- Turbo codes that are the baseline for the DTE downlink. The codes have rates of 1/2, 1/3, and 1/6, and they have frame sizes of small (1784 bits) and large (8920 bits).

¹⁹ Forward and return links are used for communications between an orbiter and a lander. The forward link is from an orbiter to a lander. A return link is from a lander to an orbiter. Completing the communications path between the Earth and the orbiter are the DSN uplink and downlink.

²⁰ MSAP is the multi mission system architectural platform. MSAP is a JPL program supporting multiple projects that uses a RAD 750 computer for subsystem development. The goal of the MSAP Program itself is to develop and demonstrate reusable and evolvable core architecture for JPL in-house missions.

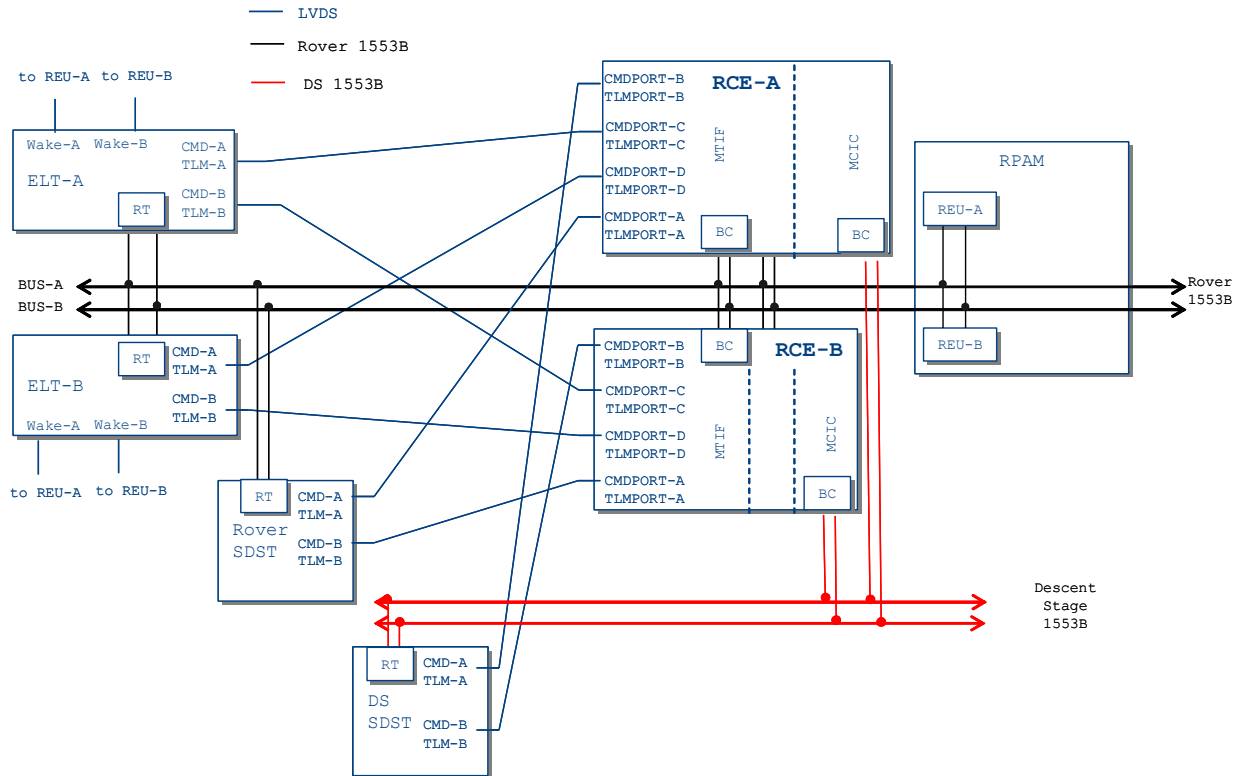


Figure 2-4. Telecom LVDS and 1553B interfaces.

- Reed Solomon encoding (interleave depth 1 and 5) that can be used for the DTE downlink (in concatenation with convolutional $[7, 1/2]$ coding²¹ that is performed by the SDST).

The MTIF card controls the SDST downlink data rate by flowing data to the SDST at the desired downlink rate. The UHF return link data rate is controlled by the UHF radio (Electra-Lite) through the Prox-1 protocol, not by the MTIF (see section 2.4).

Both ELT and SDST provide redundant uplink (command) and downlink (telemetry) low-voltage differential signaling (LVDS) high-speed digital data transfer interfaces, which are cross-strapped to the MTIF (each MTIF has four command/telemetry ports). The active downlink port on the telecom side must be selected via a serial data bus Mil Std 1553 serial bus command [12]. Both uplink ports in ELT and SDST are always active.

The rover bus controller (BC) on the MTIF controls the primary 1553 bus to which the rover SDST is connected via the remote terminal (RT). The BC for the Descent Stage SDST is part of the Motor Controller Interface Card (MCIC). Both the MTIF and the MCIC reside in the rover Computer Element (RCE). Data flows include command (CMD) and telemetry (TLM).

²¹ In telecommunication, a convolutional code is a type of error-correcting code in which (a) each m -bit information symbol (each m -bit string) to be encoded is transformed into an n -bit symbol, where m/n is the code rate ($n \geq m$) and (b) the transformation is a function of the last k information symbols, where k is the constraint length of the code (from http://en.wikipedia.org/wiki/Convolutional_code) For MSL, the code parameter values are $k = 7$, $m = 1$, and $n = 2$; the resulting code is abbreviated $(7, 1/2)$.

The “wake” in Figure 2-4 refers to the ELT receiving a “hail” from a Mars orbiter requesting the rover to wake up. The wake signaling is from the ELT to the remote electronics unit (REU) of the RPAM in the avionics subsystem. The RPAM must stay powered at all times to receive the wake signal.

2.3.2 X-Band Key Hardware Components

The telecom component descriptions in the following paragraphs are organized by the stages in the Figure 1-3 graphic. The telecom block diagram (Figure 2-1) shows the four spacecraft stages (“slices”) that contain the telecom subsystem elements. These four are Cruise, Backshell or Parachute Cone, Descent, and Rover. The heat shield stage contains no telecom components.

2.3.2.1 Cruise Stage X-Band Telecom Components

2.3.2.1.1 Medium-gain Antenna

The MGA, called out in Figure 1-2., is used for mid- to late-cruise communications. The MGA is a built-to-print of the MER MGA, fed by a septum polarizer for circular polarization (CP) operation. The MSL MGA operates either right-hand or left-hand circularly polarization (RCP or LCP), depending on which side of the polarizer is connected to the receiver or transmitter²².

The MGA, which is attached on the cruise stage, will separate from the rest of the X-Band telecom subsystem at Cruise Stage Separation. In the top left drawing of Figure 1-2, the light blue surface on top of the cruise stage is the annulus-shaped solar array with the MGA at its center.

Table 2-3 states some of the RF characteristics of the MGA.

Table 2-3. MGA RF characteristics.

Parameter	Value
Receive frequency, MHz	7150.8 (DSN channel 4)
Transmit frequency, MHz	8401.4 (DSN channel 4)
Gain, boresight, dB	18.1 ± 0.4 receive 19.2 ± 0.4 transmit
Polarization	RCP or LCP
3 dB-beamwidth, deg	± 10.3 receive ± 9.3 transmit
Axial Ratio, on boresight, dB	1.01 receive; 0.27 transmit
Axial Ratio, 20 deg off boresight, dB	6.29 receive; 7.53 transmit
Design	RF conical

²² Right-circular polarization (RCP) refers to an electromagnetic wave that propagates such that the tip of the electric field appears from the source to describe a circle in the clockwise direction. Left-circular polarization is the opposite; the tip of the electric field is seen from the source as describing a circle in the counterclockwise direction. A polarizer converts the RF beam traveling through a waveguide to an electromagnetic wave of a specific polarization. In this case the septum polarizer converts a linearly polarized wave in the waveguide run to a circularly polarized wave to be transmitted by the antenna.

Figure 2-5. and Figure 2-6 provide uplink and downlink patterns of gain as a function of angle from MGA boresight. These are based on measurements on a MER mock-up. The gain is down 3 dB from its peak at about 10 deg from boresight, as compared with about 5 deg from boresight for the rover HGA. “Beamwidth,” commonly defined in terms of a total angular range on both sides of boresight, is double the above numbers.

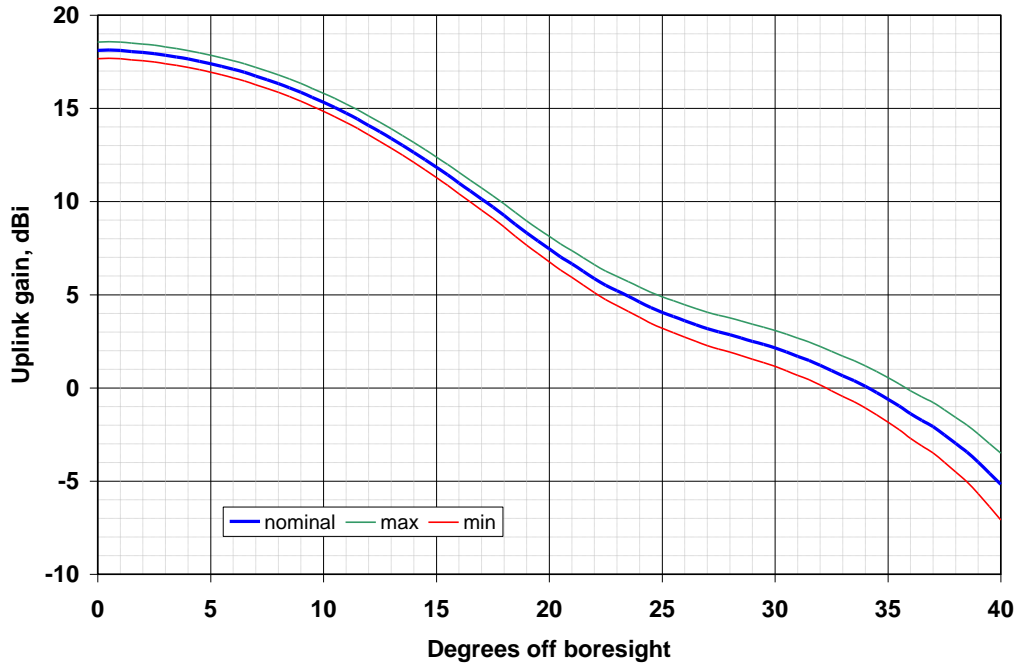


Figure 2-5. MGA uplink gain.

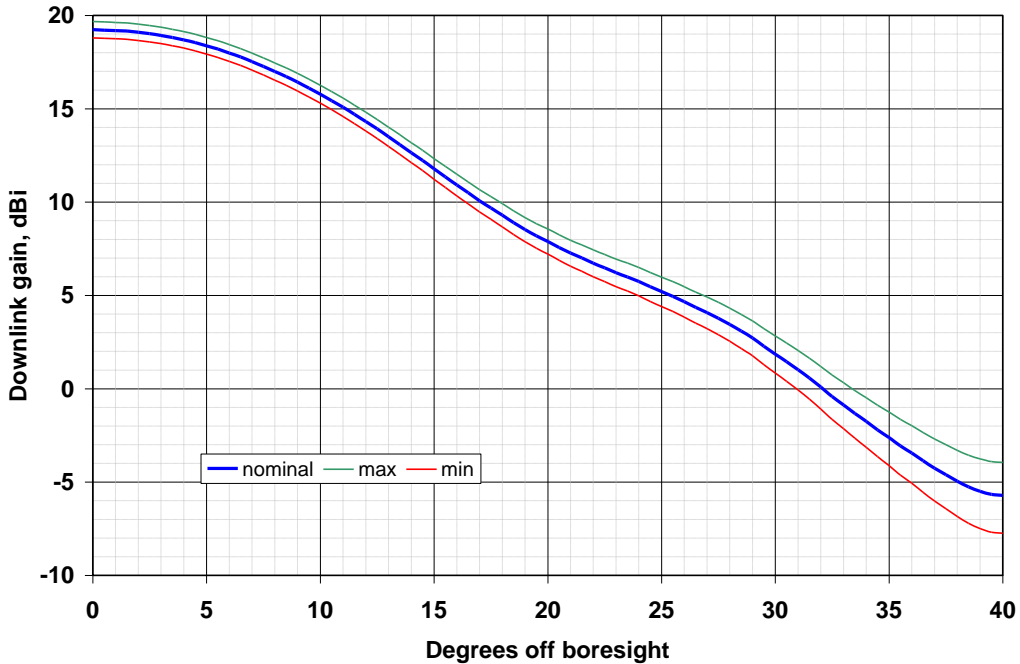


Figure 2-6. MGA downlink gain.

2.3.2.2 Parachute Cone X-Band Telecom Components

The telecom block diagram (Figure 2-1) shows the telecom components on the Parachute Cone, as well as on three other stages. Note that names beginning with P refer to parachute, those with D to descent, and with R to rover.

2.3.2.2.1 Waveguide Transfer Switches (P-WTS-1 and P-WTS-2)

All switching between X-band transponders, power amplifiers, and antennas is with waveguide transfer switches (WTS). The switches are used to connect transmit and receive functions to the proper antennas

On the parachute cone, P-WTS-1 selects the TLGA and P-WTS-2 selects between PLGA and MGA.

2.3.2.2.2 Parachute Low-Gain Antenna

Figure 2-7 shows where the PLGA and the TLGA are installed.

The PLGA is used for early cruise communications and fault responses. It also used during EDL communications. The PLGA boresight is aligned along the $-Z$ axis of the spacecraft, as shown in Figure 1-3.

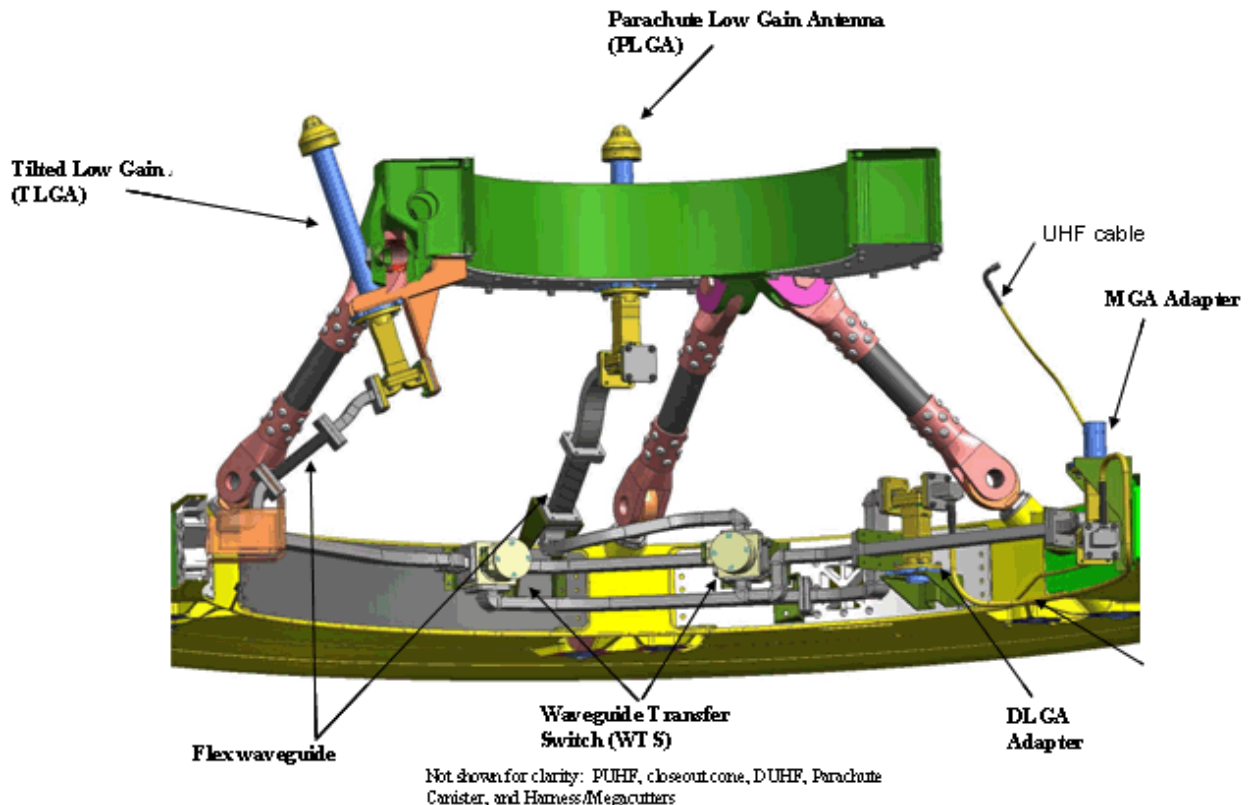


Figure 2-7. Locations of the low-gain antennas.

The design of all MSL X-band low-gain antennas (except for the DLGA), TLGA, and RLGA are each an open-ended waveguide with chokes and parasitic drooping

dipoles. However, the proximity effects of spacecraft components near each LGA result in their individual patterns being quite different from one another.

The parasitic dipoles have the effect of broadening the pattern, as compared to the MER design. Figure 2-8 and Figure 2-9 show, respectively, the uplink and downlink patterns of the PLGA (measured on a spacecraft mock-up). Both the maximum gain over all roll angles (red curve) and the minimum gain (blue) are shown. As the spacecraft spins, the peak-to-peak link performance will vary by at least several decibels roughly every 15 seconds.

For the very early launch dates with a type II trajectory, antenna angles are as large as 120 deg. For these cases, communications are only possible for the first few hours after trans-Mars injection, when the range loss has not yet become too high.

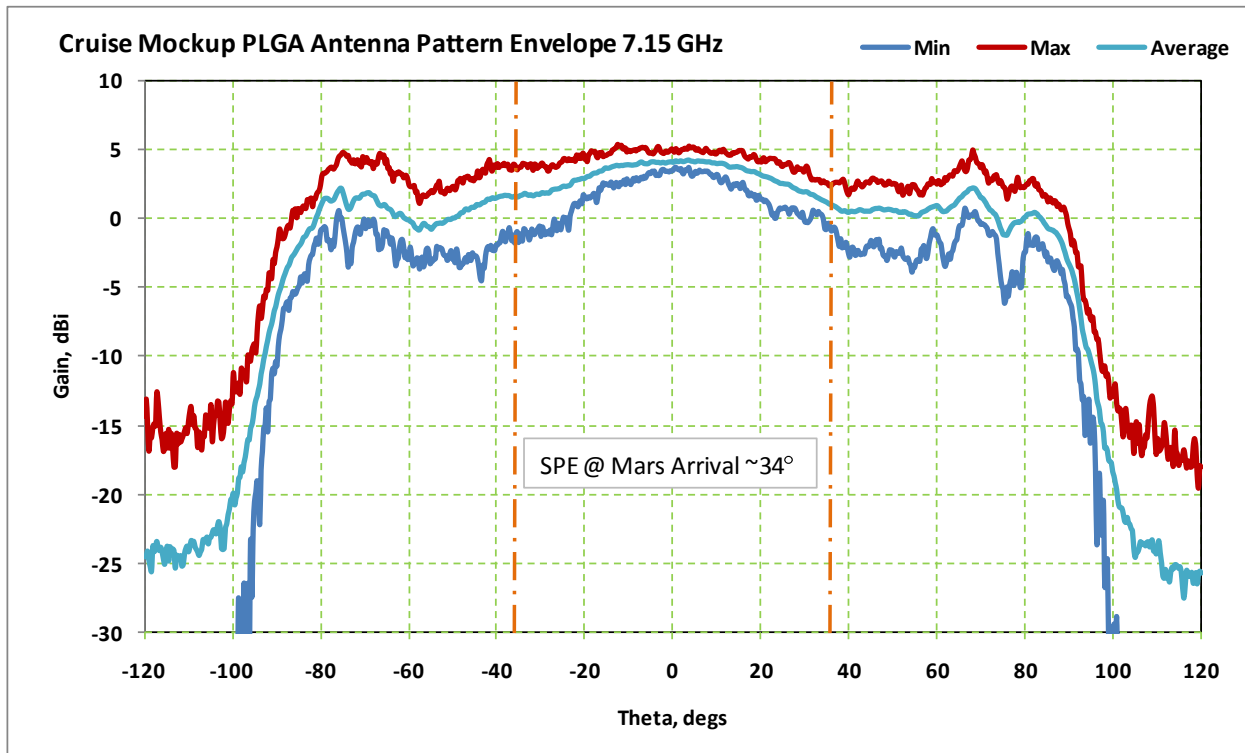


Figure 2-8. PLGA X-Band uplink gain with spacecraft mock-up, RCP, 4/30/09.

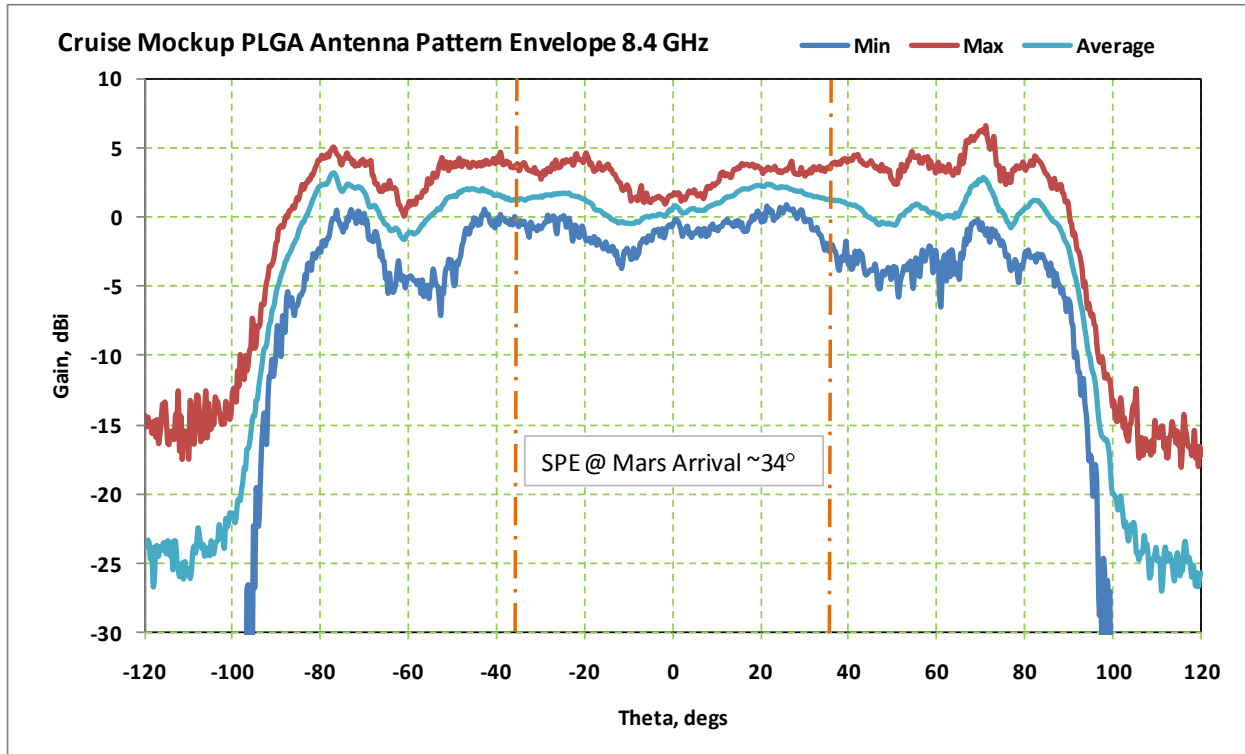


Figure 2-9. PLGA X-Band downlink gain with spacecraft mock-up, RCP, 4/17/09.

2.3.2.2.3 Tilted Low-Gain Antenna

The TLGA has the same design as the PLGA; one difference, however is that the TLGA’s boresight is ‘tilted’ with respect to the spacecraft –Z axis, by 17.5 deg, which will bring it close to the average anti-velocity vector direction during post entry banking maneuvers. This minimizes the span of Earth-to-boresight angles and, therefore, the link-signal level variation during the critical hypersonic and banking phases. Figure 1-18 illustrates the geometry involved for the EDL maneuvers when the TLGA is in use.

2.3.2.3 Descent Stage X-Band Telecom Components

The telecom block diagram (Figure 2-1) shows the telecom components on the Descent stage, as well as on three other stages. Note that names beginning with D- refer to “descent.”

The descent stage (DS) contains two active telecom components, the D-SDST and the TWTA, as well as the DLGA. In addition, there are several components involved in routing the high-powered TWTA RF output and the much weaker RF input destined for the SDST receiver.

Figure 2-10 shows the overall layout of the DS telecom components. Most are on a telecom plate, shown in a contrasting color and detailed in Figure 2-11. Both the TWTA (on the far side of the plate) and the TWTA’s electronic power conditioner (EPC) are planned to be powered on throughout cruise. These items dissipate relatively large amounts of spacecraft power as heat that is carried away by the cruise stage thermal control system (the heat rejection system [HRS]).

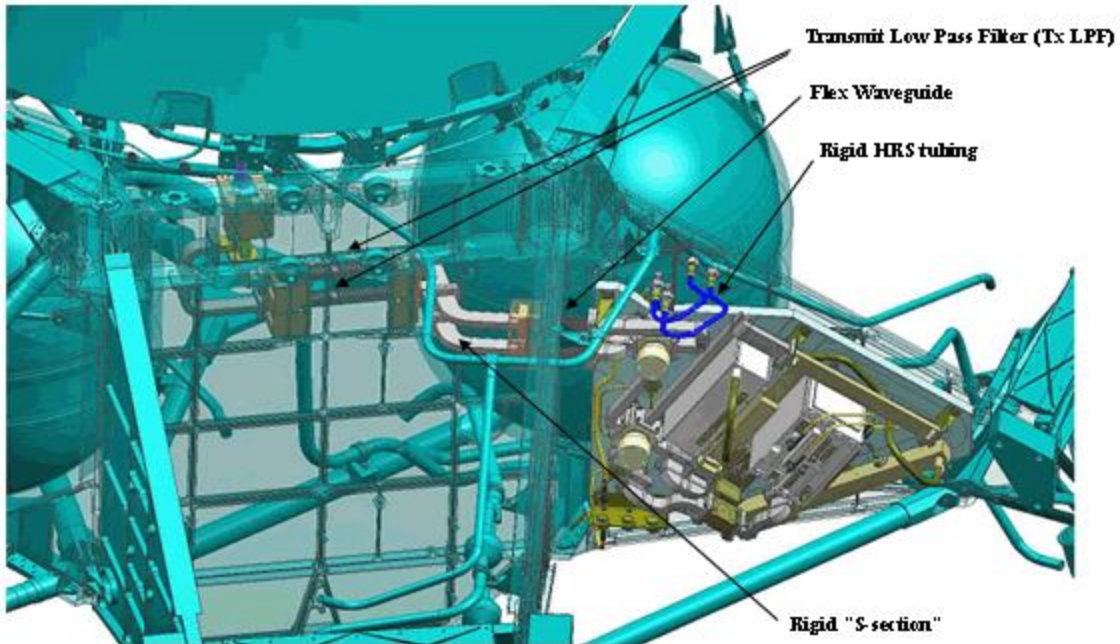


Figure 2-10. Descent Stage X-band layout.

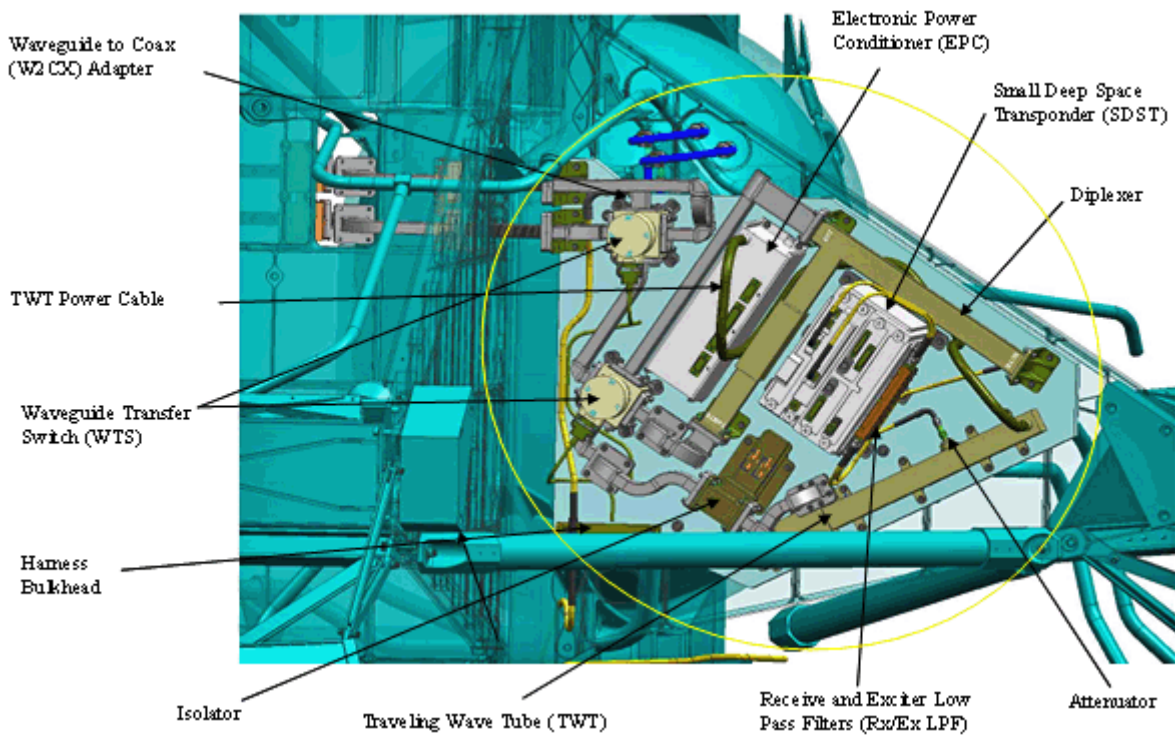


Figure 2-11. Telecom plate assembly.

2.3.2.3.1 Descent Low-Gain Antenna

The design of the descent low-gain antenna (DLGA) (Figure 2-12) is an open-ended waveguide with chokes. The relatively broad pattern of the DLGA will suffer significant distortion from

interaction with the surrounding structure of the descent stage. A study²³ of this was done using the General Reflector Antenna Scatter Program (GRASP) antenna scattering software to envelope the range of pattern variation. Figure 2-13 shows the GRASP model used to generate the pattern.

The actual view angles for DTE during the powered descent phase can vary widely, depending on the landing site chosen and descent geometry (such as the large tilt during the divert maneuver). Far off boresight view angles are not impossible. For some trajectories, the Earth is quite close to the horizon at touchdown and, therefore, the antenna pattern near 90 deg from boresight is of interest.

The resultant pattern as shown in Figure 2-14 shows that the variation is worst near the 75-deg off-boresight angle.

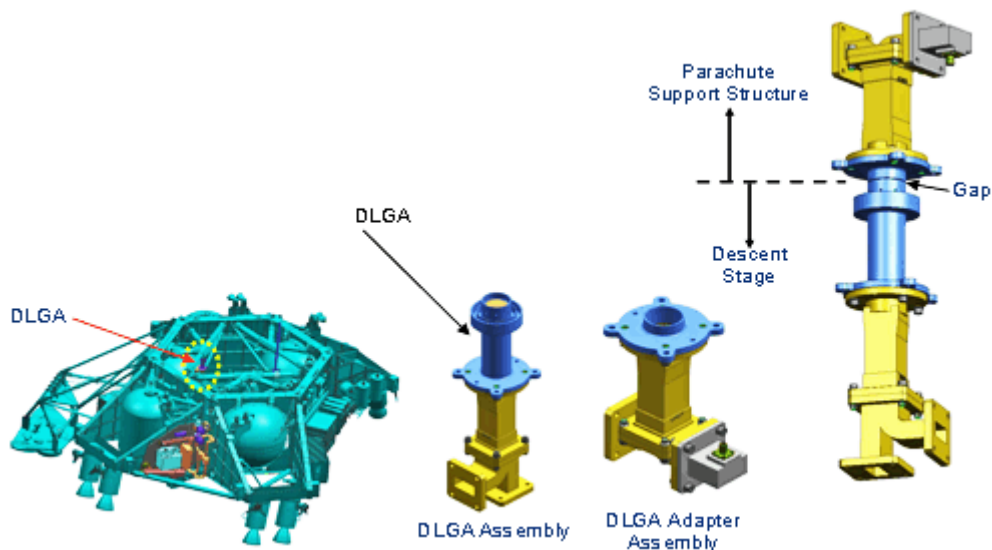


Figure 2-12. DLGA and DLGA adapter overview.

²³ “DLGA on the Descent Stage: 8.400 GHz”, Dan Hoppe, April 21, 2008 (internal MSL project document) GRASP is an acronym for general reflector antenna scatter program (http://www.ticra.com/script/site/page.asp?artid=33&cat_id=30)

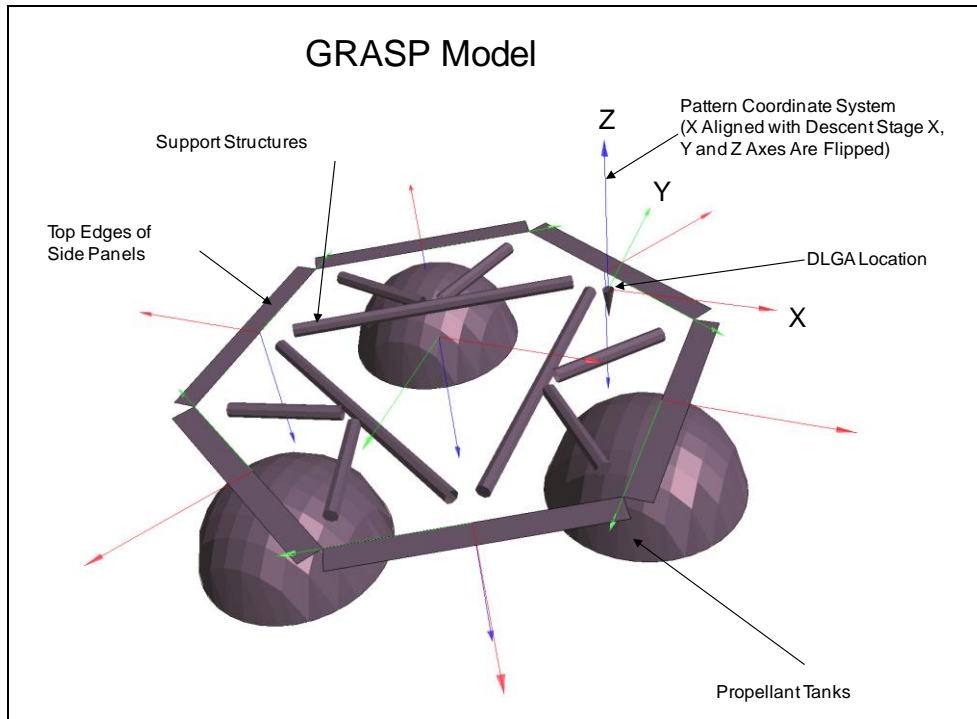


Figure 2-13. GRASP model for DLGA scattering study.

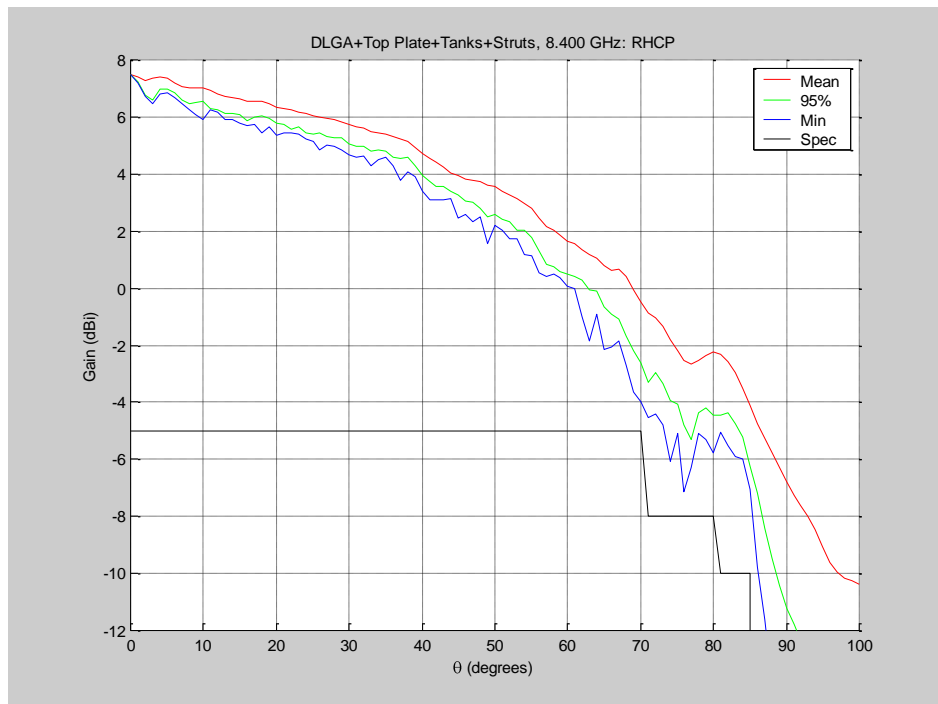


Figure 2-14. MSL DLGA downlink pattern modeled from GRASP model.

2.3.2.3.2 Descent Stage Waveguide Transfer Switches

D-WTS-1 selects one of two polarization signal paths: RCP and LCP.

D-WTS-2 is a ‘diplexer-bypass’ switch, to be used for EDL. With the switch in the bypass mode, the diplexer is bypassed and there is no X-band uplink-receive capability. The bypass mode avoids the problem of the diplexer suffering coronal breakdown for 100-W RF from the TWTA at critical pressure encountered during passage through Mars’ atmosphere during EDL.

2.3.2.3.3 *Traveling Wave Tube Amplifier*

The TWTA has two components: the traveling wave tube (TWT) and the electronic power conditioner (EPC) that provides the voltages required by the tube. The TWTA is of MRO heritage.

The TWT must provide at least 100 W of RF output to support X-band communications and radiometric requirements during cruise and during EDL until rover separation. The MSL flight unit has RF output of 104.7 W, which is 50.2 dBm (decibels referenced to 1 milliwatt).

As with other deep-space TWTAs, when the spacecraft bus voltage is switched to the EPC, there is a delay (between 200 and 240 s) before the EPC applies high voltage to the TWT. During this period, the On/Standby Mode control signal is overridden to prevent RF output.

Because the TWTA operates with high voltages and high power levels, it has three kinds of internal protection:

- **Helix Current Trip:** The TWTA trips when the TWT body (helix) current exceeds safe values (set by the TWT manufacturer). If a trip occurs, the TWTA initiates an automatic restart function (ARF) sequence. The ARF turns off the electron beam in the TWT. Within 50 ms, the electron beam comes back on and the TWTA returns to nominal operations; if a second trip occurs within 180 seconds, the TWTA will go to the start-up sequence described above. During the shutdown period the TWTA indicates its status as Body Current Trip.
- **Bus Undervoltage Trip:** This will happen when the spacecraft bus voltage at the EPC input goes below 20.5 V \pm 0.5 V. During the shutdown, period the TWTA indicates status as Under Voltage Trip. The TWTA initiates a start-up sequence when the bus input voltage rises above 21.5 V.
- **Converter Current Trip:** The TWTA trips when the high-voltage converter exceeds a safe current value. The TWTA initiates an ARF as specified above

2.3.2.3.4 *X-Band Diplexer*

The design of the diplexers in the descent stage and the rover is the same. They provide for the separation of the receive frequency from the antenna and the transmit frequency to the antenna.

The power handing capability of the diplexer at critical pressure is insufficient for use with the TWTA during EDL. Breakdown occurred at 85 W in test, lower than the 100-W nominal output. The bypass design avoids this problem during descent into the atmosphere.

2.3.2.3.5 *Transmit Low-Pass Filter*

There are two transmit low pass filters (Tx LPF), 2 branches out of D-WTS-1, one for each polarization.

The Tx LPF is a waveguide filter and has two purposes:

- For near-Earth operations, the filter reduces out-of-band emissions from the TWTA. This function is similar to MRO, which also has a 100-W TWTA of the same design.
- During EDL, the filter reduces TWTA emissions into the landing radar, especially in three frequency bands of 16.7 to 17 GHz, 25.2 to 25.5 GHz, and 33.4 to 34 GHz. Tests with the LPF early in 2009 verified that radar operation will not be degraded by TWTA emissions into its sensitive frequency bands.

Table 2-4 documents the RF characteristics of the transmit LPF.

Table 2-4. Transmit low-pass filter RF characteristics.

Parameter	Value
Receive passband* Insertion loss	0.2 dB at 7.1-7.2 GHz
Transmit passband Insertion Loss	0.2 dB at 8.35 to 8.5 GHz
Transmit attenuation of 2 nd harmonic (16.7 to 17 GHz)	> 50 dB
Transmit attenuation of 3 rd harmonic (25.0 to 25.4 GHz)	> 35 dB
Transmit attenuation of 4 th harmonic (33.4 to 34 GHz)	> 30 dB
Group delay variation, over 1 MHz in receive (7.1–7.2 GHz) and transmit (8.354-8.5 GHz) passbands (*)	1 nanosecond (ns)
* A passband is the portion of the spectrum, between limiting frequencies, that is transmitted with minimum relative loss or maximum relative gain by a filtering device.	

2.3.2.3.6 Exciter Low-Pass Filter

This filter attenuates the SDST exciter broadband spurious emissions. This filter works together with the Tx LPF so the overall out-of-band emissions at the output of the TWTA are sufficiently attenuated at the input of the landing radar. The radar operates at a center frequency of 35.75 GHz.

2.3.2.3.7 Receiver Low-Pass Filter

The receiver low-pass filter (Rx LPF, Table 2-5) is intended to reject TWTA ‘ring-around’ noise (power reflected from the diplexer) so that the SDST can detect very weak uplink signals. The SDST threshold is –155 dBm, as contrasted with the +50 dBm RF output of the TWTA.

By its design, the diplexer passes any signal in the receive band to the receiver while attenuating TWTA output at other frequencies. To complete the job, the Rx LPF attenuates TWTA output at frequencies lower than the transmit band.

Table 2-5: Receive low-pass filter RF characteristics.

Parameter	Value
Insertion loss	< 0.2 dB at 7.1 GHz
Transmit attenuation	> 70 dB

2.3.2.3.8 Waveguide

The waveguide between the TWTA isolator output and D-WTS-2 was redesigned to cut off TWTA emissions in the receive band that ‘sneak back’ into the SDST. The redesign was necessitated by the addition of the diplexer bypass switch D-WTS-2. Addition of the switch had introduced a new sneak path that allowed TWTA noise at the receive frequency band into the diplexer receive arm.

2.3.2.3.9 Descent Stage SDST

The SDSTs in the descent stage and the rover are both of the same “group buy III” design. The D-SDST and R-SDST transponders are discussed together in the next section.

2.3.2.4 Rover X-Band Telecom Components

The telecom block diagram (Figure 2-1) shows the telecom components on the rover stage, as well as on three other stages. Note that names beginning with R- refer to “rover.”

The figure shows that the rover has two active components (the Rover SDST and the SSPA), two antennas (RLGA and HGA), the gimbal to point the HGA, and several microwave components (filters, etc.). Figure 2-15 shows the overall placement of the rover’s X-band and UHF components, and the figure provides detail regarding the components. The UCXS in Figure 2-15 is a UHF coaxial transfer switch.

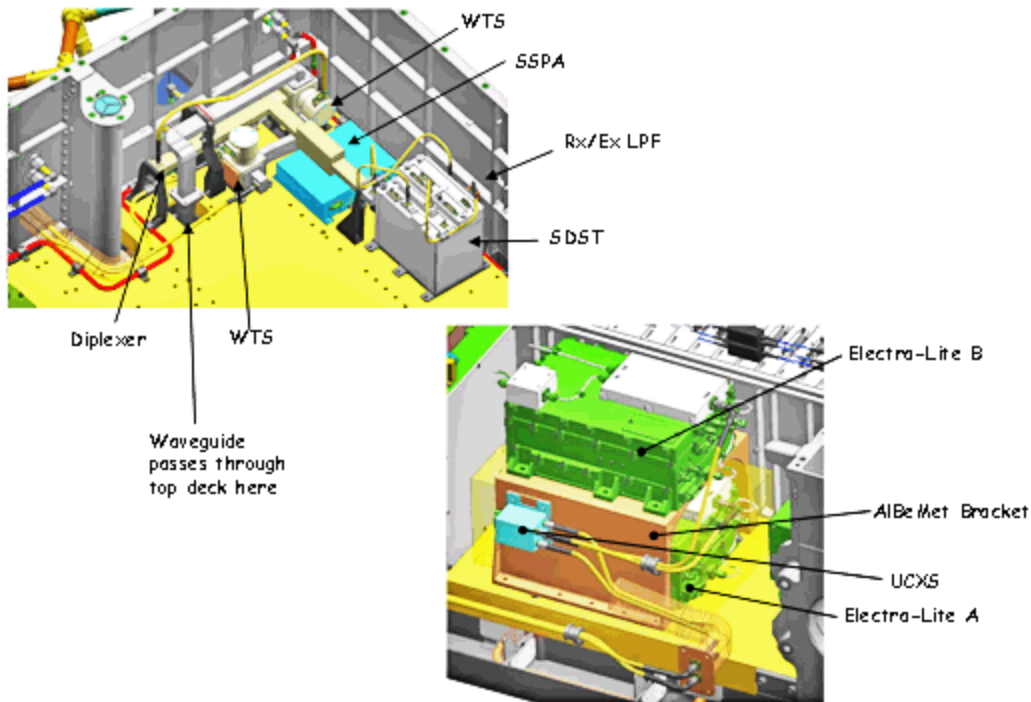


Figure 2-15. Rover telecom internal layout showing overall placement of the X-band and UHF components.

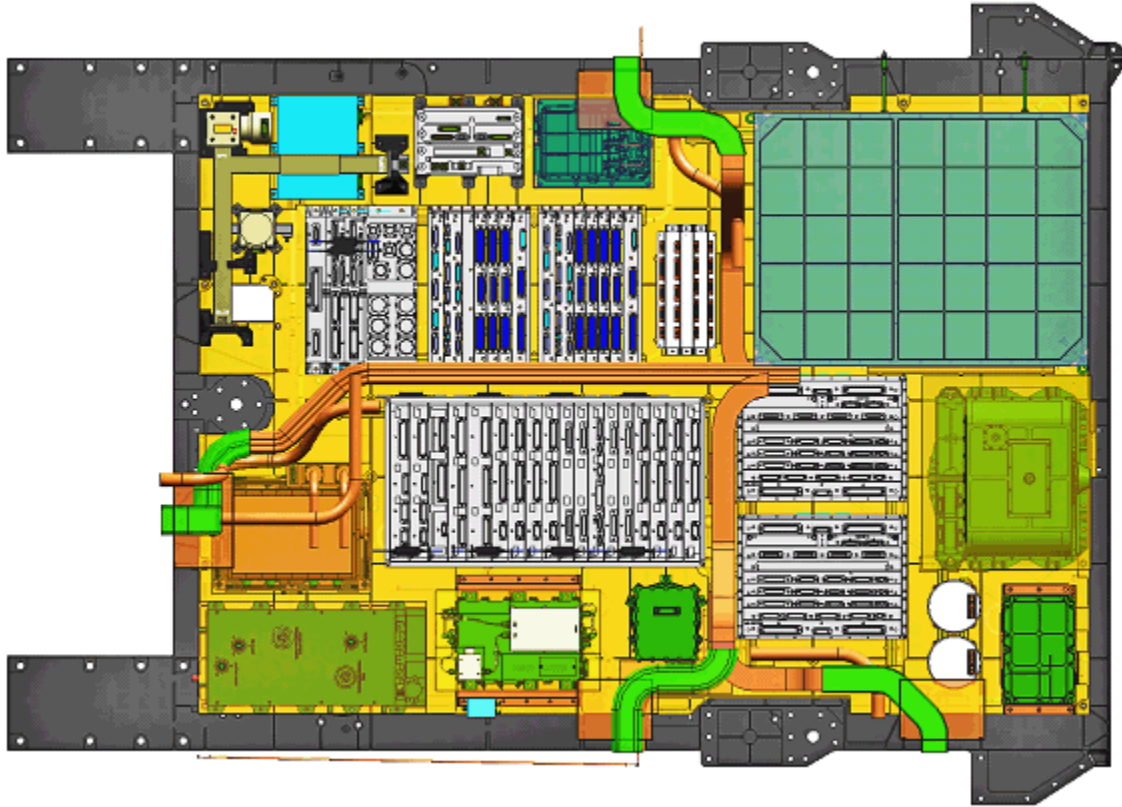


Figure 2-16. Rover detailed internal layout.

2.3.2.4.1 Rover Waveguide Transfer Switches

The rover waveguide transfer switches have the designators R-WTS-1 and R-WTS-2.

Referring to the X-Band telecom block diagram (Figure 2-1), position 1 of R-WTS-1 selects the RLGA.

R-WTS-2 selects between the HGA and the “through-path” that connects the signals to the descent stage SDST for use with antennas in the cruise stage or the parachute cone.

2.3.2.4.2 Rover Low-Gain Antenna

The RLGA is of the same design as the PLGA and TLGA. The RLGA can be used for safe-mode communications on the surface. The RLGA can also support low-rate uplink from a 34-m antenna with a standard 20-kW transmitter in case the HGA view of the Earth is obstructed or the HGA is not functional.

A simplified RLGA pattern analysis [15] was performed prior to the critical design review (CDR) to evaluate the basic pattern performance using the WIPL-D commercial high-frequency electromagnetic modeling software package [16] (WI = wires, PL = plates, D = dielectrics). Only a few key components were included in the model since the structure is large compared to the wavelength (see Figure 2-17). The pre-CDR analysis, with the pattern shown in Figure 2-18, includes ground-plane effects. The patterns are relatively smooth; however, the worst-case variations are quite high, on the order of 10 dB over a very small percentage of the coverage region.

Figure 2-19 compares the pre-CDR gain pattern for the MSL RLGA with the design and with the minimum gain value for the MER RLGA. A detailed MSL RLGA pattern analysis with a rover deck mock-up using GRASP (similar to the DLGA analysis discussed above) has not yet been done.

A more complete modeling using GRASP scattering software is planned before MSL launch.

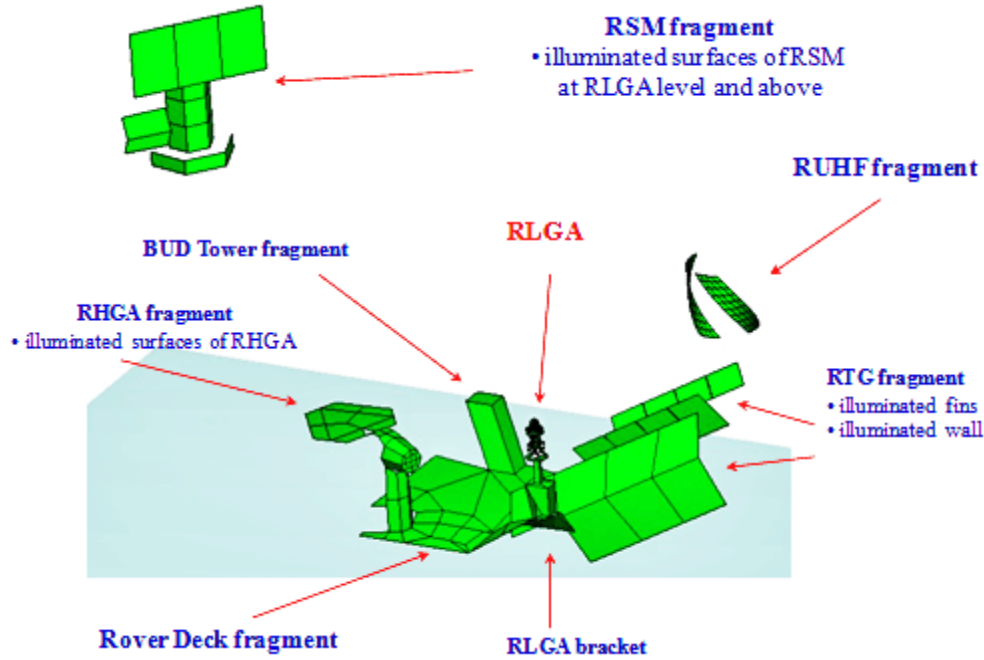


Figure 2-17. WIPL-D model of RLGA on rover deck.

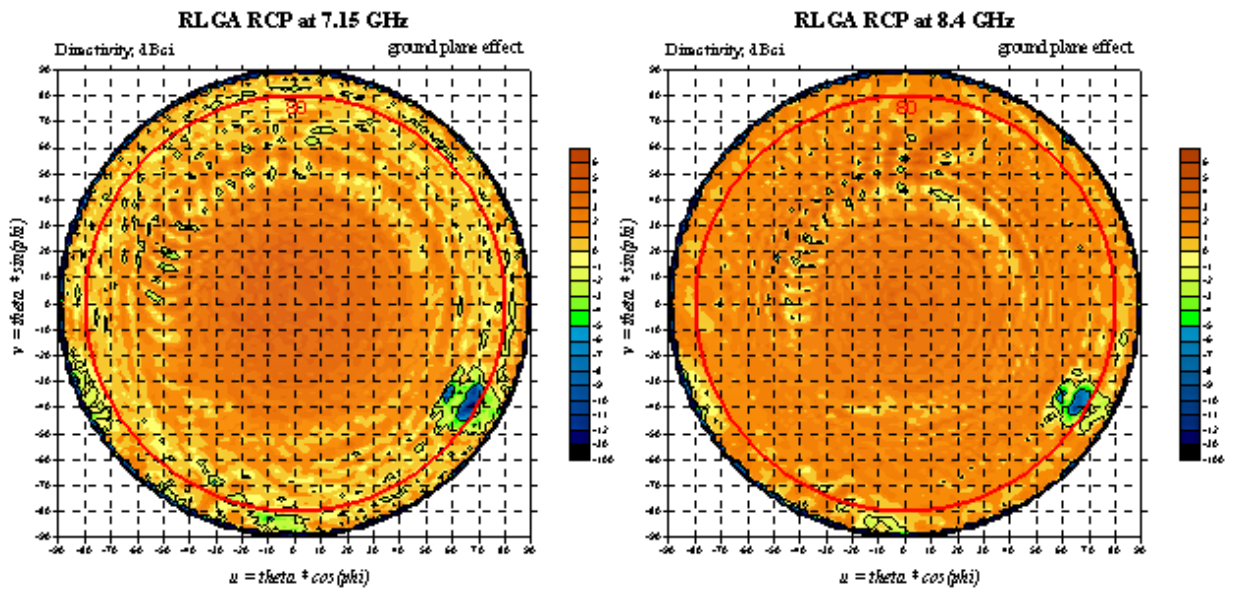


Figure 2-18: RLGA patterns modeled by WIPL-D (includes ground-plane effects).

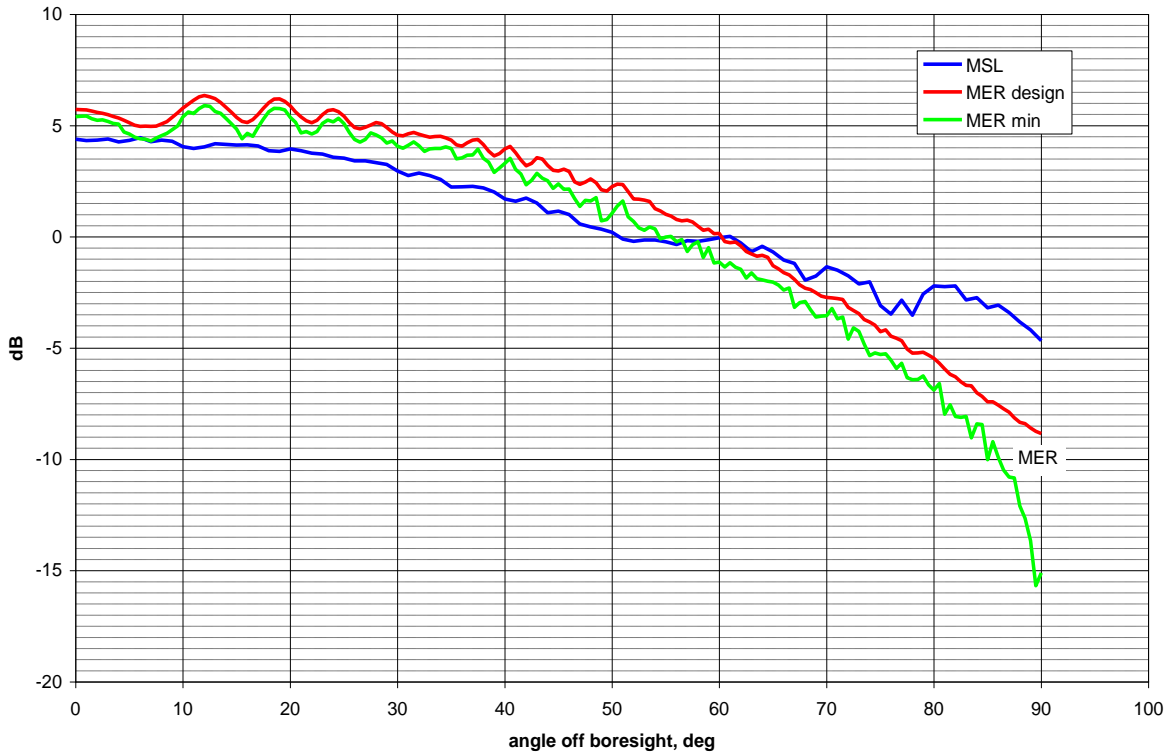


Figure 2-19. Free-space uplink gain comparison between MER RLGA and MSL RLGA

2.3.2.4.3 High-Gain Antenna

The HGA is mounted on a two-axis gimbal (Figure 2-20) located on top of the rover deck. The 48-element microstrip patch HGA radiating element is the six-sided flat structure to the left. The antenna was provided by the European Aeronautic Defense and Space Company (EADS CASA ESPACIO).

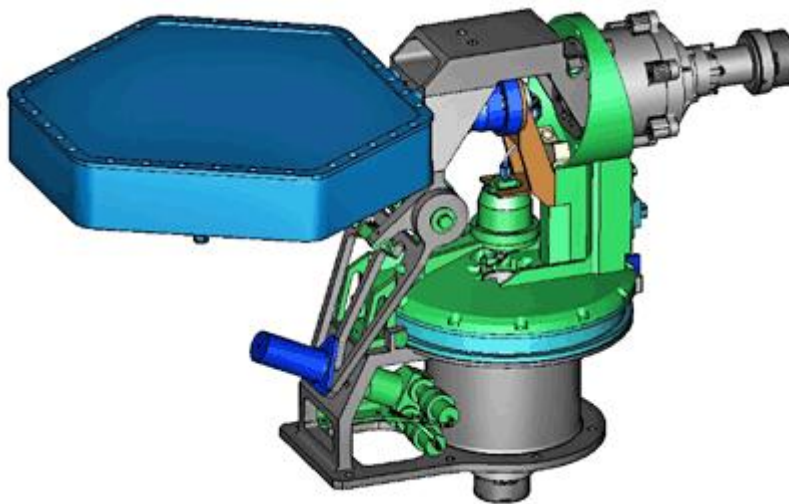


Figure 2-20. HGA and gimbal assembly.

The HGA is deployed after the rover lands. Table 2-6 provides the rover HGA RF characteristics.

Table 2-6. Rover HGA RF characteristics.

Parameter		Value	Conditions
Dimensions	cm	25.5 by 29.4	
Transmit gain	dBi	25.5 24.1 20.4	0 deg off boresight 2 deg off boresight 5 deg off boresight
Receive gain	dBi	20.2 19.7 17.3	0 deg off boresight 2 deg off boresight 5 deg off boresight
Loss in gimbals	dB	1.2 dB	
Polarization		RCP	
Transmit axial ratio		3.0 dB	Within 5 deg from boresight
Receive axial ratio		2.4 dB	Within 5 deg from boresight

Note that Table 2-6 separates out the “circuit loss” in the gimbals from the antenna gain.

Figure 2-21 and Figure 2-22 show the uplink directivity at a frequency of 7145 MHz. Similarly, Figure 2-23 and Figure 2-24 show the downlink directivity (gain relative to the gain at boresight) at a frequency of (8395 MHz). These X-band frequencies are representative of the X-band uplink and X-band downlink frequencies that MSL will use.

In the patterns, theta is the angle from boresight. The multiple curves apparent in the sidelobes of the patterns represent equally spaced cuts around phi (the axis orthogonal to theta).

2.3.2.4.4 Rover Diplexer

The design of the diplexers in the descent stage and the rover is the same. They provide for the frequency separation of receive and transmit signals coming from or going to the selected antenna.

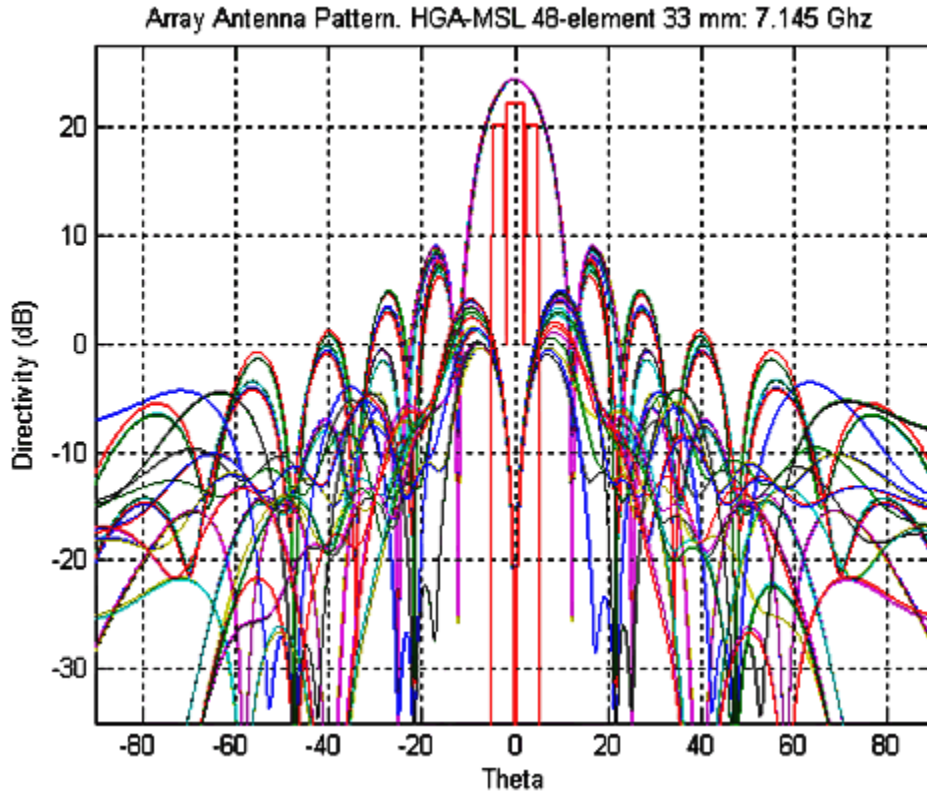


Figure 2-21. HGA Uplink Directivity showing first several sidelobes.

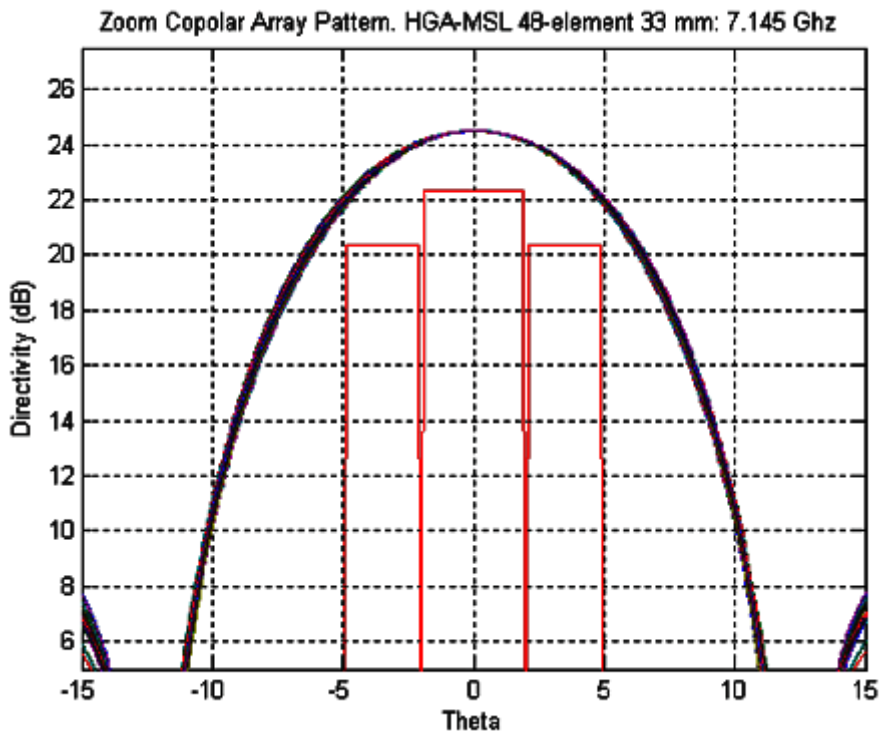


Figure 2-22. Detail of the uplink main lobe HGA directivity.

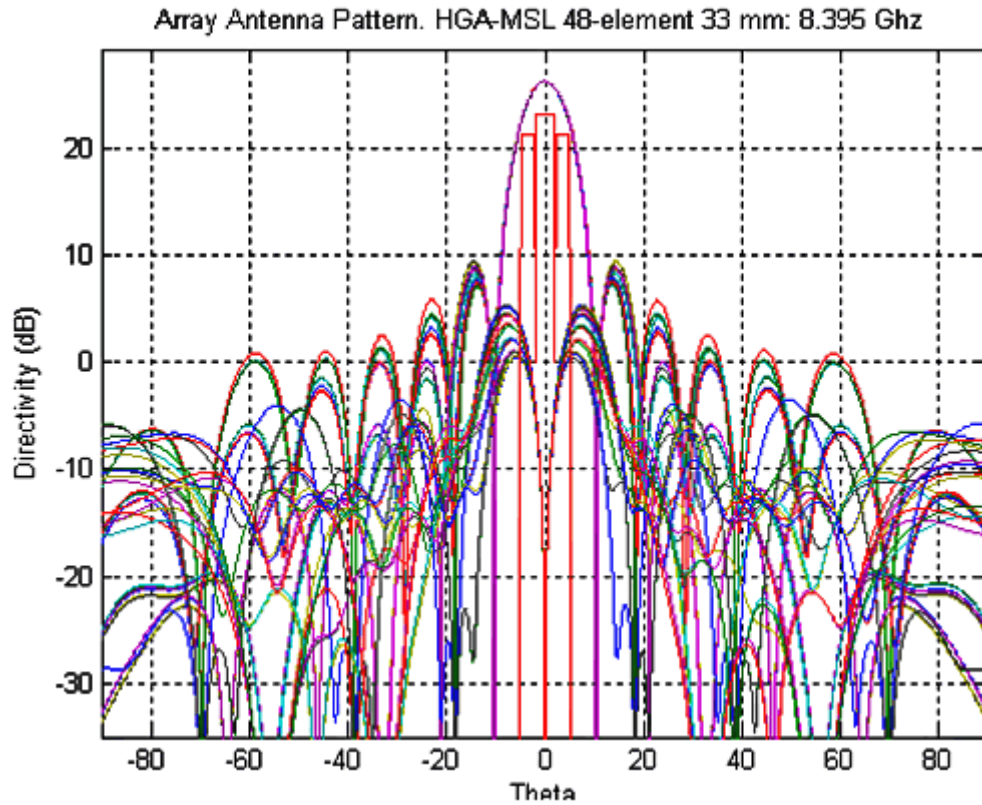


Figure 2-23. HGA downlink directivity showing first several sidelobes.

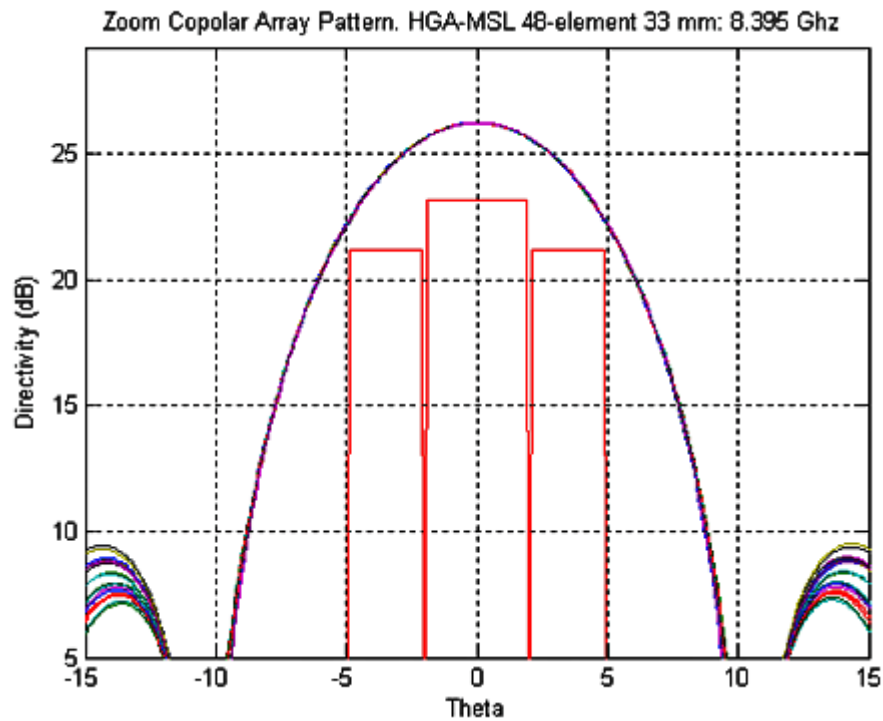


Figure 2-24. Detail of HGA main lobe downlink directivity.

2.3.2.4.5 Rover Small Deep Space Transponder

This paragraph describes the rover SDST (shown in some figures as RSDST) and the identical descent stage SDST (DSDST). In flight, only one or the other of these SDSTs would be powered on at a time.

To distinguish from earlier SDST designs, the MSL SDST is in the “Group Buy III.” Relative to earlier designs, Group III transponders have two major improvements. First, a problem has been fixed with the digital-to-analog converter in the receiver tracking loop (the “DAC glitch”)²⁴. This makes receiver acquisition of a swept uplink carrier frequency at any temperature easier than on MER. Second, Group III transponders have much less coherent leakage compared to those used on MER. As a result, the receiver static phase error (SPE) does not drift when the receiver is not locked. This also makes uplink carrier sweeps easier to plan compared to MER.

Figure 2-25 shows an Group III SDST.



Figure 2-25. Group III small deep space transponder.

²⁴ When the digital representation of the receive frequency changes from a mixture of 1s and 0s to nearly all 0s, this can cause a voltage spike at the analog output in earlier designs. This spike, more prominent at cold temperatures, can knock an already acquired SDST receiver out of lock on the uplink, particularly with sweeps in the positive direction.

The SDST is composed of four different modules: the digital processing module (DPM), the downconverter module²⁵, the power module, and the exciter module.

The DPM has three main functions:

- Convolutionally encode the data (if “coding” is enabled by 1553 control).
- Provide X-band baseband telemetry and ranging signals to the exciter module.
- Convert the analog output of the downconverter module into binary data.

Each MSL SDST has two oscillators that can drive the downlink: a voltage-controlled crystal oscillator (VCXO) whose frequency is controlled by the loop’s error voltage and is, therefore, related to the uplink frequency transmitted to the rover; and an auxiliary oscillator (aux osc) for which the frequency is generated on board and, therefore, varies with temperature (and to a lesser extent, atmospheric pressure).

The power converter module provides a set of steady voltages to the other SDST modules.

The downconverter module takes the 7.183-GHz received uplink signal and converts it to an intermediate frequency (IF) signal at $4/3 F1$ ²⁶. The uplink signal, which may be modulated with command and ranging waveforms, gets sampled by an analog-to-digital converter (ADC) at the input of the digital processor module. These samples are provided to three “channels” to use the old analog terminology:

- The carrier channel (for uplink carrier tracking).
- The command channel (for demodulating the command signal).
- The ranging channel.

The command channel has a ± 2 kHz bandpass filter centered around 2 kHz.

The ranging samples of the baseband uplink are put through a DAC so as to produce an analog signal. The resulting analog signal is a “turn-around” ranging waveform that modulates the downlink carrier.

Table 2-7 lists some of the SDST requirements relevant to the uplink (receive) telecom link performance. Reference [14] provides a more complete listing of the SDST functional specifications.

²⁵ In a receiver, a downconverter is used to transform the signal from the passband back to the baseband for further processing. Baseband refers to the original frequency spectrum of the signal before modulation or up-conversion.

²⁶ In SDST nomenclature, F1 is the fundamental frequency from which the uplink and downlink frequencies are derived. For example, the X-band downlink is 880 times F1 and the X-band uplink is 749 times F1. For MSL, operating on X-band channel 4 [13], F1 will be approximately 9.59 MHz. The VCXO output is at two times F1.

Table 2-7. SDST receive functional characteristics.

SDST Receive Parameter	Value
Receive signal maximum power	-70 dBm (for performance specs) +10 dBm (no damage)
Carrier loop threshold bandwidth	2 bandwidth (BW) settings: 20 ± 2 Hz at receiver threshold (varies with carrier loop signal to noise ratio (SNR); max bandwidth is ~120 Hz at strong signal, 100 dB SNR) 50 Hz ± 5 Hz at receiver threshold
Noise Figure	< 3.2 dB over Temp, Aging, and Radiation, 2.1 dB typical at beginning of life (BoL), room temp
Carrier Tracking Threshold at BLF and 0-dB loop signal-to-noise ratio	-157.7 dBm typical -155.0 dBm worst case
Data Rates	7.8125 to 4000 bps
Telemetry Modulation Index	0.5 to 1.5 radians peak (64 steps, about 0.7 deg resolution) should be able to get 0 deg

The exciter's RF power output to the SSPA or the TWTA can be an unmodulated or (almost always) a modulated carrier. The exciter module phase modulates the downlink carrier with any combination of three inputs:

- Telemetry (from the DPM; this is a binary phase shift key (BPSK)-modulated square-wave subcarrier).
- Turn around ranging (analog, from the DPM, after its D/A converter).
- Differential one-way ranging (DOR) (analog, a 2 F1 [~ 19 MHz] sinewave continuous wave [CW] signal, generated in the exciter module). In this case, CW refers to an analog signal as opposed to a discrete-time signal.

Table 2-8 lists some of the SDST requirements relevant to the downlink (transmit) telecom link performance.

Table 2-8. SDST exciter characteristics at 880f1.

X-Band 880f1 Transmit Parameter	Value
Output power level of X-band exciter	13.0 + 3/-2 dBm over temperature, tolerance, end of life, radiation
Phase noise	< -20 dBc/Hz @ 1 Hz (aux osc mode)
Aux Osc short term frequency stability	0.06 ppm at any constant temp from 10°C to 40°C (1 sec integration measured at 5 minute intervals over 30-min span)
NCO subcarrier tone short term stability	1 ppm (as of July 2009)
NCO subcarrier tone long-term stability	50 ppm (as of July 2009)
Harmonics	< -50 dBc
In-band and out-of-band spurious	< -50 dBc
Minimum symbol rate	0 sps for subcarrier; 2000 sps for direct modulation
Maximum symbol rate	Filtered mode: 4.4 Msps Wideband (unfiltered) mode: > 4.4 Msps
Modulation Index accuracy	± 10%
Ranging modulation indices (peak)	4.375, 8.75, 17.5, 35, 70 deg
Ranging modulation Index accuracy	± 10%
Ranging modulation index stability (over temp., radiation, and EOL)	< ±20%
Ranging delay variation over flight acceptance (FA) temperature range	< 20 ns typical
DOR modulation index (peak)	70 deg nominal
DOR modulation index accuracy	± 10%
DOR modulation Index stability (over temp., radiation, and EOL)	< ±25%

2.3.2.4.6 Rover Receiver Low-Pass Filter

The rover Rx LPF is of the same design as the descent stage Rx LPF. The filter is intended to reject SSPA ‘ring-around’ noise (power reflected from the diplexer) so that the rover SDST can detect very weak uplink signals.

2.3.2.4.7 Solid State Power Amplifier

The MSL SSPA is of the same design as the MER units. Figure 2-26 is an SSPA block diagram (© 2005 IEEE). The X-band SSPA consists of a solid-state RF amplifier, an electronic power converter (EPC), mode control and telemetry circuitry, and input and output isolators. Table 2-9 shows key characteristics. More detail, diagrams, and photographs of the MER SSPA are in Ref. [17].

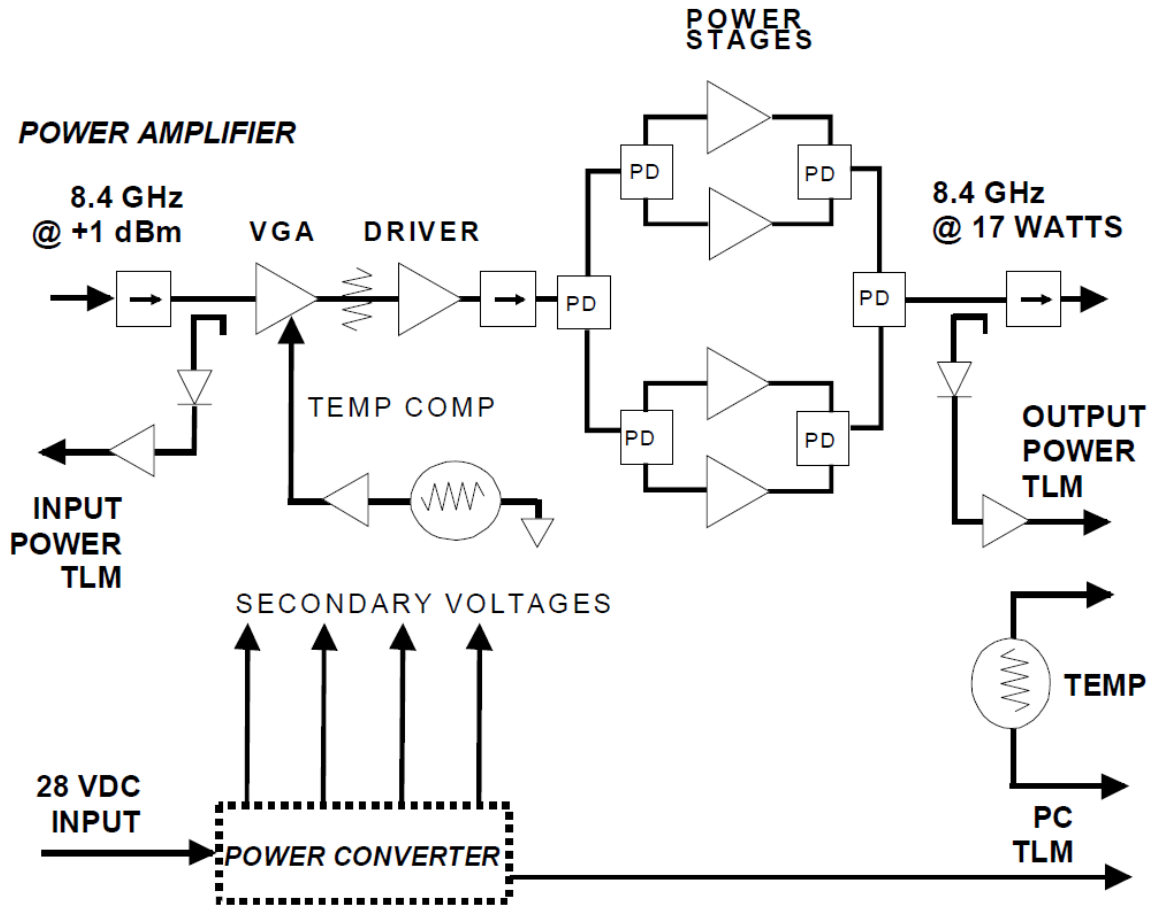


Figure 2-26. MSL SSPA block diagram.

Table 2-9. SSPA key characteristics.

Parameter	Value
Frequency Range	8.395–8.455 GHz
Output Power (RF)	15 W
DC Input Power	55 W nominal, 64 W max
Output voltage standing wave ratio (VSWR)	1.5:1 max

2.3.3 Functional Redundancy (Rover as Backup to Descent Stage)

The MSL RF switch complement allows the rover SDST to act as a back-up to the descent stage. The downside is that the rover has a weaker transmitter (15-W SSPA rather than 100-W TWTA) and more circuit losses. The total transmitting difference between rover and descent stage is about 9 dB in effective isotropic radiated power (EIRP). All functions are available through either path (except, of course, no “diplexer bypass” is required when using the SSPA during EDL). The diplexer can handle the SSPA RF power level.

2.3.4 Encoding Modes/Frame Sizes

The X-band downlink has three Turbo codes (1/2, 1/3, and 1/6); the data rates range from 10 bps to 62,500 bps. RF spectrum bandwidth limitations prevent use of the combination of 62,500 bps bit rate with turbo 1/6 coding. That combination would produce too high a symbol rate; for Mars missions, the symbol rate is limited to 300,000 sps.

An effort was made to reduce the telemetry frame size (1784 bits) at low rates while keeping some coding efficiency. MSL can use an interleave depth of 1, whereas MER had only an interleave depth of 5.

From these limits, the effective information rate (R_{eff} , a dimensionless information bits/bits of frame) on MER was $1760/3040 = 0.58$; on MSL it is $1784/2072 = 0.86$, an improvement of 1.7 dB. The improved efficiency means there is much less frame overhead on MSL at 10 and 40 bps.

2.4 UHF Flight Subsystem Description

2.4.1 UHF Interfaces with MSL Control and Data Systems

Figure 2-4 shows the data and control interfaces of the Electra-Lite (ELT) radios. The main interface to both the ELT radios is the MSAP-delivered Telecommunications Interface (MTIF) card for all data transfer functions. The MTIF interfaces for UHF and X-band are shown in Figure 2-4.

The ELT (used for relay) differs from the SDST (used for DTE/DFE) in that the transmitted data rate is controlled by the radio, not the MTIF. The MTIF clocks data into the ELT internal buffer. When the buffer-fill threshold (a settable parameter) is passed, the ELT forces the data flow control line high and the MTIF stops clocking in data until the line drops again. MSL has selected three ELT buffer fill rates as baseline:

- 8250 Hz used for low transmit data rates to minimize latency (primarily for use during EDL), with a telemetry frame size of 1784 bits.
- 33,000 Hz used for transmit data rates between 2 kbps to 32 kbps (primarily for safe-mode low-latency applications), with a telemetry frame size of 1784.
- 2,062,500 Hz for normal operations, with a telemetry frame size of 8920 bits. This fill rate can keep up with even the highest transmit rates of 2 Mbps.

Two kinds of data encoding are possible for the UHF links:

- Reed Solomon encoding (interleave depth 1 and 5) that can be used for unreliable (bit-stream or non-Proximity-1 protocol) MSL-to-Orbiter communications.
- Checksum-frame that is used for nominal reliable (Proximity-1) mode UHF downlink and for UHF EDL downlink.

The ELT has redundant uplink (command) and downlink (telemetry) LVDS interfaces, which are cross-strapped to the MTIF card (each MTIF has four command/telemetry ports). The active downlink port on the telecom side must be selected via a 1553 command. Both uplink ports in ELT are always active.

The Rover bus controller (BC) on the MTIF controls the primary 1553 bus. ELTs are connected via the remote terminal (RT). The MTIF resides in the rover computer element (RCE).

2.4.1 UHF Key Hardware Components

The telecom component descriptions in the following paragraphs are organized by stage. The telecom UHF block diagram Figure 2-1 shows four stages (“slices”), three of which have UHF hardware: parachute cone, descent, and rover.

2.4.1.1 Parachute Cone UHF Telecom Components

2.4.1.1.1 Parachute UHF (PUHF) Antenna

The PUHF is used only from the CSS to the backshell deployment portion of EDL. Refer to Figure 1-16 for this part of EDL. The antenna provides communication with relay orbiters over a wide range of view angles. In the event of a major spacecraft failure during EDL, such as an event resulting in a tumbling attitude, the antenna would permit reconstruction data to be received in all but the most extreme attitudes.

The PUHF (see Figure 2-27) is a wrap-around antenna of the type used on launch vehicles and previously used successfully on the Phoenix lander during EDL. It was designed and manufactured by Haigh-Faar of New Hampshire, in close cooperation with JPL.

The antenna is manufactured as four segments individually mounted on the parachute cone, and connected via a one- to-four power divider. Each segment has two radiating patch antenna elements, making a total of eight radiating patch antennas in a conical array.

Excitation of the antenna is via a coaxial cable between the descent stage switch D-UCTS and the one- to-four power divider mounted on the inside of the parachute cone.

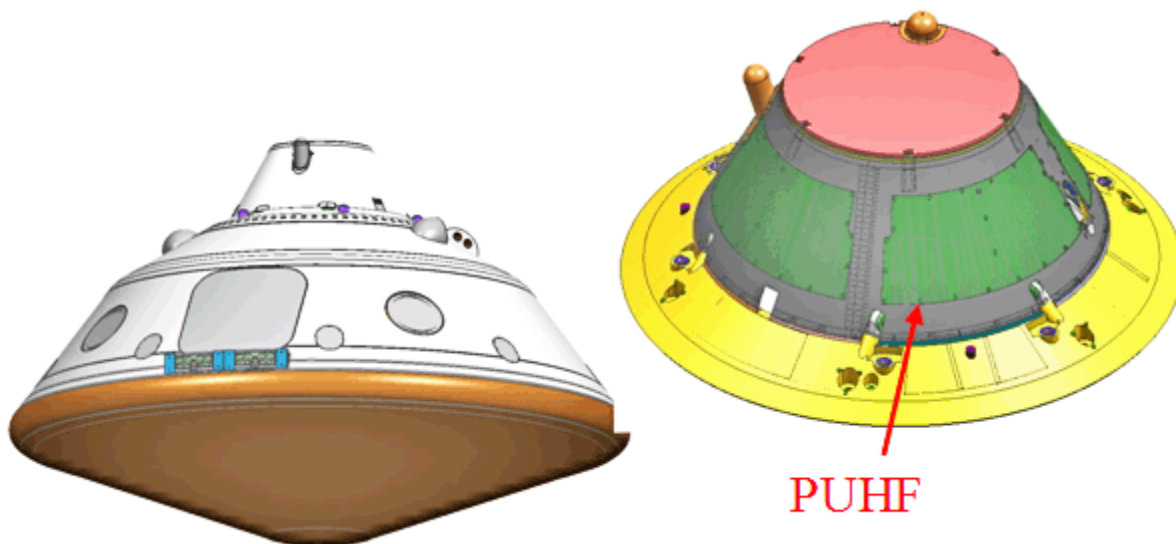


Figure 2-27. PUHF antenna mounted on parachute cone.

The pattern is semi-omnidirectional, roughly azimuthally symmetric, with a null aligned with the spacecraft $-Z$ axis. Pattern cuts for different azimuth angles (rotation about the $-Z$ axis) overlaid are shown in Figure 2-28. The antenna has a narrow but deep null along the $-Z$ axis, and its performance in the directions about the $+Z$ axis is highly variable and unreliable.

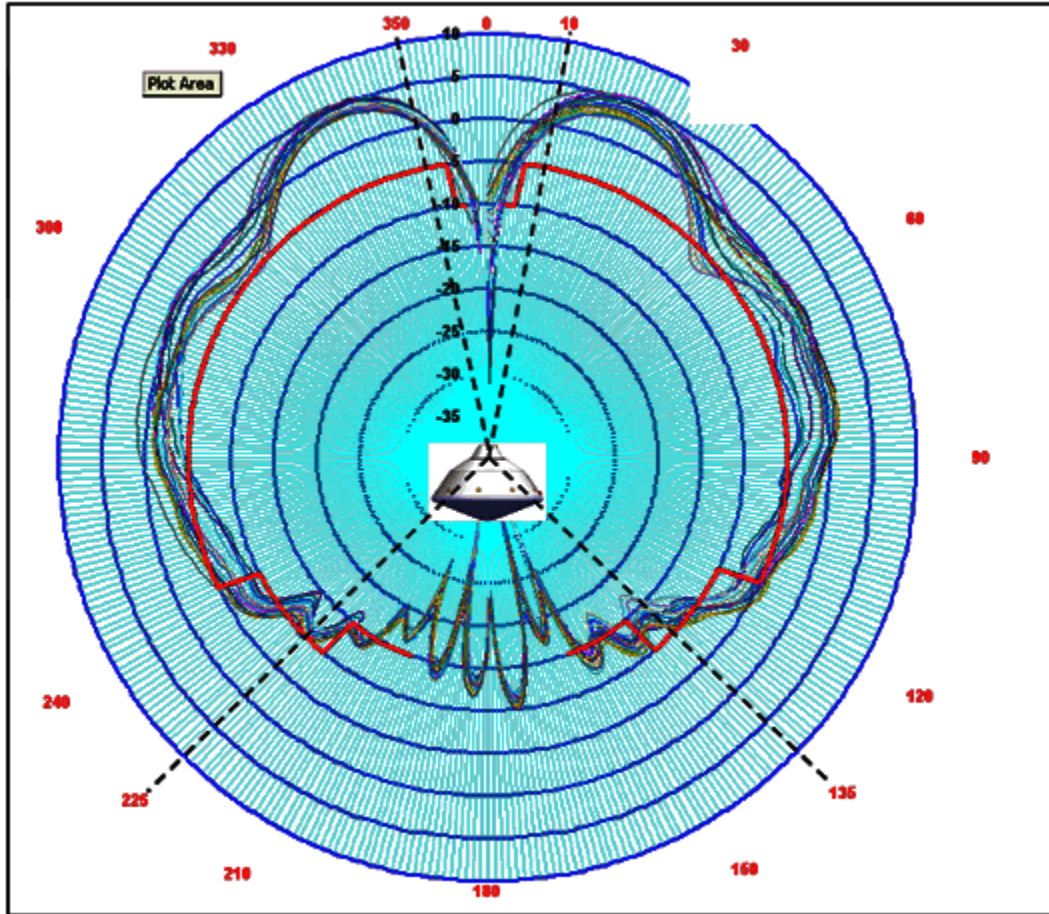


Figure 2-28. PUFH antenna radiation pattern.

2.4.1.2 Descent Stage UHF Telecom Components

The UHF components on the descent stage are the D-UTS switch and the DUHF antenna (plus connecting cables). Mounted on the descent stage, the DUHF (Figure 2-29) is a sleeve dipole design that provides an azimuthally symmetric pattern.

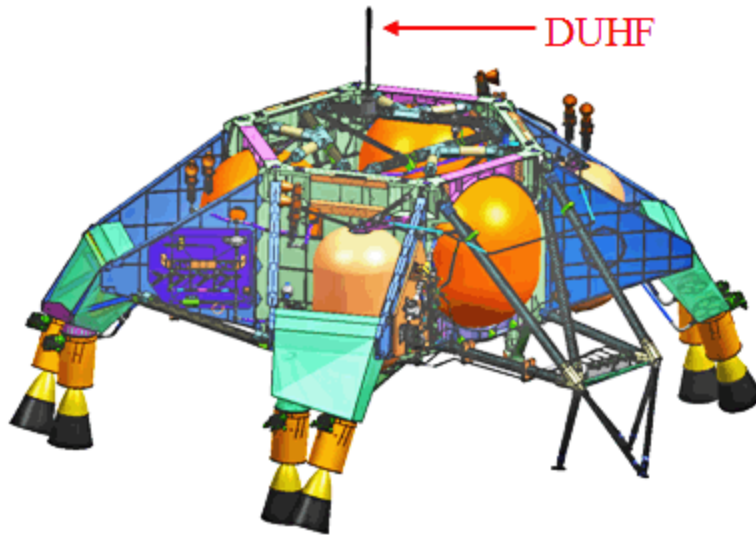


Figure 2-29. DUHF antenna mounted on descent stage.

As shown in Figure 2-30, the DUHF transmit pattern is significantly affected by the descent stage hardware [18]. Scattering from the descent stage distorts and moves the dipole null from along the $-Z$ axis. The pattern coverage will provide a high probability of closing the link to the relay assets during the critical few minutes of powered descent and sky crane activity.

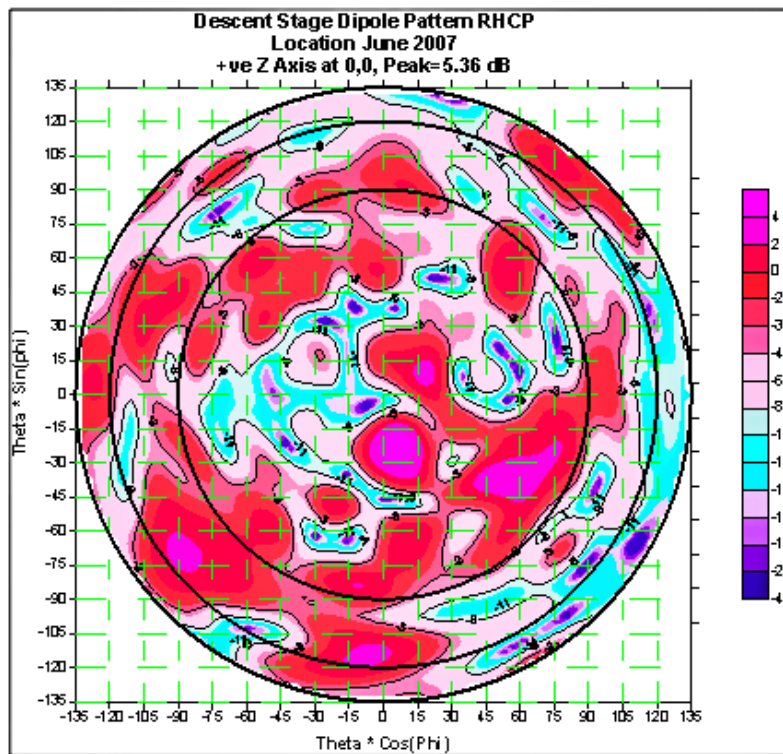


Figure 2-30. DUHF antenna pattern as mounted on descent stage.

The D-UTCS provides for switching from the PUHF to the DUHF at backshell deployment. There will be a brief break in the relay link during this switch. Stopping transmission briefly while the switch actuates avoids “hot switching” of the D-UCTS.

The cable from the rover and the other cable to the parachute cone pass through the mega-cutters and are severed at rover separation and backshell deployment, respectively.

2.4.1.3 Rover UHF Telecom Components

The Electra-Lite radios are mounted inside the rover web, as shown in Figure 2-31.

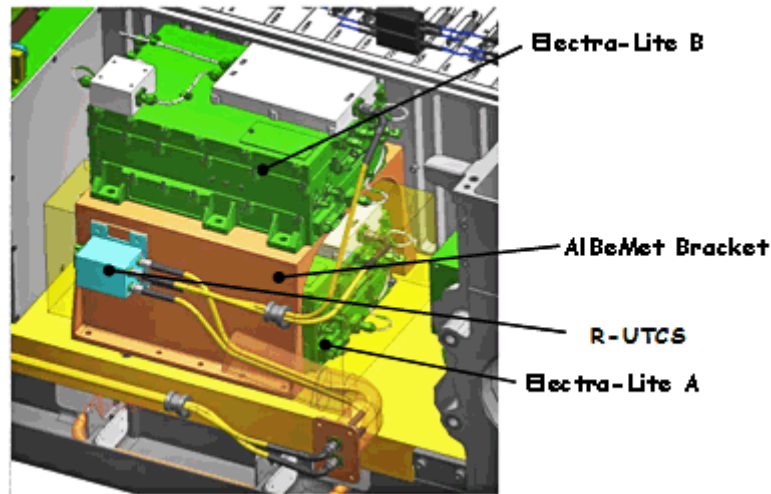


Figure 2-31. UHF hardware in rover WEB.

The ELT-B radio is mounted on a bracket (made from AlBeMet²⁷) above the ELT-A radio. The R-UCTS mounts on the side of the bracket. Because there is extra thermal isolation of the ELT-B due to the bracket, the thermal constraints on ELT-B are slightly harder than for ELT-A. This would only be an issue if ELT-B had to used, due to an ELT-A failure, and the WEB thermal environment was severe.

The R-UTCS switches between the RUHF and the line running to the descent stage.

For the sky crane activity, the relay transfers from the DUHF to the RUHF. The RUHF, a quadrafilier helix antenna specially designed for the MSL mission, is used for all of the surface activities in the mission. Figure 2-32 shows the RUHF mounted on the rover. Figure 2-33 shows a detailed view of the antenna itself.

²⁷ AlBeMet is the trade name of the Brush Wellman company for a beryllium and aluminum composite material derived by a powder metallurgy process. AlBeMet is formed by heating fine beryllium and aluminum powder under high pressure to form a uniform material. These alloys are significantly less dense than aluminum. (<http://en.wikipedia.org/wiki/AlBeMet>)

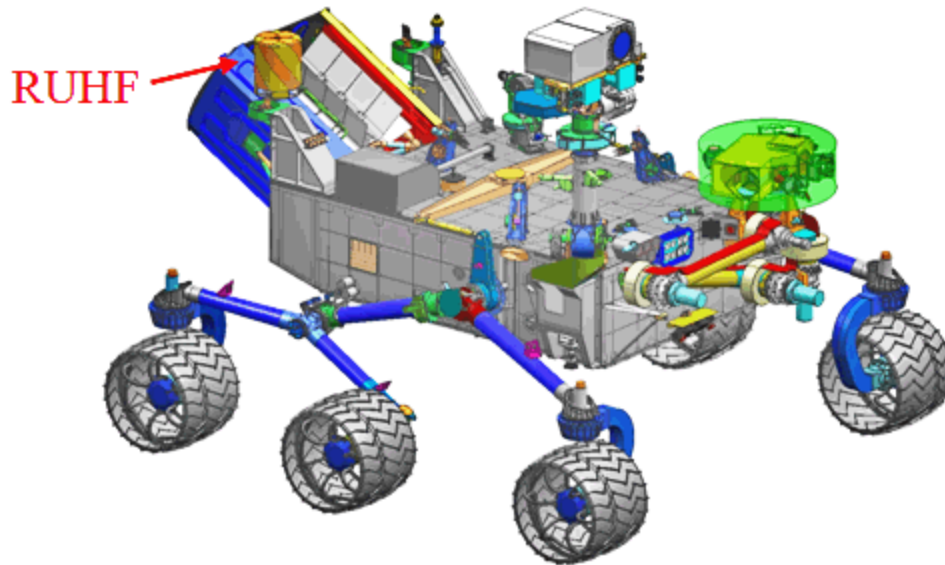


Figure 2-32. RUHF antenna mounted on rover.



Figure 2-33. MSL RUHF Quadrafil helix antenna.

The RUHF pattern is quite broad: and during surface operations, the RUHF provides coverage at RCP over most of the sky to very low on the horizon.

A WIPL-D analysis [16] was carried out early in the telecom development to assess the pattern distortion due to the rover deck, the RTG, and other objects in close proximity to the antenna (Figure 2-34 shows the WIPL-D model). At the UHF frequencies, most of the deck and its payload can be considered close to the antenna.

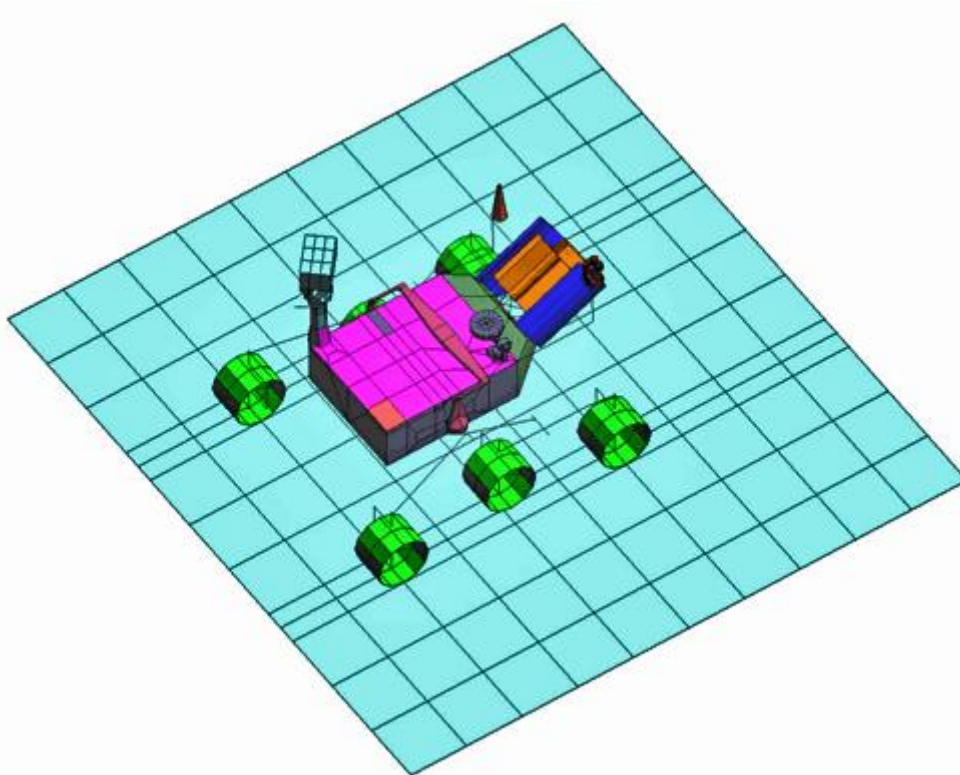


Figure 2-34. WIPL-D model for RUHF pattern analysis.

Figure 2-35 and Figure 2-36 show the analysis results, including ground effects [19]. The patterns are significantly better than the MER UHF monopole pattern, with no real nulls except at the low elevation angles near the horizon.

Because the RUHF performance on the Martian surface is critical to the mission and the flight team would like to have accurate data volume prediction tools available for planning sol-to-sol activities, the RHUF patterns will be measured using an MSL mockup in a fashion similar to the measurements made for the Phoenix lander mission [20].

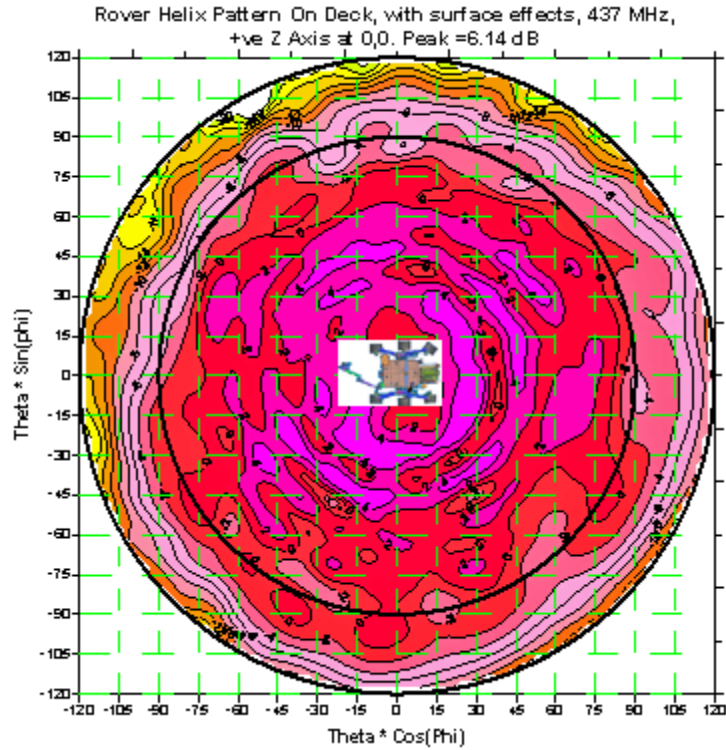


Figure 2-35. Surface RUHF antenna pattern, Rx.

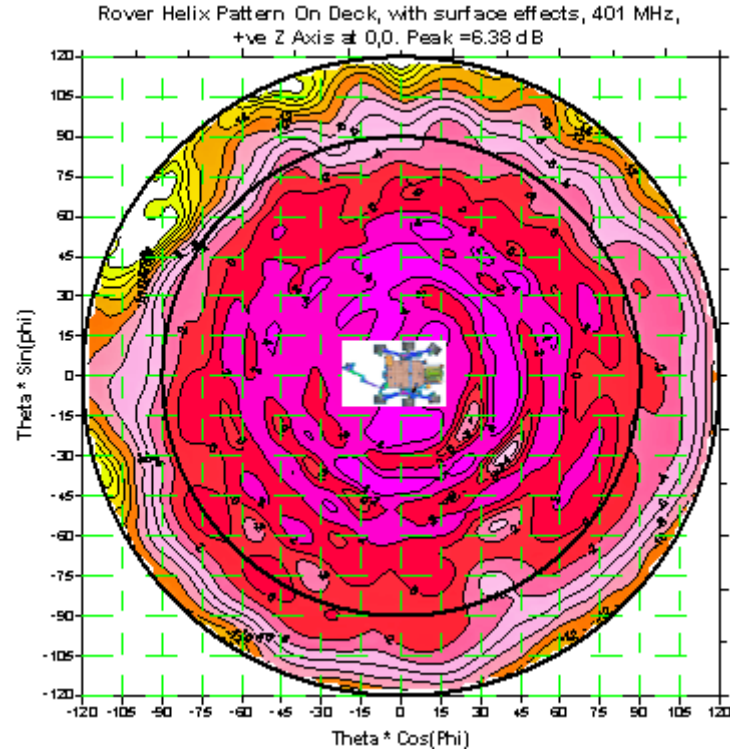


Figure 2-36. Surface RUHF antenna pattern, Tx.

The RUHF will be used during the sky crane maneuver [Figure 2-37]; however, the RUHF will be shadowed partially (and to a varying degree) by the descent stage above it. To study the effects on the pattern, we performed an analysis using WIPL-D at three representative heights (distances) below the descent stage (as illustrated in Figure 2-37). The results are shown in Figure 2-38, where it is evident that, as expected, the pattern shows much distortion when close to the descent stage, but approaches the relatively undistorted surface pattern near the end of the sky crane deployment. In the figure, BUD refers to the bridle, umbilical, descent rate limiter device.

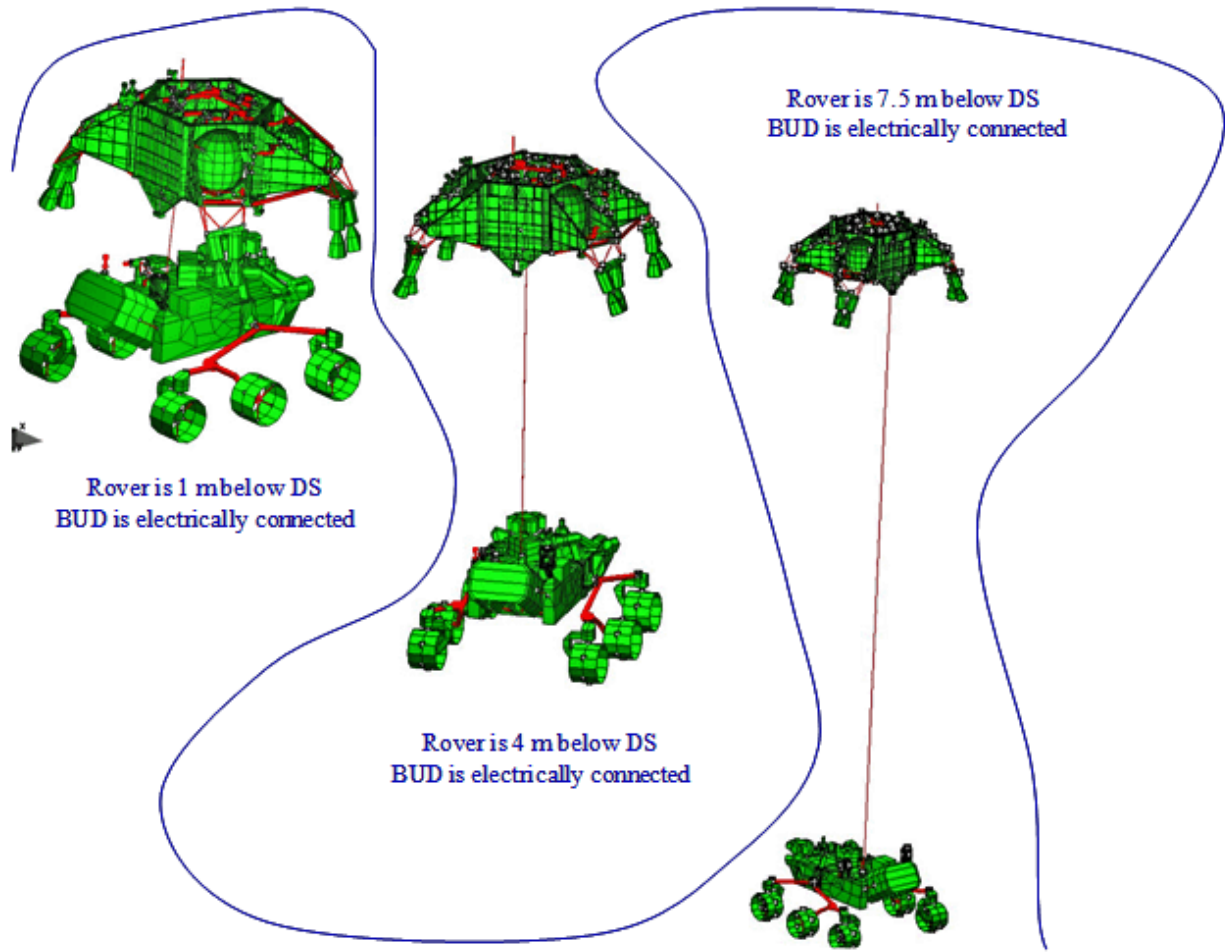


Figure 2-37. RUHF pattern study for sky crane.

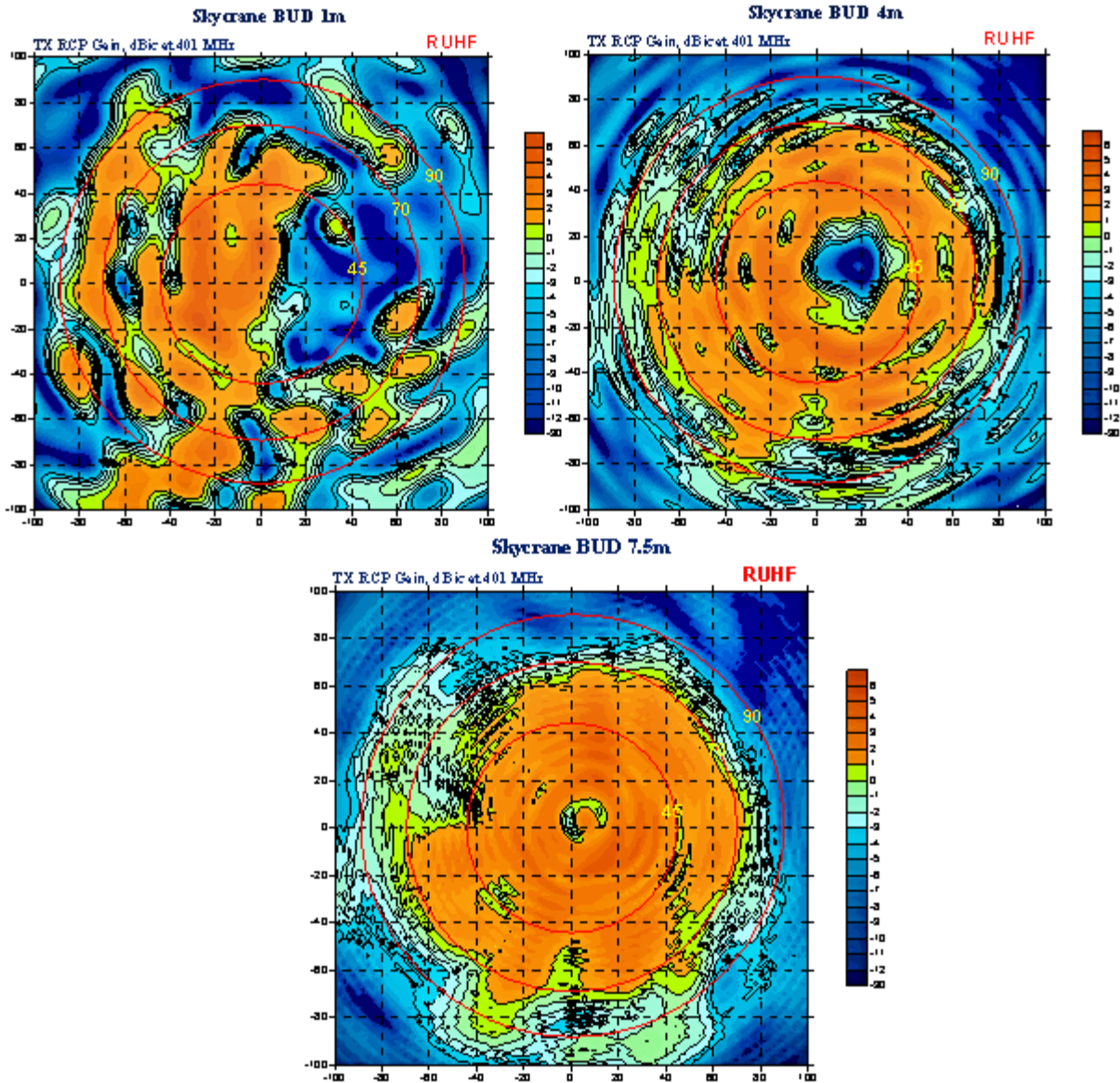


Figure 2-38. RUHF pattern analysis results for sky crane.

2.4.1.3.1 *Electra-Lite (ELT) UHF Transponders*

The UHF relay uses dual-redundant Electra-Lite (ELT) radios. The ELT implements the functions for relay communications with the Mars Odyssey and MRO orbiters (and other compatible orbiters such as MEX).

The ELT is a variant of the JPL Electra style software defined radio (SDR). The ELT is a somewhat stripped down version of the Electra radio and is intended for use in landers. Compared with the standard Electra on MRO, the MSL Electra-Lite is less capable, but it is also less massive and less power hungry.

Unlike the MSL X-band subsystem with its transponders and its separate power amplifiers (TWTA or SSPA) and diplexers, each ELT has an integrated transponder, power amplifier, and diplexer.

The flight radio FM-002 is shown in Figure 2-39. Ref. [21] provides more detail on the Electra and Electra-Lite radios.

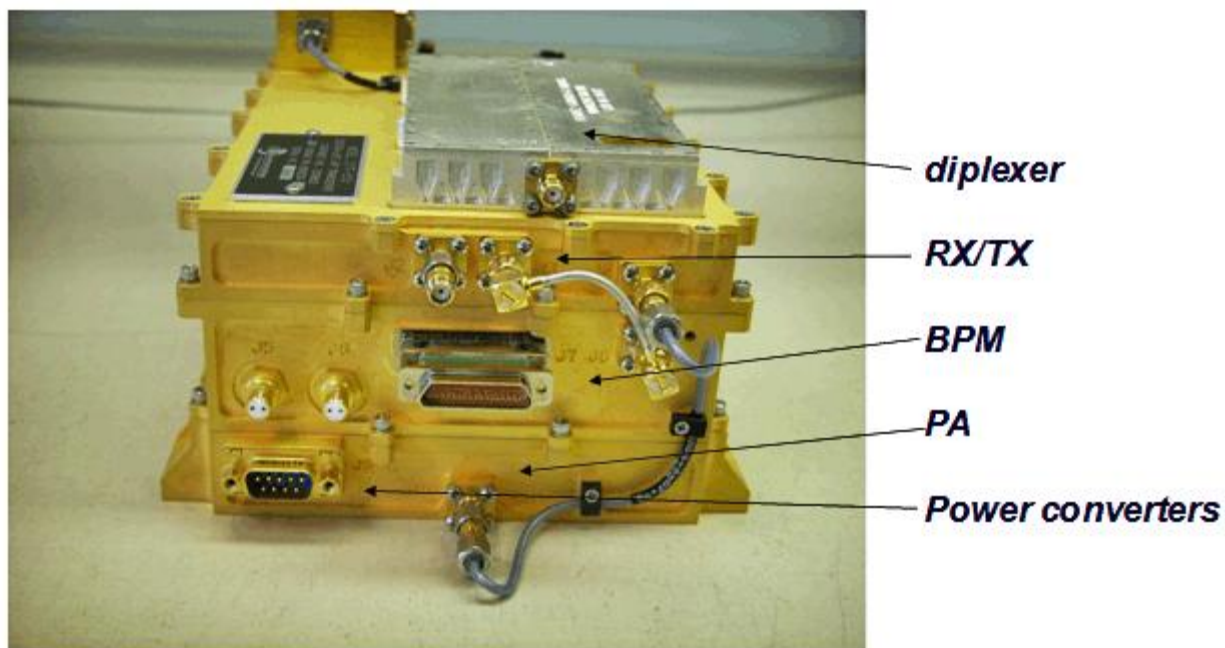


Figure 2-39. Electra-Lite FM-002.

The RF power delivered out of the diplexer is greater than 8.5 W. The downlink and uplink operational parameters are summarized in the next two subsections, followed by summaries of the Prox-1 parameters, buffer data management, and some miscellaneous information.

2.4.1.3.1.1 ELT Downlink

Downlink is the link from MSL to the orbiter, also referred as the return link.

- Downlink rates from 2 kbps to 2048 kbps are available. The CE505 radio onboard Odyssey can only support rates of 8, 32, 128, and 256 kbps. The planned nominal return link with MRO will use suppressed carrier modulation with adaptive data rates (ADR) during a relay pass or contact (overflight). Odyssey links must use residual carrier with a fixed data rate for each contact.
- Throughput efficiencies at either the MRO or MSL end of the link, or both, limit the effective maximum rate to approximately 1.35 Mbps, depending on whether there is significant forward data being sent by MRO.
- Bypass and $(7,1/2)$ convolutional coding.
- Three (CCSDS standard) frequency channels [22]: Channel 0: 401.585625 MHz; Channel 1: 404.4 MHz; or Channel 2: 397.5 MHz (CCSDS is the Consultative Committee for Space Data Systems).
 - Channel 0 is the baseline and the only one compatible with Odyssey. However, this downlink frequency plan is under review due to

electromagnetic interference/electromagnetic compatibility (EMI/EMC) issues onboard MRO. Channel 1 and Channel 2 will be used with MRO only if EMI prevents operation on Ch 0.

- Modulation: Residual Carrier with fixed modulation index (with biphasic-L baseband modulation), and suppressed carrier (with non-return to zero, NRZ).
- Coherency enabled/disabled.

2.4.1.3.1.2 ELT Uplink

Uplink is the link to MSL from the orbiter, also referred as the forward link. The planned nominal forward link with MRO will use residual carrier modulation at 32 kbps. Odyssey links must use residual carrier.

- Uplink rates are from 2 to 256 kbps.
 - The following UHF uplink rates can be used by MSL: 2, 8, 16, 32, 64, 128, 256 kbps.
 - Only 8 and 32 kbps is supported by Odyssey.
- Bypass and (7,1/2) convolutional coding.
- Three (CCSDS standard) frequency channels [22]: 0: 437.1 MHz, 1: 435.6 MHz, 2: 439.2 MHz.
 - Channel 0 is the baseline and the only one compatible with Odyssey. Channel 1 and Channel 2 will be used with MRO only if EMI prevents operation on Channel 0.
- Modulation: Residual carrier with fixed (with biphasic-L), and suppressed carrier (with NRZ)
- Coherency is enabled/disabled.

2.4.1.3.1.3 Proximity-1 Parameters (Forward and Return Links)

- Sequence controlled (reliable) link is the nominal protocol.
- Bit stream (unreliable) mode that bypasses the Proximity-1 protocol is available for off-nominal cases and for EDL.
- The adaptive data rate mode (ADR), available when relaying between MRO and MSL, will take advantage of the ability of the Proximity-1 protocol to command different data rates on the fly. (Only the return link data rates will be changed this way; the baseline forward rate between MRO and MSL will be 32 kbps).
- The baseline hailing interaction data rate for MSL is 8 kbps.

2.4.1.3.1.4 Buffer Data Management (Forward and Return Links)

- ELT provides a transmit (downlink) flow control signal to the MTIF using an additional LVDS line (“ready for data”) so that the ELT transmit buffer does not overflow. Flight software (FSW) can also set various buffer parameters (buffer depth and two watermarks) to control the latency in the transmit link.

- On the MSL receive (forward link) side, there is no flow control. The content of the Proximity-1 transfer frame data field is sent out of the LVDS line as soon as the frame is validated.

2.4.1.3.1.5 Other ELT Functions

- Collection of Proximity-1 time-packets via the 1553B interface is nominally expected during every overflight.
- Collection of radiometric data via 1553B is nominally used only in troubleshooting scenarios.
- Send “spacecraft wake-up” signal to LVDS upon receipt of Proximity-1 hail from an orbiter. Wake signaling is baselined for use only in a fault-protection situation.

2.4.1.3.1.6 UHF Coaxial Transfer Switches (D-UCTS and R-UCTS)

The switches (in the Figure 2-2 UHF block diagram) are used to switch between the antennas during EDL and to choose between ELT-A and ELT-B. They are manufactured by Sector Microwave. They are double-port double-throw (position 1 and position 2) switches.

The switch in the rover stage allows the flight team to choose to connect radios to either the descent stage switch or to the RUHF antenna. The switches have a port-to-port isolation of >60 dB and a maximum insertion loss of 0.2 dB. Their switching time is < 50 ms. They are rated to handle as much as 15 W of RF power, with a maximum return loss of –20 dB.

2.5 Terminal Descent Sensor (Landing Radar) Description

The MSL terminal descent sensor (TDS) is a six-beam Ka-band pulse-Doppler radar designed to measure the three-axis velocity and altitude of the spacecraft from about 100 m/s and 4 km altitude until rover touchdown [7]. Specifically, the radar provides line-of-sight velocity and range for each radar beam to the spacecraft’s navigation filter, which computes the three-axis velocity and altitude of the descent stage.

Figure 2-40 is a system overview block diagram of the TDS. Table 2-10 details the TDS high-level performance and physical characteristics.

Ref. [7] provides the high-level sensor specifications and physical characteristics of the TDS.

Table 2-10. TDS high level characteristics.

Parameter or condition	Value
Center frequency	36 GHz
Antenna beamwidth	3 deg
Transmit power (per beam)	2 W
Pulse width	4 to 16 ns
Altitude above Mars	6 to 3500 m
Velocity of descent stage	200 m/s maximum
Spacecraft bus power	30 W
Transmitting	120 W
Mass	25 kg
Dimensions	1.3 x 0.5 x 0.4 m

Although the TDS is not book kept as part of the telecom subsystem, it transmits and receives RF power. The MSL X-band telecom subsystem has an exciter low-pass filter and transmitter low-pass filters to ensure that the radar's performance is not degraded by the simultaneous operation of the X-band SDST and TWTA during the powered descent and sky-crane portions of the descent.

The TDS hardware consists of the TDS Digital Stack (TDS), TDS RF Stack (TDSR), the RF power combiner and divider, and the antenna (TDSA). The block diagram shows the electrical interfaces among the TDS, TDSR, and the TDSA.

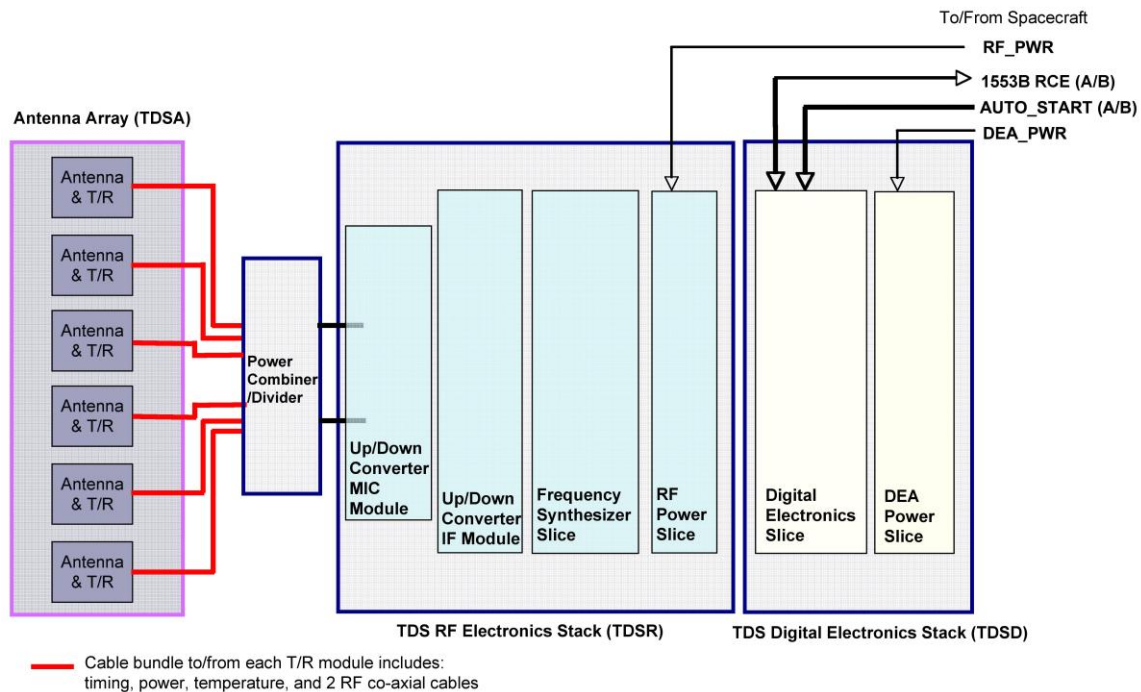


Figure 2-40. System overview block diagram of the TDS.

The TDSA consists of six separate antennas, each with its own front-end filter assembly (FFA) and transmit/receive module (TRM). Figure 2-41 shows the mechanical configuration of the TDS, with the locations of the electronic assemblies and the antennas.

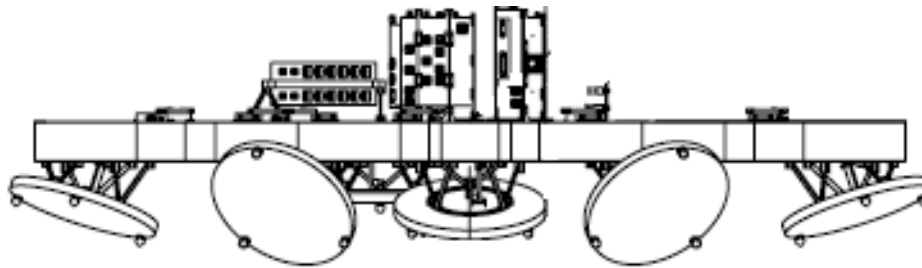


Figure 2-41. TDS antenna locations and pointing directions.

The TDS is a stack of two “slices” of electronic assemblies: the digital electronics assembly (DEA) slice and the digital power distribution unit (DPDU) slice.

The TDSR is a stack of four “slices” of electronic assemblies: the RF power distribution unit (RPDU) slice, the frequency synthesizer slice, the up/down converter intermediate frequency (IF) module (UDIM) slice, and the up/down converter MIC module (UDMM) slice.

The power slices supply conditioned direct current (DC) voltages to the electronic assemblies. The frequency synthesizer slice consists mainly of a voltage-controlled oscillator and supporting circuitry to generate the reference frequencies for the DEA slice and the RF electronics. The frequency upconverter generates the Ka-band pulse for the transmitter, and the frequency downconverter module converts the received signal down to video frequency for digitization.

The DEA serves as the controller and digital signal processor of the TDS. The DEA consists of a 1553 transceiver chip supporting 1553B command and telemetry transfers and a large (~ 1 mega gates) reprogrammable field-programmable gate array (FPGA), referred to as the radar processor (RP), for generating timing signals for the TDS and handling all the digital signal processing of radar data. A 12-bit ADC is utilized to digitize radar video signal with a bandwidth as high as 240 MHz. A radiation-hardened scalable processor architecture (SPARC) processor serves as the radar controller (RC); this item handles spacecraft commands, time tagging, post-processing, packaging of telemetry messages, and other functions.

The TDS cycles through the antenna beams, making measurements with the six antenna beams one at a time at 20 Hz (50-ms intervals). A limited number of beam sequences are pre-stored in the TDS memory and can be recalled by using a beam sequence table ID command. The use of the beam sequence allows the exclusion of an anomalous beam or a blocked beam.

In Normal mode, the TDS is set up to make line-of-sight velocity and range measurements at 20-Hz rate by cycling through the radar beams according to the specified beam-cycling pattern. The Normal mode of TDS operation includes Acquire, Dop1, and Dop2 dwells. A dwell consists of a group of radar pulses with identical radar parameters. The Dop1 and Dop2 dwells are executed only if a target was detected (valid range) in the Acquire dwell. In Dop1, the TDS determines the Doppler velocity by using the pulse-pair Doppler technique. In Dop2, the TDS uses a different inter-pulse period (IPP) to resolve the Doppler velocity ambiguity. We also determine the slant range in Dop2.

2.6 MSL Telecom Hardware Mass and Power Summary

2.6.1 X-Band Mass

Table 2-11. lists the current best estimate (CBE) masses for the major X-band telecom assemblies. The table is organized by the stages previously defined: cruise, EDL (combined parachute cone and descent), and rover.

Table 2-11. X-band telecom mass summary.

Spacecraft Stage	X-Band Subsystem Element	Quantity	Unit Mass (kg)	Total Mass (kg)
Cruise	MGA and adapter	1		0.65
EDL backshell	PLGA	1		0.4
	TLGA	1		0.4
	WTS	2	0.45	0.9
	Microwave components			2.8
EDL descent	DLGA	1		0.35
	Microwave components			2.5
EDL descent telecom plate	TWTA	1		2.5
	WTS	2	0.45	0.9
	SDST	1		3.0
	Telecom plate	1		6.6
	Microwave components			2.5
Rover X-band	SDST	1		3.0
	SSPA	1		1.4
	WTS	2	0.45	0.9
	RLGA	1		0.4
	HGA	1		1.4
	HGA gimbal	1		6.6
	Microwave components			3.7
TOTAL				40.9

2.6.2 X-Band Spacecraft Power Consumption

Table 2-12 summarizes the power consumption of the active subsystem elements (SDSTs and power amplifiers) at a nominal bus voltage of 28 V.

Table 2-12. X-band telecom spacecraft power consumption.

descent stage DC power consumption

Subassembly	Descent Stage Telecom Subsystem Mode	Nominal Bus Voltage (28.0 V)
DSDST	RX	11.4
	RX + Non-Coherent TX (TLM Only: SAFE_MODE)	14.7
	RX + Coherent TX (TLM Only: CRUISE_MODE)	14.4
TWTA	Preheating (standby)	4.6
	Quiescent (no RF drive) [exciter OFF]	62.4
	Operating (with RF drive) [exciter ON]	175.2

rover DC power consumption

Subassembly	Descent Stage Telecom Subsystem Mode	Nominal Bus Voltage (28.0 V)
RSDST	RX	11.3
	RX + Non-Coherent TX (TLM Only: SAFE_MODE)	14.8
	RX + Coherent TX (TLM Only: CRUISE_MODE)	14.2
SSPA	exciter OFF (no RF drive)	45.1
	exciter ON	62.9

The SDST values are indicated for receiver-only operation, receiver and exciter in the non-coherent mode, and receiver and exciter in the coherent mode. The exciter is required for a downlink, and the non-coherent mode also requires the auxiliary oscillator to be powered. Normally, one SDST at a time is powered.

The power amplifier values are for two modes: quiescent (the unit producing no RF output) and operating. When they are off, the units draw no power. Normally during cruise, the TWTA is outputting RF. During surface operations, the rover outputs RF from the SSPA or the SSPA is powered off.

2.6.3 UHF Mass and Power Consumption

The as-measured mass of the UHF radios is about 3 kg each.

The UHF coaxial transfer switches have a mass of about 130 gr. In operations, the switches are operated with a pulse duration of 0.2 s and can be operated in the range from 22 to 36 V. At 28 V, they will draw about 0.25 A and, therefore, consume about 7 W during the switch pulse.

The ELTs each draw about 21 watts in standby mode and about 69 W when transmitting.

2.6.4 TDS Power

The TDS has four power states²⁸:

- **Off** – Both power switches from the 28V spacecraft bus are open (no power to the TDS).
- **Low** – The power switch to the digital power distribution unit (DPDU) is closed while the power switch to the RF power distribution unit (RPDU) remains opened. At this lower power state, only the DEA is powered on and the RP (Xilinx²⁹ field programmable gate array (FPGA) is not running because there is no 1 GHz clock to the FPGA. The power draw in this state is about 30 W.
- **Quiescent** – Both power switches are closed, essentially powering up both the DEA and the RF electronics. The TDS is standing by where high-power amplifiers in the TRMs are properly biased but are not transmitting.
- **Full** – Radar timing is running in the RP and pulsing the TRMs to transmit RF power. The power usage is about 120 W.

²⁸ The TDS is powered off during cruise, except for self-checks when its other power modes are active for brief periods. The TDS modes are controlled by an onboard sequence during EDL.

²⁹ Xilinx, Inc. is the inventor of the field programmable gate array (FPGA). A field-programmable gate array (FPGA) is a semiconductor device that can be configured by the customer or designer after manufacturing—hence the name "field-programmable". FPGAs contain programmable logic components called "logic blocks," and a hierarchy of reconfigurable interconnects that allow the blocks to be "wired together"—somewhat like a one-chip programmable breadboard. (<http://en.wikipedia.org/wiki/Xilinx> and http://en.wikipedia.org/wiki/Field-programmable_gate_array)

3 Ground Systems

3.1 X-Band Operations: the Deep Space Network

This section illustrates and summarizes some of the main characteristics of the DSN of importance to MSL flight operations, particularly new capabilities not previously discussed in previous articles of this series. This section also briefly mentions the EDL Data Analysis (EDA) ground hardware and software that will be a rebuild of the nearly 10-year-old MER EDA.

In 2008, the DSN celebrated its 45th anniversary. The DSN currently includes ground stations, called Deep Space Stations (DSS), at three Deep Space Communications Complexes (DSCC) around the world:

- CDSCC near Canberra, Australia
- MDSCC near Madrid, Spain
- GDSCC at Goldstone in the California desert.

Figure 3-1, from [23], is an aerial view of the Canberra complex showing the 70-m and 34-m stations. This document also has photos of other DSN sites and their stations.

Each site³⁰ includes a complement of 34-m stations, referring to the diameter of the antenna in meters, and one 70-m station. Individual stations at a site may be arrayed together to provide more downlink margin (and currently experimentally also for the uplink). Each site also has a central control hub with operators who communicate with DSN control in Pasadena, California and with each mission's control center during tracking support of that mission.

The MSL mission intends to use single (non-arrayed) 34-m stations for most purposes. The 70m stations can be scheduled for mission activities requiring their greater capability, such as to reduce the time to uplink major command loads (by using as much as four times the data rate achievable by a 34-m station) or to receive the downlink when the vehicle is in safemode using its low gain antenna.

Though many of the stations provide receive or transmit capability at lower and higher carrier frequencies, MSL's SDSTs can use only the DSN's X-band uplink and downlink capability.

The 34-m beam waveguide (BWG) antennas are the latest generation of antennas built for use in the DSN. These antennas differ from more conventional antennas (for example, the 34-m high-efficiency [HEF] antennas also used for tracking MSL) in the fact that a series of mirrors, approximately 2.4 m in diameter, direct microwave energy from the region above the main reflector to a location in a pedestal room at the base of the antenna. The pedestal room is located below the azimuth track of the antenna and is below ground level.

³⁰ The Canberra site's antennas are designated by two-digit numbers in the 30s and 40s, the Madrid site in the 50s and 60s, and the Goldstone site in the 10s and 20s. Though not pertinent to MSL, each site also has antennas with diameters other than those described here.



Figure 3-1. Canberra Deep Space Communications Complex (CDSCC) showing 70-m and 34-m stations.

The capabilities of each antenna differ significantly depending on the microwave, transmitting, and receiving equipment installed. For X-band, the stations can receive either right circular polarization (RCP) or left circular polarization (LCP), and they can transmit at the same or the opposite polarization as is configured for receiving. In most modes, MSL transmits and receives RCP. In all cases, the downlink and uplink are the same polarization at the spacecraft at a given time. The normal configuration for a tracking station is its diplexed mode, which allows for simultaneous uplink and downlink with MSL. Some newer 34-m BWG stations do not require use of an actual diplexed mode for simultaneous uplink and downlink, and their receiving system noise temperature is accordingly lower.

Prediction of MSL link capability takes into account the configuration of the tracking station and time-varying factors, such as elevation angle and the spacecraft antenna angle to the station. As

has been done for other deep space missions, MSL and the DSN will develop an initial acquisition plan that includes managing the “hot downlink” to the station and the strong uplink at the SDST receiver caused by the relatively small spacecraft-station distance.

Figure 3-2, from [24], is a block diagram of one of the 34-m BWG stations (DSS-24). This station has recently implemented an X-band acquisition aid system, as shown in the “new” red box at the top, including a separate 1.2-m antenna aligned with the main dish. The broader beamwidth of this antenna increases the probability of a quick acquisition of the MSL cruise stage downlink after launch, and this acquisition will be used to orient the main antenna to the actual spacecraft location. The acquisition aid capability does not include uplink; therefore, the 20-kW transmitter will operate at 200-W output through the main antenna for uplink.

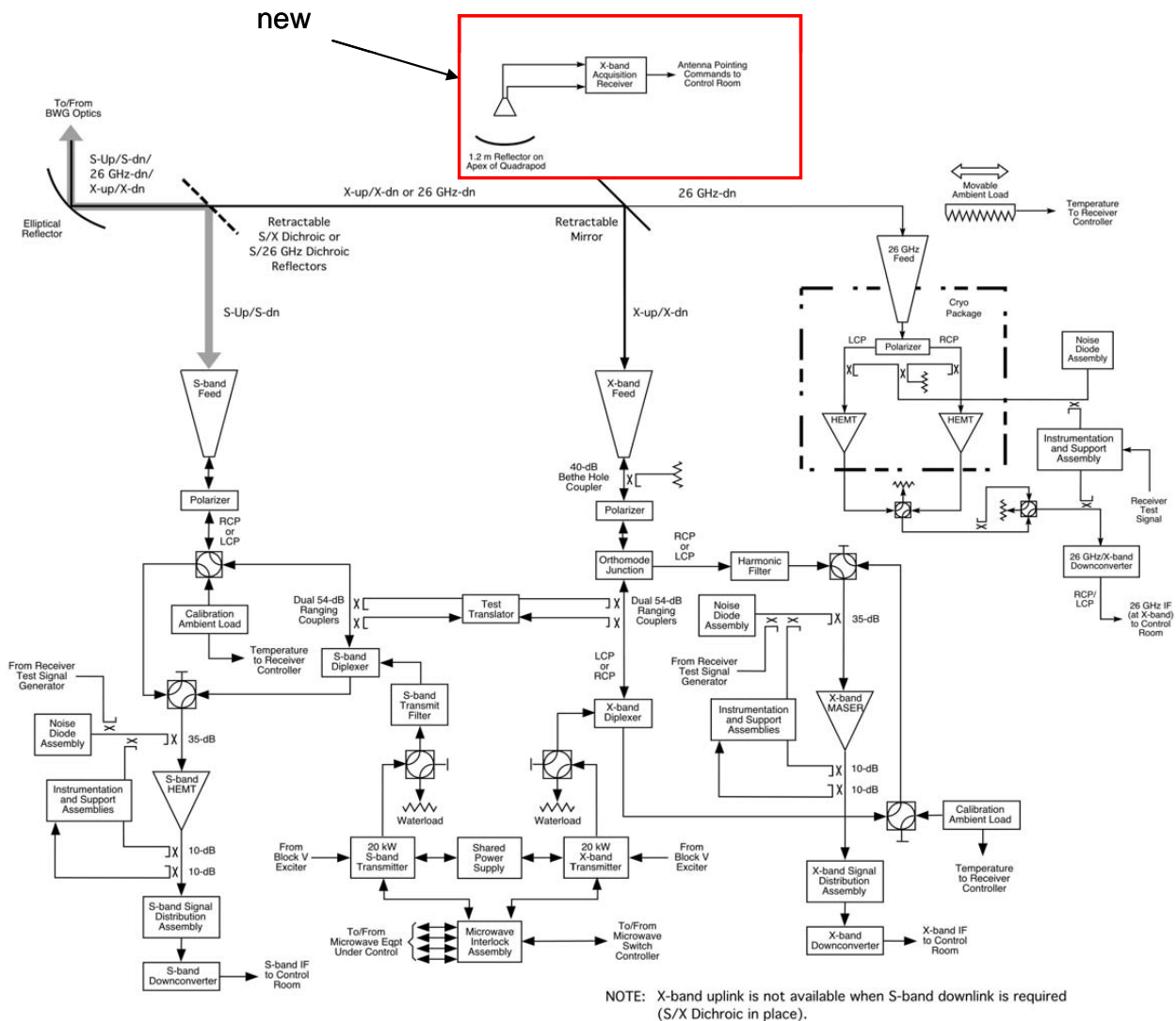


Figure 3-2. Block diagram of DSS-24 station at Goldstone.

Because of the station antennas' narrow beamwidths (hundredths of a degree), control of the antenna pointing is customized³¹ to meet the requirements and constraints of the MSL mission. For most tracking conditions, MSL will use the conical scanning (conscan) mode. This depends on developing an error signal while tracking a stable carrier downlink as the antenna moves in a small cone about the nominal direction. The MSL downlink carrier may vary in level over the short term, such as during TCM turns or with some near-Earth strong-signal modulation conditions. At these times, the station is instructed not to use conscan, and control relies solely on predicted pointing angles delivered to the station prior to the track³².

Through a series of improvements made in the processing of turnaround ranging, the DSN now specifies a threshold downlink ranging power to noise spectral density ratio (Pr/No) of -20 dB-Hz. A decade ago, project navigation teams counted on ranging only when the Pr/No was greater than about -8 dB-Hz. MSL requires the lower threshold for ranging during cruise (Section 4).

3.2 EDL Operations: EDL Data Analysis (EDA)

EDL is a critical and the most anticipated communications mission phase. Obviously, for purposes of redundancy and signal diversity, all possible communications paths will be used to their fullest extent. Both X-band and UHF will be on. The DSN will be operating with multiple redundant antennas. The UHF will communicate with the MRO as primary, but UHF assets on Earth, such as the Greenbank Observatory³³ in West Virginia, USA, could also be involved in tracking the carrier.

In addition to the standard closed loop receivers, the DSN antennas will also be connected to a special EDL Analysis (EDA³⁴) system that performs fast Fourier transform (FFT) signal processing on the signal captured by the open-loop radio science recorder (RSR) receivers. The EDAs built for MER (an example is shown in Figure 3-3) were constructed as parallel processing arrays and are mostly inoperative now due to age and neglect.

Refer to the Mars Exploration Rover article in this series [6]. Also a NASA Tech Brief [25] documents the MER EDA, described as a system of signal-processing software and computer hardware for acquiring status data conveyed by M-FSK tone signals transmitted by a spacecraft during descent to the surface of a remote planet.

³¹ The DSN is also developing a monopulse tracking capability, initially at Ka-band where the antenna beam is much narrower and the conscan motion would cause significant pointing loss.

³² The conscan system functions properly only when the carrier-signal received-power variation conscan causes (by station antenna movements) is not confused in the conscan algorithm with variation from external causes such as the TCM.

³³ Greenbank's UHF capability was last used for the Phoenix EDL. The Greenbank Observatory has a 100-m fully steerable radio telescope and a cryogenically cooled front-end. <http://www.gb.nrao.edu/GBT/GBT.shtml> provides more information.

³⁴ The RSR is a system for carrier and tone detection and tracking, specially developed for MER for the high Doppler-dynamics and low-SNR environment of EDL. It will be adapted as needed for MSL.

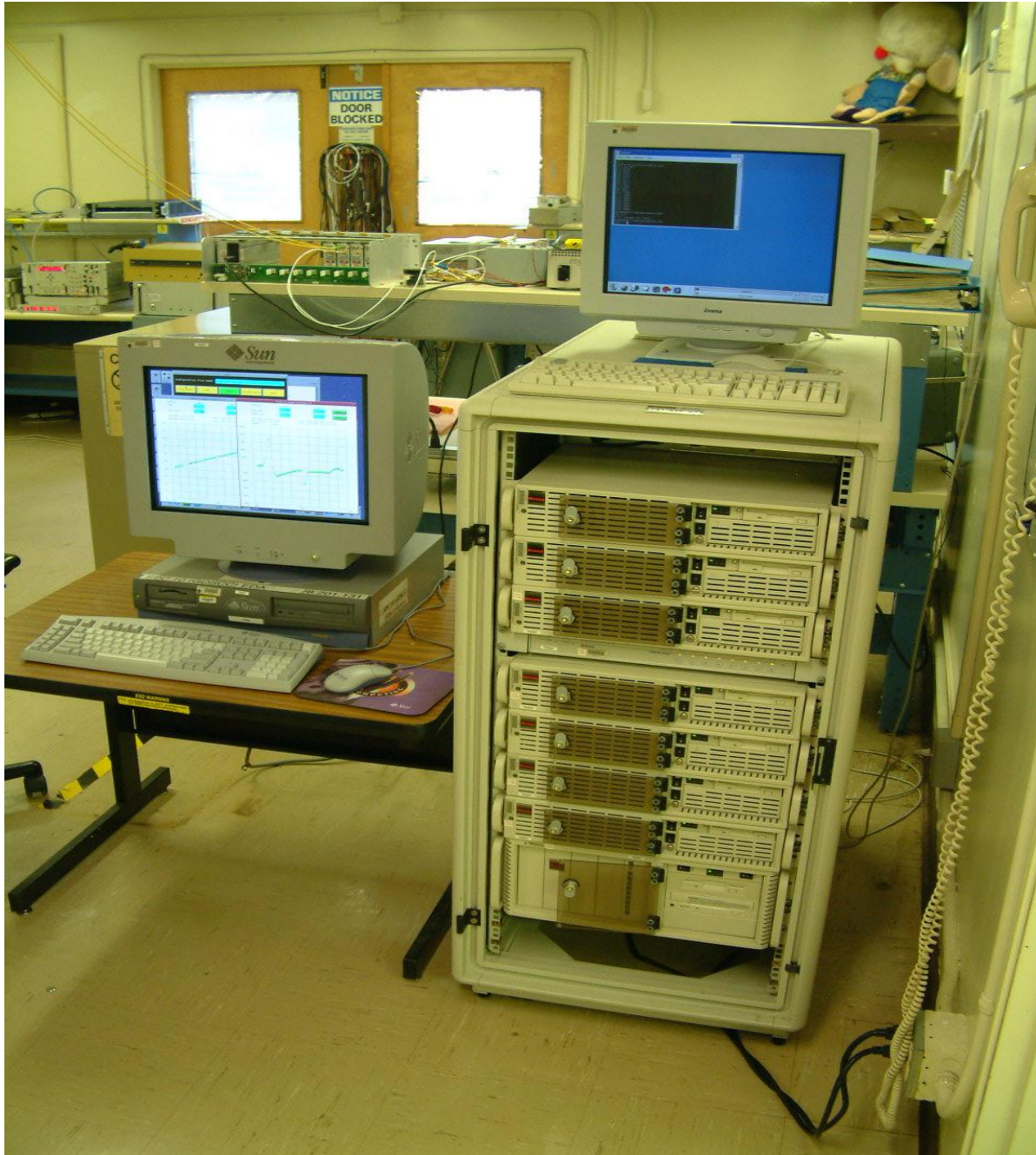


Figure 3-3. MER EDA computer array.

The design of the EDA meets the challenge of processing weak, fluctuating signals that are Doppler-shifted by amounts that are only partly predictable. The software supports both real-time and post processing. The software performs fast-Fourier-transform integration, parallel frequency tracking with prediction, and mapping of detected tones to specific events. The use of backtrack and refinement parallel-processing threads helps to minimize data gaps. The design affords flexibility to enable division of a descent track into segments, within each of which the EDA is configured optimally for processing in the face of signal conditions and uncertainties. A dynamic-lock-state feature enables the detection of signals using minimum required computing

power: less power when signals are steadily detected, more when signals fluctuate. The hardware is modular, making it possible to increase computing power by adding computers.

The purpose of the EDA built for MER was to take the measured signal data stream from the radio science receivers (RSR) at the DSN stations (Goldstone and Canberra) and resolve the frequency of the successive transmitted tones³⁵ throughout the EDL phase. For MER, the EDAs were co-located at the DSN stations, and only the results were transmitted back to JPL in real time for immediate evaluation. An upgrade to the DSN network system since the MER EDL event will allow the MSL EDAs to be located at JPL, rather than co-locating them at the DSN complexes.

MSL has undertaken an EDA rebuild to use modern computer hardware and the latest Linux operating system. For the 2011 MSL launch, work on rebuilding the EDA for MSL has been postponed until FY10 at the earliest. The MSL mission will adapt the MER EDA software with very few changes, apart from porting the software to the new computers. Minor improvements that are planned include the ability to modify parameters (such as the integration times). The user interface will also be upgraded and improved.

A forthcoming DESCANSO article on MSL telecom operations, planned for release after the surface mission begins in late 2012, will describe the MSL EDA and the results of its operations.

³⁵ On MER, each tone lasted 10 seconds, and represented certain pre-determined nominal or off nominal states of the entry vehicle. (On MER, the raw data stream from the RSR was also recorded on site for future analysis).

4 Telecom Subsystem Link Performance

4.1 X-Band

4.1.1 Cruise Link Performance

Telecom performance prediction and analysis plays a major role during cruise and approach. In particular, many of the checkout and subsystem maintenance activities scheduled during these mission phases require relatively high telemetry data rates with the consequent low link margin.

There are five main X-band functions: downlink carrier tracking, uplink command, downlink telemetry, differential one-way ranging (delta-DOR), and turnaround ranging. Because the turnaround ranging signal levels, may be low relative to threshold (especially on the downlink), ranging is the most difficult of the functions to achieve.

Sequential ranging is a two-way measurement. Ranging is degraded by three sources of thermal noise:

- Noise on the uplink (from the finite SNR on the uplink).
- Noise in the transponder ranging channel.
- Noise in the station receiver.

Of these, the noise in the ranging channel is the largest contributor because of the channel's bandwidth. The double-sided bandwidth is 3 MHz, adequate to pass a ranging waveform that has a clock-component fundamental frequency of 1 MHz. The receiver noise results from a relatively low spacecraft transmit power and consequently low SNR.

Fortunately, the DSN can now process ranging samples at signal levels as low as Pr/No of -20 dB-Hz, albeit at the cost of integration times that increase as Pr/No decreases. Figure 4-1. shows that the collection of each ranging point (the cycle time) becomes very large as the Pr/No goes below -10 dB-Hz. Cycle time is defined in the ranging module [24] of the *DSN Telecommunications Link Design Handbook*. Cycle time is given by the equation:

$$\text{Cycle time in seconds} = T1 + 3 + (L - C) * (T2 + 1)$$

where $T1$ is the integration time of the clock component and

$T2$ is the integration time of each of the other components,

L is the component number of the last (lowest frequency) ambiguity resolving component, and

C is the component number of the range.

During the cruise mission phase, the telecom lead on the Spacecraft Team will interact several times with the Navigation Team lead and with the DSN to define suitable ranging integration times $T1$ and $T2$ to use for the next series of tracking passes. These times are not only a function of the changing Pr/No but also of factors such as the change in round-trip light time (RTLTL) during a maximum-duration station pass and the ambiguity resolution required.

Tcyc vs Pr/No, sigma 3m, Pacq 99%

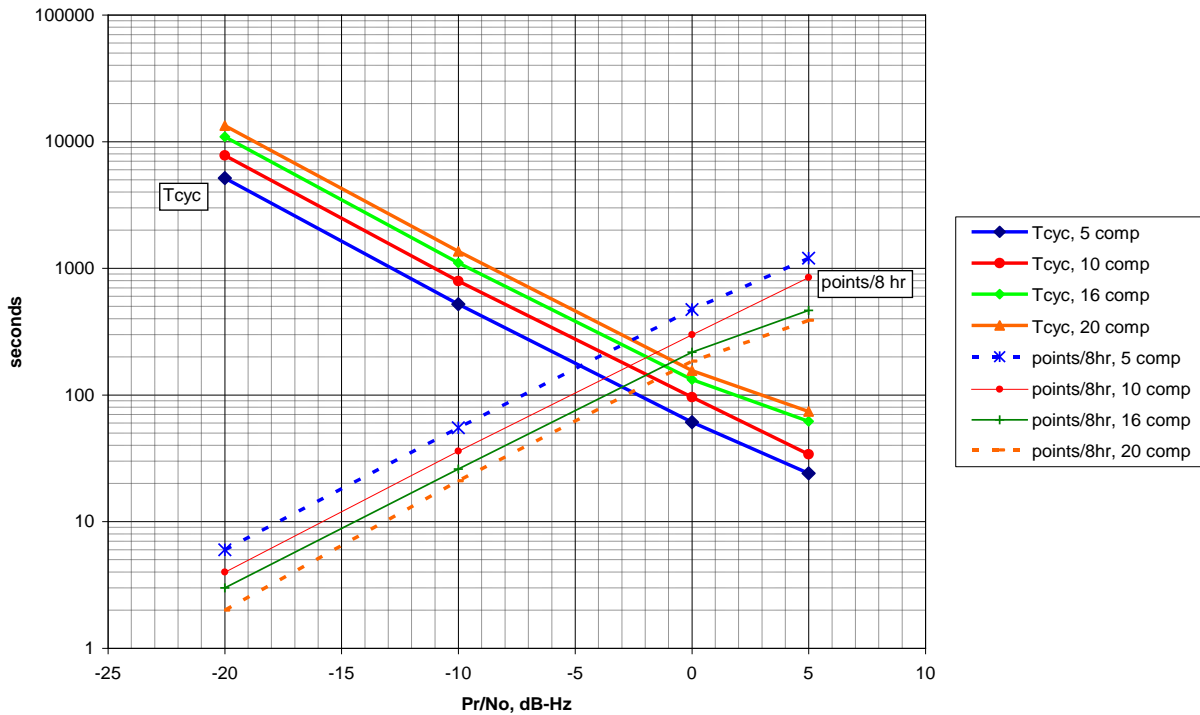


Figure 4-1. Required ranging cycle time as a function of Pr/No.

The Pr/No available at a given time and station/spacecraft geometry and configuration can be increased by:

- Increasing the uplink ranging modulation index.
- Increasing the downlink ranging modulation index.
- Lowering the telemetry modulation index (or even turning telemetry off).
- Increasing the ground station size from 34 m to a 70 m.

In early cruise, while the spacecraft is on the PLGA, the $-Z$ axis must be pointed within 80 deg of Earth to provide telecom coverage, as discussed relative to off-boresight angle (SPE angle for the PLGA) in section 1.3 and shown in Figure 1-15. Beyond 80 deg, significant scattering off the spacecraft makes antenna pattern modeling for prediction unacceptably unreliable.

At a spacecraft distance of approximately 0.2 AU from Earth (typically around 3 months after launch), the ranging performance drives a telecom configuration change from the PLGA to the MGA. Pointing requirements on the MGA are significantly tighter, as the Earth must be within 15 deg of the $-Z$ axis immediately after the transition from the PLGA and to 9 deg later in the cruise.

The telecom subsystem capability drives much of the scheduling of station coverage during cruise, as key events require 70-m coverage to satisfy real-time data rate requirements or additional 34-m coverage to return larger data volumes.

Figure 4-2 is a prediction of uplink data rate capability from launch to Mars arrival. The figure is for a launch at window-open (Day 1) for a type II trajectory as the most challenging for telecom capability. The 2-kbps maximum rate shown is the highest that the SDST can support.

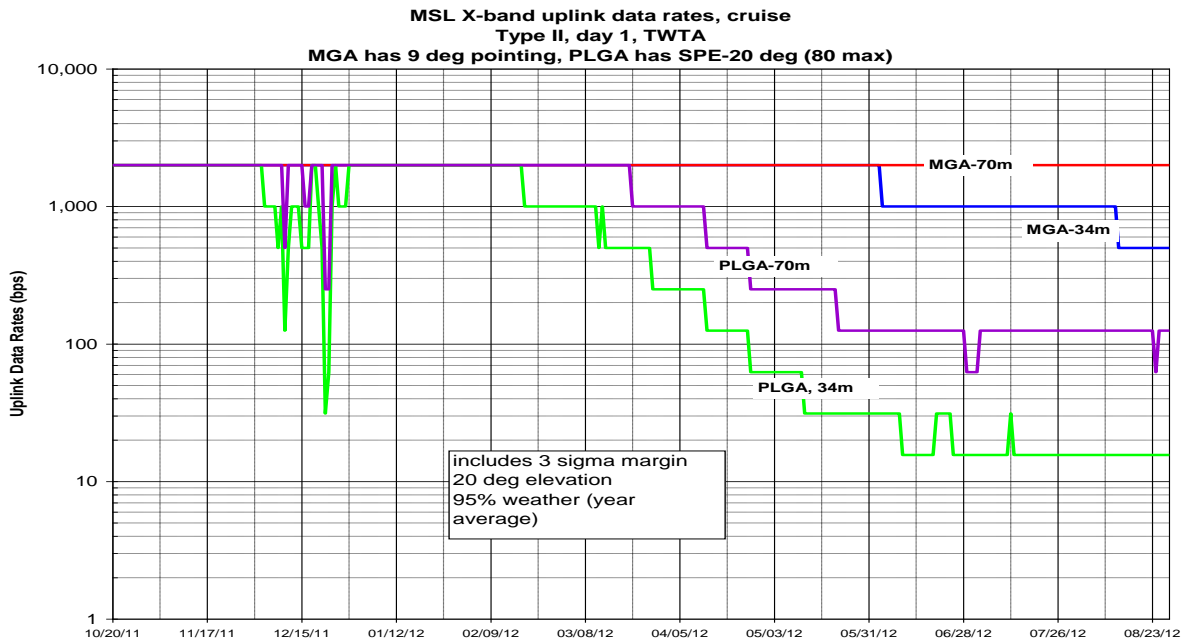


Figure 4-2. MSL X-band uplink data rates during cruise, type II day 1.

Figure 4-3 shows the corresponding set of predictions for the downlink data rates. MSL can produce telemetry rates higher than the maximum 10 kbps shown, but this is the highest that is required for cruise.

The pointing conditions for each antenna in each figure are indicated. Given this pointing, the stair-step fall-off in capability is due to going through thresholds for each bit rate as the Earth-spacecraft distance steadily changes.

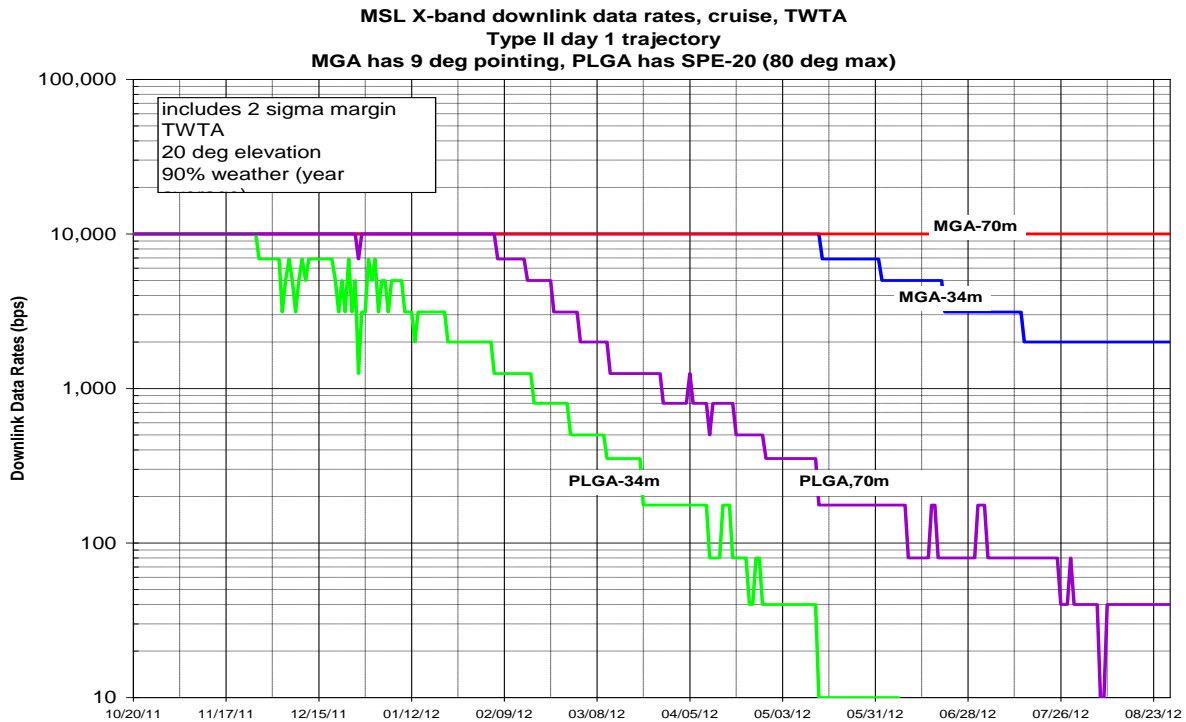


Figure 4-3. MSL X-band downlink data rates during cruise, type II day 1.

Figure 4-4 shows the ranging capability for the same conditions as the preceding uplink command and downlink telemetry figures. The figure has the following purposes:

- To show the flexibility available in controlling the ranging performance depending on the link configuration. MSL might use either of the cruise antennas, might change the ranging modulation index on either the uplink or downlink, or might turn the telemetry modulation off.
- To introduce a new term “IR” meaning ‘improved ranging’. IR is shorthand for a mode that:
 - Sets the station uplink ranging mod index to 5 dB carrier suppression, the highest available.
 - Configures the SDST downlink ranging modulation index at 35 deg.
 - Decreases the telemetry modulation index to 45 deg.
- To introduce a second new term ‘RM’ meaning ‘ranging max.’ RM does everything to maximize ranging performance. RM differs from IR in that RM:
 - Sets the SDST ranging modulation index to its highest value of 70 deg, and turns off the telemetry modulation,.
 - Turns off the station command modulation, with the station ranging mod index set to 5-dB carrier suppression.

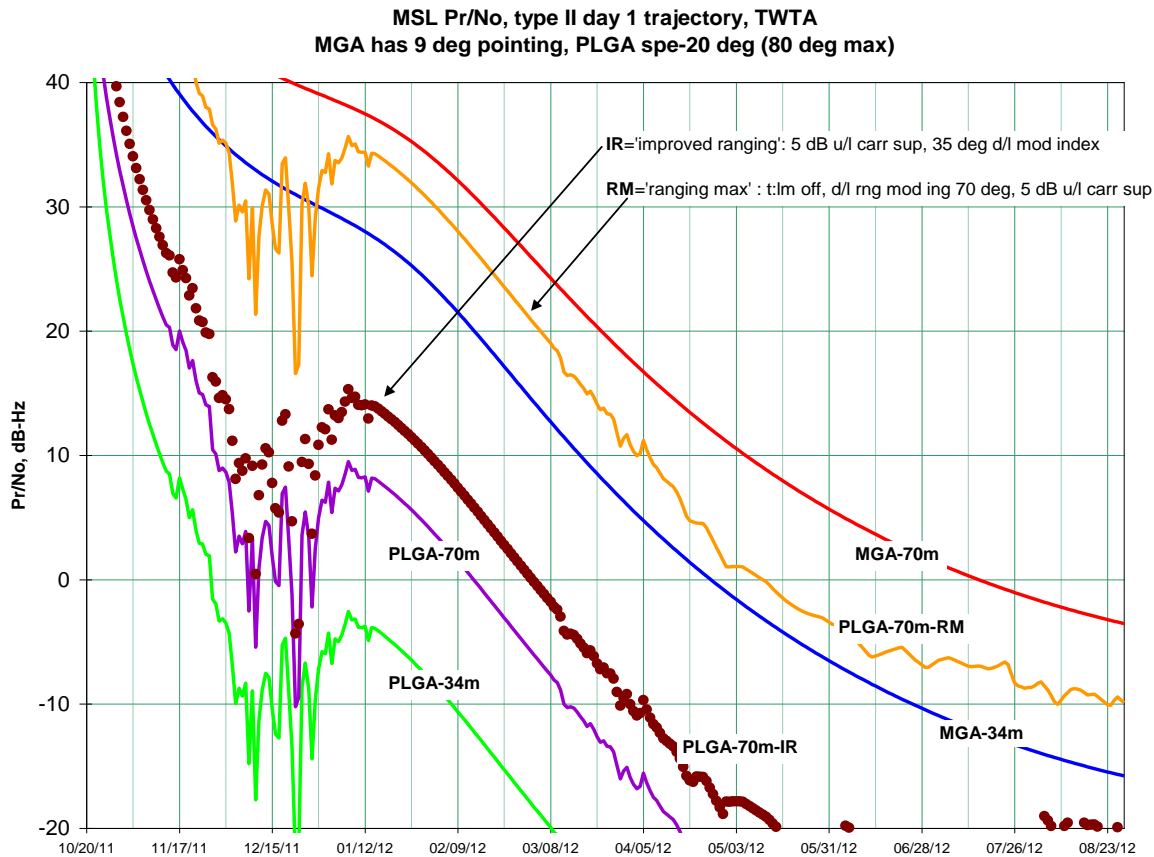


Figure 4-4. MSL X-band ranging Pr/No during cruise, type II day 1.

Except for RM, these ranging configurations account for the possibility that the station uplink command modulation might be required simultaneously with ranging at any time³⁶. These configurations guarantee commandability and ranging capability together. If a particular pass does not require commandability, it might be possible to make additional trades among link usages, operating with standard ranging instead of IR (but with command off), or operating with IR rather than RM (but with command off).

4.1.2 EDL (X-Band) Performance

During the EDL phase, the X-Band subsystem will transmit information to Earth concerning the state of the spacecraft in the form of discrete frequencies (so-called MFSK tones). Each tone, also referred to as a semaphore, is actually an unmodulated subcarrier of the normal SDST transmitted signal. In operations, the SDST telemetry mode is set to “TLM_OFF,” which means the normal telemetry stream from the EH&A will not modulate the outgoing signal. The FSW sets the subcarrier frequency to the appropriate value for the event information to be transmitted. Each timeline segment of EDL has its unique event schedule (parachute deployment, for

³⁶ Use of command together with ranging on the uplink (compared with use of one or the other) typically (1) reduces command performance by the decibel amount of the uplink ranging suppression and (2) reduces ranging performance as a function of the uplink carrier suppression.

example), and each segment will have a unique set of nominal and off nominal tones. The collection of tones, of which 256 are available, constitutes the MFSK dictionary³⁷.

The geometry of EDL is challenging for DTE links, with large view angle variations during the descent. The plot in Figure 1-22 illustrates the type of angle variation we can expect for DTE for nominal operations. Because the RTL is significantly longer than the EDL duration, EDL is entirely pre-programmed. Observers on the Earth are simply along to observe the ride that starts after all the actions have been completed at Mars. Consequently, the real value and purpose of EDL communications (besides public outreach) is to permit reconstruction in the event of a failure.

To observe EDL as it plays out over the varying Earth view angle, we are forced to use a series of spacecraft low-gain broadbeam antennas: the PLGA, TLGA, and DLGA. Each is essentially an open-ended waveguide antenna, with the PLGA and TLGA having added parasitic dipoles to broaden the beams even more off boresight.

The ground detection system consists of the DSN antennas and radio science receivers, which record and pipe the raw received signal to the EDA computers. The EDA does the spectral analysis on the signal and extracts the tones from the noise. Figure 4-5 shows the EDA configuration at a station complex (for example, Goldstone) as used for MER: several RSRs recording data from several antenna assets and feeding data to the EDAs. As the diagram shows, the distribution of signals to the RSRs (dotted lines) is at IF via the full spectrum processing (FSP) subsystem³⁸. The diagram shows the Mars Global Surveyor (MGS) spacecraft as the relay orbiter.

³⁷ Multiple-frequency-shift keying (MFSK) is a variation of frequency-shift keying (FSK) that uses more than two frequencies. MFSK is a form of M-ary orthogonal modulation, where each symbol consists of one element from an alphabet of orthogonal waveforms. M, the size of the alphabet, is usually a power of two so that each symbol represents $\log_2 M$ bits. Like other M-ary orthogonal schemes, the required Eb/No ratio for a given probability of error decreases as M increases without the need for multisymbol coherent detection. In fact, as M approaches infinity the required Eb/No ratio decreases asymptotically to the Shannon limit of -1.6 dB. (http://en.wikipedia.org/wiki/Multiple_frequency-shift_keying)

³⁸ Distribution of telemetry and Doppler signals is via a separate IF switch to the Downlink Tracking and Telemetry (DTT) subsystem.

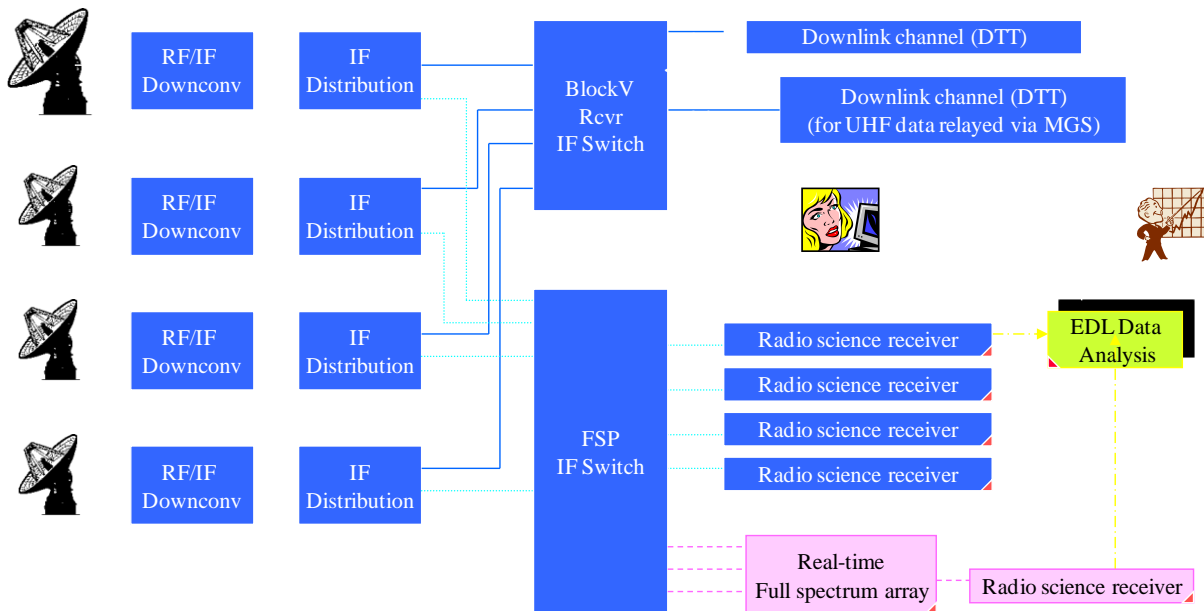


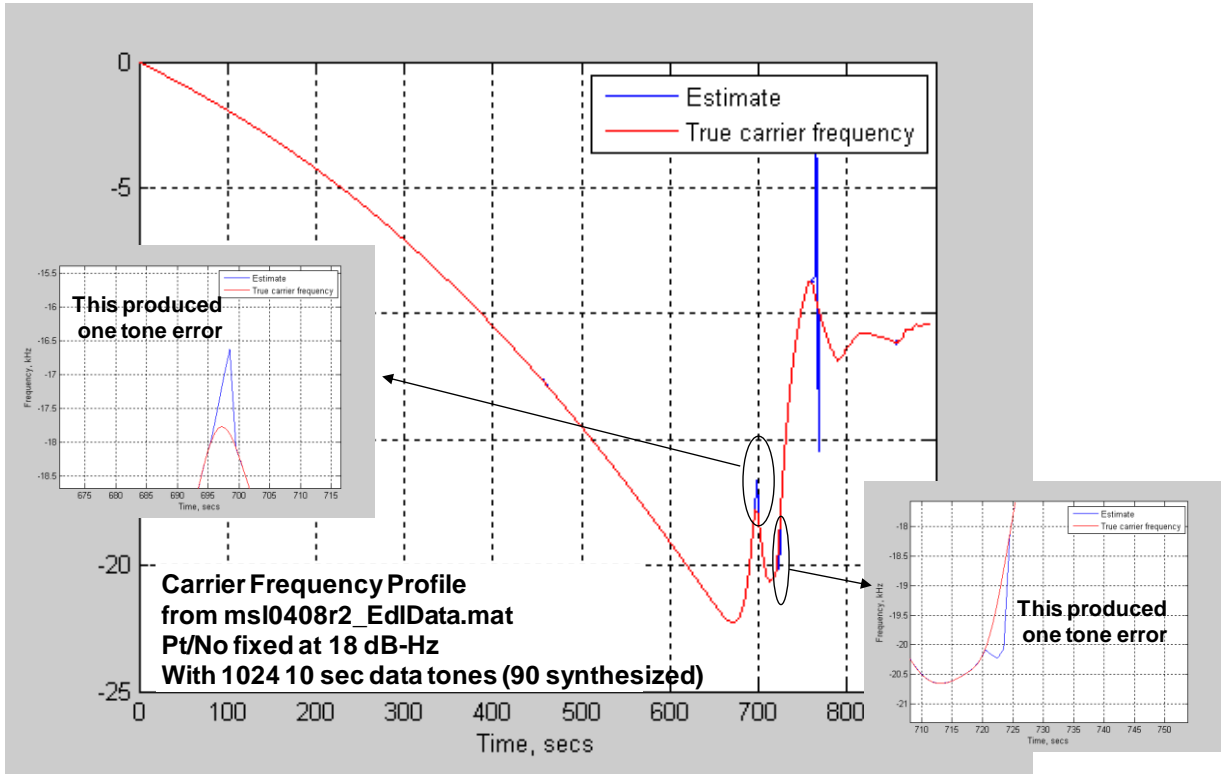
Figure 4-5. Configuration example of EDAs at DSN for EDL support.

As mentioned earlier, for MSL we might not need to co-locate the EDAs at the DSN complexes as was done for MER; in this case, the connections from the stations to the EDAs would be via the network to JPL.

To maximize the number of semaphore tones reliably detected, we would like as much off-nominal coverage and, therefore, far off-boresight coverage, as possible. Prior to the EDLs of the two MER rovers in January 2004 and again in the early studies for MSL, much analysis was performed to quantify the SNR levels that could be expected to produce acceptable tone detection probabilities. Figure 4-6 shows an example analysis simulation where challenging high Doppler events cause tones to be missed. For MSL EDL, such events might include the parachute deployment and the divert maneuver, when large Doppler rates and high off boresight angles occur.

When the SNR is strong, the job is easy. When the angles are far off boresight or the Doppler environment is challenging (such as when the Doppler rates and higher derivatives are large), the task becomes difficult or, in some cases, impossible. It is possible to array the DSN antennas during EDL to maximize the probability of tone detection if we expect difficulties in detection. DSN antenna arraying is being studied for MSL use.

**Carrier frequency tracking results using: 5 Hz FFT and 1.0 secs update with T = 1 sec integration
(with correctly interpolated Doppler profile and the nominal rate search space: +/- 40 Hz/sec)**



Note: Missed tones 70 (690-700 secs) and 73 (720-730 secs)

Figure 4-6. EDA analysis example showing missed tone cases.

Nevertheless, in some cases, and assuming nominal entry profile, the DTE signal is predicted to be reasonably strong, such as in the case shown in Figure 4-7, for the Gale landing site. (Figure 1-6 characterizes the 2009-selected landing sites, with Gale being the second listed at 4.5 deg South latitude. Use of the Gale site here is based on a 2009 launch profile, but it is representative of similar examples for the 2011 launch trajectories.)

In this example, we see the pre-entry period has a sufficiently strong DTE signal, near the 30 dB-Hz level, well above the low dynamics threshold for high-probability correct detection. This period also has very low Doppler rates, and therefore the Doppler predictions, are expected to be accurate. The left halves of Figure 4-7, Figure 4-8, and Figure 4-9 show, respectively, the signal level, the Doppler frequency, and the Doppler rate during this “low dynamics” period. In this relatively benign environment, DTE should be easily achievable.

In the subsequent “high-dynamics” period, shown in the right halves of these figures, the relayed UHF return link is expected to be the more reliable signal.

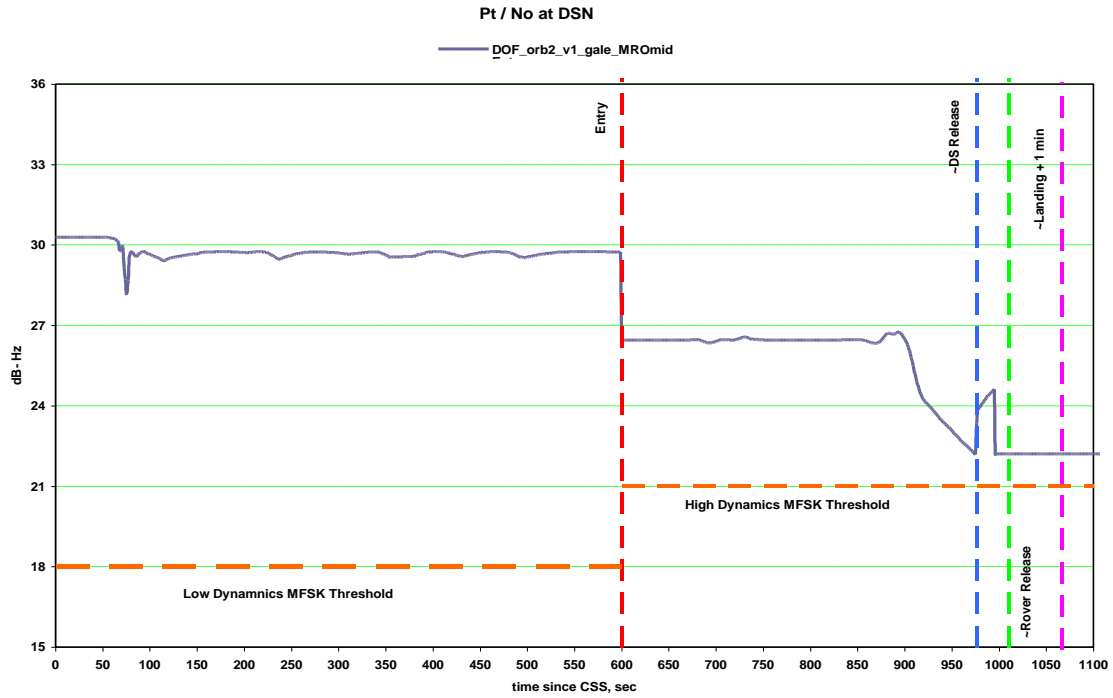


Figure 4-7. DTE Pt/No Gale site, 2009 launch.

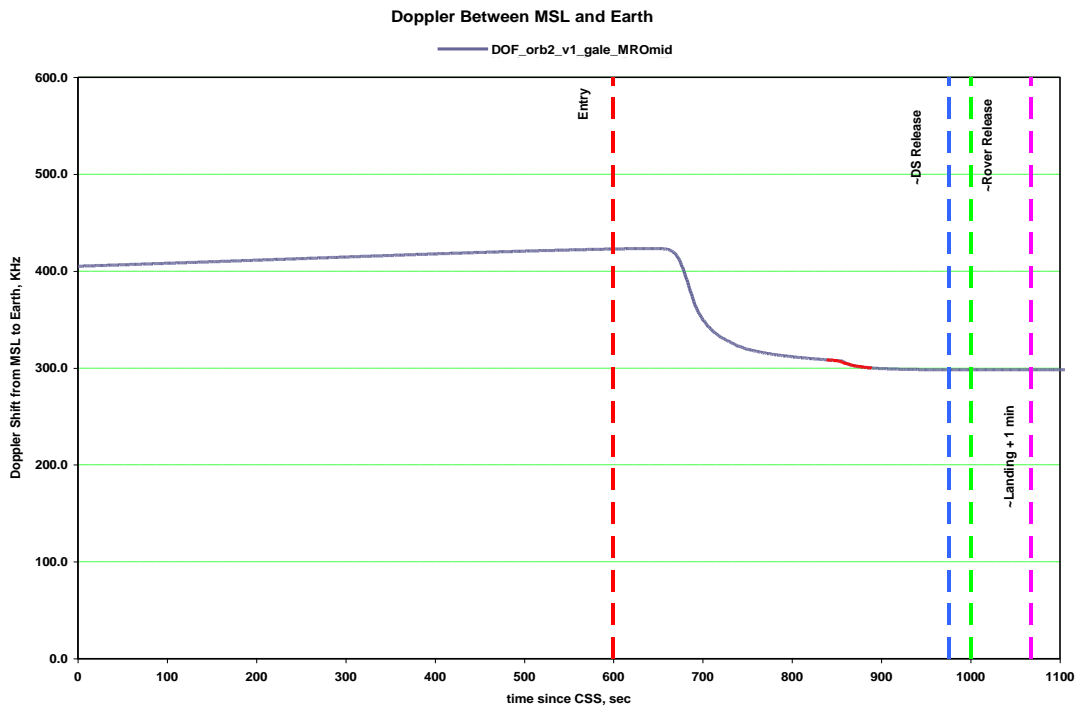


Figure 4-8. DTE Doppler Gale site, 2009 launch.

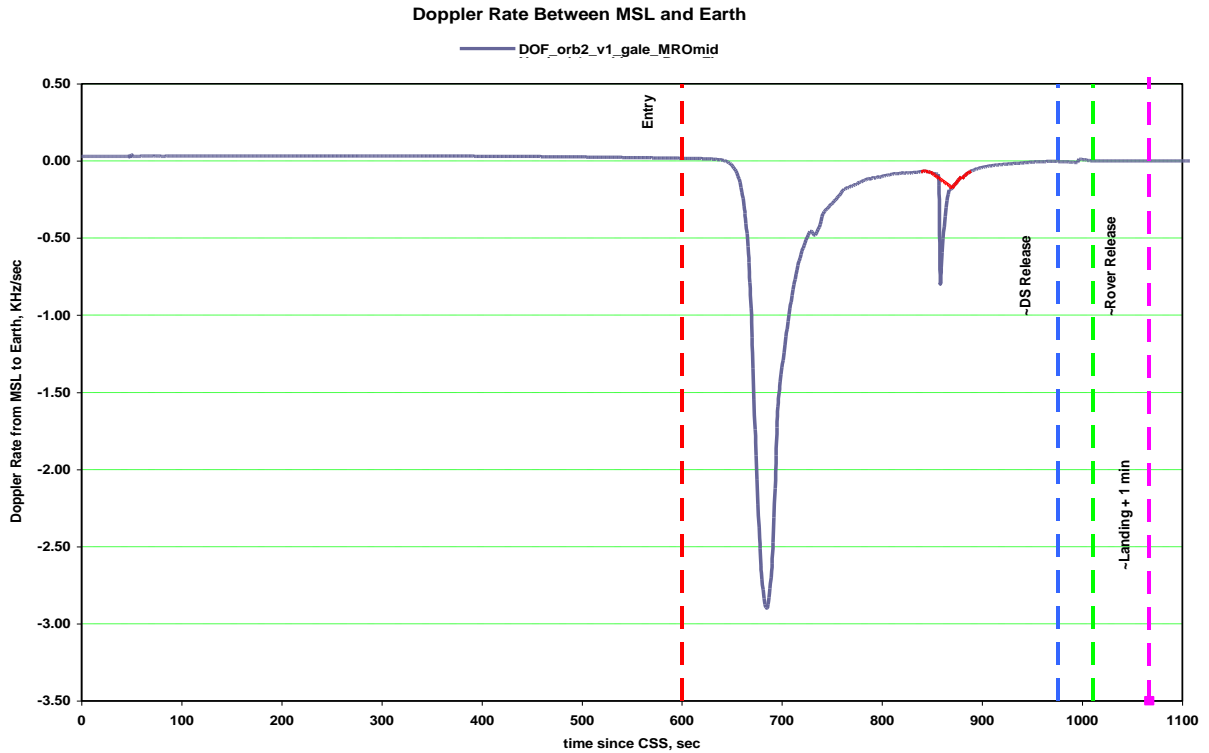


Figure 4-9. DTE Doppler rates Gale site, 2009 launch.

After entry, the large deceleration during hypersonic entry produces large Doppler rates (shown in Figure 4-9), and the view angles also become challenging. It is desirable to have reliable DTE during the period of UHF plasma blackout, which coincides with the large deceleration period. The DTE reliability, however, will depend largely on the accuracy of the profile predictions, for the receiver to be able to compensate for the Doppler changes.

Some of the landing sites will not have coverage all the way to landing + 1 minute simply due to the Earth setting below the horizon. This will also depend on the launch date.

4.1.3 Surface Performance (X-Band)

Throughout surface operations, the X-band requirements are met for:

- Data return from the HGA (160 bps at max range, 34-m BWG station, 5-deg HGA pointing error).
- Command capability via the HGA (225 kbps in 20 min, equivalent to a 190 bps uplink rate, via a 34-m, with 5-deg HGA pointing error).
- Emergency command capability via the RLGA (7.8125 bps uplink rate via a 70-m, assuming the Earth is 70 deg off the RLGA boresight).

X-band DFE uplink can be used to receive command sequences each morning, and DFE is expected to be the primary means of receiving uplinked commands. X-band communication sessions include allowance for a 15-minute preparation period to set up the communication window and a 10-minute rover activity keep-out afterwards for post-pass processing.

X-band DTE downlink can be used to send limited amounts of data to Earth independent of the relay orbiters.

DFE and DTE communications are often combined into a single pass station pass, with the pass duration made long enough to accommodate verification of DFE commanding in the DTE telemetry that follows, accounting for RTL T.

Figure 4-10. shows how uplink performance varies with time for the HGA and also with off-Earth angle for the RLGA. The DFE command data rate capability for 34-m and HGA never falls below 500 bps. In contrast, the 34-m/RLGA capability dips as low as 15.625 bps at larger Earth-Mars ranges, assuming a 40-deg off-boresight angle and as low as 7.8125 bps at a 70-deg off-boresight angle. With a 70-m station scheduled, the RLGA DFE capability is always at least 31.25 bps³⁹. Note that the “40-deg” and “70 deg” refer to different off-boresight angles.

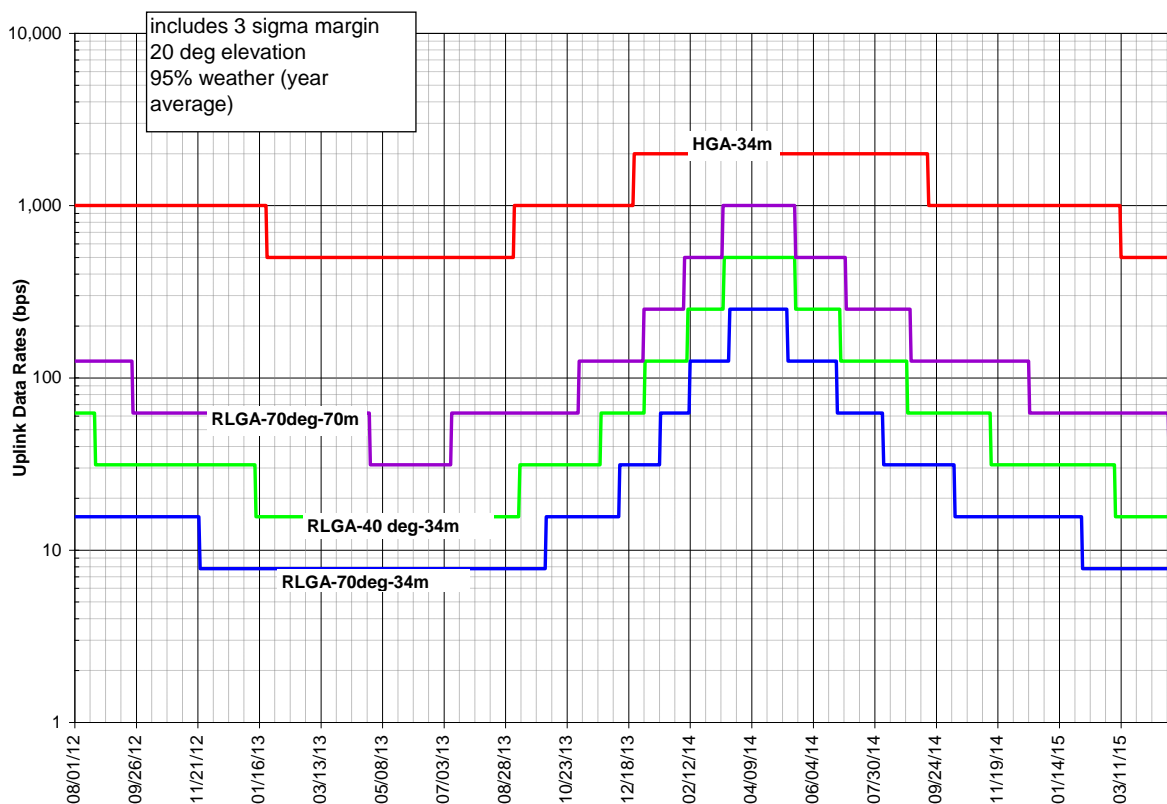


Figure 4-10. X-band uplink data rates, Mars surface.

Figure 4-11. shows how limited the X-band DTE downlink capability is; essentially, there is only an X-band downlink if the HGA is available.

³⁹ X-band surface communications, unlike cruise, assumes that turnaround ranging is never required – we know where Mars is and have other means of determining more accurately than ranging where the rover is on Mars. Therefore, these DFE command rate capabilities assume only command modulation is on the uplink.

Figure 4-12. shows that downlink Pt/No via the RLGAs is too low to support even the minimum 10 bps downlink rate at high elevation angles over a significant fraction of the Earth-Mars ranges during surface operations.

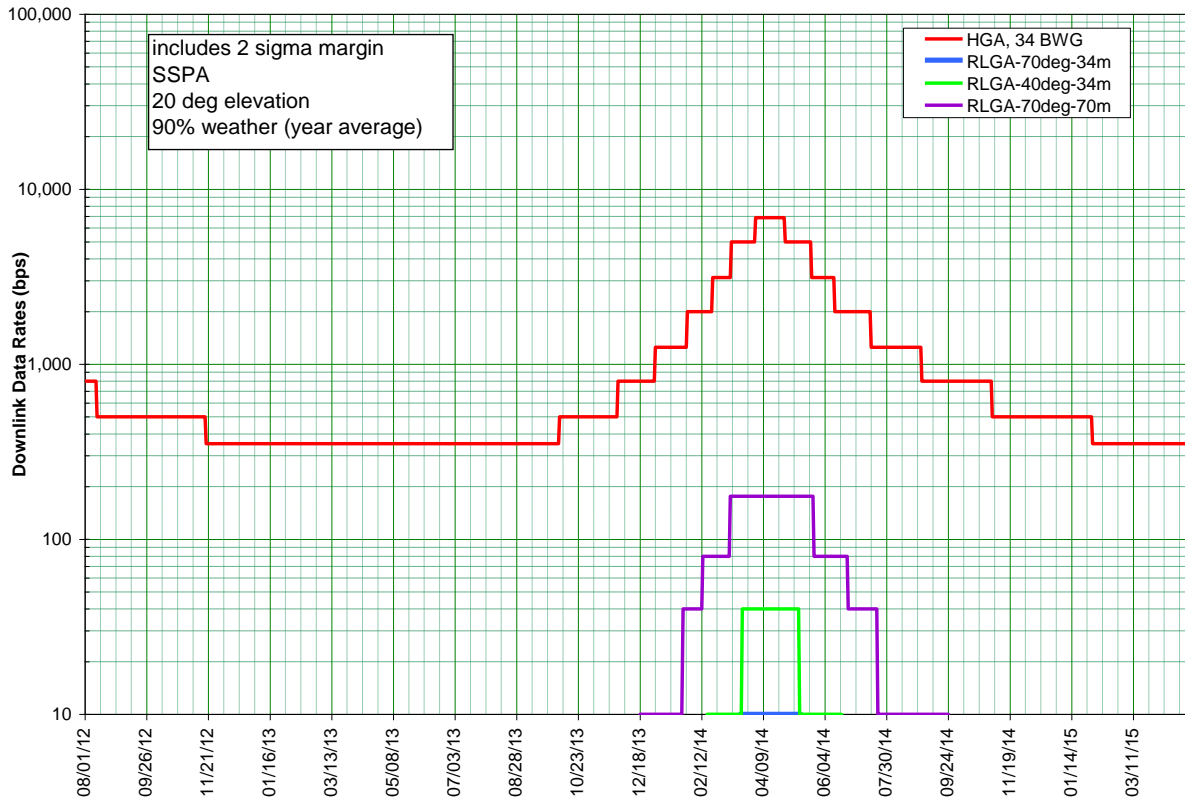


Figure 4-11. X-band downlink rates, Mars surface.

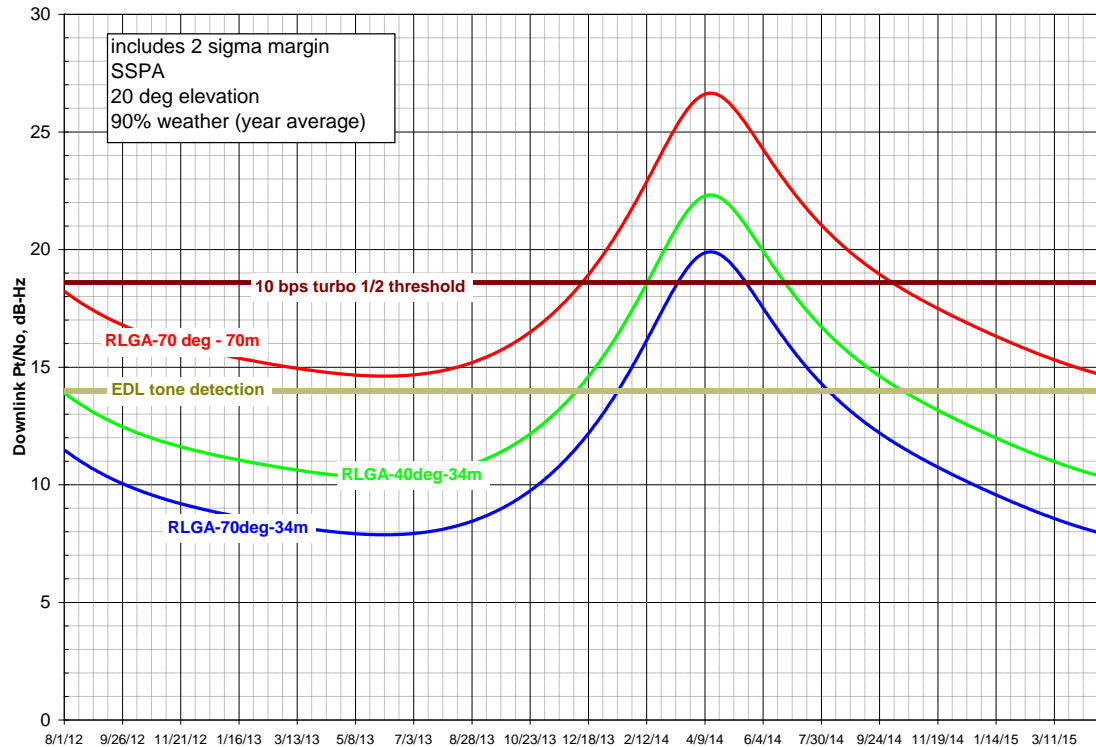


Figure 4-12. X-band downlink Pt/No via RLAGA.

If the MSL mission needs an X-band downlink capability to send discrete messages (such as “operation normal,” or “need help”) at the equivalent of very low bit rates, it will have to develop that capability. This concept is similar to an EDL-type signaling scheme, but could have much longer integration times than the minimum 10-second interval between semaphores at EDL.

4.2 UHF

The two prime functions for the UHF subsystem are relay support during EDL and surface science data relay.

4.2.1.1 EDL (UHF)

One of the top (Level 1) requirements for deep space missions is that the spacecraft provide communication to Earth of data throughout all mission critical events at a rate sufficient to determine the state of the spacecraft in support of fault reconstruction. Previous missions landing on Mars provided data communication during the critical events of EDL (Mars Pathfinder [MPF] in 1997 and MER in 2004) by making use of DTE semaphore tones to indicate the spacecraft condition. The X-band link and the semaphore tones used during EDL for the two MER spacecraft provided an increase in information content compared to that of MPF.

As compared with MER, the use of guided entry and propulsive descent on MSL requires subsystems whose status changes more quickly than on MER. These subsystems have more

moving parts that are moving more quickly than MER's airbags. The higher degree of activity results in a need for a higher information rate than tones alone can provide during EDL⁴⁰.

The addition of a UHF communications relay to a Mars orbiting asset during EDL greatly enhances communications capability by providing spacecraft telemetry. MER successfully demonstrated a UHF link with the MGS orbiter for the terminal descent (post parachute deployment) portion of EDL. However, MER did not utilize a UHF link during the earlier entry stage. The MER mission opted to not pursue any UHF capability prior to lander/backshell separation due to the significant development risks of placing a UHF antenna on the backshell.

Similar to the Phoenix EDL support, both MRO and Odyssey orbiters will be used to relay MSL lander data to the Earth.⁴¹ After extensive study of MSL visibility by asset (and redundancies) across the full range of launch and arrival periods (both primary and contingency), it was concluded that for, latitudes in the 45 deg S to 45 deg N range, DTE coverage using MFSK tones will be considered the primary planned source of information from cruise stage separation to at least entry and that MRO and Odyssey UHF relay coverage will be the primary telecom link from at least entry to rover landing. The amount of overlap — that is, the time when both links are useful — depends on the landing site selected.

MRO cannot provide delay-free (bent-pipe) relay, as it first records the return-link relay data as it is received from the descending spacecraft during the overflight and then sends the data to the DSN. Both telemetry relay (specifically, unreliable bit-stream reception at MRO for EDL and the Proximity 1 protocol [26] for normal relay) and open-loop recording (known as canister mode in CE505 radio terminology) are being considered for the relay reception onboard MRO. The current baseline is open-loop recording on MRO during EDL. However, open-loop recording was successful during Phoenix EDL. MSL will choose either Prox-1 unreliable or open loop for EDL in 2012 based on the predicted link signal level and variability.

To achieve sufficient telecom relay performance during EDL, it will be necessary for the relay orbiters to turn to point their UHF antennas at MSL to the best of their capabilities. The strategy for pointing relay assets is currently under study, but the baseline assumption is that they can point to the descending MSL within 30 deg of their UHF antenna boresights for EDL.

The UHF link will not allow all faults to be detected, particularly if the failure interferes with the spacecraft's ability to maintain the link. X-band semaphores will be used to provide information on the major events or event anomalies during EDL. This is an example of how X-band and UHF are complementary.

The UHF relay links to the orbiters in most cases will have sufficient margin to transmit at least 8 kbps (planned baseline rate). The 8 kbps MSL UHF data will be in so-called bit-stream mode (often called canister mode in the Odyssey CE505 radio). In this mode, the data is transmitted without any handshaking between the sending MSL spacecraft and the receiving orbiter. Both Odyssey and MRO will be listening to the transmitted data stream. Odyssey will operate in

⁴⁰The information rate conveyed from tones is quite limited in comparison to true spacecraft telemetry. For MSL, one tone every 10 seconds from an alphabet size of 256 has an information rate of $8/10 = 0.8$ bps. The lowest MSL X-band telemetry data rate is 10 bps, and MSL UHF telemetry will provide 8000 bps during EDL.

⁴¹The MEX orbiter may be able to provide a secondary EDL relay opportunity in addition to either MRO or Odyssey as prime.

normal telemetry demodulation mode, while MRO might be configured to record the data stream in open-loop recording mode, as was done on the Phoenix mission. The MRO data would be transmitted to Earth to be demodulated and then transferred to the flight team. One advantage of open-loop recording is that the signal will be recorded even if the carrier drops below lock threshold. Thus, the possibility exists to recover the data with non-real time analysis techniques. In contrast, with demod mode, telemetry transmitted during periods of carrier unlock is lost.

The link to the orbiter is characterized through the descent phases by a large change in range, large variations in antenna view angles, high Doppler rates, and, consequently, large changes in signal to noise ratios. The three figures that follow show these three quantities for a representative EDL to the Gale crater site for the 2009 launch. Figure 4-13 shows the range variation for the MSL to MRO relay, Figure 4-14 shows the view angle variations, and Figure 4-15 shows the received power at MRO. These results are representative of those for the 2011 launch profiles.

Figure 4-15 illustrates how there is (for most cases) sufficient margin to MRO post entry to close the link. Figure 4-16 shows the same for Odyssey. UHF blackout is likely to occur in the period from 600 to 700 seconds after CSS. A reliable X-band DTE would be desirable during the UHF blackout. Discontinuities at about 970 and 1020 seconds after CSS represent changes in predicted performance as the UHF link changes from the PUHF to the DUHF and then to the RUHF (Figure 1-19).

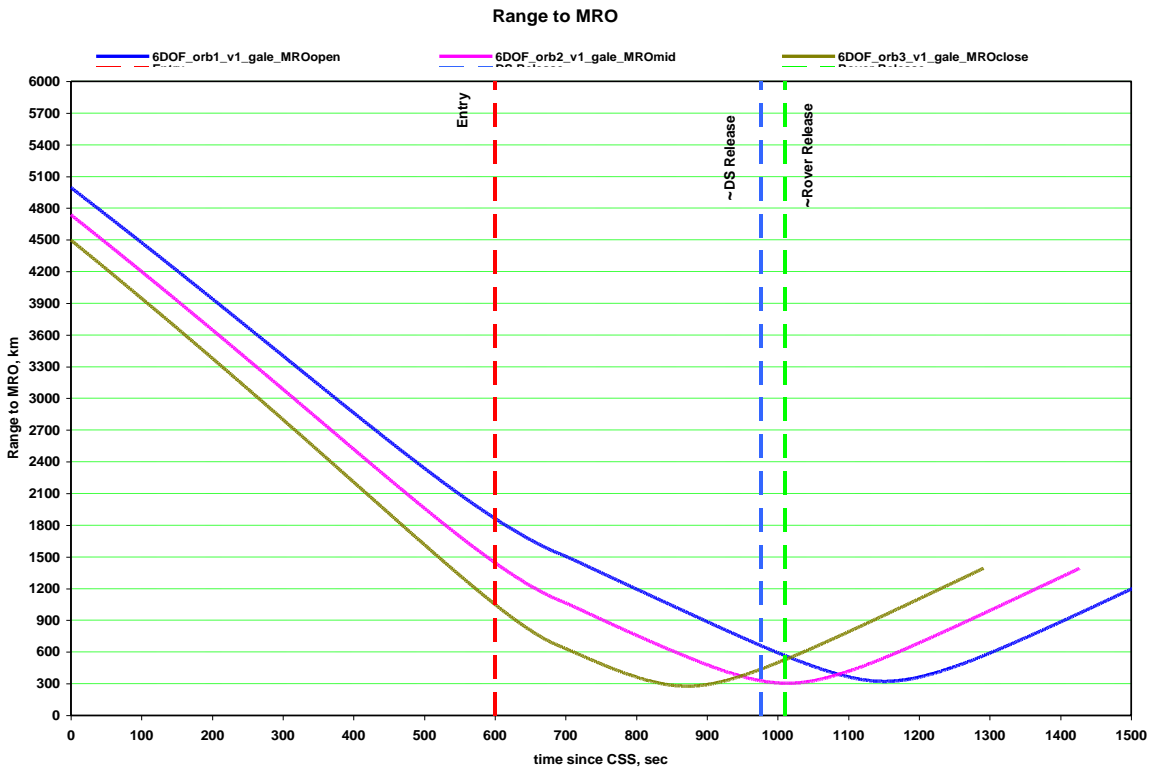


Figure 4-13. Range variations to MRO for Gale (2009 launch), three orbiter phasings.

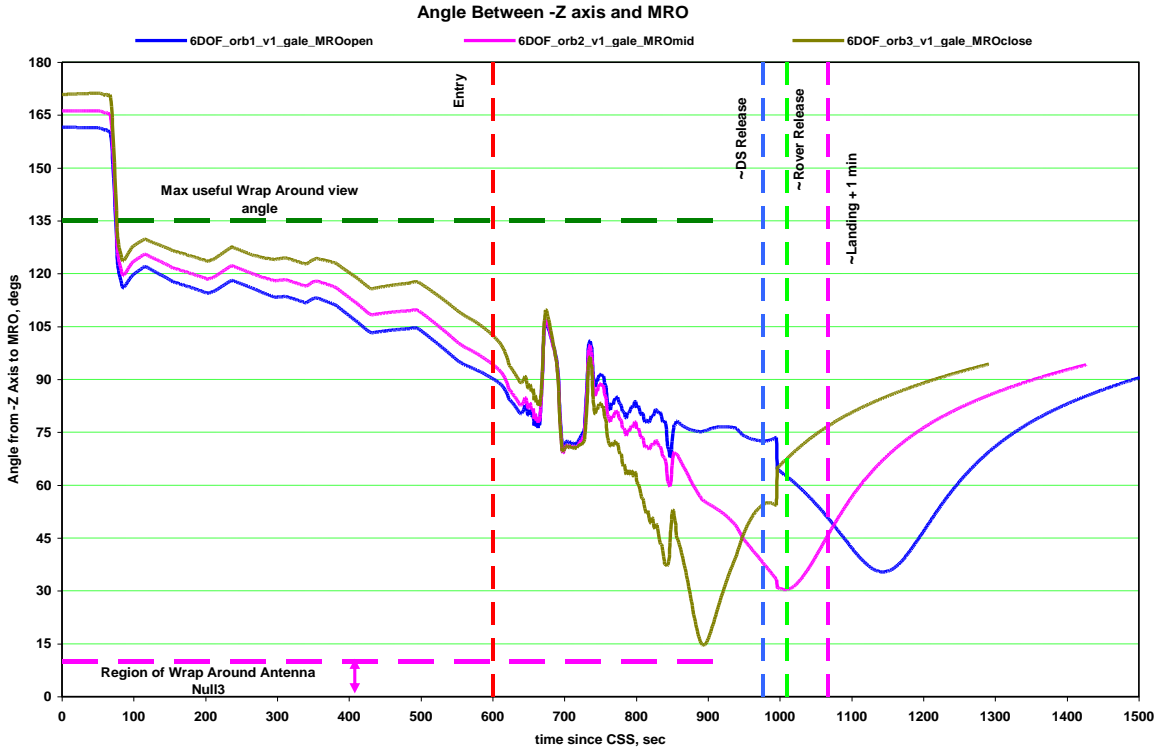


Figure 4-14. View angle variations to MRO for Gale (2009 launch), three orbiter phasings.

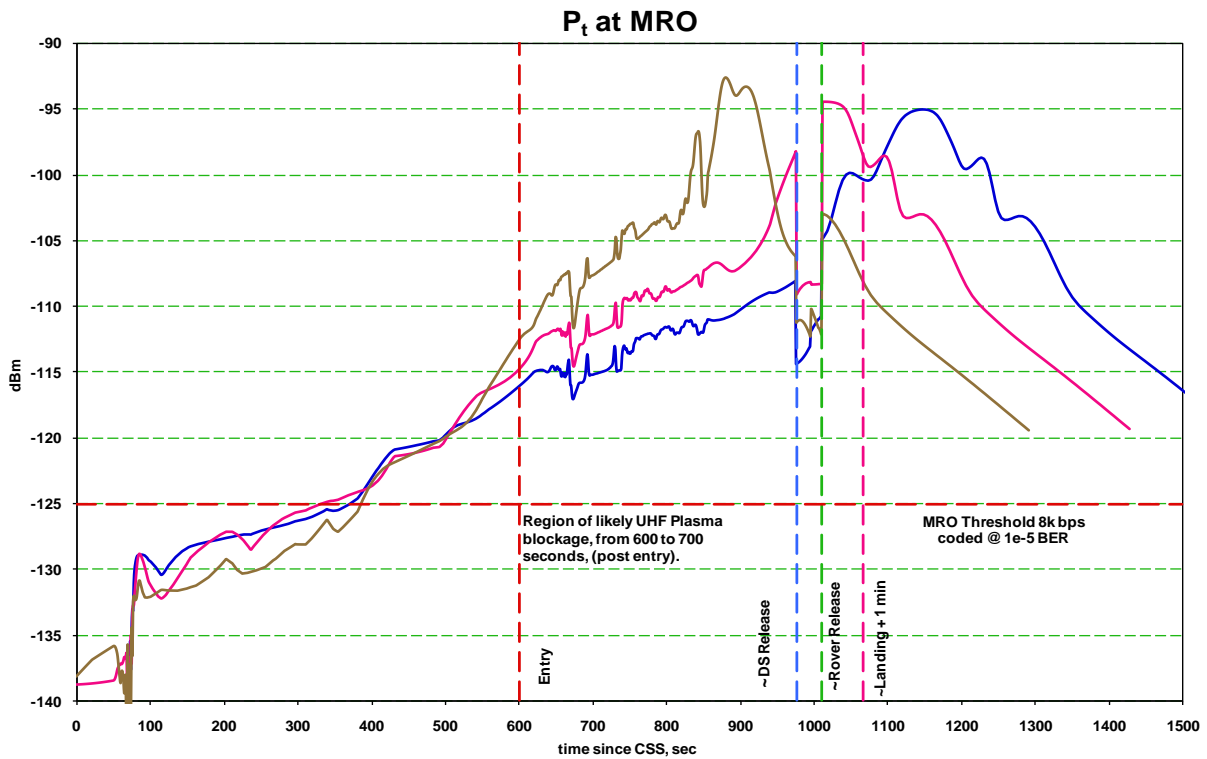


Figure 4-15. Received power at MRO for Gale (2009 launch), three Orbiter phasings.

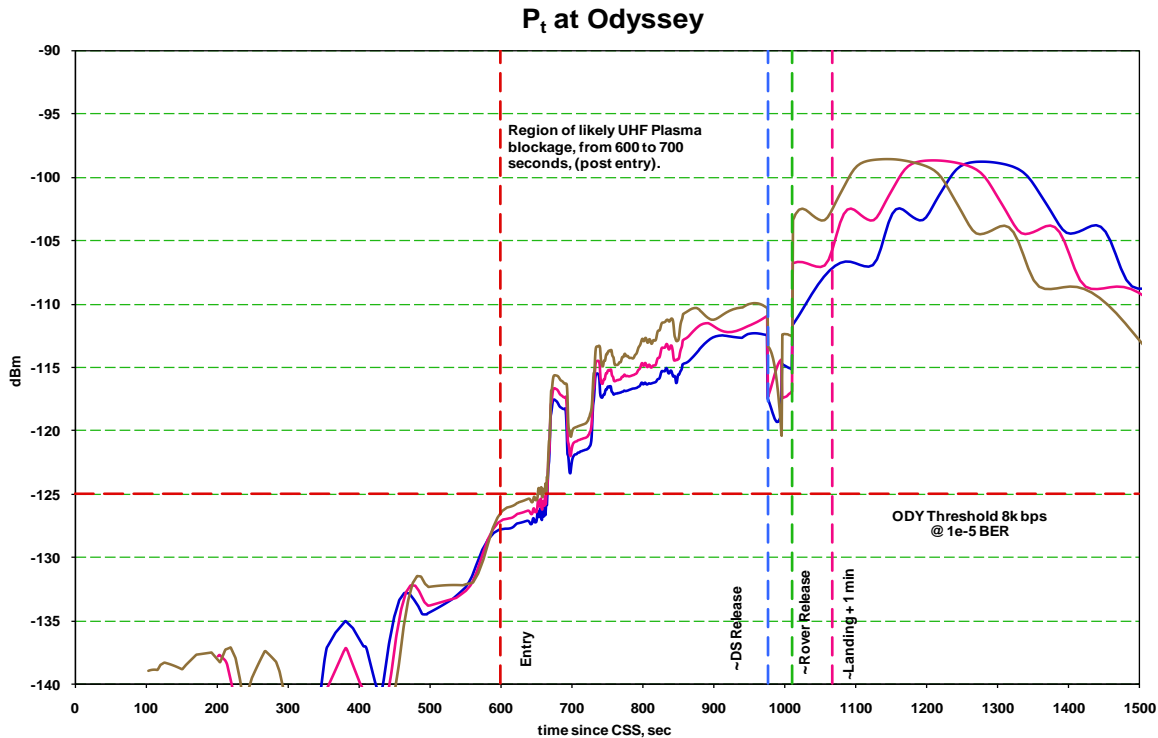


Figure 4-16. Received power at Odyssey for Gale (2009 Launch), three orbiter phasings.

The received-power plot analysis does not include “signal smearing” due to high Doppler rates, which can be many tens of hertz per second. Smearing will degrade the signal-to-noise ratio by effectively spreading the signal over many frequency bins and decreasing the signal-to-noise ratio by on the order of 10 dB in the worst cases (during maximum deceleration for example). Signal level and Doppler profile predictions will be made for the specific launch date and landing site. After-the-fact analysis of the open-loop recorded data from MRO might prove invaluable if a major entry failure occurs, making the actual Doppler rate profile significantly different from that planned. In particular, post processing might be able to recover the telemetry if the actual Doppler profile can be reconstructed.

The autonomous EDL software behavior remains in control of the spacecraft a short while after landing. The EDL behavior instructs the Spacecraft Mode Manager (SMM) to transition from EDL mode to surface mode.

The EDL UHF communication line to MRO (8 kbps in open-loop canister mode) might continue to be viable for several minutes after landing. Attempts will be made to acquire and prioritize surface-related data (e.g., Hazcam images) to be put into this stream if possible. The time limitations (to send a required amount of higher-priority data at a certain bit rate) mean that lower-priority data might not be downlinked in real time (for example, MEDLI or MARDI data). Data prioritization is defined by the flight team.

Engineering data gathered during EDL (estimated at ~ 100 Mbits) is not required to be immediately downlinked; however, this data is expected to be prioritized such that it will be played back to the DSN within 10 sols of landing to enable the EDL engineering team to complete in-depth analysis of EDL performance to feed forward to future missions.

4.2.1.2 Surface (UHF Relay)

During the surface mission, MSL will rely on UHF-relay telecommunications passes as the primary method of returning science and engineering data to Earth. Relay passes will also be used when necessary to uplink commands and software to the rover; however, surface operations are nominally designed around the use of the DFE X-band link on the Rover HGA as the primary uplink method.

UHF passes make use of MRO, which will be in a 3-p.m. ascending Sun-synchronous orbit. The MRO pass pattern repeats every 17 sols and provides anywhere from 30 to 600 Mbits per pass (100 to 1150 Mbits per sol). The expected average performance per sol is well above the 250 Mbits requirement total for the two passes.

Strategies for use of adjacent passes (when there are two low-volume passes instead of one better pass) will be addressed in subsequent updates to the mission plan and described in the DESCANSO MSL telecom operations article.

MSL will also take advantage of relay support by the Odyssey spacecraft to augment UHF passes in the event that Odyssey is still functioning when MSL arrives at Mars. Provided MRO is available, Odyssey support is not required to carry out the MSL surface mission.

Accurate daily relay data volume predictions are vital to the operations tactical process. Several tools of MER and Phoenix heritage will be updated with MSL specific data (RUHF antenna patterns, for example). The generalized telecom predictor (GTP), a variant of the much used telecom forecaster predictor (TFP), is the primary tool during operations to make UHF predictions. TFP itself will be used for X-Band DFE and DTE predictions.

Section 1.6.3 and Sections 0 and 5.3 provide some additional detail on plans for UHF relay during surface operations. The telecom operations article will describe the prediction and assessment tools for surface operations, the strategic and tactical plan development, and the data return results for the 2011 mission. Meanwhile, the MER article in this series [6] describes the corresponding surface operations that the MSL tools and plans will be based on.

5 Flight Operations (Plans)

This section comes mostly from the MSL Mission Plan [11].

5.1 Mission Operations System Approach

The flight team must staff to support intense surface operations over a 669-sol (~687 Earth days) period, some of which might be conducted on Mars time (selected staff report 40 minutes later each day) to minimize the end-to-end time between receipt of data from one sol to the uplinking of activities for the next sol.

To support a long-duration surface mission, the MSL mission operations system (MOS) uses a distributed operations concept similar to MER's. This means, in particular, that both data processing and subsequent analysis and planning might be in several locations: at JPL and at the home institutions (usually universities) of the science team members. JPL is the central data distribution hub where selected data products are provided to remote science operations sites as needed. JPL is also the central hub for the uplink process, though participants are distributed at their respective home institutions.

The uplink process is dominated by a tactical uplink process. "Tactical" refers to work that is necessary to get a final set of commands up to a rover on each sol. Analysis of yesterday's downlink data is used to decide and plan where and what today's rover activities should be. The uplink communication to the spacecraft is either with X-band DFE with the DSN or UHF through MRO. Downlink, governed by data volume requirements, is UHF relay only, as shown in Figure 5-1.

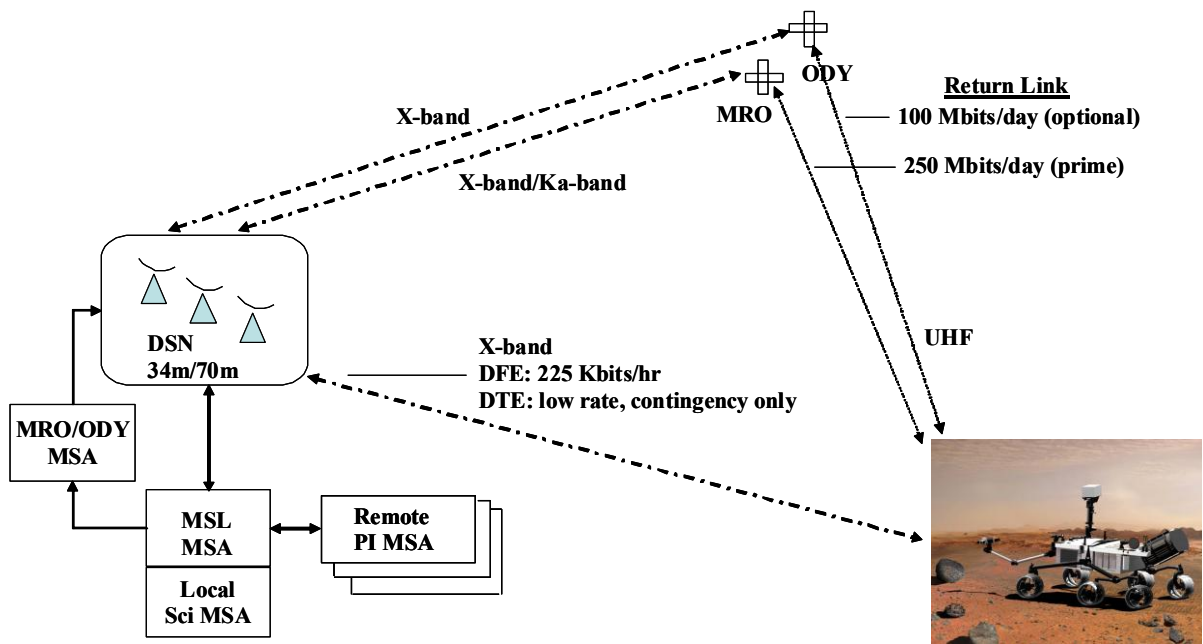


Figure 5-1. MSL surface operations MOS overview.

Figure 5-2 is a diagram identifying the elements of the operations functional architecture and the major Uplink (command) and Downlink (data) processes that they support.

To the left are science analysis and planning functions. The center has the sequencing, data collection and engineering, and navigation analysis functions. To the right are the multimission data-processing functions. The multimission ground data system (MGDS) of the Interplanetary Network Directorate (IND) at JPL interfaces with the DSN.

Each element (box) represents a set of related software and facilities, people, and local processes.

Figure 5-3 depicts the GDS subsystems and function and identifies (by the color of the sub-bullets in each box) the level of inheritance for various functions.

5.2 Initial Surface Ground Operations

For the first 60 to 90 days of operations (consisting of rover initial configuration for surface operations, rover checkout, and first surface location operations), all teams will be located at JPL. Tactical operations will be on Sol (Mars) time. This allows up to 18 hours for one-sol turnaround. Operations at JPL provide face-to-face coordination and learning. Once the rover is into steady-state operations and the operations teams have demonstrated a one shift turnaround, the flight team will transition to tactical operations on Earth time. Shortly thereafter, the team will be distributed, with science teams operating from their home sites. The tactical flight team is a virtual team, comprising members from across the organizations represented in Figure 5-2 and Figure 5-3, such as science, spacecraft, mission planning, and the Deep Space Mission System (DSMS, the parent body to the Deep Space Network (DSN)). The virtual team is a focused, multi-disciplinary group that is formed from members across the MSL mission to work a particular issue (in this case, carrying out the tactical uplink process). In these particulars, the MSL Flight Team will be similar to how the MER Flight Team was organized and deployed. In addition, the organization of and allocation of activities within the MSL team is intended to increase integration and reduce the total number of separate teams and inter-team interfaces. MSL will utilize the JPL Multi-mission Operations (MMO) capability where possible, in preference to designing MSL unique team operations.

5.3 Tactical Operations after First 90 Sols

The MSL Tactical Surface Operations are tailored to support nearly daily commanding of the rover, based on today's science evaluation of yesterday's returned data.

Figure 5-4 shows the command and data flow and is a top-level timeline of the tactical process.

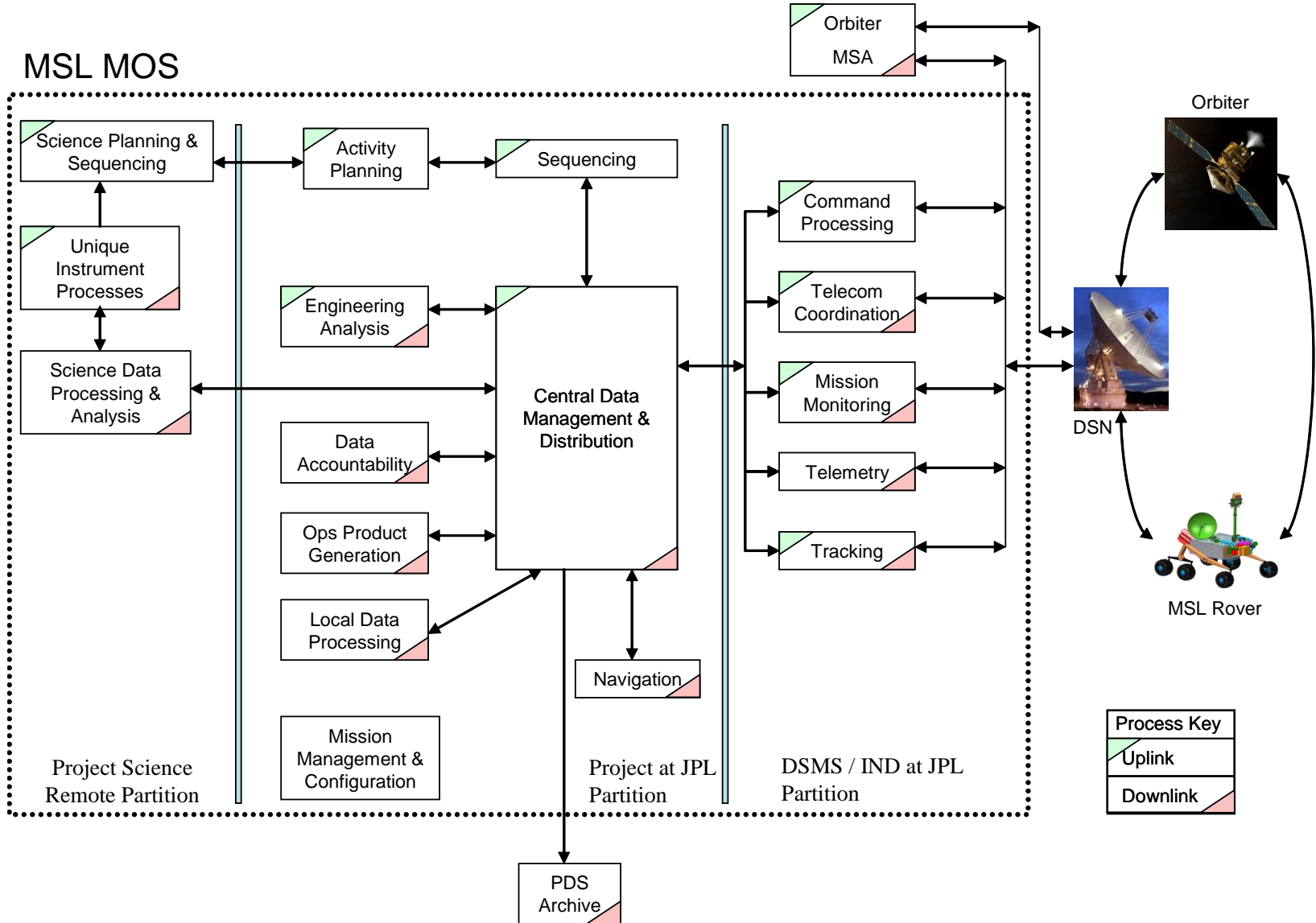


Figure 5-2. Functional architecture of MSL MOS.

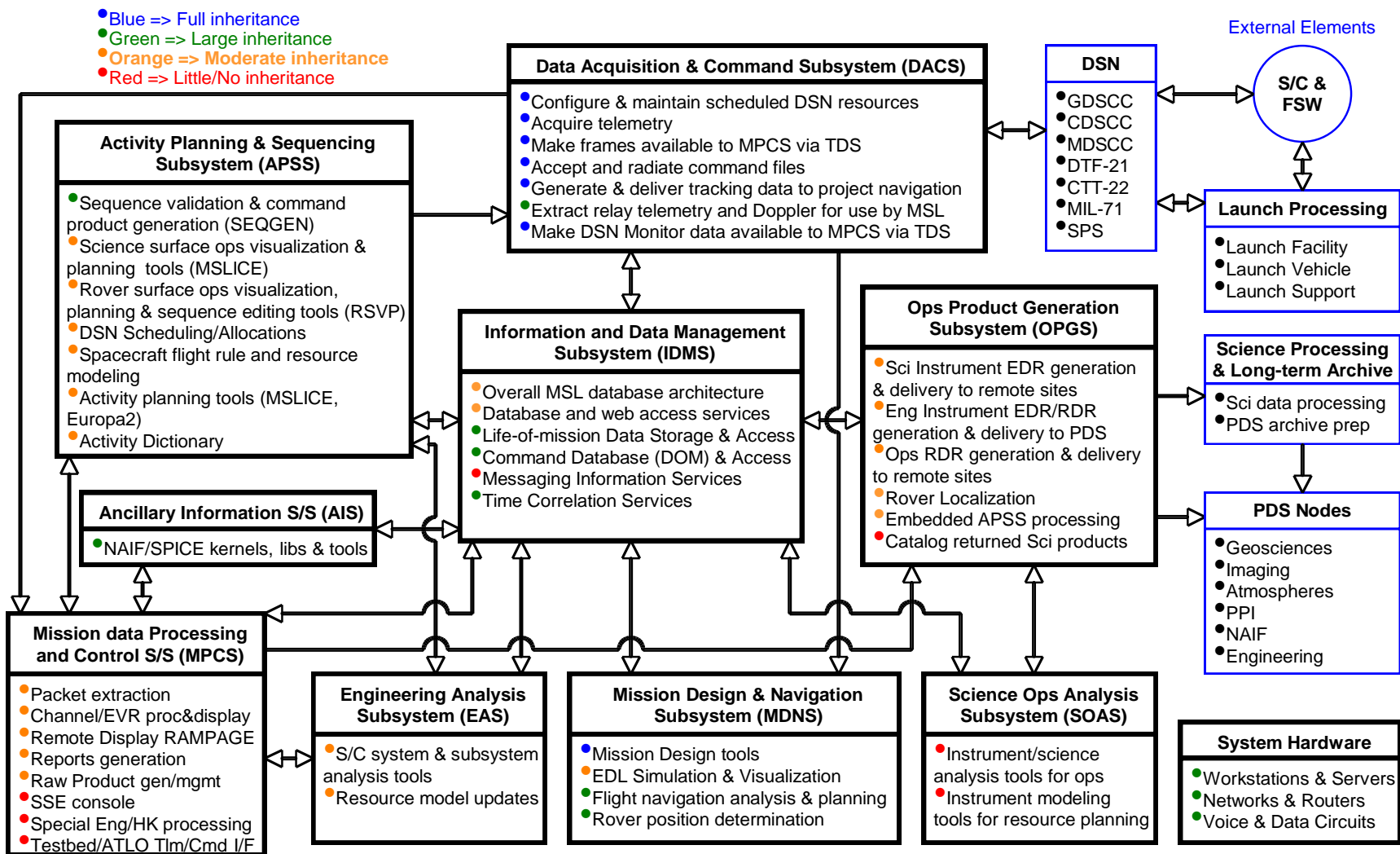


Figure 5-3. Subsystems and functions of MSL MOS.

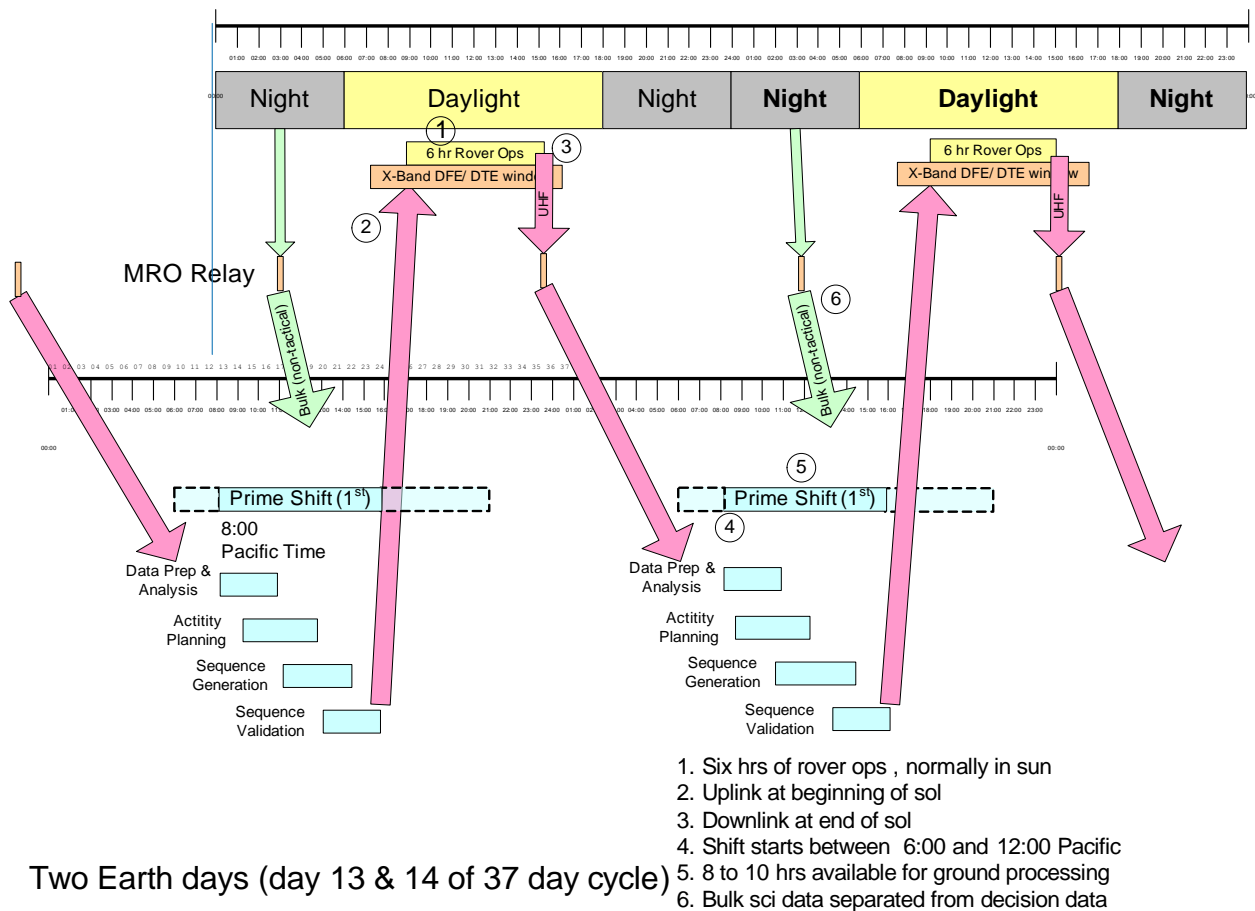


Figure 5-4. MSL tactical process during surface ops (at top level).

The steady state tactical process is performed 7 days per week through the prime surface mission. Based on the evolution of the MER surface team, the core of the tactical team works four 10-hour shifts per week, with a sliding start time between 6 a.m. and 1 p.m. The driver for the sliding start time is to have a “modified” prime shift at JPL. This is more conducive to family life over the long duration and also helps maintain normal sleep cycles. The start time will stay as close to 8 a.m. as possible. The normal uplink cycle is 8 hours between receiving telemetry data in the MSL MSA to uplink approval. This enables 1-day turnaround cycles. There will be a small number of tactical planning templates developed to facilitate the rapid turnaround. Some examples of activities are site recognizance, target approach, sample acquisition and processing, science instrument analysis on acquired sample, and traverse to new science site. These templates will initially be developed in response to the Mission Scenarios described elsewhere in this document. After landing, the process becomes discovery-driven. The MOS approach and GDS tools provide for re-use of Sequences and conversion of Sequences into Activities for future use.

5.4 UHF Telecom Constraints

The relay orbiters can be used to uplink sequences, flight software, and any other data we might need to send to the rover.

With ground and surface process durations as currently defined, we will be able to use the 3 a.m. MRO pass over 50% of the time to uplink our sequences. Data cleanup commands, which may be large and which are usually not time critical, will typically be sent in time for relay to the rover during the 3 a.m. pass.

MSL relies on UHF communication with relay orbiters to downlink the data generated during surface operations. For planning purposes, it is assumed that the downlink relay bandwidth averages 125 Mbits per pass for a total of 250 Mbits per sol and that the volume of decisional data collected each sol does not exceed 100 Mbits.

Figure 5-5 shows the expected return link data volume the MRO relay orbiter. Relay capacity follows a 5 or 6 sol pattern of two low-volume followed by three or four high-volume passes.

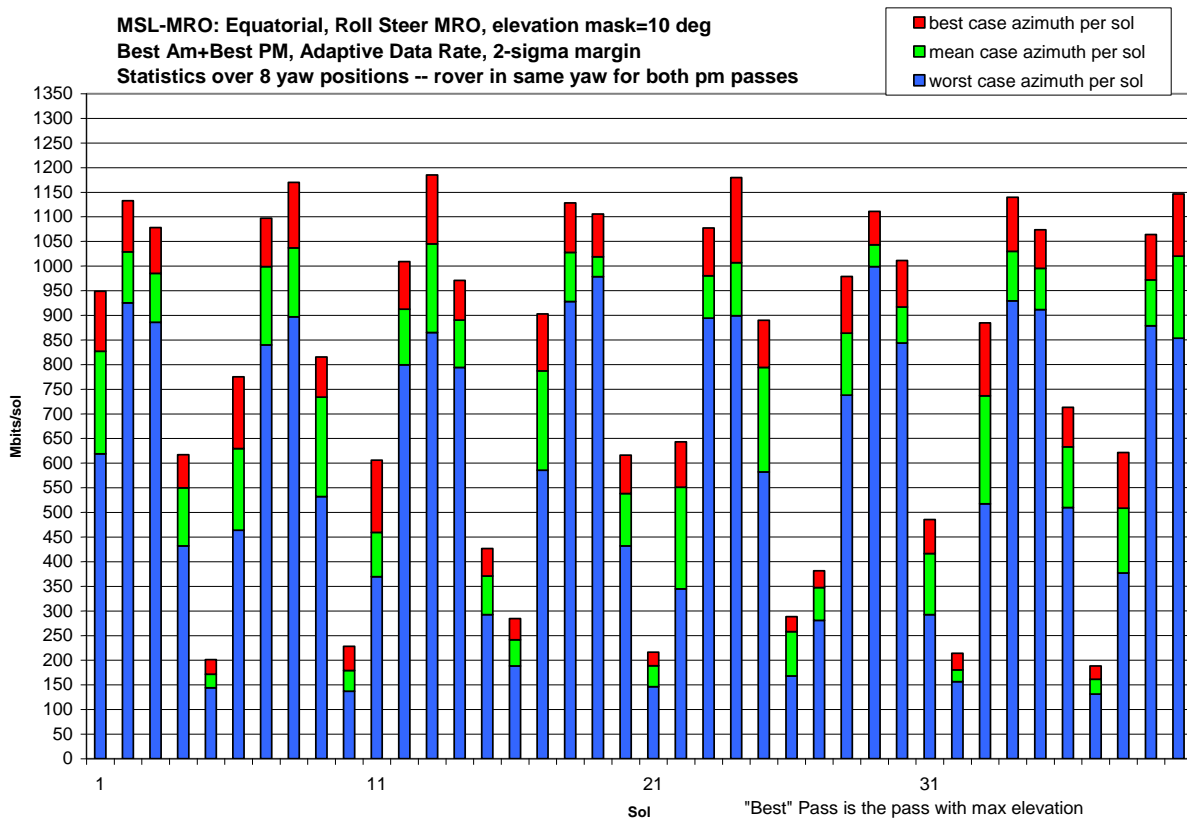


Figure 5-5. Estimated sol-by-sol return data volume through MRO.

This figure is based on the following assumptions regarding MRO performance:

- Every pass, MRO performs a roll maneuver, up to 30 degrees, to point its UHF antenna as close as possible to MSL.
- The rover is at the Equator.
- MRO must rise at least 10 deg above the horizon to communicate with MSL.
- The relay link utilizes adaptive data rates.
- Performance is based on the best morning and evening passes.
- A 2-sigma margin for the return link is applied.

Given these assumptions, the worst-case performance is no less than 125 Mbits per sol and the average performance is 687 Mbits per sol. On days when the expected return link volume is less than 100 Mbits, decisional data will be downlinked according to the priority assigned by the Science Operations Working Group (SOWG). On days when the expected volume is large, any backlog of decisional data can be downlinked using the additional capacity over 125 Mbits.

In addition to data volume constraints, the start time of the relay pass imposes an important constraint on surface operations. In a typical sol, the command sequence is uplinked via DFE around 9:30 local mean solar time (LMST) and any activity that produces data needed to support a decision during the next ground processing cycle must be completed prior to the afternoon MRO pass.

The actual MRO pass start times vary by about ± 1 hour around 15:00 LMST for the rover at the equator. At 30 N and 30 S, MRO pass start times can range from 1:45 to 4:00 LMST for the a.m. pass and from 14:00 to 16:15 LMST for the p.m. pass.

5.5 X-Band Telecom Constraints

For about 50% of sols, MSL will uplink sequences via an X-band DFE transmission from DSN to the high gain antenna (HGA). This transmission will typically be scheduled to arrive at the rover around 9:30 LMST and is expected to take 15 minutes or less per upload.

Although MSL has the capability to downlink small amounts of data via X-band DTE from the HGA to DSN, we do not plan to utilize this capability during typical operations.

Refer to Figure 4-10 for uplink (DFE) capability and to Figure 4-11 for downlink (DTE) capability.

5.6 Surface Relay Link Strategy and Operations

5.6.1 Orbiter Relay Support Strategy

MSL will negotiate with the Mars Program Office and MRO/Odyssey projects, as formalized in the interface control document (ICD), for orbiter relay support during all passes in view of the landing site during the first thirty days of surface operations. These passes will be used to support UHF uplink (forward link) of command loads and downlink (return link) transmission of

rover engineering and science data. Relay orbiters will arrange for DSN coverage such that end-to-end data return can occur within one hour from the time data is transmitted by the rover.

5.6.2 Surface Initial Commanding Strategy

The first few sols of operations will be based on commands/sequences that have been developed, tested, and pre-loaded before landing. A “one command cycle per sol” strategy will be in place from the time of landing, although the commanding cycle might not conform to the nominal Mars-time 16-hour turn around for first few sols. Command uplink will initially be done via a morning DFE-only pass via the RLGA until HGA X-band communication becomes available as rover attitude information improves. The team chose DFE-only because the expected downlink capability via the RLGA is very low, but uplink capability exists (up to 125 bps via a 70-m station, per Figure 4-10). During these initial surface operations, downlink will be done at UHF at much higher data rates.

The nominal plan assumes, in prioritizing spacecraft safety and operability over an early start of science return, no pressure to rush initial checkout activities. Therefore, there is no plan to require “ground-in-the-loop” near real-time go/no go commanding. The command cycles for the first few sols are basically enabling and potentially reordering predefined and preloaded sequences. The MOS ground operations will transition to developing new command sequences on the nominal tactical timeline by the end of the checkout activities.

5.6.3 Surface Initial Communications Strategy

For planning purposes, the MRO UHF relay capability is considered the prime relay link supporting ~ 03:00 and ~ 15:00 LMST 15-minute-long passes per sol at all possible landing sites. Use of the Odyssey UHF relay is considered enhancing and will be used as resources permit. The UHF relays will be used at the first opportunity with no special checkout but at low-data rates to maximize link margin until performance can be assessed by the ground team. We expect that the MRO relay performance can be brought to nominal levels (~ 250 Mbits/sol) within two command cycles for use during sol 3.

X-Band communication will be limited to the low gain antenna for the first several sols and is assumed to be capable of supporting operations without special checkout, such as X-band HGA pattern tests. The RLGA will only support very low data rates, but this is sufficient for real-time response in case an off-nominal situation should occur. An X-band communications window of several hours’ duration will be planned for the first several sols to support such communication as necessary. Once adequate attitude knowledge is attained to point the HGA with the required accuracy, the HGA will be used to support a command uplink in the morning of each sol to maximize time for ground and surface operations. The current baseline is to have the HGA in operations within 2 sols.

5.6.4 Surface Communications Operations

Continuing the initial UHF strategy, UHF is used at least twice per sol for morning and afternoon communication sessions with one or both relay orbiters. The sessions are planned to include a communication preparation period of 15 minutes before the UHF pass and 10 minutes of keep-out for processing of any uplinked data after the pass.

Both MRO and Odyssey passes will be used to maximize the data return. Any large uploads to the spacecraft (such as software builds) will most likely be done using the UHF relay. Depending

on the landing site and the Mars-Earth geometry, DTE/DFE might not be efficient or even usable, in which case the relay might be used exclusively. The Mars program office and the Phoenix and MER missions successfully verified using only using UHF only when X-band was not available.

DFE/DTE during the surface mission will rely primarily on using the HGA, since for most of the mission the X-Band low gain antenna (RLGA) will not provide sufficient link for daily activities. The RLGA is planned primarily for contingency modes and, perhaps, for small command uploads when the link performance is sufficient.

6 MSL Telecom Topics in Follow-up Article

We plan a follow-up article for mid-2013, after cruise, EDL, and a period of surface operations. This planned Mars Science Laboratory telecommunications performance article will focus on the following topics, based on continued development activities and the outcome of these mission phases:

- Launch and initial acquisition activities.
- Early cruise telecom X-band performance.
- EDA development and EDL operations.
- Communications behavior (comm windows).
- UHF (Electra) checkout.
- Electra relay communications (Proximity 1 protocol).
- Updates to surface operations plans.
- Surface operations.
- Lessons learned.

Abbreviations and Acronyms

1553 (MIL-STD-1553) a standard for digital communications published by the United States Department of Defense

A/D	analog to digital
ADC	analog to digital converter
ADR	adaptive data rates
AGL	above-ground level
Ahr	amp hour
AIS	ancillary information subsystem
AlBeMet	trade name of aluminum beryllium composite produced by Brush Wellman Inc.
ALC	automatic level control
AM	ante meridian
AOA	angle of attack
APXS	alpha particle X-ray spectrometer
ARF	automatic restart function
ATLO	assembly, test, and launch operations
ATN	attenuator
ATS	aft transition structure
AU	astronomical unit, 149.6×10^6 km
aux osc	auxiliary oscillator
BC	bus controller
BECO	booster engine cutoff
BIP	backshell interface plate
BLGA	Backshell low gain antenna on MER
BODA	burnout detection algorithm
BoL	beginning of life
BPF	bandpass filter
BPM	baseband processor module
bps	bits per second
BPSK	binary phase shift key
BSS	backshell separation
BTU	British thermal unit (1.06 kilojoule)
BUD	bridle, umbilical, descent rate limiter device
BWG	beam waveguide

C3	launch-specific energy
CAN	Canberra (Deep Space Communications Complex)
CBE	current best estimate
CBM	cruise balance mass
CBM	Communications Behavior Manager, software
CCAM	collision and contamination avoidance maneuver
CCB	common core booster
CCSDS	Consultative Committee for Space Data Systems
CDR	critical design review
CDSCC	Canberra Deep Space Communications Complex (DSCC)
CG	center of gravity
ChemCam	Chemistry and mineralogy camera
CheMin	Chemistry and Mineralogy (makes X-ray diffraction analyses of rock and soil samples)
C-ISA	Centaur interstage adapter
CMD	command
Comm	communication, or on a diplexer, common port (connected to an antenna)
conscan	conical scanning
cPCI	compact peripheral component interconnect
CSS	cruise stage separation
CTT	compatibility test trailer
CW	Continuous-wave
D/A	digital to analog
DAC	digital-to-analog converter
DACS	data acquisition and command subsystem
DAN	Dynamic albedo of neutrons (instrument to detect and analyze hydrogen in the near-subsurface of Mars)
dB	decibel
dBc	dB below carrier
dBm	decibels referenced to milliwatts
DC	direct current
DEA	digital electronics assembly
DEA	descent engine assembly
DEC	Dual-Engine Centaur
deg	degree
DFE	direct from Earth
DLGA	descent LGA

DOE	Department of Energy
DOM	Distributed object manager
DOR	differential one-way ranging
DPDU	digital power distribution unit
DPM	digital processing module
DS	descent stage
DSN	Deep Space Network
DSCC	Deep Space Communications Complex
DSDST	descent stage small deep space transponder
DSMS	Deep Space Mission System
DSS	Deep-Space Station
DTE	direct to Earth
DTF	DSN test facility
DTT	Downlink Tracking and Telemetry (subsystem)
D-UCTS	Descent UHF coax transfer switch
DUHF	descent UHF antenna
EADS	Casa Espacio, European Aeronautic Defense and Space Company (HGA vendor)
EAS	engineering analysis subsystem
EBM	entry balance mass
EDA	EDL data analysis
EDL	Entry Descent and Landing
EFPA	entry flight path angle
EH&A	engineering housekeeping, and analysis
EIRP	effective isotropic radiated power
ELT	Electra Lite transponder
EM	electromagnetic
EMC	electromagnetic compatibility
EMI	electromagnetic interference
Eng/HK	Engineering/housekeeping
EOL	end of life
EOM	end of mission
EPC	electronic power conditioner (TWTA)
EPC	electronic power converter (SSPA)
EPS	electrical power system
EUT	Electra UHF transponder
EVR	Event report
Ex	exciter (provides the RF drive to the transmitter)

F1	fundamental frequency of the SDST
FA	flight acceptance
FA	flight allowable
FET	field effect transistor
FFA	front-end filter assembly
FFT	fast Fourier transform
FPGA	field-programmable gate array
FS	Flight system
FSK	frequency-shift keying
FSP	full-spectrum processing subsystem
FSW	flight software
FY	fiscal year
GDS	ground data system
GDS	Goldstone
GDSCC	Goldstone Deep Space Communications Complex (DSCC)
GFE	Government furnished equipment
GHz	gigahertz
GNC	guidance, navigation, and control_
GRASP	General Reflector Antenna Scatter Program
GTP	generalized telecom predictor
Hazcam	hazard camera
HEF	high efficiency (antenna)
HEMT	high-electron mobility transistor
HGA	high-gain antenna
HGAG	HGA gimbal
HGAS	high gain antenna system
HRS	heat rejection system
ICD	interface control document
IF	intermediate frequency (typically below 200 MHz)
IND	Interplanetary Network Directorate
IPP	inter pulse period
IR	improved ranging
ISA	interstage adapter
ISO	isolator (at TWTA output)

JPL	Jet Propulsion Laboratory
kb	kilobit
kbps	kilobits per second
kg	kilogram
kN	kilonewton
<i>LC</i>	inductance capacitance filter
LCP	left-circular polarization
LGA	low-gain antenna
LCP	left-hand circular polarization
LH ₂	liquid hydrogen
LMST	local mean solar time (local solar time, LST, is also used)
LO ₂	liquid oxygen
LOS	loss of signal
LPF	low-pass filter
LST	local solar time (local mean solar time, LMST, is also used)]
LTST	local true solar time
LV	launch vehicle
LVDS	low-voltage differential signaling
m	meter
MAD	Madrid DSCC (Deep Space Communications Complex)
MAHLI	Mars hand lens imager (color microscopic imager)
MARDI	Mars descent imager (high-resolution color descent imager)
Mastcam	(multi-spectral, stereo imaging and video camera on MSL mast)
Mbits	megabits
MCIC	motor controller interface card
MCIF	motor controller interface
MDNS	mission design and navigation subsystem
MDSCC	Madrid Deep Space Control Center (DSCC)
MECO	main engine cutoff
MEDLI	MSL EDL instrumentation
MER	Mars Exploration Rover
MES	main engine start
MEX	Mars Express
MFSK	multiple-frequency shift keying

MGA	medium-gain antenna
MGDS	Multi-mission Ground Data System
MGS	Mars Global Surveyor
MIC	microwave integrated circuit
MIL-71	name of DSN station at Cape Canaveral (not an acronym)
MLE	Mars landing engine
MM	multi mission
MMO	multi mission operations
MMRTG	multimission radioisotope thermoelectric generator
MOLA	Mars Observer laser altimeter
MOS	mission operations system
MPCS	mission data processing and control subsystem
MPF	Mars Pathfinder
MREU	MSL remote electronics unit (also called REU)
MRO	Mars Reconnaissance Orbiter
ms	millisecond
MSA	mission support area
MSAP	multi mission system architectural platform
MSL	Mars Science Laboratory
MSLICE	MSL InterfaCE (a surface ops visualization and planning tool)
Msp/s	megasympols per second
MTC	Mars Time coordinated
MTIF	MSAP telecommunications interface board
NAIF	Navigation and Ancillary Information Facility
NASA	National Aeronautics and Space Administration
NCO	numerically controlled oscillator
NPO	NPO Energomash (Russian manufacturer)
NRZ	non-return to zero
ns	nanosecond
NVM	non volatile memory
NVM	non volatile memory/camera
OCM	organic check material
OD	orbit determination
ODY	Odyssey
Osc	oscillator

PD	passive device (in SSPA, a microwave coupler or combiner)
PDS	Planetary Data System
PEDL	pre-entry, descent, and landing
PLF	payload fairing
PI	principal investigator
PLGA	parachute low-gain antenna
PM	post meridian
PMP	payload mounting module
Pol	polarizer
PPI	Planetary Plasma Interactions
ppm	parts per million
Prox-1	Proximity 1 (data protocol)
Pr/No	turnaround ranging power to noise spectral density ratio
psf	pounds per square foot
PSS	parachute support structure
PUHF	parachute UHF antenna
rad	radian (=57.3 degree)
RAD	radiation assessment detector
RAMP	rover avionics mounting plate
RAT	rock abrasion tool
RC	radar controller
RCE	rover computer element
RCP	right-circular polarization
RCS	reaction control system
Reff	effective information rate
REMS	Rover environmental monitoring station (instrument to measure meteorological conditions and ultraviolet near the rover)
REU	Remote electronics unit (also called MREU)
RF	radio frequency
RFPDU	radio frequency power distribution unit
RLGA	rover low-gain antenna
RM	ranging maximum
RP	radar processor
RP	rocket propellant or refined petroleum (kerosene)
RPAM	rover power and analog module
RPDU	RF power distribution unit (in TDS)
rpm	revolutions per minute

RPFA	rover pyro fire assembly
RSM	remote sensing mast
RSR	radio science receiver
RT	remote terminal
RTN	return
RTG	radioisotope- thermoelectric generator
RTLTL	round-trip light time
R-UCTS	rover UHF coax transfer switch
RUHF	rover UHF antenna
R-WTS	rover waveguide transfer switch
Rx	receiver
SA	sample acquisition
SAM	sample analysis at Mars (instrument for chemical and isotopic analysis of acquired samples)
S-band	RF frequencies 2 to 4 GHz
S/C	spacecraft
SDR	software defined radio
SDST	small deep space transponder
SEC	Single-Engine Centaur
SEP	separation
SeqGen	sequence generation (spacecraft activity planning software)
SEP	Sun–Earth–Probe angle
SMM	spacecraft mode manager
SNR	signal-to-noise-ratio, in dB
SOAS	science operations analysis subsystem
SOC	state of charge
sol	Martian day
SOWG	Science Operations Working Group
SPARC	scalable processor architecture
SPaH	sample preparation and handling
SPE	static phase error
SPE	Sun–Probe–Earth (angle)
sps	symbols per second
SRB	solid rocket booster
SRBJ	solid rocket booster jettison
SSPA	solid state power amplifier
SUFR	straighten up and fly right

TCM	trajectory correction maneuver
T _{cyc}	cycle time
TDS	terminal descent sensor
TDSA	TDS antenna array
TDSD	TDS digital stack
TDSR	TDS RF stack
TFP	telecom forecaster predictor
TIP	target interface point
TLGA	tilted low-gain antenna
TLM	telemetry
TRM	transmit receive module
TTE	turn to entry
TWT	Traveling wave tube
TWTA	traveling wave tube amplifier (=TWTA + EPC)
Tx	transmitter
UCXS	UHF coaxial transfer switch
UDIM	up/down IF module
UDMM	up down MIC [microwave integrated circuit] module
UHF	ultra high frequency (300 MHz to 3 GHz)
USA	United States of America
USN	Universal Space Network
UTC	Universal Time Coordinated
UTCS	UHF transceiver coaxial switch
UV	ultraviolet
VCXO	voltage-controlled crystal oscillator (list only one)
VSWR	voltage standing wave ratio
W	watt
W2CX	waveguide to coaxial
WEB	warm electronics box
Whr	watt-hour
WIPL-D	Wires, Plates, Dielectrics (a commercial high frequency electromagnetic modeling software package)
WTS	waveguide transfer switch

X-band
XFMR

RF frequencies from 7 to 12.5 GHz
transformer

References

-
- [1] Louis D’Amario, *Mars Science Laboratory Interplanetary Baseline 2011 Interplanetary Trajectory Characteristics Document*, JPL D-27210, July 15, 2009 <https://charlie-lib.jpl.nasa.gov/docushare/dsweb/View/Collection-47223>.
- [2] *Basics of Space Flight*, web site, Jet Propulsion Laboratory, Pasadena, California, accessed November 2, 2009. <http://www2.jpl.nasa.gov/basics/bsf4-1.html>.
- [3] B. Florow, K Breitenbach, S Udomkesmalee, *Positioning, Phasing & Coordinate Systems (3PCS)*, Volume 1, *MSL Coordinate Systems*, D-34642 (JPL internal document), Jet Propulsion Laboratory, Pasadena, California, May 29, 2007.
- [4] L. D’Amario, T. Martin-Mur, *Launch/Cruise/Approach Design*, in *Launch/Cruise/approach Technical Interface Meeting*, D-64186 (internal JPL/MSL document), Jet Propulsion Laboratory, Pasadena, California, May 19, 2009.
- [5] Lockheed Martin's Atlas V Selected to Launch Mars Science Laboratory in 2009 (press release), Lockheed Martin website, June 6, 2009. <http://www.spaceref.com/news/viewpr.html?pid=20031>
- [6] J. Taylor, A. Makovsky, A. Barbieri, R. Tung, P. Estabrook, and A. G. Thomas, *Mars Exploration Rover Telecommunications*, DESCANSO Design and Performance Summary Series, Article 10, Jet Propulsion Laboratory, Pasadena, California, October 2005.
- [7] Y. Lou, *MSL Terminal Descent Sensor User’s Guide*, Ver 2.1, D-37174 (JPL internal document), Jet propulsion Laboratory, Pasadena, California, February 9, 2009. <https://charlie-lib.jpl.nasa.gov/docushare/dsweb/View/Collection-47120>
- [8] *Mars24, Technical Notes on Mars Solar Time*, website, Goddard Institute for Space Studies, New York, updated August 5, 2008. <http://www.giss.nasa.gov/tools/mars24/help/index.html>
- [9] J. Herath, “Project Overview: System Design Review (SDR),” [MSL EDL instrumentation (MEDLI) website], MEDLI-SDR-0210, University of Idaho, May 1, 2007. [“http://www.mrc.uidaho.edu/~atkinson/SeniorDesign/ThermEx/MEDLI/MEDLI_SDR_Project_Overview.pdf](http://www.mrc.uidaho.edu/~atkinson/SeniorDesign/ThermEx/MEDLI/MEDLI_SDR_Project_Overview.pdf)
- [10] *Mars Pathfinder*, fact sheet, Jet Propulsion Laboratory, Pasadena, California, http://www.jpl.nasa.gov/news/fact_sheets/mpf.pdf
- [11] *Mars Science Laboratory Mission Plan*, JPL D-27162, Rev. A (internal document, Jet Propulsion Laboratory, Pasadena, California, August 10, 2007.
- [12] Digital Time Division Command/Response Multiplex Data Bus, MIL-STD-1553B, United States Department of Defense, continual updates.
- [13] P. Illot, *Mars Science Laboratory Telecommunications Functional Design Description*, Rev. B, D-34199 (JPL/ internal document), Jet Propulsion Laboratory, Pasadena, California, October 27, 2008.

-
- [14] *Small Deep Space Transponder (SDST), Functional Specification and Interface Control Document for MSL and Juno Projects*, D-33672 (JPL/MSL project internal document), Jet Propulsion Laboratory, Pasadena, California, May 15, 2007.
- [15] N. Blyznyuk, *Mars Science Laboratory Telecom System Engineering Pre-CDR Peer Review*, Telecom Antennas Pattern Analysis,” JPL D-64361 (internal JPL/MSL document), Jet Propulsion Laboratory, Pasadena, California, April 24, 2007.
- [16] WIPL-D: *Electromagnetic Modeling of Composite Metallic and Dielectric Structures*, WIPL-D d.o.o. [The abbreviation d.o.o means limited liability company] website, Belgrade, Serbia. <http://www.wipl-d.com/faq.php>
- [17] W. Boger, D. Burgess, R. Honda, C. Nuckolls, “X-Band, 17 Watt, Solid-State Power Amplifier for Space Applications,” *IEEE MTT-S International Microwave Symposium Digest*, vol. 3, pp. 1379–1382, 2005.
<http://ieeexplore.ieee.org/stamp/stamp.jsp?arnumber=01516940>
- [18] N. Blyznyuk, *DUHF Accommodation Study*, JPL D-64238 (internal JPL/MSL document), Jet Propulsion Laboratory, Pasadena, California, June 14, 2006.
- [19] N. Blyznyuk, *RUHF Accommodation Study*, JPL D-64394 (internal JPL/MSL document), Jet Propulsion Laboratory, Pasadena, California, June 14, 2006.
- [20] P. Ilott, J. Harrel, B. Arnold, N. Bliznyuk, R. Nielsen, D. Dawson, J. McGee, “UHF Relay Antenna Measurements on Phoenix Mars Lander Mockup,” *Antenna Measurements and Techniques Association (AMTA)*, Austin, Texas, October 22–27, 2006.
- [21] C. D Edwards, Jr., T. C. Jedrey, E. Schwarzbaum, A. S. Devereaux, R. DePaula, M. Dapore, and T. W. Fischer, “The Electra Proximity Link Payload for Mars Relay for Telecommunications and Navigation,” IAC-03-Q.3.A.06, *54th International Astronautical Congress*, Bremen, Germany, 29 September 29–October 3, 2003.
<http://trs-new.jpl.nasa.gov/dspace/bitstream/2014/7832/1/03-2150.pdf>
- [22] “*Proximity-1 Space Link Protocol—Physical Layer*”, *Recommendation for Space Data System Standards*, CCSDS 211.1-B-2 (Blue Book), Consultative Committee for Space Data Systems Secretariat, National Aeronautics and Space Administration, Washington, District of Columbia, March 2006.
<http://public.ccsds.org/publications/archive/211x1b3ec1.pdf>
- [23] Deep Space Network, website, Jet Propulsion Laboratory, Pasadena, California.
<http://deepspace.jpl.nasa.gov/dsn/>
- [24] P. W. Kinman, “Sequential Ranging,” Module 203, Rev. C, October 31, 2009, *DSN Telecommunications Link Design Handbook*, JPL D-19379, Rev. E, Jet Propulsion Laboratory, Pasadena, California, January 15, 2001,
<http://eis.jpl.nasa.gov/deepspace/dsndocs/810-005/>
- [25] T. Pham, C. Chang, E. Satorius, S. Finley, L. White, P. Estabrook, and D. Fort, *Entry Descent Landing Data Analysis (EDA)*, NASA Tech Brief NPO-41220 BR, National Aeronautics and Space Administration, Washington, District of Columbia, October 13, 2004.

-
- [26] “*Proximity-1 Space Link Protocol—Data Link Layer*,” *Recommendation for Space Data System Standards*, CCSDS 211.0-B-3 (Blue Book), Consultative Committee for Space Data Systems Secretariat, National Aeronautics and Space Administration, Washington, District of Columbia, July 2006. <http://public.ccsds.org/publications/archive/211x0b4.pdf>